THE ROLE OF ATM SIGNALLING AND ITS MEDIATOR PROTEINS IN DNA DOUBLE STRAND BREAK REPAIR

A thesis submitted to the University of Sussex for the degree of Doctor of Philosophy
By Andreas David William Kakarougkas
May 2012

Declaration

I hereby declare that this thesis has not been and will not be, submitted in whole or in part to another university for the award of any other degree.

Signature ……

Andreas David William Kakarougkas

Acknowledgements

I would like to express my sincerest gratitude to Professor Penny Jeggo for giving me the opportunity to carry out my doctoral studies in her laboratory and for her invaluable support and guidance throughout this period. I would also like to thank the Medical Research Council for funding my doctoral studies. Special thanks go out to all the members of the Jeggo laboratory for their help over the past four years and for making the GDSC an amazing place to work. I am particularly grateful to Atsushi Shibata for supervising aspects of this work.

I would like to thank our families for helping and supporting us in many different ways.

Finally I would like to dedicate this thesis to the women in my life. To Amani, for her constant support and encouragement without which this work would not have been possible, and to Nadia, whose smile always helps me keep things in perspective.

UNIVERSITY OF SUSSEX

ANDREAS DAVID WILLIAM KAKAROUGKAS

DOCTOR OF PHILOSOPHY IN BIOCHEMISTRY

THE ROLE OF ATM SIGNALLING AND ITS MEDIATOR PROTEINS IN DNA DOUBLE STRAND BREAK REPAIR

SUMMARY

Although most DNA double strand breaks (DSBs) are repaired by DNA non-homologous end-joining (NHEJ), DSBs at heterochromatin (HC) regions undergo repair by homologous recombination (HR) in G2 phase. Repair of DSBs at HC regions requires ATM-dependent KAP1 phosphorylation and subsequent HC relaxation. The mediator proteins facilitate DSB repair at HC in G1 phase by retaining ATM and hence pKAP1 at DSBs until the completion of repair. In this thesis, I investigated the role of the mediator proteins in enabling DSB repair in G2 phase. I demonstrate that the mediator proteins are required for the slow component of DSB repair in G2, which represents HR. They also promote ATM-dependent pKAP1 formation in G2 as in G1. In addition, I have described a role for MDC1 in Rad51 loading and for RNF8 in DNA resection. Moreover, I demonstrate that BRCA1 overcomes an inhibitory barrier by 53BP1 to resection by promoting a G2-specific enlargement in 53BP1 foci during HR that involves 53BP1 repositioning to the foci periphery and vacation from the central core. RPA foci form in the core devoid of 53BP1. 53BP1 has opposing roles in HR; it creates a restrictive barrier to resection but promotes pKAP1 and HC relaxation. RAP80 also inhibits resection by binding to ubiquitylated histones at DSBs. I demonstrate that the DUB enzyme, POH1, is required to overcome the barrier posed to resection by RAP80 since its depletion leads to deficient 53BP1 vacation of the central core and deficient resection. BRCA1 and POH1 cooperate during G2 phase to promote resection and DSB repair by HR. Additionally; I investigated the role(s) of the chromatin remodelers BAF180 and CHD7 in transcriptional silencing following DSB induction, a process that requires ATM, RNF8 and RNF168. I demonstrate that deficient transcriptional silencing leads to a DSB repair defect at early times post IR.

Table of Contents

List of Figures

List of Diagrams

List of Tables

Abbreviations

14-3-3σ	Stratifin
3D	3 Dimensional
53BP1	p53 binding protein 1
ADP	Adenosine Diphosphate
AID	Activation induced cytidine deaminase
Alt-NHEJ	Alternative non homologous end joining
AMP	Adenosine monophoshpate
APE1	Apurinic-apyrimidinic endonuclease 1
APLF	Aprataxin and PNKP like factor
ATLD	Ataxia-telangiectasia like disorder
AT	Ataxia-telangiectasia
ATM	Ataxia-telangiectasia mutated
ATMi	Ataxia-telangiectasia mutated inhibitor
ATP	Adenosine triphosphate
ATR	ATM and Rad3-related protein
BACH1	BTB and CNC homology 1, basic leucine zipper transcription factor 1
BAF180	Polybromo 1
BAH	Bromo-adjacent homology
BAX	BCL2-associated X protein
BCL-2	B-cell CLL/lymphoma 2
BER	Base excision repair
BLM	Bloom syndrome, RecQ helicase-like
BMI1	BMI1 polycomb ring finger oncogene
BRCA1	Breast cancer associated protein 1
BRCA2	Breast cancer 2, early onset
BRCC45	Brain and reproductive organ-expressed (TNFRSF1A modulator)
BRCC36	BRCA1/BRCA2-containing complex, subunit 3
BRCT	BRCA1 C Terminus

BRG1	Brahma related gene 1
BRM	Brahma
C-NHEJ	Classical non-homologous end joining
C-terminus	Carboxyl terminus
Cdc25A	Cell division cycle 25 homolog A (S. pombe)
Cdc25C	Cell division cycle 25 homolog C (S. pombe)
CDC45	Cell division cycle 45 homolog (S. cerevisiae)
CDK	Cyclin-dependent kinase
Cdk1	Cyclin-dependent kinase 1
Cdk2	Cyclin-dependent kinase 2
cDNA	Complementary DNA
CENP-F	Centromere protein F
CFP	Cyan fluorescent protein
CHD3	Chromodomain helicase DNA binding protein 3
CHD4	Chromodomain helicase DNA binding protein 4
CHD7	Chromodomain helicase DNA binding protein 7
Chk1	Checkpoint kinase 1
Chk2	Checkpoint kinase 2
CMV	Cytomegalovirus
CPT	Camptothecin
CSA	Cockayne syndrome protein A
CSB	Cockayne syndrome protein B
CSR	Class switch recombination
CtIP	CTBP-interacting protein
Ctp1	CtIP-related endonuclease
Cul1	Cullin 1
DDR	DNA damage response
DNA	Deoxyribonucleic acid
DNA-PK	DNA dependent protein kinase
DNA-PKcs	DNA dependent protein kinase catalytic subunit
DSB	Double strand break
DUB	Deubiquitinating enzyme
E2F1	E2F transcription factor 1

ERCC1	Excision repair cross-complementing rodent repair deficiency, complementation group 1
EU	Euchromatin
Exo1	Exonuclease 1
FA	Fanconi Anaemia
FAS	Fas (TNF receptor superfamily, member 6)
FEN1	Flap structure-specific endonuclease 1
FHA	Forkhead-associated
FOK1	FOK1 endonuclease
GADD45	Growth arrest and DNA-damage-inducible
GEN1	Gen endonuclease homolog 1 (Drosophila)
GFP	Green fluorescent protein
GG-NER	Global genome NER
Gy	Gray
H3K4me3	Histone H3 trimethylated on lysine 4
H3K9me3	Histone H3 trimethylated on lysine 9
H4K20me2	Histone H4 dimethylated on lysine 20
HA	Human influenza hemagglutinin
HAT	Histone acetyltransferase
HC	Heterochromatin
HDAC	Histone deacetylase
HDAC1	Histone deacetylase 1
HDAC2	Histone deacetylase 2
HERC2	HECT and RLD domain containing E3 ubiquitin protein ligase 2
HP1	Heterochromatin protein 1
HR	Homologous recombination
IR	Ionising radiation
IRIF	Ionising radiation induced foci
JARID1A	Jumonji, AT rich interactive domain 1A
JMJD2A	Jumonji domain-containing protein 2A
K48	Lysine 48
K63	Lysine 63

KAP-1	KRAB-associated protein 1
Kb	Kilobase
L3MBTL1	Lethal(3)malignant brain tumor-like protein 1
LCI	Live cell imaging
LET	Linear energy transfer
Lig IV	Ligase 4
LIG4	Ligase 4 syndrome
MDC1	Mediator of DNA Damage Checkpoint protein 1
Mdm2	Murine double minute 2
MeCP2	Methyl CpG binding protein 2
MEF	Murine / mouse embryonic fibroblast
MERIT40	Mediator of Rap80 interactions and targeting 40 kDa
MMEJ	Micro homology mediated end joining
MMS	Methyl methanesulfonate
MRE11	Meiotic recombination 11
MRN	MRE11 Rad50 and NBS1 complex
Mus81	US81 endonuclease homolog (S. cerevisiae)
NBS	Nijmegen breakage syndrome
NBS1	Nijmegen breakage syndrome 1
NER	Nucleotide excision repair
NF-κB	nuclear factor kappa-light-chain-enhancer of activated B cells
NHEJ	Non homologous end joining
NPL4	Nuclear protein localization protein 4
NuRD	Nucleosome Remodeling Deacetylase
PARP	Poly (ADP-ribose) polymerase
pATM	ATM phosphorylated on serine 1981
PBAF	Polybromo-associated BAF
PcG	Polycomb-group
PCNA	Proliferating Cell Nuclear Antigen
PHD	Plant Homeo Domain
PIAS	Protein inhibitor of activated STAT-1
PIKK	Phosphatidylinositol 3-kinase-related kinases
pKAP1	KAP-1 phosphorylated on serine 824

Plk1	Polo-like kinase 1
PNK	Polynucleotide kinase 3′-phosphatase
POH1	Pad1 homologue
Pol I	Polymerase 1
Pol II	Polymerase 2
PTM	Post translational modification
PUMA	p53 up-regulated modulator of apoptosis
Rad18	RAD18 homolog (S. cerevisiae)
Rad50	RAD50 homolog (S. cerevisiae)
Rad51	RAD51 homolog (S. cerevisiae)
Rad51c	RAD51 homolog C (S. cerevisiae)
RAP80	Receptor associated protein 80
RIDDLE	Radiosensitivity, immunodeficiency, dysmorphic features and learning difficulties
RING	Really Interesting New Gene
RNA	Ribonucleic acid
RNF168	Ring finger protein 168
RNF169	Ring finger protein 169
RNF8	Ring finger protein 8
RPA	Replication protein A
RPA2	Replication protein A2
RS-SCID	Severe Combined Immunodeficiency with Sensitivity to Ionizing Radiation
RSC	Chromatin structure remodelling
SAE1	SUMO-activating enzyme subunit 1
SAE2	SUMO-activating enzyme subunit 2
SCE	Sister chromatin exchange
SCF	Skp1, Cul1, F-box ubiquitin ligase complex
Ser	Serine
siRNA	Small interfering RNA
Skp1	S-phase kinase- associated protein 1
SMC1	Structural maintenance of chromosomes protein 1
Spo11	SPO11 meiotic protein covalently bound to DSB homolog (S.

	cerevisiae)
SSB	Single strand break
ssDNA	Single stranded DNA
Thr	Threonine
Tip60	Tat interacting protein, 60kDa
TOPBP1	Topoisomerase (DNA) II binding protein 1
Ub	Ubiquitin
UBC9	Ubiquitin conjugating enzyme 9
UBC13	Ubiquitin conjugating enzyme 13
uH2A	Ubiquitylated histone H2A
UIM	Ubiquitin interacting motif
USP16	Ubiquitin-specific processing protease 16
UV	Ultraviolet
UVA	Ultraviolet A
V(D)J	Variable (V), Diversity (D) and Joining (J) genes
VCP	Valosin containing protein
XLF	XRCC4-like factor
XP	Xeroderma pigmentosum
XPB	Xeroderma pigmentosum group B-complementing protein
XPD	Xeroderma pigmentosum D
XPF	Xeroderma pigmentosum, complementation group F
XRCC1	X-ray repair complementing defective repair in Chinese hamster cells 1
XRCC4	X-ray repair complementing defective repair in
YFP	Yellow fluorescent protein

CHAPTER 1

Introduction

1 Introduction

1.1: Significance of research in the field of the DNA Damage Responses.

DNA is the blue print of life. Every function of every living organism is carried out using information contained in the DNA molecule. It is therefore imperative that the integrity of DNA is maintained so it can be faithfully passed on to further generations. However, this is a major challenge for cells since DNA exists in a hostile environment, and its integrity is constantly under threat due to exposure to endogenous and exogenous DNA damaging agents. Endogenous agents include reactive oxygen species, which are by-products of normal cellular metabolism, while exogenous agents include ionising and UV radiation.

Loss of ability to deal with DNA damage can have severe consequences for the cell. Cellular proliferation in the presence of DNA damage can lead to loss of genomic stability, which is a hallmark of malignant transformation. The importance of the DNA damage responses (DDR) in preventing malignant transformation is evident in individuals afflicted with syndromes leading to a defective DDR, as many display elevated cancer incidence (Table 1.1) (Jackson & Bartek, 2009). Moreover, components of the DDR pathways are frequently lost or supressed in malignant cells thus allowing them to overcome these protective mechanisms.

Scientific research in the DDR field is important in order to gain understanding of the molecular mechanisms underlying cancer development. Moreover, targeting the DDR in cancer therapy has emerged as a powerful tool in sensitising cells to existing cancer treatments (Lord & Ashworth, 2012). It is paradoxical that deficient DNA repair is the primary cause of cancer development yet cancer treatment involves introducing DNA damage through radiotherapy and chemotherapy. However, the alterations in DDR pathways that promote carcinogenesis can be manipulated for therapeutic benefit. By identifying which DNA repair pathways are suppressed in a given tumour, drugs can be used to inhibit the remaining pathway(s) upon which the tumour cells become reliant, thus selectively sensitising the tumour cells to DNA damaging agents. Therefore, gaining insight into the complex molecular mechanisms of the DDR is important not only for understanding malignant transformation but also for finding ways to improve cancer treatment.

Syndrome	Phenotypes	Mutated Genes
GGR/NER deficiency		
Xeroderma pigmentosum	Neurodegeneration and microcephaly, Photosensitivity, skin cancer	XPA-XPG Pol η
Cockayne syndrome	Microcephaly, neuron demyelination and stunted growth	CSA, CSB, XPB, XPD, XPG
Trichothiodystrophy	Neurodevelopmental defects, dysmyelination (abnormal myelin), brittle hair and nails	XPD, XPB, TTD-A
Cerebro-oculo-facio-skeletal (COFS) syndrome	Demyelination (loss of myelin), dysmyelination, brain calcification, microcephaly	XPD, XPG, CSB, ERCC1
DNA helicase deficiency		
Bloom's syndrome	Microcephaly, short stature, dysmorphic features, mild/moderate mental retardation, susceptible to infections, Elevated predisposition to all cancers	BLM
Werner's syndrome	Premature ageing, cancer predisposition	WRN
Rothmund–Thompson syndrome	Stunted growth, skeletal abnormalities, early cataracts, accelerated ageing, chromosomal instability and cancer predisposition	RECQL4
Ataxia with oculomotor apraxia 2	Ataxia, neurodegeneration and oculomotor apraxia	SETX
Exonuclease deficiency		
Aicardi-Goutières syndrome (AGS)	De/dysmyelination, brain calcification, microcephaly, elevated CSF (cerebrospinal fluid) IFN-α, CSF lymphocytosis (CSF lymphocytes increased)	TREX1, RNASEH2
NHEJ/V(D)J recombination deficiency		
Inactivation of Ku70 or Ku80 in mouse models	Premature ageing, cancer predisposition, lymphomas	Ku70 Ku80
Lig4 syndrome/Human immunodeficiency with microcephaly	Microcephaly, leukemia, immunodeficiency, and developmental and growth delay	DNA Ligase IV, XLF/Cerunnos
RS-SCID (radiosensitive-SCID)	Severe-combined immunodeficiency, lymphomas and hypersensitivity to ionizing radiation	Artemis
HR deficiency		
Breast cancer 1, early onset	Breast and ovarian cancer	BRCA1
Breast cancer 2, early onset	Breast and ovarian cancer; predisposition to pancreatic, prostate and gastric cancer and melanoma	BRCA2
DNA SSB repair deficiency		
Spinocerebellar ataxia with axonal neuropathy (SCAN1)	Ataxia, neurodegeneration, peripheral axonal motor and sensory neuropathy, muscle weakness	TDP1
Ataxia with oculomotor apraxia 1 (AOA1)	Ataxia, neurodegeneration, oculomotor apraxia and peripheral neuropathy	APTX
DNA cross-link repair deficiency		
Fanconi anaemia	Congenital abnormalities, progressive bone marrow failure, prone to AML, squamous carcinomas of head, neck or gynaecological system.	FANCA-FANCM, BRCA2 (FANCD1)
Mismatch repair deficiency		
Hereditary non-polyposis colorectal cancer (HNPCC)	Colon and gynaecologic cancers	MSH2, MSH3, MSH6, MLH1, PMS2
DNA DSB-repair and signal-transduction deficiency		
Li-Fraumeni syndrome	Soft tissue sarcomas, breast cancer, brain tumours	p53
Familial breast cancer (non BRCA1/2)	Predisposition to medium/late-onset breast cancer	Chk2, MRN, ATM BRIP1, PALB2,
Ataxia telangiectasia	Cerebellar ataxia, telangiectases, immune defects, predisposition to malignancy (mainly lymphomas but also breast cancer)	ATM
Ataxia telangiectasia-like disorder	Mild A-T like features, possibly cancer predisposed	MRE11
Nijmegen breakage syndrome (NBS)	Microcephaly, growth retardation, mental retardation, immunodeficiency, cancer predisposition	NBS1
NBS-like syndrome	NBS-like phenotype	RAD50
RIDDLE syndrome	Radiosensitivity, immunodeficiency, dysmorphic features and learning difficulties	RNF168 (RIDDLIN)
Seckel syndrome	Marked microcephaly, primordial dwarfism, dysmorphic facial features and mental retardation, possibly AML	ATR, SCKL2, SCKL3
Primary microcephaly 1	Microcephaly, mental retardation	MCPH1/BRIT1
Hutchinson-Gilford progeria syndrome (HGPS) and restrictive dermopathy(RD)	Accelerated ageing (HGPS); neonatal lethality (RD)	Lamin-A
DNA-damage-response impairment and defective DNA repair		
Down syndrome	Mental retardation, progeria	Trisomy of chromosome 21
Alzheimer's disease	Progressive neurodegeneration leading to dementia, memory loss and cognitive decline	Increased oxidative stress and damage
Parkinson's disease	Tremor, bradykinesia, posture rigidity and postural instability, degeneration of dopaminergic neurons in substantia nigra area	Mutations in α-Synuclein and Parkin variants
Huntington's disease	Progressive chorea and dementia, severe neuronal loss in the striatum and cerebral cortex	CAG repeat expansion in *huntingtin (HD)*
Several spinocerebellar ataxias	Problems with bodily movements (similar to Huntington's disease), progressive neuron loss	Expanded CAG repeats in various genes
Friedreich's ataxia	Limb ataxia, cerebellar dysarthria, sensory loss, skeletal deformities	GAA expanded repeats in *frataxin (FXN)*
Myotonic dystrophy types 1 and 2	Muscle weakness and wasting, cataracts, testicular atrophy, cognitive decline	CTG expansion (type 1), CCTG expansion (type 2)
Triple-A syndrome	Adrenal insufficiency, achalasia, alacrima, neurodegeneration, autonomic dysfunction	Mutation in *AAAS* gene
Amyotrophic lateral sclerosis	Progressive degeneration of motor neurons, muscle weakness and atrophy, leading to fatality	Defective Cu-Zn superoxide dismutase (SODC, SOD1); mitochondrial DNA

Table 1.1: Human diseases with DDR defects (Jackson & Bartek, 2009)**.**

The introductory chapter of this thesis will provide an overview of the DDR with particular emphasis on the response to DNA double strand breaks (DSBs). This will lay the ground for the choice of topics covered in subsequent chapters. The aims of this thesis are outlined at the end of the introductory chapter.

1.2: DNA damage responses. Overview of the mechanisms that cells have evolved to prevent genomic instability.

To combat the effect of DNA damage and to maintain genomic stability, cells have evolved a vastly complicated collection of processes termed the DNA damage responses (DDR) (Harper & Elledge, 2007). These processes function to monitor DNA status integrity, to safeguard and to ensure that a complete and error free copy of the entire DNA molecule is passed on to the daughter cells following cell division. Owing to the frequency of genomic insult and to the size and complexity of their genome, this is a formidable challenge for mammalian cells. However, through sensors, mediators, transducers and effectors, mammalian cells repair DNA damage with incredible efficiency. Moreover, when DNA repair is not possible, the damaged cells are able to undergo apoptosis or enter senescence, thereby ensuring that damaged DNA is not passed on to further generations. Here I will summarise the processes responding to DNA damage.

1.2.1: Cell cycle checkpoints

Following the detection of DNA damage, cells activate a signalling cascade that leads to a halt of cell cycle progression (Diagram 1.1). Cell cycle checkpoints prevent cells from undertaking processes such as DNA replication and mitosis in the presence of DNA damage. Moreover, by inhibiting cell cycle progression, cell cycle checkpoints provide the cells with valuable time in which to attempt DNA repair before DNA replication or mitosis ensue (Jeggo & Löbrich, 2006). Cell cycle checkpoints function by inhibiting the activity of cyclin- dependent kinases (CDK), which drive cells through the cell cycle. In the presence of DNA damage, cells can inhibit entry into S-phase via the G1/S checkpoint and entry into mitosis via the G2/M checkpoint. In addition, if DNA damage is detected in S-phase, the intra-S-phase checkpoint causes a transient, reversible

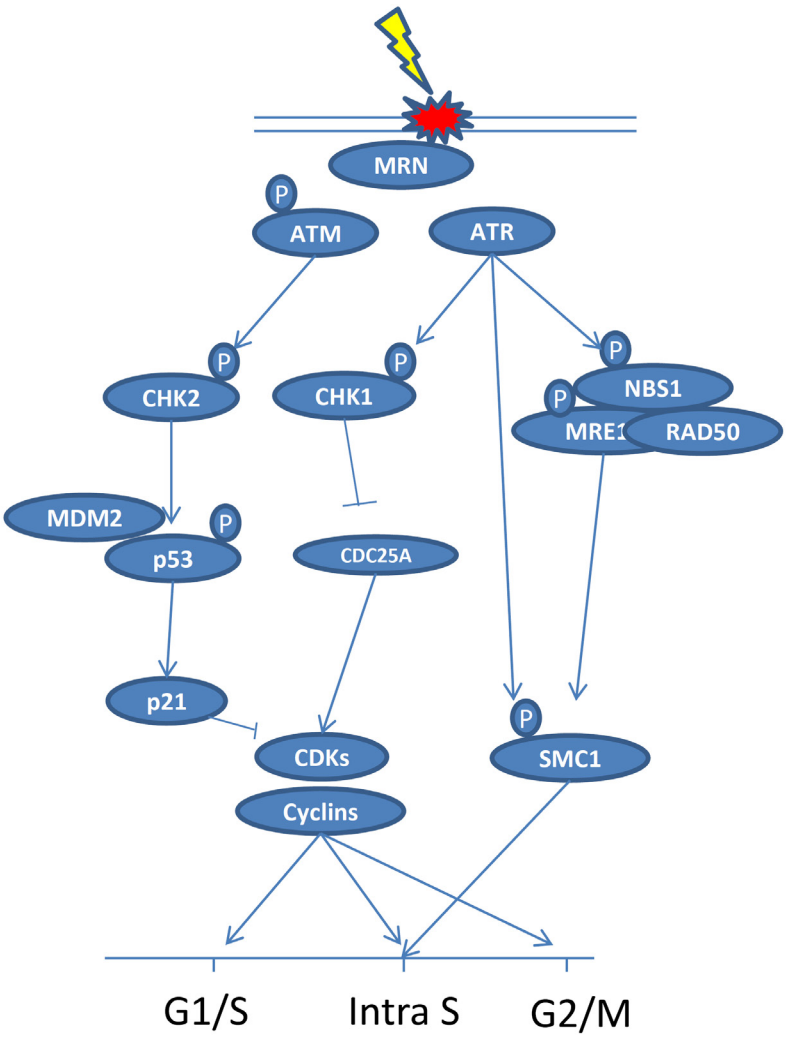

Diagram 1.1: Cell cycle checkpoint overview.
Detection of DNA damage leads to the activation of cell cycle checkpoints at the G1/S and G2/M boundaries, but also in S-phase. The PIKK kinases, ATM and ATR regulate the activation of the checkpoints by phosphorylating the effector kinases Chk2 and Chk1, respectively. The G1/S and G2/M checkpoints can both be rapidly activated by phosphorylation of the CDC25 phosphatases. This modification leads to their degradation and prevents the removal of inhibitory phosphorylations from the CDKs that promote cell cycle progression. When a more sustained checkpoint response is required, p53 is hyper-accumulated and drives the up regulation and accumulation of the effector p21, which is an inhibitor of the CDKs. In S-phase, DNA synthesis can be inhibited via the ATM/ATR and Chk2/Chk1 pathway which prevents origin firing. Alternatively, activation of the intra-S-phase checkpoint can be achieved via NBS1 and the cohesion protein SMC1. The mediator proteins are thought to facilitate these pathways by promoting the amplification and maintenance of the ATM/ATR signalling cascades. Adapted from (Kastan & Bartek, 2004).

inhibition of DNA replication by slowing on-going DNA synthesis and by preventing new origin firing (Zhou & Elledge, 2000).

The PIKK kinases, ATM and ATR, lie at the heart of the signalling cascades that make up the DDR. As will be discussed in more detail later, these kinases function in every facet of the DDR including cell cycle arrest, chromatin remodelling, DNA repair, and apoptosis (Shiloh, 2003). They carry out these functions via regulatory modification of a large numbers of downstream mediators and effectors. In the case of cell cycle regulation, the key effector kinases are Chk2 and Chk1, which are phosphorylated in response to DNA damage by ATM and ATR, respectively. Here an overview of the ATM-ATR co-ordination of DNA damage induced arrest at different cell cycle stages is provided (Diagram 1.1).

1.2.1a: G1/S checkpoint.

Following the activation of a checkpoint response, cell cycle progression can be halted in a transient way, or in a more sustained or even permanent way. This depends on which signalling pathway leading to a checkpoint response it utilised by the cell. In G1, the signalling pathway involving the phosphatase Cdc25A results in a transient response, while the signalling pathway involving the transcription factor p53 leads to a more sustained arrest. The Cdc25A signalling pathway can rapidly halt progression from G1 into S-phase in response to DNA damage, thus allowing time for the synthesis and accumulation of the factors required for the sustained p53 dependent arrest.

Under normal physiological conditions, entry into S-phase is driven by the removal of an inhibitory phosphorylation on the Cdk2 cyclin kinases by the Cdc25A phosphatase. However, following the detection of DNA damage in G1 phase, ATM and ATR phosphorylate Chk2 or Chk1, respectively, which in turn phosphorylate Cdc25A on several residues. This phosphorylation promotes further ubiquitylation of Cdc25A by the Skp1, Cul1, F-box ubiquitin ligase complex (SCF), which targets Cdc25A for proteasomal degradation (Sørensen *et al*, 2003; Busino *et al*, 2004). The dephosphorylation of the Cdk2 cyclin kinases (Cyclin E/A) is required for the recruitment of the pre-replication complexes to chromatin and for the initiation of DNA synthesis. Therefore the degradation of Cdc25A prevents this process by maintaining Cdk2 phosphorylation (Mailand *et al*, 2000; Falck *et al*, 2001). This branch of the G1/S checkpoint functions independently of p53 and rapidly inhibits cell cycle progression.

However, since Cdc25A normally functions to promote S-phase entry by dephosphorylating the Cdk2 cyclin kinases, its expression levels peak in late G1. Moreover, Cdc25A mediated cell cycle arrest is transient and can only prevent entry into S-phase for several hours. It appears that this is a fast acting response that is able to block late G1 phase cells from entering S-phase until the p53 branch of the checkpoint becomes active.

The expression levels of p53 under normal conditions are negatively regulated by the ubiquitin ligase, Mdm2, which binds and ubiquitylates p53 thus targeting it for degradation. However, following DNA damage induction, ATM or ATR phosphorylate Mdm2 thereby inhibiting its interaction with p53 (Maya *et al*, 2001). In addition, p53 is phosphorylated by Chk2 and directly by ATM and ATR leading to its stabilisation and hyper-accumulation (Hirao *et al*, 2000). As a result, p53 drives the up regulation and accumulation of the effector p21, which is an inhibitor of the Cdk2 cyclin kinases(Sherr & Roberts, 1999). Although this response requires several hours for the critical levels of p21 to be reached, the resulting inhibition of cell cycle progression is more sustained and even permanent. In conclusion, the Cdc25A and p53 branches of the G1/S checkpoint arrest cooperate to ensure that cells do not enter S-phase harbouring unrepaired DNA damage.

1.2.1b: Intra-S-phase checkpoint.

During DNA replication, cells are particularly vulnerable to genotoxic exposure. This is in part due to changes in chromatin structure that facilitate DNA replication, but mainly due to the consequences of active replication forks encountering damaged DNA regions. Stalled and collapsed replication forks can have devastating effects on the maintenance of genomic stability and, as a result, cells have evolved elegant mechanisms to attempt replication fork restoration (Petermann & Helleday, 2010). In addition, to prevent replication forks from encountering damaged DNA regions, cells activate an intra-S-phase checkpoint response. Similar to the G1/S checkpoint, the intra-S-phase checkpoint is comprised of two signalling branches, which cooperate to delay replication fork progression and to prevent the firing of new replication origins (Kastan & Bartek, 2004).

The first signalling pathway is identical to the transient branch of the G1/S checkpoint and involves ATM/ATR and Chk2/Chk1. By promoting the degradation of

Cdc25A, Cdk2 remains phosphorylated and inhibited. In turn, this prevents the loading of CDC45 onto chromatin, which is required for the recruitment of DNA polymerase α to the pre-replication complexes. Under these conditions, origin firing cannot take place and DNA synthesis is inhibited (Bartek *et al*, 2004).

The second branch of the intra-S-phase checkpoint response involves the phosphorylation of the MRN component NBS1 and the cohesin protein SMC1 by ATM (Lim *et al*, 2000; Yazdi *et al*, 2002). In this pathway, NBS1 functions as an adaptor protein and promotes the phosphorylation of SMC1, which is required for the intra-S phase checkpoint activation after IR. This branch of the S-phase checkpoint is distinct to the ATM/Chk2/Cdc25A pathway, but is clearly important since NBS cells display checkpoint defects in S-phase (Yazdi *et al*, 2002).

1.2.1c: G2/M checkpoint.

The G2/M checkpoint functions to prevent cells harbouring DNA damage from entering mitosis and attempting cell division. Entry into mitosis in the presence of DNA damage can lead to cell death by mitotic catastrophe or to genetic rearrangements and/or deletions, that contribute to the loss of genomic stability. Similar to the other cell cycle checkpoints, cell cycle arrest in G2 can be achieved transiently via post-translational modification of adaptor and effector proteins, or in a sustained way via the transcriptional regulation of such factors.

The transient activation of the G2/M checkpoint is mechanistically similar to the equivalent responses in the G1 and S phases of the cell cycle. Following activation of ATM/ATR, Chk1/Chk2 are phosphorylated and in turn go on to phosphorylate phosphatases (CDC25A-C). This phosphorylation initially impairs their activity and subsequently targets them for degradation (Lukas *et al*, 2004b). Degradation of the phosphatases prevents dephosphorylation of the Cdk1 kinase cyclin B, which is required to drive cells into mitosis (Kastan & Bartek, 2004).

Following exposure to IR in G2 phase, ATM and ATR co-operate in the transient G2/M checkpoint response, while the sustained checkpoint response is primarily ATR dependent (Brown & Baltimore, 2003). This is likely due to cells damaged in S-phase progressing to the G2/M boundary where the presence of ssDNA, due to erroneous or incomplete replication, maintains ATR activation and leads to a

sustained G2/M checkpoint response. Moreover, cells damaged in G2 phase can undergo repair by Homologous Recombination (HR), which involves the generation of ssDNA that activates ATR. The generation of ssDNA by resection appears to be a molecular switch that activates ATR and leads to a sustained G2/M checkpoint response (Shiotani & Zou, 2009).

The sustained G2/M checkpoint response is less well understood and is distinct to the G1/S checkpoint. Although the activation and maintenance of the G1 checkpoint is p53 and p21 dependent, cells lacking p53 are still able to activate the G2/M checkpoint indicating that p53 is not essential for this process (Taylor & Stark, 2001). On the other hand, p53 appears to play a role in the maintenance of the G2/M checkpoint via transcriptional regulation of GADD45 and 14-3-3σ (Taylor & Stark, 2001). GADD45 inhibits entry into mitosis by impacting on Cdk1 cyclin B and Cdc25A activity, since overexpression of either of these factors can overcome the GADD45 block on mitotic entry (Wang *et al*, 1999). 14-3-3σ is also thought to impact on Cdk1 cyclin B and Cdc25A activity and has been shown to be upregulated in a p53 dependent manner in response to DNA damage, leading to G2 arrest (Hermeking *et al*, 1997).

The importance of a proficient checkpoint response on the maintenance of genomic stability is highlighted by the fact that p53 is frequently downregulated in tumours. However, despite their importance, both the G1/S and G2/M checkpoints have limitations. The G1/S checkpoint is highly sensitive and can be activated by a single DSB, however, the initial 'rapid' response is leaky and some damaged cells are able to progress into S-phase. Moreover, and particularly following higher radiation doses, the G1/S checkpoint is not maintained efficiently thus allowing cells with residual damage to progress into S-phase (Deckbar *et al*, 2010). The G2/M checkpoint is less sensitive than the G1/S checkpoint meaning that there is a threshold of DNA damage that is required for its activation. Moreover, G2/M checkpoint maintenance is also not complete thus allowing cells with unrepaired DNA damage to enter mitosis (Deckbar *et al*, 2007; 2011; Stewart *et al*, 2009). Another limitation of the checkpoint response to DNA damage is the ability of certain cells to inactivate the checkpoint via a process termed 'checkpoint adaptation'. The process of checkpoint adaptation involves the inactivation of a sustained checkpoint in cells harbouring DNA damage thus allowing them to enter mitosis (Syljuâsen, 2007). In this process, polo kinase 1 (Plk1) overcomes Chk1 dependent checkpoint maintenance by promoting its de-phosphorylation, while at the same time it promotes mitotic entry by phosphorylating and activating Cdc25C

(Syljuâsen, 2007). The process of checkpoint adaptation might be activated during malignant transformation thus allowing cells with DNA damage to continue dividing.

Under normal physiological conditions, cell cycle checkpoints efficiently prevent genomic instability but their function alone is not sufficient. They form an important part of the DDR and are coordinated with other components of the response such as DNA repair, apoptosis and senescence.

1.3: DNA repair.

DNA repair forms an integral part of the DDR. Following the detection of damage and activation of cell cycle arrest, components of the DNA repair machinery are recruited to the damage sites and attempt to repair the damaged region(s). Owing to the variety of types of DNA damage that can arise, cells have evolved several different repair mechanisms to deal with this damage. Here I will provide a brief overview of these repair processes and will then focus on DSB repair in a separate section.

1.3.1: Nucleotide excision repair.

Nucleotide excision repair (NER) is the repair mechanism that responds to DNA damage affecting base pairing or general helical structure. Such damage normally arises following exposure to exogenous agents such as UV light and bulky lesions caused by chemical mutagens. NER can be divided into global genome-NER (GG-NER) and transcription coupled repair (TCR), which specifically responds to DNA damage that interferes with elongating RNA polymerases. The mechanisms of GG-NER and TCR are identical and require the same factors, except that in TCR when a polymerase-blocking lesion is detected, the affected polymerase is first removed by CSB and CSA. Next, in both pathways, the helicases XPB and XPD unwind and open up a DNA region of ~30bp around the damage site and RPA rapidly binds the exposed region to stabilise the molecule. The endonucleases XPG and ERCC1/XPF cleave either side of the generated flap on the DNA strand that contains the damage (Svejstrup, 2002) . Finally, polymerase(s) are recruited to fill in the excised region by using the undamaged strand as a template (Ogi *et al*, 2010).

The importance of the NER pathway in the maintenance of genomic stability is highlighted by human disorders resulting from mutations in factors of the NER

pathway. Xeroderma pigmentosum (XP) results from mutations in the XP genes and results in a 1000 fold increase in the incidence of skin cancer as a direct result of defective UV induced DNA damage repair (Friedberg, 2001). Cockayne syndrome, results from mutations in the CSA and CSB genes and consequently only affects the TCR branch of the NER pathway (Hoeijmakers, 2001).

1.3.2: Base excision repair.

As with NER, base excision repair (BER) responds to and repairs lesions affecting only one strand of the DNA molecule. BER mainly deals with endogenous DNA damage that arises as a consequence of normal cellular metabolism. By-products of these metabolic processes include reactive oxygen species, which damage DNA with high frequency on a daily basis. The BER pathway responds to small chemical alterations, abasic sites and single-strand DNA breaks (SSB) and repairs them by a core reaction followed by a short or long-patch version of the BER pathway. Base alterations are detected and excised by a family of glycosylases resulting in the formation of an abasic site. Abasic sites are then processed by the core BER reaction, which involves incision of the DNA strand at the abasic site by the endonuclease APE1 (Almeida & Sobol, 2007). The resulting SSB is then processed by short or long-patch BER. In a parallel pathway responding to SSBs, XRCC1, PARP1 and PNK process the SSB ends into a substrate that can be repaired by the BER machinery (Caldecott, 2003). The small patch BER pathway, involves the removal of the baseless sugar residue, followed by a gap filling reaction by polymerase β and ligation by the XRCC1-ligase 3 complex. The long patch BER pathway, involves the generation of a 2-10 base pair flap that is excised by the endonuclease FEN1. The excised region is filled in by polymerases (β,δ,ε) using the undamaged strand and ligase 1 carries out the ligation step (Fortini & Dogliotti, 2007).

Recently, a hereditary neurodegenerative disorder in which SSBs are defectively repaired indicates that the BER pathway might have a neuroprotective function (El-Khamisy *et al*, 2005).

1.4: Apoptosis.

Following the completion of DNA repair, cell cycle checkpoints are deactivated and cell cycle progression resumes. However, there are cases when attempts to repair DNA fail.

When such a situation arises, cells either permanently halt their cell cycle progression (senescence), or they undergo programmed cell death (apoptosis). There are many factors that determine which of these outcomes take place, including cell type and the extent of DNA damage.

There are several lines of evidence indicating that an inability to repair DNA damage is a strong trigger of apoptosis. Indeed, human cells defective for the NER, BER and DSB repair pathways all show elevated levels of apoptosis in response to DNA damage (Christmann *et al*, 2003). Moreover, cells that are transfected with restriction enzymes that induce DSBs also trigger an apoptotic response (Lips & Kaina, 2001). However, the induction of apoptosis does not always coincide with an inability to repair DNA damage. Certain cell types trigger apoptosis following the induction of low number of DSBs despite being proficient in DNA repair. An example of such a cell type are neuronal and progenitor cells, which during embryonic neuronal development are hypersensitive to radiation induced apoptosis (Gatz *et al*, 2011).

ATM and ATR play a critical role in the signalling response leading to apoptosis. As mentioned earlier, following the induction of DSBs, ATM and ATR are activated and phosphorylate downstream targets including p53. This leads to cell cycle arrest via p53 dependent transcriptional upregulation of factors such as p21. However, following the induction of large amounts of DNA damage or in the presence of persistent DNA damage, p53 can also drive the expression of pro-apoptotic factors such as BAX, PUMA and the FAS receptor (Lane, 1992). BAX interaction with mitochondria leads to the release of pro-apoptotic factors such as cytochrome c which leads to the activation of caspases whose protein degradation function leads to cell death (Tafani *et al*, 2002). The dual role of p53 in checkpoint and apoptotic signalling makes it hard to decipher whether it is a pro or anti-apoptotic factor. In some cell types, loss of p53 leads to resistance to DNA damage due to a supressed apoptotic response, whereas in other cell types loss of p53 sensitises cells to apoptosis (Roos & Kaina, 2006).

The ATM-ATR-p53 signalling pathway is important for the initiation of apoptosis, but the fact that ATM and p53 deficient cells are able to undergo apoptosis suggests that backup pathways exist. One pathway leading to apoptosis independently of p53 involves the activation of E2F1 by Chk1/Chk2. E2F1 activation drives the expression of the p53 homologue p73 whose pro-apoptotic function drives the expression of PUMA and BAX, thus leading to apoptosis (Melino *et al*, 2004). Another p53 independent pathway leading to apoptosis involves NF-κB, which can induce the

expression of the FAS receptor. The FAS receptor is expressed on the cellular surface but when activated and internalised it leads to caspase activation and subsequently apoptosis (Huang *et al*, 1996). Finally, apoptosis can be triggered by the degradation of BCL-2. However, the details of this pathway are not fully understood (Roos & Kaina, 2006).

In combination with the other components of the DDR, apoptosis plays an important role in the preservation of genomic stability. Eliminating cells harbouring DNA damage prevents cells from carrying out processes, such as replication or mitosis, in the presence of DNA damage, which can lead to genomic rearrangements and ultimately malignant transformation.

1.5: Senescence.

Replicative senescence is the process whereby cells undergo permanent arrest and no longer progress through the cell cycle. One way to trigger senescence is by telomere shortening which occurs progressively as a result of incomplete telomere replication in S-phase. With each cell cycle, telomeres become progressively shorter until replicative senescence is induced and cells stop cycling to protect the cells from loss of genomic material (Harley *et al*, 1990). This phenomenon can be counteracted by the function of telomerase, which is a reverse transcriptase able to restore telomere ends using telomeric RNA as a template. Cells with a high replicative potential such as stem cells and tumour cells, display high levels of telomerase activity (Cong *et al*, 2002). By the same mechanism, cultured cells such as fibroblasts that enter senescence after a set number of passages can escape this process and continue dividing when overexpressing telomerase.

In addition to replicative senescence, cells can also enter senescence as a result of DNA damage. It is thought that when cells accumulate DNA damage above a certain threshold, they enter senescence despite normal telomere length. This hypothesis is supported by the finding that cells lacking components of the DSB repair pathways display accelerated senescence (Lombard *et al*, 2005).

DNA damage induced and replicative senescence are induced by similar mechanisms. As discussed earlier, the detection of DNA damage leads to activation of ATM/ATR and cell cycle arrest via the Chk1/Chk2-p53/p21 signalling pathway. Interestingly, cells entering replicative senescence are positive for DNA damage

markers indicating that shortened telomeres activate the DDR (Takai *et al*, 2003). Indeed, shortened telomeres are recognised by the DSB repair machinery and trigger a DDR leading to senescence that is similar to the checkpoint response following DNA damage (Dimitrova *et al*, 2008). Consistent with this, cells with mutated p53 display extended lifespan while senescent cells in which ATM/ATR and/or Chk1/Chk2 is depleted are able to escape senescence and begin DNA synthesis (Herbig & Sedivy, 2006; Herbig *et al*, 2004).

Cellular senescence represents a protective mechanism whereby cells that have accumulated DNA damage, undergo a permanent checkpoint response. In addition, aging cells that have undergone a set number of passages enter senescence by activating a similar pathway, presumably as a way of protecting the cells from attempting DNA replication and mitosis in the presence of accumulated DNA damage. The importance of these mechanisms in preventing genomic instability is highlighted by tumour cells, which circumvent these protective mechanisms by blocking p53 function and upregulating the expression of telomerase.

1.6: Double strand break repair.

DNA double strand breaks (DSBs) are the most challenging DNA lesion that a cell can be faced with owing to the fact that both DNA strands are damaged. In addition, DSBs are the most toxic type of DNA damage as a single DSB can potentially lead to cell death. DSBs can be induced directly in all cell cycle phases by exposure to agents such ionising radiation (IR) or can result from replication forks encountering SSBs in S-phase. Cell have evolved two main repair pathways to deal with DNA damage, Non Homologous End Joining (NHEJ) and Homologous Recombination (HR).

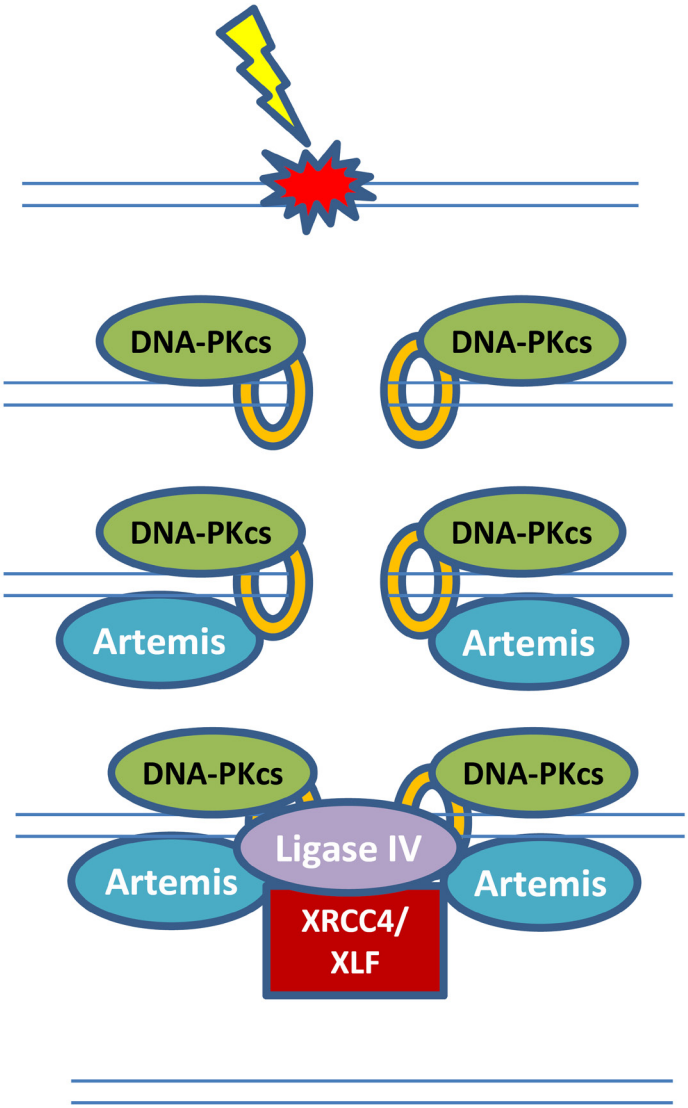

Diagram1.2: Classical non homologous end joining
In Non-Homologous End Joining (NHEJ) DSBs are recognized by the Ku 70/80 heterodimer that binds to the strand ends, which tethers them and leads to the recruitment of other proteins. The catalytic subunit of the DNA-dependent protein kinase, DNA- PKcs, then binds to the strand ends and activates the nuclease Artemis by autophosphorylation. Artemis then processes the ends possibly leading to loss of genetic information thus making NHEJ an error prone pathway of DSB repair. Finally XLF, Ligase IV and XRCC4 ligate the strands back together.

1.6.1: Classical Non Homologous End Joining.

NHEJ is the DSB repair pathway that repairs the majority of DSBs in the G1 and G2 cell cycle phases (Beucher *et al*, 2009). There are several factors that determine whether a DSB can be accurately repaired by NHEJ, but following exposure to IR approximately 80% of induced DSBs undergo efficient end processing (most likely without involving resection) and are repaired by classical NHEJ (C-NHEJ) (Diagram 1.2).

The first step of the NHEJ pathway involves the recruitment of the Ku70/Ku80 heterodimer which binds to the broken DNA ends and prevents their resection (Mimori & Hardin, 1986). Next, the Ku heterodimer translocates along the DNA molecule and recruits the DNA-dependent protein kinase catalytic subunit (DNA-PKcs) (Gottlieb & Jackson, 1993). DNA-PKcs is a key kinase in the DDR and regulates many downstream substrates. In classical NHEJ where CtIP dependent resection of DNA ends is not required prior to ligation, DNA-PKcs regulates the interaction of Ku with the DNA end ligation complex which is comprised of XRCC4, Ligase IV and XLF (Costantini *et al*, 2007). DNA-PKcs enhances the interaction between the heterodimeric form of Ku and the BRCT domain of Ligase IV (Costantini *et al*, 2007). In turn, ligase IV directly interacts with XRCC4 via two BRCT domains that are present in the C-terminal region of DNA ligase IV (Critchlow *et al*, 1997). The final component of the ligation complex is XLF which has been shown to directly interact with DNA ligase IV-XRCC4 and may function to tether the DSB ends (Ahnesorg *et al*, 2006). The DNA ligase IV-XRCC4-XLF complex is then able to ligate the DNA ends and seal the lesion. The ligation reaction involves the transfer of an AMP moiety by the DNA ligase IV/XRCC4 complex to the 5' phosphate of the DNA molecule leading to a donor DNA-adenylate complex. The reaction is then completed by the formation of a phosphodiester bond between the 5' phosphate donor and the 3' hydroxyl of the acceptor. XLF functions to re-adenylate the DNA ligase IV/XRCC4 complex thus allowing it to carry out further ligation reactions (Riballo *et al*, 2009).

The reaction described above repairs approximately 80% of IR induced DSBs with fast kinetics in the G1 and G2 phases of the cell cycle. However, approximately 15-20% of IR induced DSBs are repaired with slow kinetics and require additional repair factors for their efficient repair (Riballo *et al*, 2004). These factors include ATM, Artemis and the mediator proteins. The role of ATM and the mediator proteins in promoting the repair of this subset of DSBs will be discussed in detail in a later section.

There seems to be several contributing factors that determine whether a DSB requires additional processing prior to ligation. These include the chromatin structure surrounding the DSB as well as the complexity of the DNA lesion and whether the DSB end termini require additional processing prior to ligation (Riballo *et al*, 2004; Goodarzi *et al*, 2008). The endonuclease Artemis has been shown to be required for the efficient repair of this subset of breaks but the mechanism of how it achieves this has remained elusive. ATM and the NHEJ machinery also function in V(D)J recombination which is a process of genetic recombination that takes place during the production of the immune system. In this process, Artemis cleaves DNA hairpin structures in an DNA-PK dependent manner (Ma *et al*, 2002). The endonuclease activity of Artemis is facilitated by DNA-PK autophosphorylation, which is thought to remodel the DNA ends thus making them compatible for nucleolytic cleavage. The requirement for the endonuclease activity of Artemis in DSB repair is unclear (Goodarzi *et al*, 2006). As will be discussed later, the role of Artemis in the repair of a subset of DSBs is required in both the G1 and G2 phases of the cell cycle and is independent on the chromatin structure surrounding the DSB.

1.6.2: Micro Homology Mediated End Joining

Micro homology mediated end joining (MMEJ) is a backup end joining repair pathway that is thought to function when C-NHEJ is inhibited (Liang *et al*, 1996) (Diagram 1.3). This pathway of DSB re-joining is thought to be error prone due to deletions resulting from excessive DNA degradation (Liang & Jasin, 1996). Moreover, MMEJ is associated with the formation of chromosomal translocations (Bennardo *et al*, 2008). The mechanism of MMEJ is poorly understood but is thought to involve 5’ to 3’ DNA end resection of both DNA ends to generate 3’ DNA tails containing regions of microhomology that can then be used to ligate the break (McVey & Lee, 2008). The resected regions are not recovered, and it is this 5’ to 3’ resection that is thought to result in the deletions associated with MMEJ. The mechanism that carries out the re-joining remains unclear. However, the Lobrich and Jeggo laboratories have evidence that this can arise via a process dependent upon NHEJ proteins. There is also evidence that re-joining can occur via a process involving DNA ligase I/III and XRCC1 and PARP1 (described as Alt-NHEJ).

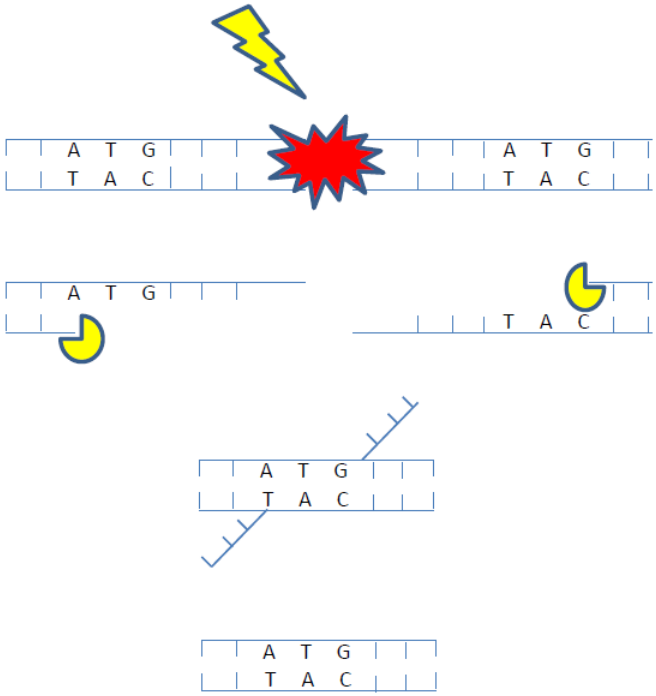

Diagram 1.3: Micro homology mediated end joining.
In order for the DNA ends to be ligated, they must be processed into substrates that are compatible with the ligation reaction. In order for the DNA ends to be complementary, microhomology regions are generated at DNA ends via the insertion or deletion of nucleotides. Alternatively, when microhomology regions are present further from the DNA ends, DNA resection can take place in order to expose the microhomology regions that allow the DNA ends to be ligated. This repair pathway is termed micro homology mediated end joining (MMEJ) and is thought to be error prone due to deletions resulting from excessive DNA degradation.

As will be discussed in detail later, DNA resection is the first step of DSB repair by HR in the G2 phase of the cell cycle and requires CtIP and the nuclease MRE11 (Shibata *et al*, 2011). Recent findings indicate that these factors also operate in resection associated with MMEJ suggesting a similar mechanism (Rahal *et al*, 2010). Moreover, the notion that CtIP and MRE11 function in the resection step of MMEJ is supported by recent findings showing that the increased translocations of Ku70 deficient cells are suppressed by CtIP depletion (Zhang & Jasin, 2010).

Ku is recruited to DSBs with very fast kinetics where it binds to DNA ends with high affinity (Smith *et al*, 1999). Ku appears to compete with PARP, another DNA binding factor. When DNA ends become bound by Ku, they are protected from DNA end resection and C-NHEJ ensues. When Ku is absent, PARP-1 is able to bind to DNA ends and initiate MMEJ (Alt-NHEJ) leading to deletions and chromosomal translocations (Wang *et al*, 2006). It is not clear whether Alt-NHEJ has a normal physiological function or whether it is an erroneous backup pathway that is only employed when NHEJ is compromised. There is strong evidence however, that by binding to DNA ends, Ku modulates DSB pathway choice and in the majority of cases promotes C-NHEJ in both G1 and G2 (Fattah *et al*, 2010).

1.6.3: Homologous Recombination.

HR is a repair pathway that utilises homologous sequences on the sister chromatid and uses them as a template for repair. Consequently, HR can only be utilised once the DNA region containing damage has been replicated. HR is considered an error free pathway that accurately repairs DNA lesions without loss of genetic information. The HR pathway plays an important role in the repair of one-ended DSBs arising at collapsed replication forks and appears to be the repair pathway predominantly used in S-phase (Petermann & Helleday, 2010) (Diagram 1.4). Work from our laboratory has indicated that HR is not as extensively used to repair two-ended DSBs following IR (X or γ-rays) exposure in G2 phase, where it functions to repair ~20% of induced DSBs (Beucher *et al*, 2009; Jeggo *et al*, 2011). Similar to the fraction of DSBs in G1 that require ATM, Artemis and the mediators proteins, this subset of DSBs in G2 also requires ATM and Artemis and is repaired with slow kinetics (Beucher *et al*, 2009). One of the major aims of this thesis was to investigate the role(s) of the mediator proteins in the repair of these DSBs in G2.

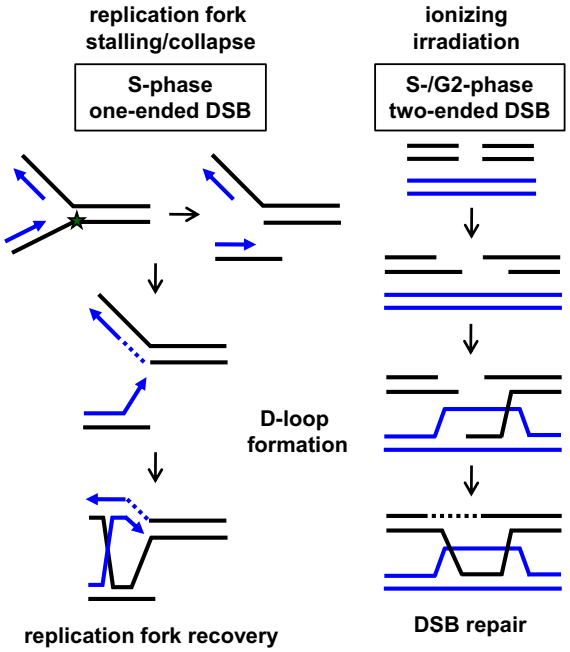

Diagram 1.4: Homologous recombination repair of one-ended and two-ended DSBs.
Homologous recombination (HR) repairs one ended DSBs arising in S-phase, but also two ended DSBs in G2 phase. In G2 phase HR, the DSB break is recognized by the MRN complex (Rad 50, Mre11 and NBS1), which then recruits ATM to the DSB site. Following ATM mediated resection and coating of single stranded DNA by RPA, members of the 'Rad' family together with BRCA1 and BRCA2, search the intact sister chromatid for a homologous region. Once the region has been located on the sister chromatid it is used as a template and the gaps are filled in by a polymerase without lose of genetic information. Finally the strands are ligated. In S-phase, the HR pathway is thought to be utilised for the restoration of collapsed replication forks that lead to the formation of one-ended DSBs. This process requires the core HR components (Rad family, BRCA1, BRCA2) and leads to the formation of a D-loop that can lead to the formation of an SCE upon resolution. Adapted from (Jeggo *et al*, 2011).

The HR pathway is initiated by extensive 5'to3' resection of the DNA ends to generate single stranded DNA overhangs (Elgin & Grewal, 2003). The process of resection is regulated by many factors and will be discussed in more detail in chapter 4. Briefly, the nuclease activity of MRE11 is thought to initiate resection while CtIP and ATM have also been shown to be required for this process (Mimitou & Symington, 2009b; Shibata *et al*, 2011). Recent evidence from yeast studies indicates that this first step functions to remove Ku and the MRN complex from DNA ends, thus allowing further nucleases to access the break and extend the resected regions (Langerak *et al*, 2011). The extension step of resection seems to involve the function of further nucleases and helicases such as Exo1 and BLM (Nimonkar *et al*, 2008; Mimitou & Symington, 2009a). In addition, multiple factors function to ensure that extensive resection does not take place as this could have deleterious consequences for the cell (Hu *et al*, 2011). How the process of resection is regulated and the interplay between key factors of the process is a main aim of this thesis and is analysed in chapter 4.

Once the ssDNA overhangs have been generated, they are quickly bound to and coated by RPA which protects the overhangs from further degradation and prevents the formation of secondary structures (Fanning *et al*, 2006). In addition, RPA coated DNA leads to ATR activation, which is important for the checkpoint response. Next, RPA becomes displaced and Rad51 is loaded onto the ssDNA region. BRCA2 has been shown to be an important factor for loading Rad51 on RPA coated DNA and for initiating the homology search on the sister chromatid (Liu *et al*, 2010; Jensen *et al*, 2010). The exact mechanism of how the homology search step is completed in not fully understood but recent evidence suggests that the process is facilitated by increasing the mobility of the damaged chromosomes thus enabling them to locate their homologous pair (Miné-Hattab & Rothstein, 2012). Next, Rad51 dependent strand invasion of the homologous region takes place which is then used as a template for filling in the resected regions (Holthausen *et al*, 2010). Finally, the strands are separated and restored via Holliday junction resolution in a process that requires the endonucleolytic function of Mus81 and GEN1 (Rass *et al*, 2010).

1.7: Relevance of the DDR in human disease.

Efficiently dealing with DNA damage and maintaining genomic stability plays an important role in the prevention of human disease. DNA damage and loss of genomic

stability is a hallmark of malignant transformation indicating that the DDR has an important role in preventing cancer formation. In addition, defects in the response to DNA damage also results in microcephaly and/or neurodegeneration suggesting that efficient DNA repair processes are important during embryonic neuronal development and/or the maintenance of a functional nervous system. Further still, the DDR machinery function in a diverse range of biological functions including the generation of immune system diversity, and the production of gametes. Consequently, inherited DDR defects can lead to increased cancer incidence, neurodegeneration, immune deficiency and infertility (Jackson & Bartek, 2009).

The human disorders associated with mutations in genes that function in the DDR are summarised in table 1.1, but below I will focus on human disorders associated with defective DSB repair.

1.8: Human disorders associated with defective DSB repair.

Ataxia Telangiectasia (AT) is an early onset autosomal recessive neurodegenerative disorder resulting from mutated ATM. AT is characterised by progressive ataxia but it is currently unclear whether ATM prevents this via its role in the DDR. AT patients also display increased cancer incidence and clinical radiosensitivity which are attributed to the central role of ATM in the DDR (Chun & Gatti, 2004).

The progressive neurodegeneration of AT patients is due to Purkinje cell loss, but it is not clear whether this results from a defective DSB response. Evidence that this might be the case comes from another human disorder resulting from mutated MRE11. MRE11 is a member of the MRN complex that is required for ATM activation in response to DSB induction and functions in the ATM dependent DSB repair pathway (Lee *et al*, 2010). Inheritance of defective MRE11 results in ataxia telangiectasia-like disorder (ATLD) which presents as a mild form of AT (Taylor *et al*, 2004). ATLD patients display neurodegeneration similar to AT patients, indicating that this phenotype might result from a deficient DNA DSB response. Cultured cells from AT and ATLD patients display radiosensitivity and a defective checkpoint response (Lavin, 2008). In addition, cultured cells from AT and ATLD patients display a similar DSB repair defect following IR exposure indicating that these proteins function in the same pathway responding to DNA DSBs (Goodarzi *et al*, 2008; Lee *et al*, 2010).

Nijmegen breakage syndrome (NBS) is another disorder resulting from a defective component of the MRN complex. In this syndrome, mutations in NBS1 result in a disorder characterised by microcephaly, clinical radiosensitivity and increased cancer predisposition (Saar *et al*, 1997). The cellular features of NBS cells are similar to those of AT cells, consistent with findings that NBS1 is involved in the activation and recruitment of ATM to DSBs where they directly interact via the C terminus of NBS1 (Berkovich *et al*, 2007). Importantly however, the clinical features of NBS and AT patients are very different. Although microcephaly is seen in NBS patients, they do not display ataxia and are therefore distinct to AT patients.

Another human disorder associated with defective DSB repair is LIG4 syndrome. LIG4 syndrome is a disorder that arises from mutation in the DNA ligase IV gene, which, as discussed earlier, is a component of the ligation complex that functions in NHEJ. The clinical features of LIG4 syndrome patients include microcephaly, a global developmental delay and immunodeficiency (O'Driscoll *et al*, 2001). Unlike ATM, MRE11 and NBS1 whose role in NHEJ is limited, ligase IV plays an important role in the ligation step of all DSBs and consequently LIG4 knockout MEFs display a severe DSB repair defect (Riballo *et al*, 2004). In contrast, ligase IV is dispensable for ATM signalling and as a result LIG4 deficient cells have a normal checkpoint response (O'Driscoll *et al*, 2004). Moreover, since NHEJ functions in V(D)J recombination, LIG4 patients also display immunodeficiency (O'Driscoll *et al*, 2001). Another distinction is that unlike AT patients where neurodegeneration is progressive, LIG4 patients are microcephalic but display no neurodegeneration post birth, indicating a role for ligase IV in embryonic neuronal development. Recent work from our laboratory using a LIG4 syndrome mouse model, suggests that the microcephaly in LIG4 syndrome, results from apoptosis triggered by unrepaired DSBs that arise in rapidly proliferating cells during neurogenesis (Gatz *et al*, 2011).

As discussed earlier, Artemis is a nuclease that functions in the repair of a subset of DSBs but also functions to cleave hairpin structures during V(D)J recombination (Riballo *et al*, 2004; Ma *et al*, 2002). As a result of these functions, radiosensitive severe combined immunodeficiency (RS-SCID) patients, who have mutated Artemis, are severely immunodeficient and cells from these patients display radiosensitivity in culture (Moshous *et al*, 2001; O'Driscoll *et al*, 2004). However, Artemis deficient cells are distinct to LIG4 deficient cells as Artemis is only required for the repair of a subset of DSBs. They are also distinct to AT cells as they display a

proficient checkpoint response and RS-SCID patients are not microcephalic (Riballo *et al*, 2004).

Seckel Syndrome is an autosomal recessive disorder with clinical features that include severe microcephaly, developmental delay and characteristic facial features (Goodship *et al*, 2000). Seckel Syndrome results from defective ATR which, as discussed previously, is a key component of the signalling response to DNA damage (O'Driscoll *et al*, 2003). ATR is activated by ssDNA and is the primary kinase responding to UV damage that leads to replication stalling in S-phase. ATR-Seckel cells display deficient ATR signalling resulting in a defective G2/M checkpoint following UV exposure as well as elevated micronuclei formation and nuclear fragmentation (Alderton *et al*, 2004). However Seckel Syndrome cells do not display increased sensitivity to IR because the ATM-dependent signalling transduction pathway responds directly to induced DSBs.

In summary, the DDR signalling pathways play important roles in limiting malignant transformation by preventing the accumulation of DNA damage and maintaining genomic stability. In addition, important roles for components of the DDR exist in the development of the neuronal and immune systems as well as in the prevention of neurodegeneration.

1.9: The DDR in cancer and cancer therapy.

The importance of the DDR in preventing genomic instability and malignant transformation is highlighted in the syndromes described above and others such as Fanconi anaemia and Bloom's syndrome where radiosensitivity and elevated cancer incidence are observed due to defective DSB repair (Lord & Ashworth, 2012). Moreover, several tumour types exist where DDR defects have been identified in a proportion of sporadic tumours and are believed to have contributed to the malignant transformation of these tumours. Examples of such tumour types include colorectal tumours and ovarian adenocarcinomas where loss of function mutations and epigenetic silencing lead to defective mismatch repair and HR, respectively (Lord & Ashworth, 2012; Cancer Genome Atlas Research Network, 2011).

In addition to defects identified in sporadic tumours, several familiar cancers are associated with defective HR with a prime example being hereditary breast cancer. The HR defect in familial breast cancers most frequently results from mutations in the

BRCA1 and BRCA2 genes, which as discussed earlier function in the HR pathway responding to DSBs (Powell & Kachnic, 2008). Individuals with BRCA associated breast cancer predisposition carry heterozygous mutations in the germ line and during their lifetime have an 80% risk of developing breast cancer. This malignant transformation entails loss or inactivation of the active wild type allele (Clarke *et al*, 2006).

There is substantial evidence indicating that the DDR is defective in the majority of cancers, resulting in the genetically unstable phenotype of tumour cells. One model as to how this arises suggests that the first step to malignant transformation is the activation of oncogenes. Activation of these genes leads to rapid proliferation, which is associated with DNA damage in S-phase. Uncontrolled replication can lead to the formation of DSBs when replication forks collide or when the dNTP pool is depleted leading to fork stalling and/or collapsing (Halazonetis *et al*, 2008). In support of this model, elevated levels of endogenous damage have been detected in precancerous lesions using DSB markers such as γ-H2AX foci (Halazonetis *et al*, 2008). However the intact DDR responses should be able to halt cell cycle progression and ensure that these lesions are efficiently repaired. It appears that the progression of precancerous lesions to malignant tumours is marked by the inactivation of DDR mechanisms that allow these cells to rapidly proliferate in the presence of DNA damage (Halazonetis *et al*, 2008).

The inactivation of DDR components allows tumour cells to proliferate in the presence of DNA damage, but also sensitises them to cancer treatments where DNA damaging agents such as platinum salts are used. For example, ovarian cancers with BRCA defects are sensitive to cross linking agents since there is a requirement for the HR pathway in the repair of the induced DNA damage (Lord & Ashworth, 2012). A greatly promising research area in cancer therapy is the development of drugs that can selectively target the intact DDR pathways of tumour cells. Using such drugs in conjunction with DNA damage inducing radiotherapy/chemotherapy can greatly increase the effectiveness of these treatments. Topoisomerase and PARP inhibitors are examples of drugs that target aspects of the DDR (Pommier *et al*, 2010; Rouleau *et al*, 2010). In both cases, these drugs lead to defective repair of SSBs that upon entry into S-phase can be converted to toxic DSBs when replication forks encounter these lesions. There is a great requirement for the HR pathway for the repair of these DSBs, thus making tumours with defective/suppressed HR particularly sensitive to these drugs.

There are several on-going clinical trials where DDR targeting drugs such as the PARP inhibitors are used for the treatment of cancers with known HR defects (Lord & Ashworth, 2012). However, since the proportion of cancers with known DDR defects is relatively small, these drugs do not have widespread use. To increase the usage of DDR inhibitors, the DDR defect of individual tumours needs to be identified and advances in whole-genome sequencing is making this possible. By identifying the DDR defect of a given tumour, the appropriate DDR inhibitor can then be used to sensitise the tumour to therapy. There is a long way to go and many obstacles to overcome, but these studies highlight the great potential of targeting components of the DDR for therapeutic gain.

1.10: Post-translational modifications in the DDR.

Many cellular processes are regulated via post-translational modifications (PTMs) as they can lead to the activation, deactivation, degradation, recruitment and interaction of factors functioning in these processes. In the DDR, PTMs play a key role in the orchestration of the multitude of factors that function to repair and/or respond to DNA damage (van Attikum & Gasser, 2009). There are numerous PTMs but here I will provide an overview of those that have been demonstrated to function in the DDR.

1.10.1: Poly(ADP-ribosyl)ation.

ADP-ribosylation involves the addition of ADP-ribose moieties to a protein. In a process termed PARylation, poly (ADP-ribose) polymerases (PARPs) can add multiple moieties to form poly (ADP-ribose) chains, which are the earliest PTM detectable at DNA damage sites (Polo & Jackson, 2011). Histone PARylation leads to the recruitment of downstream DNA repair factors including XRCC1 and APLF, which are particularly important for single-strand DNA repair (Okano *et al*, 2003; Rulten *et al*, 2008). PARylation is also likely to play a role in DSB repair as it has been reported to lead to the recruitment of chromatin remodelling factors and the MRN complex to DSBs (Polo *et al*, 2010; Haince *et al*, 2008).

1.10.2: Phosphorylation.

Protein phosphorylation, involves the post-translation modification of a target protein through the addition of a phosphate group. This modification is carried out by a protein kinase, which transfers the γ-phosphate from ATP to a serine, threonine or tyrosine residue on the target protein. There are a vast number of protein kinases in eukaryotic cells, which together with protein phosphatases regulate many cellular processes through reversible phosphorylation (Johnson, 2009; Barford, 1996). ATM, ATR and DNA-PKcs are key protein kinases in the DDR and are members of the phosphoinositide 3-kinase related kinase (PIKK) family (Abraham, 2004). These kinases can phosphorylate either serine (S) or threonine (T) residues, but show strong affinity for sites followed by a glutamine (Q) residue i.e. SQ/TQ sites. Interestingly, related kinases that are not involved in the DDR do not show the same affinity for these regions. Therefore identification of SQ/TQ sites on proteins can be indicative of involvement in the DDR (Matsuoka *et al*, 2007). Many such targets have been identified and implicated in the DDR where their modification by phosphorylation can directly regulate their structure and activity. Moreover, phosphorylation of DDR components can act as docking sites for the recruitment of downstream components that possess phospho-binding motifs such as BRCT and FHA domains (Mohammad & Yaffe, 2009).

1.10.3: Ubiquitylation.

Ubiquitylation involves the attachment via an isopeptide bond of a 76 amino acid polypeptide called ubiquitin to a target protein. Ubiquitin is bound to the target protein via its C-terminus and usually to the amino group of a lysine residue on the target protein in a three-step process. First, ubiquitin is adenelated on its C-terminus in an ATP dependent process by an enzyme known as an E1 ubiquitin ligase. Adenelated ubiquitin is then transferred to an E2 ubiquitin ligase before being ligated to the target protein in a process catalysed by an E3 ubiquitin ligase. E3 ubiquitin ligases may have direct enzymatic activity or may catalyse the ligation of ubiquitin by promoting the interaction of the E2 ligase and the target protein (Al-Hakim *et al*, 2010).

Ubiquitylation is similar to phosphorylation in that both utilise ATP hydrolysis. In addition, like phosphorylation, the process of ubiquitylation is involved in many cellular processes including cell cycle regulation, transcription, protein degradation and DNA repair (Trempe, 2011). The involvement in such an array of processes is due to the versatility in the formation of the ubiquitin conjugates on target proteins resulting from a variety of E2 and E3 complexes. Depending on the desired outcome, a single ubiquitin moiety may be attached (monoubiquitylation) or several ubiquitin moieties at different lysine residues (poly-monoubiquitylation). Furthermore, ubiquitin itself possesses seven lysine residues which themselves can be ubiquitylated resulting in the formation of ubiquitin chains (polyubiquitylation). These chains may lead to the cellular relocalisation of the target protein or may act as a recruitment platform for other proteins possessing ubiquitin interacting motifs. Finally, cells utilise de-ubiquitin enzymes to make the process reversible therefore adding a further layer of regulation (Ulrich & Walden, 2010).

1.10.4: Sumoylation.

Sumoylation is another post-translational modification that has been implicated in aspects of the DNA damage response (Gareau & Lima, 2010). Similar to the ubiquitin pathway, sumoylation involves the conjugation of sumo moieties (sumo 1 and sumo 2/3) onto target proteins via the cooperation of E1, E2 and E3 sumo ligases. However unlike the ubiquitin pathway, the sumo pathway only involves two E1 ligases, SAE1 and SAE2, and one E2 ligase, UBC9. There are however several E3 sumo ligases including the PIAS1-4 family.

1.10.5: Methylation.

Methylation is the addition of methyl group(s) to target proteins. When methylation is carried out on a lysine residue by a methyltransferase, it can involve the addition of one (mono) two (di) or three (tri) methyl groups. Methylated histones have been reported to play a role in the DDR where they function as recruitment sites for factors that contain TUDOR, PHD or chromodomains all of which can bind to methylated residues (Polo & Jackson, 2011). Such factors include 53BP1 and Tip60, which contain TUDOR and chromodomains, respectively. There are currently conflicting reports on whether *de*

novo histone methylation is carried out at DNA damage sites or whether existing methylated histones become exposed as a result of other PTMs such as ubiquitylation (Pei *et al*, 2011; Botuyan *et al*, 2006; Stewart, 2009). A recent study indicated that JMJD2A, a factor that binds methylated histones via its tandem TUDOR domain, competes with 53BP1 for methylated residues. However, upon the induction of DSBs, JMJD2A is ubiquitylated by RNF8 and RNF168 and targeted for proteasomal degradation thus allowing 53BP1 to bind to the exposed methylated histones and accumulate at DSB sites (Mallette *et al*, 2012).

1.10.6: Acetylation.

Histone acetylation at DSBs has been well studied by many different groups (Polo & Jackson, 2011). Through the joint function of histone acetyltransferases (HATs) and histone deacetylases (HDACs), histones at DSBs are modified to facilitate DNA repair. It is not currently clear whether HATs and HDACs cooperate at all DSBs or whether the function of one or the other is required depending on factors such as chromatin compaction and transcriptional status at the damaged DNA site. HDACs have been implicated in DSB repair by NHEJ as their depletion leads to defective DSB repair (Miller *et al*, 2010). This is believed to contribute to the radio sensitising effects of HDAC inhibitors which are being developed for cancer treatment.

Histone acetylation is associated with transcription, where it promotes chromatin remodelling leading to chromatin relaxation. Similarly, the HAT Tip60 has been reported as an important factor in facilitating DSB repair by HR by acetylating histones at DNA damage sites and thus increasing chromatin accessibility (Murr *et al*, 2006).

1.11: Chromatin structure.

In cells, DNA does not exist as a naked linear molecule but is rather packaged in a highly organised protein-DNA complex called chromatin. Cellular metabolic processes in which access to DNA is required need to contend with the highly compact structure of chromatin. Chromatin modifications that enable processes such as transcription and DNA repair, are generally achieved via histone post-translational modifications and chromatin remodellers (Bannister & Kouzarides, 2011; Berger, 2007; Clapier & Cairns,

2009). Chromatin can be broadly divided into euchromatin (EU) and heterochromatin (HC) (Diagram 1.5).

EU represents genomic areas that are relatively decondensed and which are frequently transcriptionally active. However, EU is still heterogeneous in nature with different areas enriched for particular modifications at any given time. There are numerous PTMs that can occur on chromatin including methylation, acetylation, phosphorylation, ubiquitylation, sumoylation and more (Bannister & Kouzarides, 2011). These modifications play an important role in transcriptional regulation by acting as recruitment platforms for proteins containing domains that bind to the different modifications (Bannister & Kouzarides, 2011). The regulation of transcription is highly complex as a given modification can act either as an activator or repressor of transcription depending on which residue of a given histone it is bound to (Berger, 2007). Moreover, the possibility of multiple modifications on a single residue as well as cross-talk between histone PTMs provide further regulatory layers (Bannister & Kouzarides, 2011).

Histone modifications and chromatin remodelling in EU are important components of the DDR to DSBs arising in EU (van Attikum & Gasser, 2009; Xu & Price, 2011). However, ATM, Artemis and mediator proteins appear to be dispensable for DSB in EU following exposure to X or gamma radiation. As will be discussed later, these components are important for the repair of DSBs that arise within HC regions (Goodarzi *et al*, 2008).

1.11.1: Heterochromatin.

HC reflects areas of the genome that remain particularly condensed throughout the cell cycle. HC was first distinguished from EU by its darker nuclear staining patterns and it was hypothesised that it corresponds to transcriptionally inactive areas (Trojer & Reinberg, 2007). In higher eukaryotes, HC is mainly made up of repetitive DNA, while specifically in humans, HC accounts for approximately 10-25 % of the genome (Miklos & John, 1979). HC can be divided further into constitutive and facultative HC.

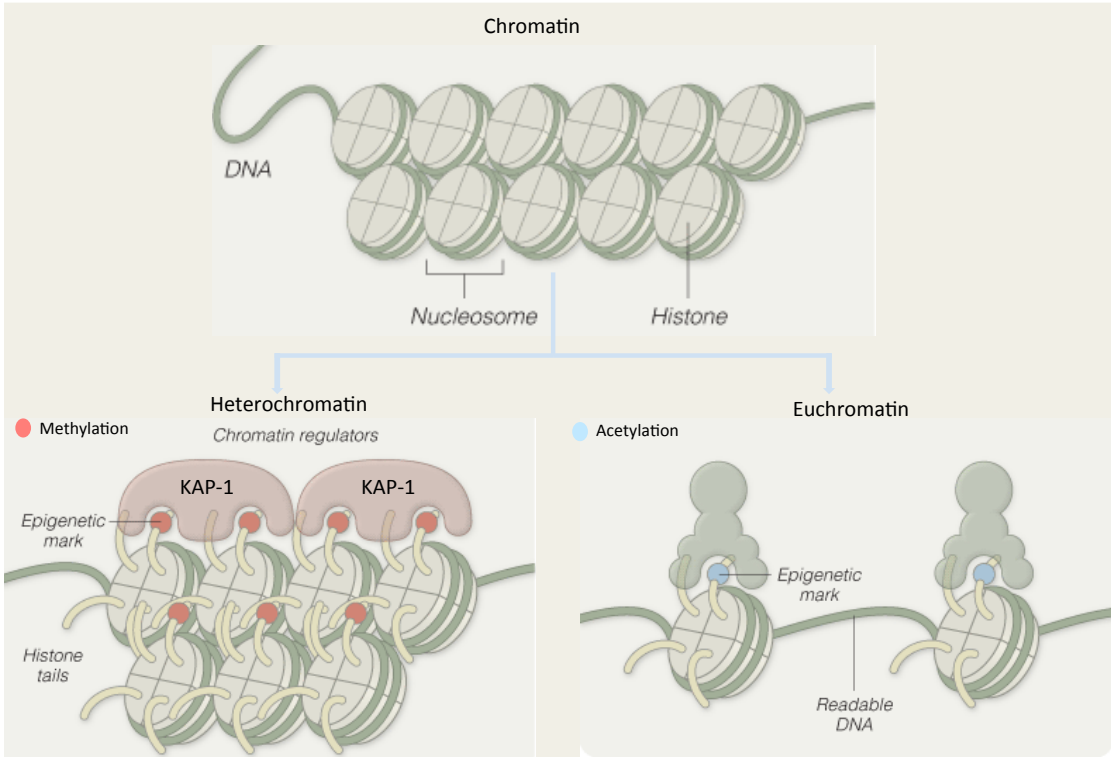

Diagram 1.5: Overview of chromatin structure.
Chromatin can be divided into euchromatin (EU) and heterochromatin (HC). EU represents genomic areas that are relatively decondensed and which are transcriptionally active. Moreover, these regions are enriched for epigenetic marks that are associated with transcription, such as histone acetylation. These epigenetic marks can act as recruitment platforms for transcriptional factors.
Heterochromatin reflects areas of the genome that remain particularly condensed throughout the cell cycle. These areas enriched for epigenetic marks that are associated with transcriptional silencing, such as histone methylation. These epigenetic marks recruit repressors, which in turn interact with co-repressors and together these factors lead to the formation of the dense HC superstructure.

Constitutive HC corresponds to genomic areas that are transcriptionally inactive and are permanently silenced, such as the telomeres and centromeres (Grewal & Jia, 2007). In addition to permanently silenced genes, these regions contain repetitive and non-coding sequences known as satellite DNA. The highly repetitive nature of satellite DNA enables the formation of secondary structures that are thought to be important for the establishment of constitutive HC (Metzler-Guillemain *et al*, 2003).

Facultative HC is dynamic in nature and provides regulatory control over gene expression. Genomic areas that are normally in EU and transcriptionally active, can become heterochromatinised and transcriptionally silenced. This is particularly prevalent during development and a prime example is the inactive X-chromosome in female mammalian cells, which is silenced by the establishment of HC (Yunis & Yasmineh, 1971). Another example is the silencing of genomic regions during cellular differentiation thus leading to functional specificity in differentiated cells (Trojer & Reinberg, 2007).

The formation of HC is a highly regulated process that involves the function of (i) transcriptional repressors and their associated corepressors, (ii) histone PTM modifiers such as histone deacetylases (HDACs) and histone methyltransferases (HMTs), (iii) adapter molecules such as HP1 and Polycomb and (iv) accessory factors such as ATP-dependent chromatin remodellers (Craig, 2004; Grewal & Jia, 2007). The first step in the process involves the recruitment of transcriptional repressors to gene promoters via their DNA-binding motifs, most commonly zinc finger domains (Urnov, 2002). Next, via protein-protein interaction domains, repressors recruit corepressors, which in turn recruit further HC components. An example of such an interaction which is particularly important in the DDR, is the interaction of the transcriptional corepressor Kruppel-associated box (KRAB)-associated protein (KAP-1) with zinc finger repressors containing a KRAB domain (Craig, 2004). In turn, transcriptional corepressors such as KAP-1 interact with modifiers including HDACs and HMTs as well as accessory factors such as ATP-dependent chromatin remodellers. The combined function of HDACs and HMTs lead to HC areas becoming enriched for chromatin modifications associated with transcriptional silencing such as H3K9me3 and diminished for transcription associated histone acetylation (Trojer & Reinberg, 2007; Berger, 2007). These histone modifications lead to the recruitment of adapter molecules including HP1 and Polycomb that further establish and maintain the HC superstructure by promoting nucleosome interactions (Maison & Almouzni, 2004).

The combined action of the factors outlined above lead to the establishment and maintenance of the HC superstructure. However, there are instances when chromatin accessibility is required, such as following the induction of DNA damage. In such cases, ATP-dependent chromatin remodellers can be recruited to DNA damage sites via interactions with transcriptional repressors or corepressors where they use the energy from ATP hydrolysis to remodel nucleosomes and increase chromatin accessibility (Craig, 2004; Goodarzi *et al*, 2011). In recent years, chromatin remodelling has emerged as an important aspect of the DDR and a major aim of this thesis is to investigate how repair of DSBs associated with HC is achieved in G2 phase (Downs *et al*, 2007).

1.12: The ATM signalling cascade to DSBs.

Following DSB induction, a complex signalling cascade is initiated that involves sensors, mediators, transducers, and effectors. These factors cooperate to carry out DNA repair within the context of chromatin and to interface DNA repair with other cellular processes such as transcription and DNA replication (Diagram 1.6).

Sensor proteins including the Ku70/80 heterodimer and the MRN complex detect DSBs following IR exposure and mark the first step in the DDR to DSB induction (Mimori & Hardin, 1986; Lavin, 2007). The recruitment of these factors is thought to stabilise the break and prevents the DNA ends from drifting apart. The MRN complex binds to DSBs as a heterotetramer, and tethers the DNA ends by direct interaction between the two Rad50 molecules (Moreno-Herrero *et al*, 2005). The MRN complex also plays an important role in the recruitment of ATM to DSB sites via a direct interaction between the C-terminal region of NBS1 and ATM (Berkovich *et al*, 2007; You *et al*, 2005).

ATM is recruited to DSBs as a dimer, where it undergoes autophosphorylation on serine 1981 leading to dimer disassociation and activation of its kinase activity (Bakkenist & Kastan, 2003). Following activation of its kinase activity, ATM phosphorylates many downstream substrates including the histone variant H2AX on serine 139 (γ-H2AX) (Rogakou *et al*, 1998). This phosphorylation triggers a cascade of events leading to the recruitment of an ever-expanding family of proteins that enable

efficient DSB repair by mediating chromatin remodelling, DSB repair pathway choice, checkpoint maintenance and more (Harper & Elledge, 2007).

Following the phosphorylation of histone H2AX, MDC1 is recruited to DSBs where it directly binds to the C-terminal region of γ-H2AX via its BRCT domains (Stucki *et al*, 2005). In addition to BRCT domains, MDC1 also possesses an FHA domain capable of phosphospecific interactions but this is dispensable for its association with γ-H2AX. The formation of γ-H2AX and the recruitment of MDC1 occur with fast kinetics and are visible within minutes following DSB induction (Bekker-Jensen & Mailand, 2010). Binding of MDC1 to γ-H2AX prevents γ-H2AX from being dephosphorylated, but also allows MDC1 to act as a binding platform for the recruitment of downstream factors. NBS1, which directly binds ATM, interacts with MDC1 via its FHA domain and this interaction retains ATM, leading to the spread of γ-H2AX over megabases (Lukas *et al*, 2004a; Stucki & Jackson, 2006; Rogakou *et al*, 1999). MDC1 also possesses conserved T-Q-X-F clusters, which as discussed earlier, are ATM/ATR substrate motifs (Mailand *et al*, 2007). Phosphorylated MDC1 is recognised and bound by the E3 ubiquitin ligase, RNF8, via RNF8's FHA domain (Mailand *et al*, 2007). This initiates the component of the ATM signalling cascade that is controlled by ubiquitin signalling.

RNF8 possesses a RING finger domain as well an FHA domain. The RING finger domain of RNF8 is dispensable for focal accumulation but is required for its ubiquitin ligase activity (Mailand *et al*, 2007). Following RNF8 recruitment, its ubiquitin ligase activity is stimulated by HERC2 (Bekker-Jensen *et al*, 2010). HERC2 is phosphorylated in response to DNA damage by either ATM, ATR or DNA-PK on Thr 48227 and this triggers its recruitment to DSB sites via an interaction with the FHA domain of RNF8 (Bekker-Jensen *et al*, 2010). HERC2 is thought to catalyse and stabilise the interaction between the RING finger domain of RNF8 and the E2 enzyme UBC13, an interaction that is required for the ubiquitin ligase activity of RNF8 (Bekker-Jensen *et al*, 2010). As mentioned previously, ubiquitin chains can form on a number of lysine residues, but only interaction with the E2 ligase UBC13 results in RNF8 mediated K63 linked ubiquitin chains (Plans *et al*, 2006). Therefore HERC2 catalyses the interaction between UBC13 and RNF8 and promotes K63 linked ubiquitin chain formation (Bekker-Jensen *et al*, 2010).

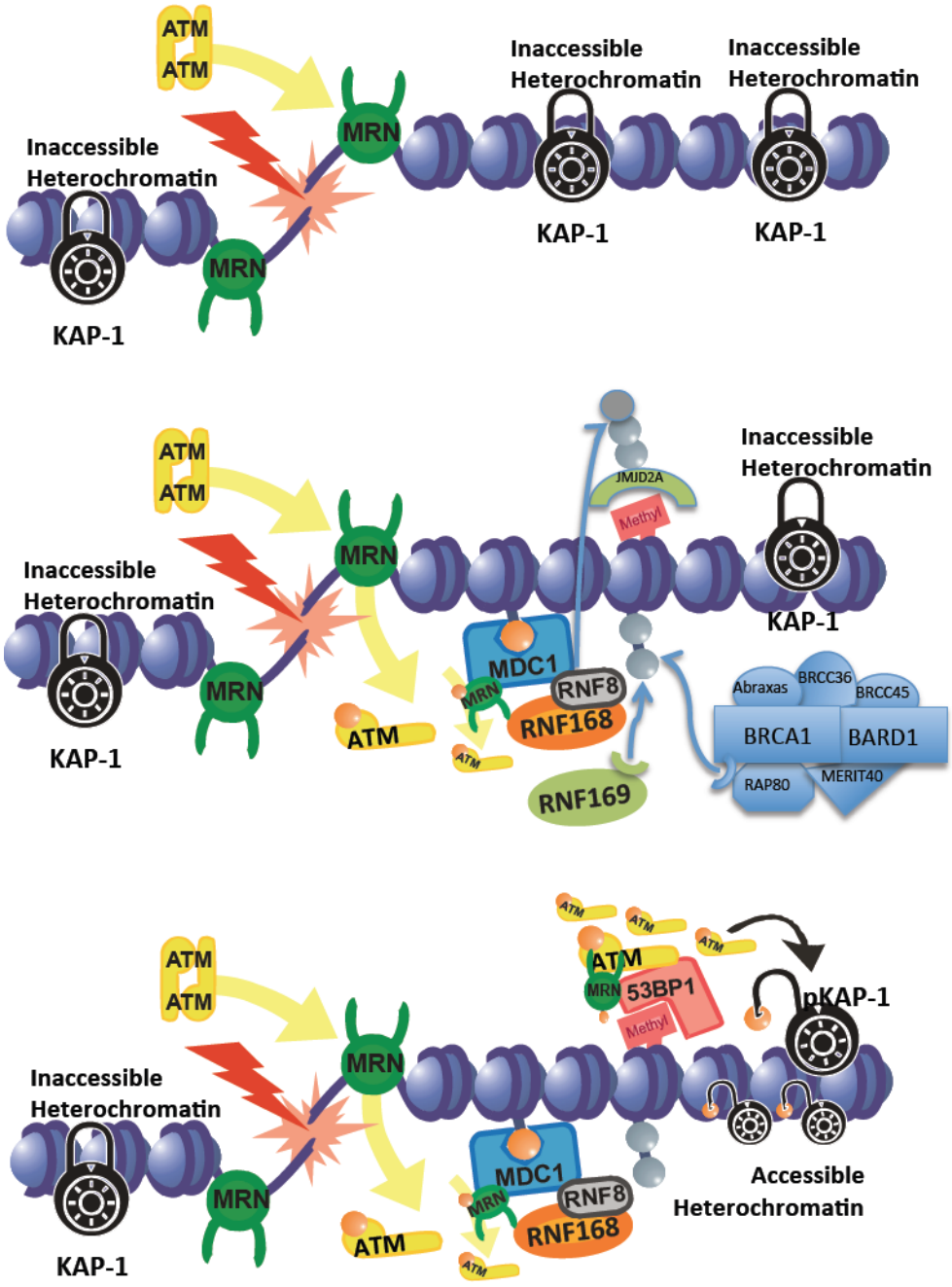

Diagram 1.6: The ATM signalling cascade to DSBs leading to HC relaxation
Upon the induction of a DSB, the lesion is detected by the MRN complex, which then recruits inactive dimer ATM to the DSB site. Once at DSB sites, ATM undergoes autophosphorylation, leading to its monomerisation and activation. Upon activation, ATM phosphorylates downstream targets including histone H2AX. Phosphorylated H2AX is recognised and bound to by MDC1, which then acts as a scaffold for the recruitment of further repair factors including RNF8 and RNF168. RNF8 ubiquitylates downstream substrates such as histone H2A and JMJD2A, leading to the formation of K63 and K48 ubiquitin chains respectively. RNF168 amplifies the RNF8 signal and catalyses the formation of K63 linked polyubiquitin chains which are then recognised and bound to by factors such as RNF169 and RAP80 which contain UIM motifs. RNF8 catalysed K48 linked ubiquitylation, targets substrates such as the methyl binding factor JMJD2A for proteasomal degradation, thus exposing methylated histones and leading to the recruitment of 53BP1 to these regions. 53BP1 interacts with the MRN complex via a direct interaction between its BRCT domains and the Rad50 subunit of the MRN complex (Lee *et al*, 2010). This interaction results in tethering of activated ATM at DSBs since ATM interacts with NBS1, another subunit of the MRN complex (You *et al*, 2005). 53BP1 dependent tethering of ATM at DSBs leads to concentrated and localised KAP1 phosphorylation (pKAP1), which leads to HC relaxation and allows the repair machinery to access the DSB. Original diagram by A.A Goodarzi.

Following the activation of its E3 ligase activity, RNF8 ubiquitylates chromatin surrounding the DSB predominantly on histones H2A and H2AX (Mailand *et al*, 2007; Huen *et al*, 2007). This results in the accumulation of K63 linked ubiquitin conjugates at DSBs (Kolas *et al*, 2007; Wang & Elledge, 2007; Zhao *et al*, 2007). Interestingly, the ubiquitin pathway appears to function in parallel to the SUMO pathway since the E3 SUMO ligases PIAS1 and PIAS4 also accumulate at DSBs and form SUMO1 and SUMO2/3 conjugates (Galanty *et al*, 2009). PIAS1 and PIAS4 are dispensable for RNF8 recruitment to DSBs but their depletion compromises the formation of ubiquitin conjugates, suggesting that SUMOylation might regulate RNF8 ubiquitin ligase activity (Galanty *et al*, 2009). The formation of ubiquitin conjugates at DSBs is required for the recruitment of downstream factors via motifs capable of interacting with ubiquitin. One such factor is the ubiquitin ligase RNF168, which is mutated in RIDDLE syndrome (Stewart *et al*, 2009). RNF168 possesses a RING finger domain but also two interacting with ubiquitin (UIM) motifs which target it to the ubiquitylated histones flanking DSBs (Doil *et al*, 2009). Once at DSB sites, RNF168 interacts with UBC13 and amplifies the RNF8 initiated ubiquitin response by further ubiquitylating histones H2A and H2AX leading to the recruitment of 53BP1 and BRCA1 (Doil *et al*, 2009; Stewart *et al*, 2009). Interestingly, a recent study demonstrated that RNF169, another E3 ubiquitin ligase paralogous to RNF168, is recruited to DSBs downstream of RNF8 and RNF168 (Poulsen *et al*, 2012). RNF169 is recruited to RNF8/RNF168 catalysed ubiquitin chains via its UIM and appears to compete with BRCA1 and 53BP1 for ubiquitin modified chromatin at DSBs (Poulsen *et al*, 2012). Since 53BP1 has been described as a factor that is inhibitory to HR, it is suggested that by delaying its accumulation to DSBs, RNF169 inhibits NHEJ and promotes repair by HR (Poulsen *et al*, 2012). The ubiquitin ligase activity of RNF169 appears to be dispensable for this function, as well as for the formation of the ubiquitylation products that lead to the recruitment of 53BP1 and BRCA1 (Poulsen *et al*, 2012).

The recruitment of BRCA1 to DSB sites is promoted via its interaction with RAP80, a factor that possesses a UIM capable of binding to ubiquitin chains (Sobhian *et al*, 2007). However, recent studies have suggested that RAP80 is enhancing but not essential for BRCA1 recruitment to DSBs (Hu *et al*, 2011). Conversely, the mechanism of 53BP1 recruitment to DSBs has remained elusive although RNF8/RNF168 and the upstream signalling response are clearly important (Stewart, 2009). The mystery surrounding the recruitment of 53BP1 to DSBs stems from the fact that 53BP1 does not

possess a motif capable of interacting with ubiquitin but rather binds to histone H4 dimethylated on lysine 20 (H4K20me2) via its TUDOR domain (Botuyan *et al*, 2006). Moreover, there have been conflicting reports on whether this modification increases following DNA damage, or whether other modifications such as histone ubiquitylation lead to the exposure of the methylated histones to which 53BP1 binds (Pei *et al*, 2011; Botuyan *et al*, 2006). The results of three recent studies, support a model whereby 53BP1 recruitment is facilitated via the disassociation or degradation of factors bound to H4K20me2 at DSBs, thus allowing 53BP1 recruitment (Acs *et al*, 2011; Meerang *et al*, 2011; Mallette *et al*, 2012). Acs *et al* demonstrate that the VCP-NPL4 complex is recruited to DSBs via the interaction of NPL4 with ubiquitylated histones. Once at DSB sites, this complex interacts with ubiquitylated L3MBTL1, a Polycomb protein that binds H4K20me1/2. The ATPase activity of VCP then promotes the disassociation of L3MBTL1 from chromatin thus exposing H4K20me2 and allowing 53BP1 assembly (Acs *et al*, 2011). Interestingly, Meerang *et al* indicated that the recruitment of the VCP-NPL4 to DSBs depends on RNF8 mediated K48 and not K63 ubiquitylated chains (Meerang *et al*, 2011). Moreover this study demonstrates that the ATPase activity of VCP is required to extract K48 ubiquitylated proteins from DSBs and that this is required for the accumulation of 53BP1 and BRCA1 (Meerang *et al*, 2011). Given this, it is likely that the ubiquitylation of L3MBTL1 results in K48 linked ubiquitin chains resulting in its disassociation from chromatin by VCP. Finally, Mallette *et al* demonstrated that JMJD2A, a factor that possesses a TUDOR domain, binds to H4K20me2 and competes with 53BP1 for these sites. However, following DNA damage, JMJD2A is ubiquitylated by RNF8/RNF168 leading to the formation of K48 linked ubiquitin chains (Mallette *et al*, 2012). This modification targets JMJD2A for proteasomal degradation thus leading to its removal from chromatin and allowing 53BP1 to bind the vacant H3K20me2 sites. In summary, these studies provide a model for the recruitment of 53BP1 to DSB sites but also highlight the significance of both K63 and K48 linked RNF8/RNF168 mediated ubiquitin modifications in the DDR.

Once recruited to DSBs, 53BP1 interacts with the MRN complex via a direct interaction between its BRCT domains and the Rad50 subunit of the MRN complex (Lee *et al*, 2010). This interaction results in tethering of activated ATM at DSBs since ATM interacts with NBS1, another subunit of the MRN complex (You *et al*, 2005). 53BP1 dependent tethering of ATM at DSBs is important for the maintenance of G2/M checkpoint arrest following IR exposure >3Gy, but also for the repair of DSBs at HC

regions (Shibata *et al*, 2010; Noon *et al*, 2010). DSBs at HC regions require concentrated and localised KAP1 phosphorylation (pKAP1) for HC relaxation and 53BP1 mediates this process by concentrating active ATM at these sites (Noon *et al*, 2010). During heterochromatin formation, SUMOylated KAP1 interacts with the nucleosome remodeller CHD3 which promotes nucleosome compaction. However, KAP1 phosphorylation on Ser 824 following DNA damage, generates a motif that disturbs the CHD3-KAP1 interaction leading to the disassociation of CHD3 from chromatin, which in turn results in chromatin relaxation (Goodarzi *et al*, 2011).

Several of the factors described in this signalling response to DSBs have additional roles in the DDR and do not simply function to mediate ATM dependent HC relaxation. In addition, other factors such as BRCA1 are recruited as part of this signalling cascade but are, in fact, dispensable for pKAP1 formation (see chapter 4). Nevertheless, the ATM signalling cascade resulting in HC relaxation is an important part of the DDR and is required for the repair of DSBs residing at HC regions. Such DSBs account for ~20% of X and gamma ray induced DSBs.

Chromatin decondensation is particularly important for the repair of DSBs localised at HC regions, but this is not to say that it does not take place in EU also. Indeed, chromatin structure has been shown to be inhibitory to processes such as transcription, and large-scale chromatin decondensation is required to facilitate these processes (Müller *et al*, 2001). Similarly, chromatin remodelling at DSBs appears to be important for the recruitment of repair factors such as RNF168 and BRCA1. Interestingly, a recent study demonstrated that RNF8 functions together with the chromatin remodeller CHD4 to promote the extensive chromatin decondensation that is required for the recruitment of downstream repair factors (Luijsterburg *et al*, 2012). RNF8 recruits CHD4 to DSB sites via its FHA domain where the chromatin remodelling activity of CHD4 functions to decondense chromatin in a manner dependent upon its ATPase activity (Luijsterburg *et al*, 2012). Although the recruitment of CHD4 and the associated chromatin decondensation does not depend upon the ubiquitin ligase activity of RNF8, the ATPase activity of CHD4 promotes the RNF8 mediated ubiquitin modifications required for the accumulation of downstream factors (Luijsterburg *et al*, 2012). Therefore, it appears that chromatin decondensation is important for DSB repair both in HC and EU, although ATM function appears to be dispensable for RNF8-CHD4 mediated chromatin remodelling.

1.13: DSB repair pathway choice.

As discussed previously, cells have evolved two main mechanisms for repairing DSBs, NHEJ and HR. However, the presence of multiple repair pathways raises an important question. What are the factors that determine DSB repair pathway choice, and how is the choice of repair pathway regulated? Recent work has provided insight into these questions but several unanswered questions remain. There appear to be two main determinants of DSB repair pathway choice. The first is the position of the cell in the cell cycle, and the second is whether or not DNA resection is initiated (Symington & Gautier, 2011). The regulation of resection has emerged as an intricately controlled process that affects DSB repair pathway choice in all cell cycle phases (Shibata *et al*, 2011; Mimitou & Symington, 2011; Yun & Hiom, 2009; Zhang & Jasin, 2010).

Until recently, the only known determining factor of DSB repair pathway choice was cell cycle phase. The general view was that G1 cells utilise the NHEJ pathway while in S/G2 phase, HR is the predominant repair pathway since the presence of a homologous template on the sister chromatid can be used for accurate repair. However, in light of recent findings, this is an oversimplified model that does not take into account the effect on pathway choice of parameters such as DNA damage complexity and chromatin structure at the damaged site (Shibata *et al*, 2011). Moreover, despite HR being functional in G2 phase, NHEJ is still the dominant repair pathway in G2, as only ~20% of X and gamma ray induced DSBs are repaired by HR (Beucher *et al*, 2009). Therefore, although cell cycle phase does impact on DSB repair pathway choice, it is not the determining factor.

Recent work from our laboratory indicated that in mammalian cells, both the complexity of DNA damage and the chromatin complexity surrounding the DSB are determining factors in DSB repair pathway choice (Shibata *et al*, 2011). High LET carbon-ion induced DSBs are more ‘complex’ than etoposide induced DSBs as they lead to the formation of clustered damaged sites containing multiple DSBs and other forms of damage. Such lesions are more likely to undergo resection and repair by HR. On the other hand, etoposide induced DSBs are predominantly repaired with fast kinetics by NHEJ also in G2 phase. However, when etoposide induced DSBs are located at HC regions, they undergo resection and are repaired by HR (Shibata *et al*, 2011). Therefore, at least in G2 phase, DNA damage complexity and chromatin structure surrounding the DSB are determining factors in DSB repair pathway choice.

Following the induction of DSBs, Ku and the MRN complex rapidly bind all DSBs (Mimori & Hardin, 1986; Lavin, 2007). It appears that Ku binding to DSBs and the subsequent recruitment of DNA-PK promote fast re-joining of the DNA ends by NHEJ. However, when repair by NHEJ is not possible, DNA end resection is initiated leading to DSB repair by HR in G2 phase and by MMEJ in G1 phase (Shibata *et al*, 2011; Yun & Hiom, 2009). However, prior to the initiation of resection, Ku must disassociate from the DNA ends since its presence is inhibitory to resection (Fattah *et al*, 2010; Shao *et al*, 2012; Sun *et al*, 2012; Langerak *et al*, 2011). Although the removal of Ku from DNA ends appears to be critical for the initiation of resection, the mechanism of how this is achieved is still unclear. Work in *Schizosaccharomyces pombe* demonstrated a role for the nuclease activity of Mre11 and Ctp1/CtIP in the disassociation of Ku70/Ku80 and the MRN complex from DSB ends (Langerak *et al*, 2011). Another study monitoring the removal of the meiotic transecterase, Spo11, from meiotic DSBs in *Saccharomyces cerevisiae* also described an important role for MRE11 in this process (Garcia *et al*, 2011). This study revealed that MRE11 endonuclease activity introduces nicks up to 300 nucleotides from the DNA end, which initiates bidirectional resection by Exo1 in the 5'-3' direction and by the exonuclease activity of MRE11 in the 3'-5' direction (Garcia *et al*, 2011). This bidirectional resection leads to the disassociation of Spo11 from the DNA but also creates a ssDNA overhang. It is not yet clear whether Ku is removed from DSB ends by a similar mechanism. An alternative model is that Ku disassociates from DNA ends following PTM. Work using *Xenopus laevis* egg extract, demonstrated that Ku80 is ubiquitylated following DSB induction and that the formation of K48 linked ubiquitin chains on Ku80 is required for its removal from DSB ends (Postow *et al*, 2008). Similarly, a study using human cells demonstrated that Ku80 is ubiquitylated by RNF8 following DNA damage leading to the formation of K48 linked ubiquitin chains on Ku80. This leads to its disassociation from the DNA ends and targets it for degradation (Feng & Chen, 2012). Although the precise mechanism leading to the removal of Ku from DSB ends is not fully understood, it is an important step in the resection process and reveals important roles for MRE11 and RNF8 in the regulation of DSB repair pathway choice.

Another key factor in DSB repair pathway choice via its role in DNA resection is CtIP (Huertas & Jackson, 2009; Sartori *et al*, 2007; You *et al*, 2009; Yun & Hiom, 2009; Shibata *et al*, 2011). Specifically in the S and G2 phases of the cell cycle, CtIP is phosphorylated by CDK on Ser 327 which promotes its interaction with the BRCT

domain of BRCA1 (Yu & Chen, 2004; Huertas & Jackson, 2009). This interaction is important for an efficient checkpoint response to the induction of DNA damage and for efficient repair by HR (Yu & Chen, 2004; Yun & Hiom, 2009). During HR, CtIP is required for the initiation of resection and its function in this process is modulated by CDK dependent phosphorylation on Thr 847 (Sartori *et al*, 2007; Huertas & Jackson, 2009). Furthermore, recent work has demonstrated that in the G2 phase, ATM regulates resection via direct phosphorylation of CtIP on Ser 644/745 (Shibata *et al*, 2011). These findings demonstrate roles for CtIP, CDK and ATM in DSB pathway choice via the regulation of resection. Surprisingly, following exposure to IR in G2, if the initiation of resection is abolished via depletion of CtIP or the inhibition of ATM, then repair can ensue with faster kinetics by NHEJ (Shibata *et al*, 2011). This demonstrates that the initiation, or not, of resection is a key event in DSB repair pathway choice.

CtIP also functions in resection during MMEJ in G1 phase, but this role does not depend on its interaction with BRCA1 (Yun & Hiom, 2009). It is also not currently clear whether CDK and ATM regulate CtIP function during G1 phase resection. The slow component of repair in G1 phase is thought to correspond to DSBs that undergo resection and repair by MMEJ. A recent study demonstrated that this alternative re-joining pathway leads to chromosomal translocations that can be prevented by the depletion of CtIP, which prevents the initiation of resection and promotes repair by C-NHEJ (Zhang & Jasin, 2010). These findings suggest that in both the G1 and G2 cell cycle phases, the regulation of resection determines DSB repair pathway choice.

1.14: Interfacing DSB repair with transcription.

Collision of DNA polymerases with DNA damage during S-phase, can be particularly deleterious to the cell as this can lead to collapsed replication forks and the formation of DSBs. To prevent this happening, cells are able to block entry into S-phase via the G1/S checkpoint but are also able to slow down actively replicating cells via the intra-S-phase checkpoint. Similarly, when RNA polymerases encounter DNA damage such as bulky lesions they can become stalled. Cells are able to overcome this by transcription-coupled repair which involves the ubiquitylation and degradation of the stalled polymerase (O'Connell & Harper, 2007). The presence of DSBs can also affect the transcription machinery and conversely, the presence of the transcription machinery

at DSBs might interfere with the repair machinery. However, since transcription is active in interphase cells, cell cycle checkpoints cannot prevent this from happening. As will be discussed here, accumulating evidence suggests that through PTMs and chromatin remodelling, cells actively inhibit transcription in *cis* to DSBs and only restore it following the completion of repair.

One of the earliest events following DSB induction is the PARylation of histones by PARPs (Polo & Jackson, 2011). This modification leads to the recruitment of repair factors as well as the recruitment of the polycomb group (PcG) of transcriptional repressors, and chromatin remodellers such as the NuRD complex (Chou *et al*, 2010). As discussed earlier, these factors are associated with transcriptional repression and heterochromatinisation. Components of the NuRD complex include HDAC1/HDAC2 and the ATPases, CHD3/CHD4, all of which have been implicated in gene regulation and various aspects of the DDR (Denslow & Wade, 2007; Smeenk *et al*, 2010; Polo *et al*, 2010; Goodarzi *et al*, 2011; Larsen *et al*, 2010; Luijsterburg *et al*, 2012). It is thought that rapid accumulation of these factors to DSBs via PARylation of histones flanking DSBs, leads to the transient formation of an HC like structure that is inhibitory to transcription. In support of this model, the PARP dependent recruitment of PcG and NuRD components to UV laser microirradiation tracks is associated with the loss of nascent RNA and elongating RNA polymerases from these regions (Chou *et al*, 2010).

The mechanism whereby the PcG and NuRD complexes achieve transcriptional repression following DSB induction seems to involve histone ubiquitylation. The polycomb repressive complex 1 (PRC1) contains BMI1, RING1 and RING2 and functions as an E3 ubiquitin ligase (Ismail *et al*, 2010). Following its rapid recruitment to DSBs, the PRC1 factor BMI1 ubiquitylates histones H2A and γ-H2AX which has been shown to be important for transcriptional repression and accurate DSB repair (Wang *et al*, 2004; Ismail *et al*, 2010). On the other hand, the RING1b/RNF2 ubiquitin ligase that is the canonical ubiquitin ligase of H2A was recently shown to mediate chromatin compaction independently of its ubiquitin ligase activity (Eskeland *et al*, 2010). It is therefore currently debatable how the PRC1 complex promotes chromatin compaction and transcriptional silencing and whether this involves histone ubiquitylation. Interestingly, the recruitment of PcG and NuRD to DSBs is ATM, ATR and histone H2AX independent, indicating that the initial transient inhibition of transcription is independent of these factors (Chou *et al*, 2010).

Rapid recruitment of the NuRD chromatin-remodelling complex to DSBs has been reported to promote histone ubiquitylation. In particular the CHD4 subunit is required for RNF168 recruitment by promoting RNF8 catalysed histone ubiquitylation (Larsen *et al*, 2010; Luijsterburg *et al*, 2012). Similarly, the p400 SWI/SNF ATPase, is recruited to DSBs where it destabilises nucleosomes, a process that is required for RNF8 to ubiquitylate histones flanking DSBs (Xu *et al*, 2010). The recruitment of RNF8 and RNF168 leads to localised histone H2A ubiquitylation and to the formation of K63 ubiquitin chains. This event seems to represent a switch from the transient inhibition of transcription conferred by the PcG and NuRD complexes, to a more sustained response that is dependent on RNF8/RNF168 and histone H2A ubiquitylation (Wang *et al*, 2004; Shanbhag *et al*, 2010). Consequently, RNF8/RNF168 depletion leads to reduced H2A ubiquitylation and defective transcriptional silencing in *cis* to DSBs (Huen *et al*, 2007; Mailand *et al*, 2007; Doil *et al*, 2009; Stewart *et al*, 2009; Shanbhag *et al*, 2010). Importantly, although the transient response is ATM independent, the more sustained response is ATM dependent, since ATMi leads to defective transcriptional silencing (Shanbhag *et al*, 2010). Mechanistically ATM appears to inhibit both RNA Pol I transcriptional initiation and RNA Pol II transcriptional elongation. In a pathway involving NSB1 and MDC1, ATM appears to inhibit Pol I transcription by interfering with the assembly of the Pol I initiation complex (Kruhlak *et al*, 2007). In parallel, ATM is required for H2A ubiquitylation and the formation of K63 ubiquitin chains but is also required for the maintenance of H2A ubiquitylation (Shanbhag *et al*, 2010). ATM therefore prevents H2A DUBing in *cis* to DSBs and inhibits the chromatin decondensation associated with transcription (Shanbhag *et al*, 2010).

In summary, a complex signalling network involving chromatin remodelling and PTMs leads to a transient inhibition of transcription following DNA damage that may or may not require histone ubiquitylation. If necessary, a more sustained response is activated via RNF8/RNF168 histone H2A ubiquitylation. This response is maintained by ATM and is reversed only following the completion of repair by USP16 mediated histone DUBing (Shanbhag *et al*, 2010).

Interestingly, ATM and RNF8/RNF168 are required to prevent transcription associated chromatin decondensation in *cis* to DSBs which is distinct to their role at HC where they promote chromatin relaxation (Shanbhag *et al*, 2010; Noon *et al*, 2010). Moreover, RNF8 can also promote chromatin relaxation via its interaction with the

CHD4 ATPase (Luijsterburg *et al*, 2012). It therefore appears that these factors are able to manipulate chromatin structure in several ways depending on the organisation and transcriptional status of the chromatin surrounding a DSB.

1.15: Aims of this thesis.

Work from our laboratory has demonstrated that ATM, Artemis and the mediator proteins are required for the repair of a subset of IR induced DSBs in G1 phase (Riballo *et al*, 2004). Subsequent work demonstrated that these DSBs are repaired with slow kinetics and represent DSBs arising at HC regions. The repair of such DSBs requires ATM and mediator protein dependent localised KAP1 phosphorylation to relax chromatin surrounding these DSBs (Goodarzi *et al*, 2008; Lee *et al*, 2010; Noon *et al*, 2010; Goodarzi *et al*, 2011). Similarly, in G2 phase ATM and Artemis are also required for slowly repaired DSBs, but in G2 phase these lesions are repaired by HR (Beucher *et al*, 2009). During G2 phase DSB repair, ATM promotes HC relaxation as in G1 phase, but also has an additional role in initiating DNA resection via CtIP (Shibata *et al*, 2011). The major aim of chapter 3 in this thesis was to investigate whether the mediator proteins are also required for G2 phase HR and if so, how they function to facilitate this process.

The mediator proteins encompass a heterogeneous family of factors with a wide array of functional domains. These domains can promote protein-protein interactions or enable direct PTM of downstream substrates. Ubiquitin signalling is a PTM that has emerged as an important regulatory component of the DDR (Thomson & Guerra-Rebollo, 2010; Ulrich & Walden, 2010; Ramaekers & Wouters, 2011). In chapter 4 of this thesis I investigated the role of the ubiquitin signalling network in HR with particular emphasis on the role(s) of the ubiquitin ligases RNF8, RNF168 and BRCA1.

As discussed earlier in this chapter, the initiation of resection plays an important role in DSB repair pathway choice. The major aim of chapter 5 of this thesis was to unravel the mechanistic regulation of this process. To this end, I investigated the role of BRCA1 and its interacting proteins in positively and negatively regulating resection. Moreover, I addressed how BRCA1 and its interacting proteins interface with 53BP1 during G2 phase HR to regulate resection and facilitate DSB repair at HC.

In chapter 6, I aimed to build on recent findings demonstrating that ATM and RNF8/RNF168 are required for transcriptional silencing in *cis* to DSBs (Shanbhag *et al*, 2010). I aimed to test whether failure to silence transcription leads to defective DSB repair. Finally, I aimed to assess whether ATP-dependent chromatin remodellers are required for this process, as was previously suggested for NuRD (Chou *et al*, 2010).

CHAPTER 2

Materials and Methods

2 Materials and Methods

2.1: Cell lines and culturing conditions

The cell lines that were used in this thesis are:

- A549: Human lung adenocarcinoma epithelial cell line
- Hela: Human cervical cancer cell line
- 1Br hTERT: Immortalised human fibroblasts
- Wild type and 53BP1$^{-/-}$ mutant mouse embryonic fibroblast (MEF) cell lines
- Wild type and BRCA1 mutant (RING and BRCT) mouse embryonic fibroblast (MEF) cell lines (Brca1$^{FH\text{-}WT/FH\text{-}WT}$, BRCA1$^{FH\text{-}I26A}$ and BRCA1$^{FH\text{-}S1598F}$ MEFs)
- NIH3T3: Mouse embryonic fibroblast cell line
- U2OS: Human osteosarcoma cell line
- U20S 3-6-3: Human osteosarcoma cell line containing DSB and transcription reporter system
- HEK293: Human embryonic kidney cell line

A549, Hela, U2OS and HEK293 cell lines were complemented with MEM Complete medium made up of: 'Minimum Essential Medium' (MEM) (Gibco, UK) supplemented with 10% Foetal bovine serum (FBS) (Gibco, UK) and 1% Penicillin and Streptomycin (PEST) (Gibco, UK). MEF and 1BrhTERT cells were complemented with DMEM Complete medium. U20S reporter cells were cultured in DMEM (GIBCO) containing 10% Tet-system approved FBS (Clontech), 1% Penicillin/Streptomycin, 200 mg/ml G418, and 100 mg/ml hygromycin B. All cells were incubated at 37°C in a humidified 95% air and 5% CO2 atmosphere.

2.2: Drug treatment and irradiation

Cells were irradiated by exposure to a ^{137}Cs source at a dose rate of 1Gy/8 seconds. For G2 phase experiments 4μM Aphidicolin was added to prevent S-phase cells from progressing into G2. Where indicated, 10 μM ATM inhibitor (Calbiochem) was added

30 minutes before IR. For flow cytometry experiments camptothecin was used at a concentration range of 2-4 μM.

2.3: Small interfering RNA (siRNA) knockdown conditions

siRNA-mediated knockdown was achieved using HiPerFect Transfection Reagent (Qiagen, Hilden, Germany) using the following transfection conditions.
Per 2 x 10^5 cells in 2ml media the following was made up and added to suspended cells after a 15m incubation:

- 50-100 pmol of 25 mM stock siRNA solutions
- 6μl of Hiperfect transfection reagent
- OptiMEM to a final volume of 100 μl

The cells were then grown for 24 hours and the transfection process was repeated. The cells were then grown for an additional 48h prior to IR. Table 1 indicates the siRNA oligos used in this thesis.

siRNA	Manufacturer	Sequence
MDC1	Invitrogen	5′AAAUCCUGAGACCUCCUAAGGUUUU-3′ (nucleotides 736-760)
RNF8 A	Invitrogen	5'-GGACAA UUAUGGACAACAA-3'
RNF8 B	Invitrogen	5' -UGCGGAGUAUGAAUAUGAA-3'
53BP1	Invitrogen	5′-AGAACGAGGAGACGGUA AUAGUGGG-3′ (nucleotides 229–252)
KAP-1	Invitrogen	5'CAGUGCUGCACUAGCUGUGA GGAUA- 3' (human cDNA nt 450–475)
BRCA1	Invitrogen	5'-GGAACCUGUCUCCACAAAG-3'
BRCA1	Dharmacon SMARTpool siRNA	
Ku70	Dharmacon SMARTpool siRNA	
DNAPK	Dharmacon SMARTpool siRNA	
Artemis	Dharmacon SMARTpool siRNA	

BRCA2	Dharmacon SMARTpool siRNA	
MRE11	Dharmacon SMARTpool siRNA	
CtiP	Dharmacon SMARTpool siRNA	
H2AX	Dharmacon SMARTpool siRNA	
RAP80	Dharmacon SMARTpool siRNA	
BRCC36	Dharmacon SMARTpool siRNA	
Abraxas	Invitrogen	5'-UAUAUAAGGAAUGUUCCAGUCGAUG
POH1	Dharmacon SMARTpool siRNA	
POH1	Invitrogen	5'- AGAGUUGGAUGGAAGGUUU-3'
BRG1	Dharmacon SMARTpool siRNA	
CHD7	Dharmacon SMARTpool siRNA	
BAF180	Dharmacon SMARTpool siRNA	
ATR	Dharmacon SMARTpool siRNA	

Table 2.1: siRNA oligonucleotides used in this thesis

2.4: Immunofluorescence for foci enumeration and analysis.

Cells plated on glass slides were fixed for 10 min with fixative (3% (w/v) PFA, 2% (w/v) sucrose, 1X PBS) and permeabilized for 1 min with 0.2 % Triton X-100 in PBS. When staining for RPA or Rad51 foci, pre extraction was performed by treating the cells with 0.2 % Triton X-100 in PBS for 0.5-1 min prior to PFA fixation. Pre-extraction allows the removal of non-chromatin bound protein and thus allows clear visualisation of remaining protein. This is important for visualisation of abundant proteins such as RPA and Rad51.

Cells were rinsed with PBS and incubated with primary antibody diluted in PBS + 2% (w/v) BSA for 1 hour at 37°C. Cells were washed three times, incubated with secondary antibody (diluted in PBS + 2% (w/v) BSA) for 30 min at RT in the dark, incubated with 4',6-diamidino-2-phenylindole (DAPI) for 10 min and washed three times with PBS. Slides were mounted using Vectasheild and visualized using a Zeiss Axioplan microscope and Simple-PCI software or a Nikon e400 microscope. In each sample a minimum of 30 cells was scored blindly and error bars represent the s.d between three independent experiments.

For immunofluorescence on flow cytometry analysis, the following antibodies were used in this thesis.

Primary Antibodies:

Antibody	Manufacturer	Catalogue No.	Concentration
γH2AX	Upstate Technology	05636	1:800
53BP1	Upstate Technology	05726	1:800
53BP1	Bethyl	A300-272A	1:800
RPA	Calbiochem	NA 18	1:800
RPA	Lifespan Biosciences	LS-C38952	1:100
Rad51	Santa-Cruz Biotechnology	SC8349	1:200
BRCA1	Home made	Freire et al	1:400
pATM	Epitomics	21521	1:200
pATM	Millipore	05-740	1:200
PCNA	Abcam	PC10	1:500
CENPF	Abcam	Ab5	1:1000
pKAP1 pS824	Bethyl	A300-767A	1:200
p-Histone H3 Ser 10	Upstate Biotechnology	SC8349	1:500
FK2	Millipore	04-263	1:400

Table 2.2: Primary antibodies used in this thesis

Secondary Antibodies:

Antibody	Manufacturer	Catalogue No.	Concentration
FITC	Sigma	F0257	1:200
CY3	Sigma	C2306	1:200
Alexa 488	Invitrogen	A21208	1:400
Alexa 647	Invitrogen	A 31634	1:400
Alexa 555	Invitrogen	A21422	1:400

Table 2.3: Secondary antibodies used in this thesis

2.5: Sister Chromatid Exchanges.

2 x 10^5 logarithmically cells were grown for 48 h in 10 μM BrdU before IR. 0.2μg/ml Colcemid (plus 1mM caffeine to overcome the G2/M arrest) was added from 8 -12 h post-IR to collect mitotic cells. The cells were harvested and collected by trypsinisation and centrifugation before undergoing hypotonic treatment by being resupsended in 75mM KCl pre-warmed to 37 °C. Following 30 minutes incubation at 37 °C, the cells were centrifuged and re-suspended in fixative solution made up of 3 parts methanol and 1 part glacial acetic acid. Following three rounds of centrifugations and re-suspension in fixative solution, the cells were dropped on ethanol treated glass slides from a height of 30cm to allow good cell spreading.

Once the slides were dry, they were stained in the dark for 20m with bisbenzimide solution (Hoescht) (10μg/ml in milliQ H2O). The cells were then dipped in SSC buffer (2M NaCl, 0.3M tri-sodium citrate, pH7) to remove excess Hoescht stain and were then covered by 1ml of SSC buffer and a coverslip. The cells were then placed under a UV lamp for 1 hour at a wavelength that excited the Hoescht stain (355nm). The slides were then rinsed and incubated in 60 °C SSC buffer for 1 hour.

Finally the slides were stained for 10 minutes in 6% giemsa-solution in Sörensen buffer (1:1 mixture of 0,067M Na2HPO4 + 0,067M KH2PO4; pH 7,2) and visualised and scored using a Nikon e400 light microscope. SCEs were scored in at least 800 chromosomes from 3 independent experiments per data point. Note that the modifications from standard protocols i.e addition of aphidicolin, addition of caffeine and time of harvest, meant that only cells that were in the G2 phase of the cell cycle at the time of irradiation were scored.

2.6: Flow cytometry.

A549 cells with or without siRNA oligo were seeded in 6cm dishes at a density of 6 x 10^5 cells/4ml. Forty eight hours later cells were either treated with 10Gy IR or with 2-4 μM camptothecin for 1h. Next the cells were washed with PBS containing 1mM EDTA (to prevent cellular clumping), trypsinised and collected in universal tubes containing complete MEM. The cells were collected by centrifugation and washed two further times with EDTA containing PBS. 1ml ice cold Triton was added to the cells to permeabilise the cellular membranes and the cells were transferred to eppendorf tubes.

Following a 5-minute incubation on ice the cells were washed with PBS once more before being fixed with PFA for 10 minutes at room temperature. Following PFA fixation, the cells were washed twice with PBS.

The fixed cells were then centrifuged at 10000 rpm for 10 minutes and were then resuspended in 2% BSA containing the desired antibody (RPA 1:20) (Rad51 1:10) and incubated at room temperature for 1 hour. Next the cells were washed with PBS and then the secondary antibody was added (Alexa 488 1:200) for 1 hour at room temperature. Finally, a PI mix (180μl PBS + 20 μl PI + 2 μl RNAse) was added and following a twenty minute incubation, the cells were analysed by a flow cytometer FACS CANTO flow cytometer. For each condition a minimum of 10000 events was recorded.

2.7: Plasmid transfection and expression parameters.

The following plasmid constructs were transfected and transiently overexpressed in this thesis:

- pLPC-puro vector containing amino acids 1220–1711 of 53BP1 fused to the fluorescent label mCherry (Dimitrova et al, 2008)
- GFP vector containing histone H2B
- M-Cherry vector containing the FOK1 endonuclease
- EGFP-vector containing full length BAF180 cDNA
- EGFP vector containing BAF180 cDNA with site directed mutations

Transient expression of the above constructs was achieved by transfecting the indicated cell lines using the Hiperfect transfection reagent. 1µg of DNA was added to optiMEM to a final volume of 100 µl. After a 5 minute incubation, 6 µl of Hiperfect was added and the mixture was incubated for 15 minutes before being added to 2 x 10^5 adherent cells in 2ml of media. Depending on which construct was used, the cells were then allowed to express the construct for 24-48 hours.

2.8: Live cell imaging.

Live cell imaging was carried out on a Applied Precision® Delta Vision® RT Olympus IX70 deconvolution microscope and softWoRx® Suite software fitted with an environmental chamber. The environmental chamber kept the cells at 37 °C whilst the cells were kept in CO2 independent medium (Gibco UK) for the duration of the experiment. Analysis of the live cell imaging data was carried out using the BitPlane Imaris software.

2.9: 3D rendering and foci volume quantification.

For 3D foci analysis, Z-stack imaging was carried out using an Applied Precision® Delta Vision® RT Olympus IX70 deconvolution microscope and softWoRx® Suite software. Z-stacks were set at 2 µm and individual nuclei imaged using 100x magnification. Following image acquisition, deconvolution was carried out using the Huygens Professional image processing software. The deconvolution parameters were set as follows: PSF- Theoretical Max iterations- 400 Quality change threshold- 0.01.

Following deconvolution by the Huygens Professional image processing software package, Z-stack images were imported into softWoRx® Suite software for 3D representation. This was achieved using the model function (A) and then selecting the 2D Polygon finder (B). Within the 2D polygon finder, the desired channels (e.g. RPA, 53BP1) were selected and then the software detected the 2D representation in each Z-stack for each channel (B). The 3D object builder was then selected (B), and the 2D polygons were combined to create a three dimensional model (C). The 3D model was then viewed by selecting the model function (C). By opening the options window found within the ‘view’ tab individual channels could be selected and there attributes

altered (E). In the example shown in (E), the attributes of the 53BP1 signal are changed to ‘wireframe’, from ‘solid’ which they were in (D), allowing visualisation of the underlying structure of the 3D objects by making them transparent. In addition this allows visualisation of enclosed objects, in this case RPA foci.

A)

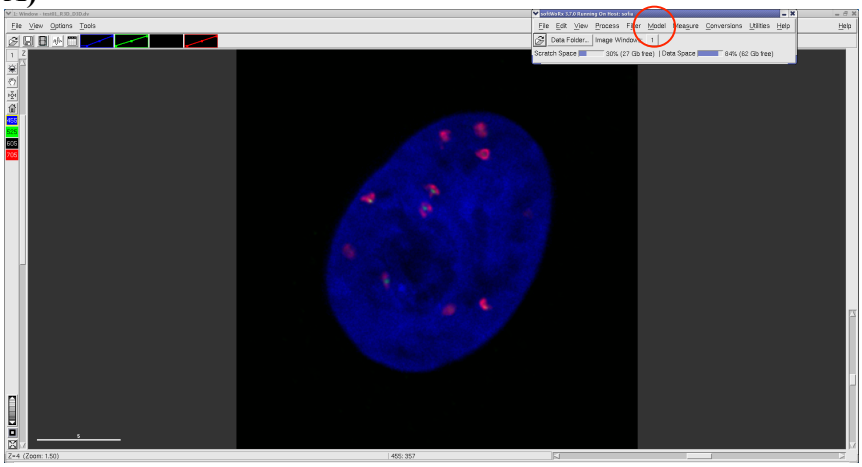

B)

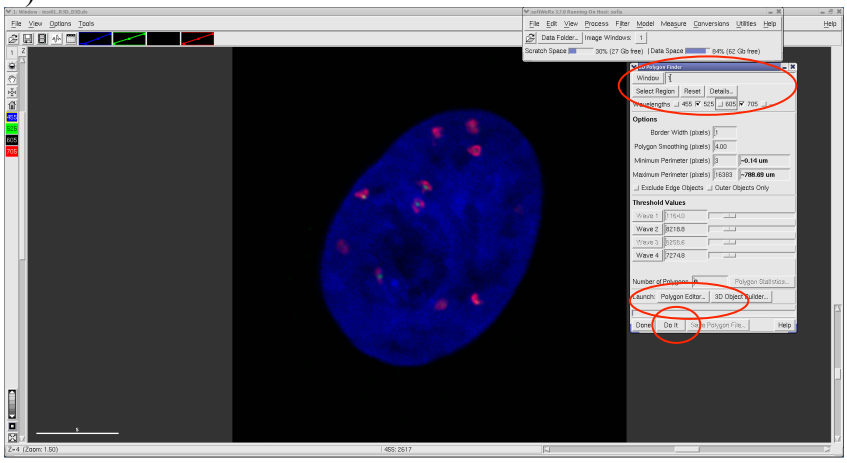

C)

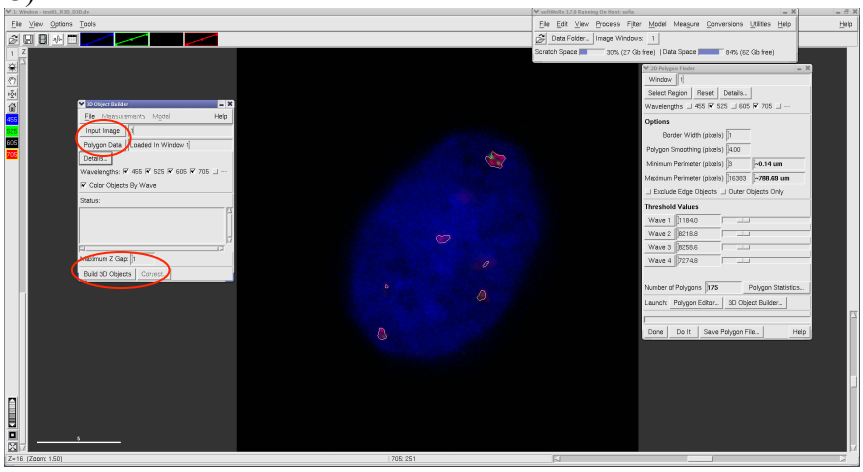

D)

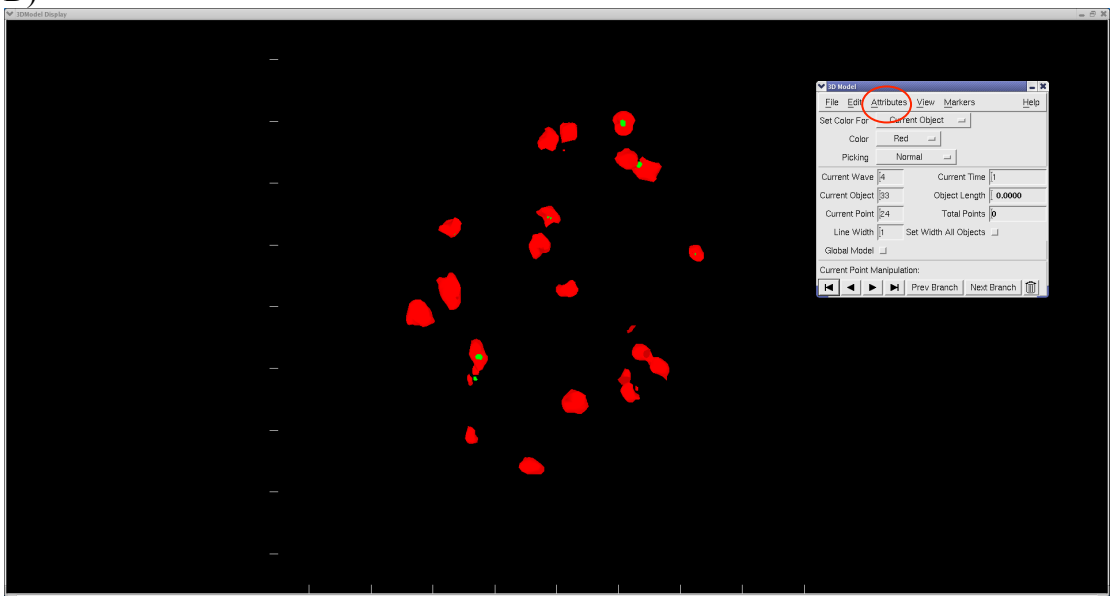

E)

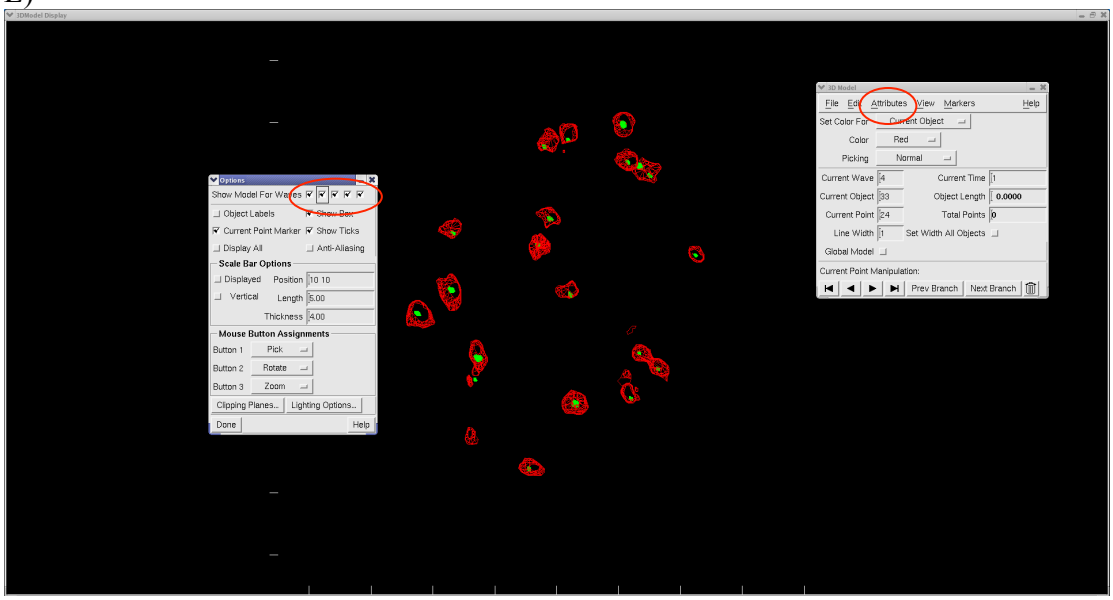

Figure 2.1: Foci 3D imaging parameters

2.10: Foci quantifications Parameters.

Following deconvolution by the Huygens Professional image processing software package, Z-stack images were imported into BitPlane Imaris software for foci volume quantitation. The Z-stack images were represented in 3D using the 'Surpass' option, whilst the channels to be analysed were selected from the display adjustment function (A). Next, the 'surfaces' tool was used to detect the foci in the selected channels (B). Finally, statistical parameters (e.g. volume) for the detected objects were exported and analysed (C). In each sample a minimum of 10 cells were analyzed and quantified and error bars represent the s.d between three independent experiments. Error bars represent the minimum values and maximum valid values. Maximum valid values, determined as the highest datum still within 1.5 the interquartile range of the upper quartile, were used to eliminate abnormally large values arising from foci 'clumping' and resolution limitations.

A)

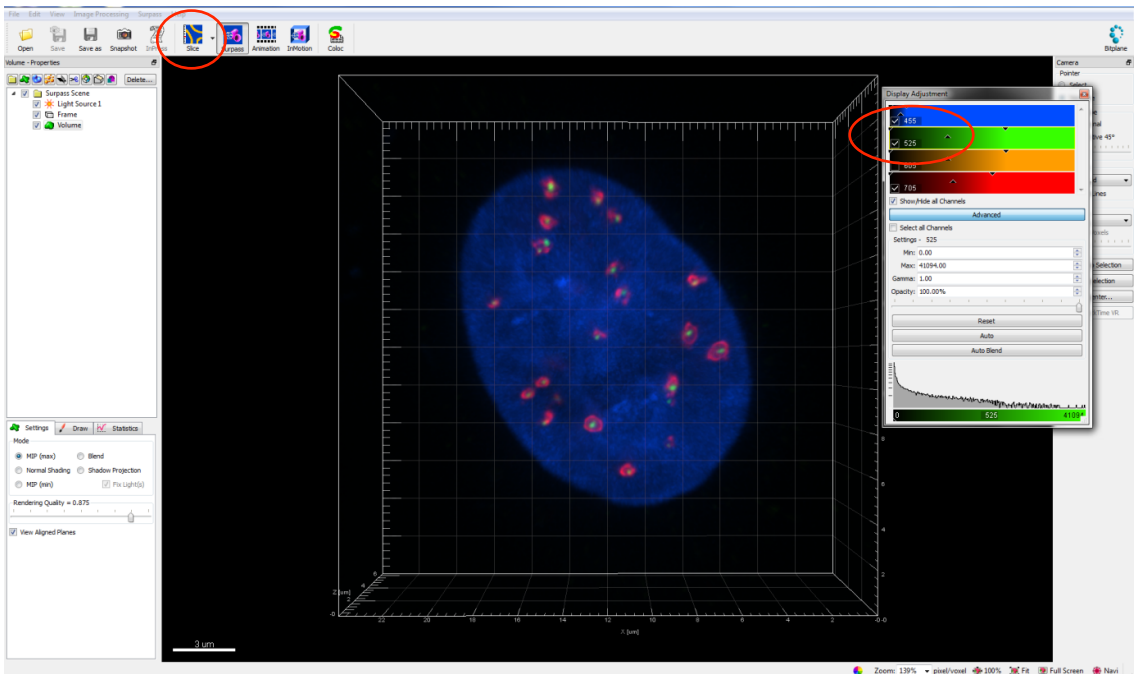

B)

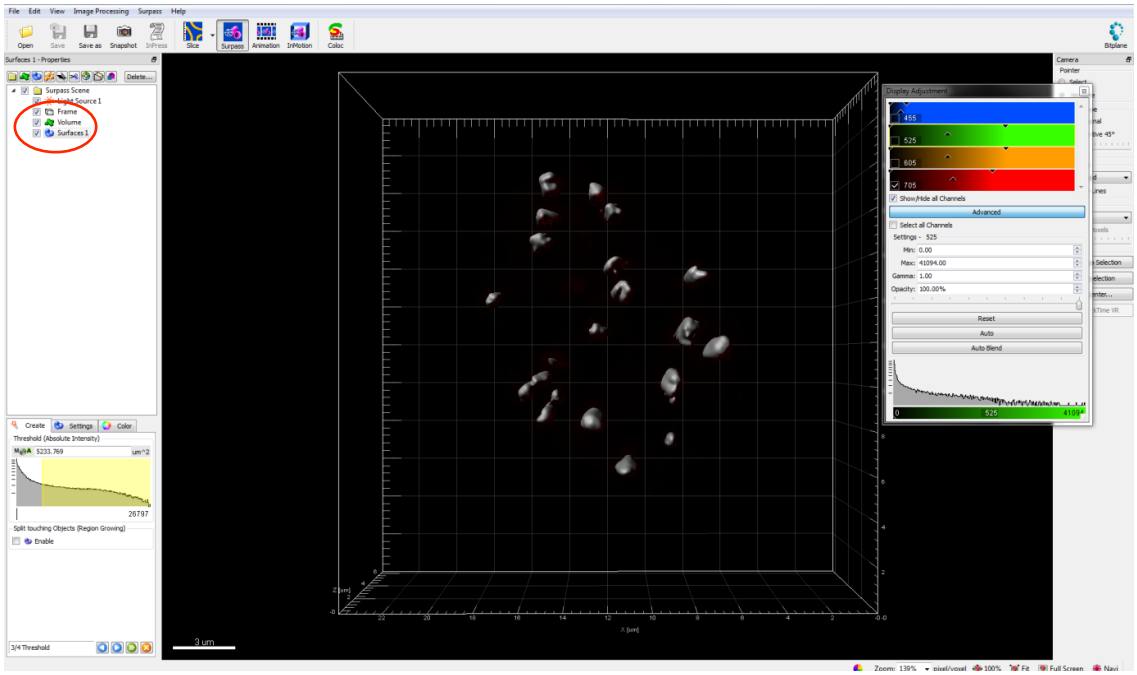

C)

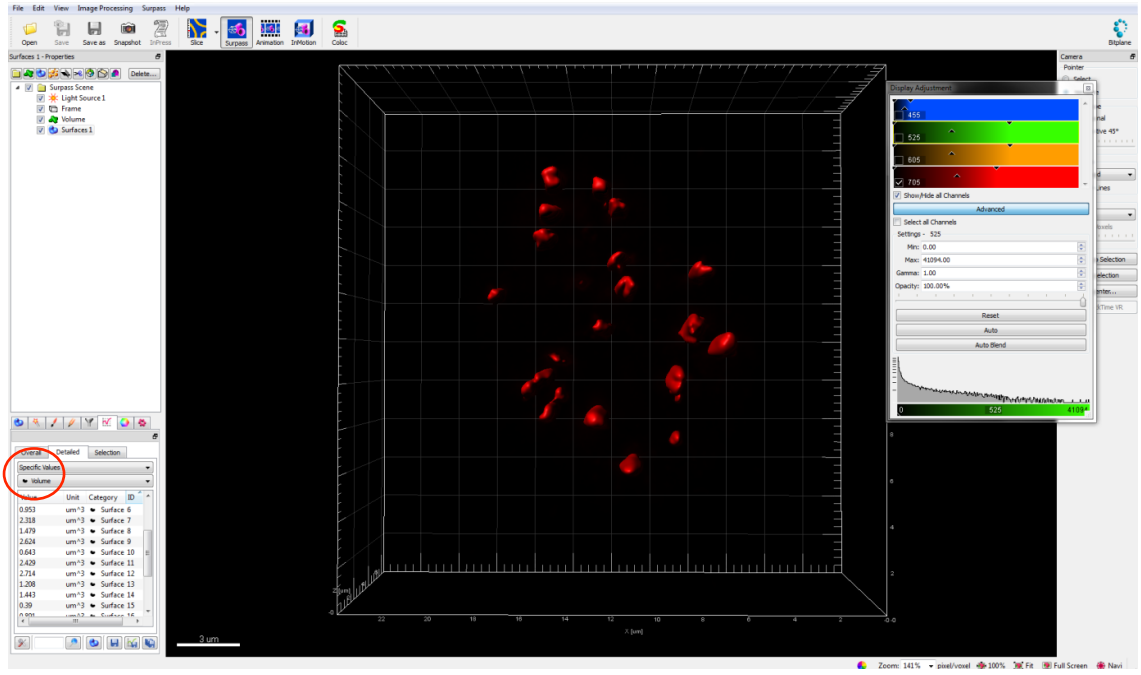

Figure 2.2: Foci 3D volume quantification parameters

2.11: Site directed mutagenesis.

The phosphomimic and phosphomutant BAF180-GFP constructs were generated using the QuikChange® Multi Site-Directed Mutagenesis Kit following the manufacturers protocol. The following mutagenic primers were designed and used in these experiments.

BAF180 S115 to A: 5'-aggcttacatcgcacatacgcccaggactgtagctttaaa-3'
BAF180 S115 to E: 5'-ctcaggcttacatcgcacatacgagcaggactgtagctttaaaaaca-3'

The region where the mutations were introduced was sequenced to ensure that the mutational changes were successfully introduced. This was achieved using the following primers and conditions:

Forward primer: G C C A G G A C T G T A G C T T T A A A A A C A
Reverse primer: T T C T A G A A A T T T T C G T G T A G C C A G

2.12: Laser microirradiation.

Exponentially growing human HEK293 cells were plated onto 35mm glass-bottom dishes (MatTek) and transfected with EGFP-BAF180 constructs using Hiperfect according to the manufacturers protocol. The cells were allowed to express the constructs for 24h and were then incubated with 10 μg/ml Hoechst 33285 for 1 h at 37 °C before irradiation. EGFP positive cells were irradiated with a 351nm ultraviolet A (4.36 J/m^2) laser channeled through a ×40/1.2-W objective using a Zeiss ConfoCor 2/LSM510 combi meta point scanning confocal microscope. Ultraviolet A was focused to an area of approximately 12 μm×0.1μm, and images were captured at 15s intervals following laser damage for a total time of 200s. EGFP signal intensity along the irradiation track was quantified using the LSM 520 Meta software.

2.13: Transcription reporter system.

Transcription reporter U2OS cells (Shanbhag *et al*, 2010), were treated with siRNA oligonucleotide where indicated. 48h later, the cells were transfected, or not, with the mCherry-FOK1 endonuclease plasmid. 24h later, 1 μg/ml doxycycline was added to the cells to drive transcription and the cells were harvested 4h later. The cells were then visualized on a fluorescent microscope. Doxycycline driven transcription was visualized as YFP-MS2 protein binding to MS2 nascent transcript. In cells expressing FOK1, DSBs were visualized by FOK1 focal accumulation and transcription in these cells was monitored by YPF-MS2. Where indicated, ATMi was added 30m prior to doxycycline treatment. The presence or absence of nascent transcripts was analysed in a minimum of 30 cells per condition and the data represent the mean and standard deviation of three independent experiments.

CHAPTER 3

The role of the mediator proteins in Homologous Recombination

3 The role of the mediator proteins in Homologous Recombination

3.1: Introduction.

Homologous Recombination (HR) functions in the repair of DSBs in the S and G2 phases of the cell cycle by using the intact sister chromatid as a template for repair. However, contrary to the widely held view that HR is the predominant DSB repair pathway in G2 phase, HR only repairs 20% of the X and γ ray induced DSBs (Beucher *et al*, 2009). These lesions require ATM and Artemis function for their efficient repair and are thought to arise at HC regions (Beucher *et al*, 2009; Shibata *et al*, 2011). However it is not clear whether other members of the ATM signalling response are also required to mediate HR at HC regions in G2 phase. Moreover, ATM appears to have distinct roles in facilitating DSB repair at HC in G1 and G2 phase. In G1 ATM facilitates HC repair via KAP1 phosphorylation and although ATM also has this function in G2 phase HR, it also functions to initiate resection (Goodarzi *et al*, 2008; Shibata *et al*, 2011). It is therefore important to establish whether the mediator proteins, which promote HC DSB repair in G1 phase, also promote this process in G2 phase and whether like ATM they also have additional functions. In this chapter I examine the role of the mediator proteins 53BP1 and MDC1 in facilitating DSB repair by HR in G2 phase.

In addition to repairing a fraction of DSBs in G2 phase, the HR pathway is also employed to restore replication forks that have stalled/collapsed during S-phase (Saintigny *et al*, 2001). Replication forks can become stalled and ultimately collapse when they encounter obstacles such as SSBs or secondary DNA structures (Petermann & Helleday, 2010). Agents such as topoisomerase poisons and PARP inhibitors prevent the repair of SSBs thus leading to the formation of toxic one-ended DSBs when replication forks encounter these lesions (Lundin *et al*, 2002; Saleh-Gohari *et al*, 2005). HR appears to be the dominant repair pathway of one ended DSBs since HR deficient cells are highly sensitive to agents that lead to replication fork stalling/collapse (Groth *et al*, 2012). HR at collapsed replication forks involves the 5'-3' resection of the one ended DSB to produce a ssDNA overhang that becomes coated initially by RPA and subsequently by Rad51 (Lundin *et al*, 2003). Similar to HR repair of two ended DSBs in G2 phase, this triggers the invasion of the sister chromatid which is used as a

template for the repair of the resected regions (Helleday, 2003). The resulting Holliday junction is resolved in a Mus81 dependent manner that may or may not lead to crossovers and the formation of an SCE (Roseaulin *et al*, 2008; Helleday, 2003).

The requirement of core HR components such as BRCA2 for the repair of one-ended DSBs is demonstrated by the sensitivity of cells deficient for these factors to drugs such as PARP inhibitors (Bryant *et al*, 2005). However, the role(s) of the mediator proteins in the repair of one-ended DSBs by HR has not been previously assessed. In this chapter I examine the role of the mediator proteins 53BP1, and MDC1, in DNA resection in S-phase cells following camptothecin treatment. Moreover, I examine the requirement of CtIP and ATM for this process as well as the requirement for the other PIKK kinases, DNA-PK and ATR.

As mentioned previously, HR defective cells are highly sensitive to one-ended DSBs that arise following replication fork collapse. One model for this sensitivity, is that it results from erroneous re-joining of distant one-ended DSBs by NHEJ (Helleday *et al*, 2007). Here I use live cell imaging (LCI) to monitor the repair of methyl methanesulfonate (MMS) induced DSBs in HR proficient and deficient S-phase cells. In addition, I assess whether 53BP1 has a role in the distant rejoining of one-ended DSBs. 53BP1 has previously been shown to facilitate long range rejoining events in telomere end to end fusions, during V(D)J recombination and in Class Switch Recombination (CSR) (Dimitrova *et al*, 2008; Difilippantonio *et al*, 2008; Bothmer *et al*, 2011). Therefore, establishing whether long-range rejoining events during S-phase contribute to the genomic instability of HR defective cells, and if 53BP1 is required for these events, are important outstanding questions.

3.1.2: Monitoring HR in G2 phase.

Traditional plasmid assays have been predominately used to monitor repair of DSBs by HR. These involve the integration of a reporter substrate containing an I-SCE1 site within one of two defective GFP genes. Following transfection of the I-SCE1 endonuclease and DSB induction, if the homologous region of the second GFP gene is used for repair, this leads to restoration of GFP functionality. Flow cytometry can then be used to estimate the frequency of these events within a population of cells and the requirement of genetic factors for the process can be determined (Pierce *et al*, 2001;

Stark *et al*, 2002; Moynahan *et al*, 2001). However, the limitation of such systems is that chromatin structure at the cutting site is defined and does not emulate the heterogeneity of chromatin structure and its impact on DSB repair pathway choice and outcome.

One goal of this chapter was to investigate the role of the mediator proteins in homologous recombination in G2 phase. However, since experiments in G1 had indicated that the function of these proteins in DSB repair is to modify HC structure, I could not use the traditional I-SCEI based assays to assess these functions.

First, I needed to ensure that I was able to monitor HR specifically in G2 phase cells. Since HR also functions in S-phase it was important to prevent cells irradiated in S-phase from progressing into G2. I achieved this by adding aphidicolin to cells prior to irradiation. As previous work from our laboratory has shown, this reversible DNA polymerase inhibitor leads to S-phase arrest and to a characteristic γ-H2AX panuclear staining probably due to DSBs from collapsed or stalled replication forks (Beucher *et al*, 2009). In order to identify G2 phase cells, I used a CENP-F antibody. CENP-F protein levels peak in G2 phase and are then rapidly degraded after completion of mitosis. Subsequently it is a good G2 marker as protein levels are low in G1 and high in G2 phase (Liao *et al*, 1995). Additionally, I was also able to use the γ-H2AX pattern after aphidicolin treatment to exclude S-phase cells from analysis, which would be identified by their panuclear staining for γ-H2AX.

DNA end resection resulting in the formation of single stranded DNA is the first step of HR (Symington & Gautier, 2011) . There appear to be several nucleases and other proteins that are involved in this process that has at least two distinct steps (Mimitou & Symington, 2011). The first step, is the initiation of resection that seems to require the MRE11 nuclease and CtIP whose function is seems to be required to remove Ku from DNA ends (Langerak *et al*, 2011; Sartori *et al*, 2007). The second step involves CtIP and Exo1 which is the 5'-3' exonuclease that carries out the elongation step of resection in HR (Nimonkar *et al*, 2008; Shibata *et al*, 2011). The resulting single stranded DNA is then rapidly coated by RPA to stabilize the molecule, to protect it from further degradation and potentially to prevent it from forming secondary structures (Fanning *et al*, 2006). RPA coated single stranded DNA can be visualized is G2 phase by immunostaining with an RPA antibody (Shibata *et al*, 2011). By two hours after exposure to IR in G2, DSBs undergoing repair by HR have accumulated sufficient levels of RPA protein for distinct IRIF to be visualized. These foci can be enumerated

and provide a clear indication of the efficacy with which this HR intermediate is formed. No RPA foci are observed in the absence of CtIP suggesting that RPA foci are a good read out for resection (Shibata *et al*, 2011).

Similarly, Rad51 foci also form in G2 phase at DSBs that are repaired by HR (Forget & Kowalczykowski, 2010). Following single strand DNA formation and RPA coating, Rad51 displaces RPA and initiates the homology search on the undamaged template. As for RPA, cells that are deficient in HR fail to form Rad51 foci correctly indicating a defect in the process (Yuan *et al*, 1999) . However, use of Rad51 foci allows analysis of a specific HR intermediate and provides insight into which step of the process a given factor functions. An example of this is the comparison of BRCA1 and BRCA2. Mutant cells for either BRCA1 or BRCA2 display defective HR when measured by plasmid based systems (Moynahan *et al*, 1999; 2001). However, when RPA foci are specifically measured, only BRCA1 mutant cells display an RPA foci formation defect (Schlegel *et al*, 2006; Shibata *et al*, 2011). In contrast, when Rad51 foci are measured both BRCA1 and BRCA2 mutant cells are defective (Schlegel *et al*, 2006; Shibata *et al*, 2011; Beucher *et al*, 2009). These assays allow a distinction to be made as to where in the HR pathway specific factors function. BRCA2 seems to function downstream of BRCA1 and is dispensable for resection while BRCA1 is required for both these processes.

Finally as readout of the completion of HR, I monitored sister chromatid exchange (SCE) formation. SCEs form following Holliday junction resolution and represent successful recombination events (Conrad *et al*, 2011). This is a useful tool as different factors display varying degrees of dependency for RPA or Rad51 foci formation. Therefore if cells defective for a given protein display a minor RPA foci defect, looking at SCEs can monitor the impact of this on the overall outcome of HR. I used these assays to assess the direct role(s) of the mediator proteins in G2 phase DSB repair by HR, as well as their indirect role in the process via chromatin modifications.

3.2: Results

3.2.1: IR induced DSBs associated with HC are repaired via HR in G2 phase.

We have previously demonstrated that the mediator proteins are required for ATM dependent DSB repair in the G1 phase of the cell cycle. The orchestrated accumulation of these proteins at DSB sites results in the tethering of activated ATM and the subsequent robust phosphorylation of KAP1 at HC DSBs (Noon *et al*, 2010). Localised phosphorylation of KAP1 results in chromatin relaxation, which is important for repair of DSBs at dense HC regions. In G1 phase, such DSBs are repaired with slow kinetics and, in addition to ATM and the mediator proteins, they also require the nuclease Artemis for efficient repair (Riballo *et al*, 2004). We recently demonstrated that as in G1, a fraction of IR induced DSBs in G2 (~20%), also require ATM and Artemis (Beucher *et al*, 2009).

DSB repair in G2 phase is also biphasic consisting of a fast and slow component. Interestingly however, the slow component of repair in G2 corresponds to DSBs being repaired by HR whilst the fast component corresponds to those repaired by NHEJ. The observation that ATM and Artemis are required for the slow component of DSB repair in G2 raised the interesting possibility that these factors may also function in HR. This notion gained favour when analysis was carried out using core components of the HR pathway (BRCA2, Rad51) and an epistatic relationship to ATM and Artemis was observed (Beucher *et al*, 2009). We have subsequently demonstrated that ATM is a key regulator of DSB repair pathway choice in G2 phase by initiating the process of DNA end resection through phosphorylation of the nuclease CtIP (Shibata *et al*, 2011).

In addition to its role in initiating resection, ATM function is also required for chromatin de-condensation at DSB sites in G2 and, as in G1, this role can be overcome by KAP1 depletion (Beucher *et al*, 2009). It therefore appears that IR induced DSBs in G2 that are associated with HC are specifically repaired by HR. To further substantiate this finding, I aimed to show that late repairing DSBs in G2 colocolise with RPA foci (depicting ongoing HR) and pKAP1 foci (depicting HC) (Figure 3.1a). Due to changes in chromatin superstructure following DNA replication, G2 phase cells have low chromatin bound KAP-1 making pKAP1 foci analysis difficult. To visualise pKAP-1 in

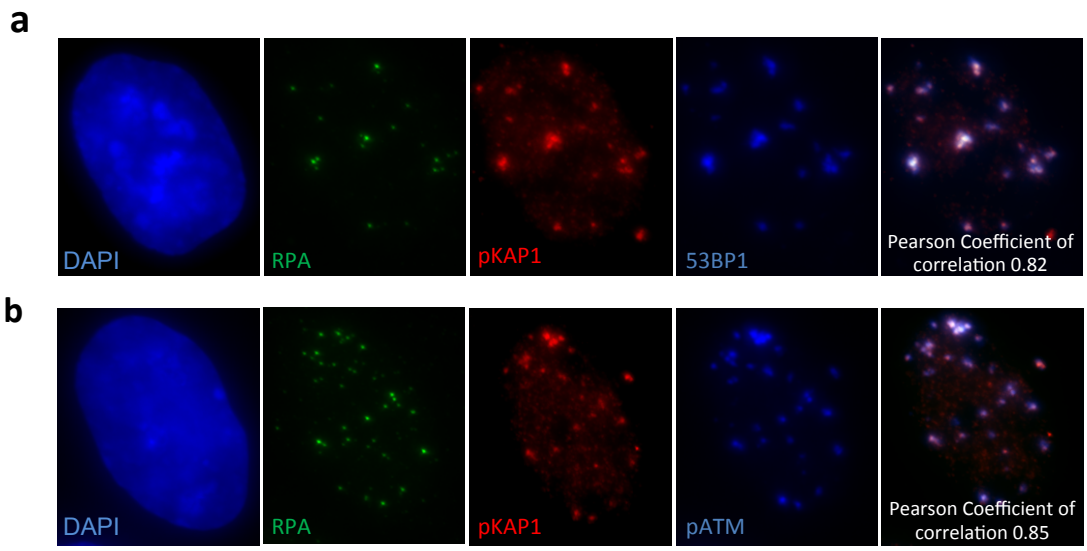

Figure 3.1: Co-localization analysis of 53BP1, pATM, RPA and pKAP1 IRIF in G2 phase 1BRhTERT cells.
1BRhTERT cells were harvested 8 h post exposure to 3 Gy IR and immunostained with the indicated antibodies. Aphidicolin was added to prevent S phase cells progressing into G2 during analysis. Analysis was undertaken in G2 phase cells. S phase cells were excluded from analysis by their pan-nuclear RPA staining which arises as a consequence of aphidicolin addition. G1 cells do not show RPA foci. Co-localization between pKAP1 and 53BP1 (a) and pATM (b) was carried out using softWoRx® Suite software. The Pearson Coefficient of Correlation indicates how closely the two intensities are colocalised on a pixel-by-pixel basis (full colocalisation is 1.0). RPA foci overlapped with all the above IRIF indicating that these lesions are repaired by homologous recombination. G2 phase cells have low chromatin bound KAP-1 making pKAP1 foci analysis difficult. To visualize pKAP-1 in G2 cells, the cells were subjected to MeCP2 siRNA, which as previously observed allows greater foci expansion and visualization of pKAP1 in G2.

G2 cells, the cells were subjected to MeCP2 siRNA, which as previously observed, allows greater foci expansion and subsequently allowed visualisation of pKAP1 foci (Brunton *et al*, 2011). At late time points (8h) post damage induction, DSB sites marked by 53BP1 foci strongly colocalise with pKAP1 foci and RPA foci (Figure 3.1a). Additionally, and consistent with previous data, pATM was also retained at DSB sites and strongly colocolised with pKAP1 and RPA foci (Figure 3.1b).

To further substantiate the notion that HR in G2 phase repairs only HC DSBs, I decided to artificially increase the fraction of breaks repaired by HR. To achieve this I co-depleted Ku80 and DNA-PKcs by siRNA treatment. Ku80 is a component of the Ku heterodimer that rapidly and efficiently binds DNA ends whilst DNA-PKcs is a core component of the NHEJ pathway. By depleting Ku80, which is believed to be a barrier to DNA resection and by inhibiting NHEJ via DNA-PKcs depletion I was able to increase the fraction of breaks repaired by HR in G2 (Langerak *et al*, 2011). Following Ku80 and DNA-PKcs co-depletion I observed a significant increase in the number of RPA and Rad51 foci as wells as SCEs compared to control cells (Figure 3.2a-c). Significantly, although very high co-localisation is observed between pKAP1 and RPA foci in control cells, this decreases following Ku80 and DNA-PKcs depletion (Figure 3.2d). I interpret this to suggest that euchromatic DSBs that would normally be repaired by NHEJ undergo resection and are repaired by HR when Ku80-DNA-PKcs is lost. This confirms that pKAP1 does not form at all DSBs and that in normal cells most HR occurs at DSBs harbouring pKAP1 foci.

In conclusion, this data provides strong evidence that IR induced DSBs in G2 phase located at HC regions are repaired by HR. It is conceptually plausible that the highly repetitive sequences of HC may be favourable to the HR pathway in which a homology search on the sister chromatid needs to be carried out.

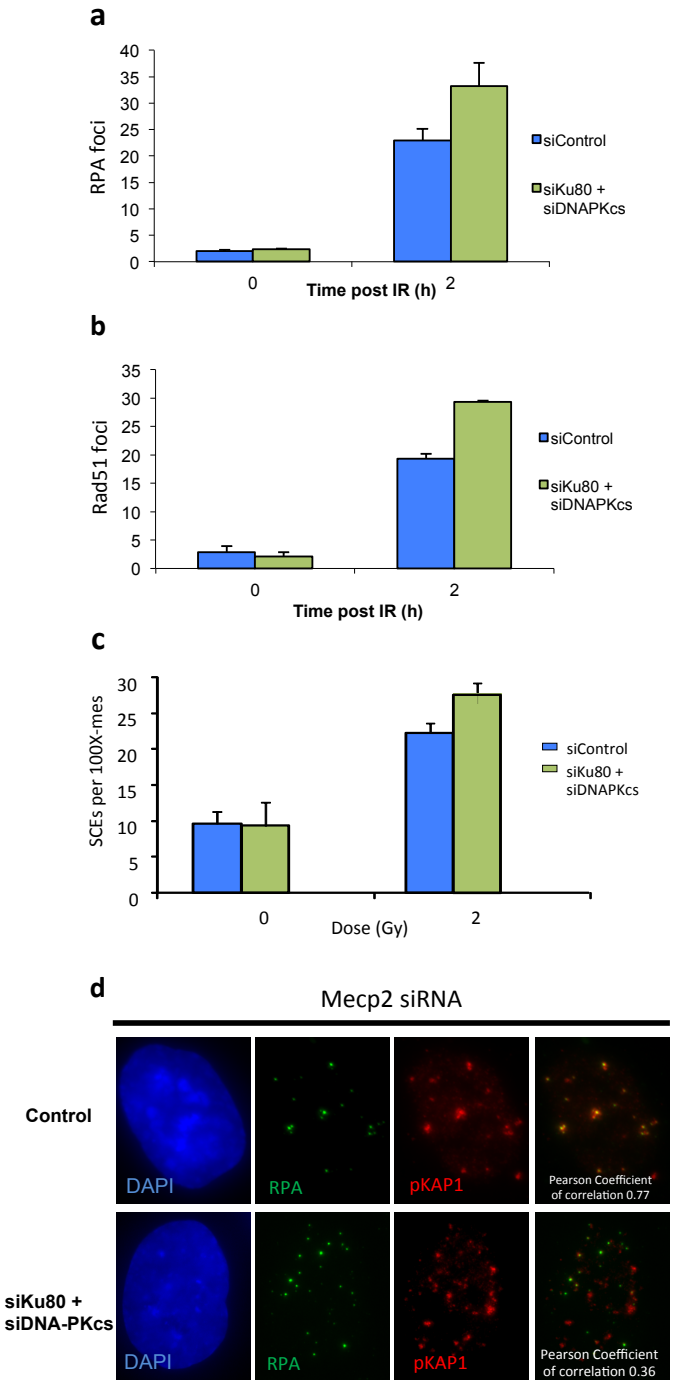

Figure 3.2: SCEs, RPA and Rad51 foci enumeration in G2 phase A549 cells.
(a-c) SCEs as well as RPA and Rad51 foci were enumerated in control cells and in cells depleted for Ku80 and DNA-PKcs. In G2 phase control cells RPA and Rad51 foci reach maximum numbers at approximately two hours post IR and represent DSBs repaired by HR. For SCEs, the cells were grown in BrdU for forty-eight hours and aphidicolin was added prior to IR to prevent S-phase from progressing to G2. The cells were harvested twelve hours post IR and SCEs were scored in colcemid arrested mitotic cells. Exposing G2 phase cells to 2Gy leads to a two-fold increase in the number of SCEs.
Cells depleted for Ku80 and DNA-PKcs have elevated numbers of RPA and Rad51 foci in G2 as well as increased numbers of radiation induced SCEs (a-c) compared to control cells. This is a consequence of impaired NHEJ resulting in euchromatic DSBs undergoing repair by HR. Consistently there is a reduction in the co-localisation of RPA and pKAP1 signals as resection in no longer restricted to HC regions (d). Enumerated data represent the mean and standard deviation of three independent experiments.

3.2.2: 53BP1, MDC1 and H2AX are required for IR induced HR in G2 phase.

As a first step in determining whether the mediator proteins function in HR, I decided to investigate whether they are required for efficient DSB repair in G2 phase. To achieve this, I monitored the loss of γ-H2AX foci at defined times (2h,8h) following exposure to 3Gy IR. Timpeoints beyond 8h can not be analysed in G2 since cells start to enter mitosis, particularly in ATMi or mediator siRNA treated cells due to a defective G2/M checkpoint (Shibata *et al*, 2010). Foci were only scored in G2 phase cells which were identified by CENP-F staining (Figure 3.3a). Addition of aphidicolin prior to irradiation prevented S-phase cells from progressing to G2 and ensured that only cells in G2 at the time of irradiation were analysed.

siRNA mediated depletion of either 53BP1 or MDC1 led to a mild DSB repair defect in G2, similar to that observed in G1 phase cells (Figure 3.3b). Importantly, as in G1, depletion of 53BP1 or MDC1 only affected the slow component of repair since the number of γ-H2AX foci at two hours post IR was indistinguishable to that in control cells (Figure 3.3b). This result suggested that 53BP1 and MDC1 function in the slow, ATM dependent repair pathway in both G1 and G2. To verify this I carried out epistasis analysis by adding the ATM inhibitor to 53BP1 and MDC1 depleted cells and monitoring loss of γ-H2AX foci (Figure 3.3b). As expected, addition of ATMi did not lead to an additive repair defect indicating that these proteins function in an ATM-dependent DSB repair pathway in G2.

The role of ATM in G2 is distinct to that of G1, since in G2 ATM also regulates the initiation of resection through phosphorylation of CtIP. Resection, the first step of HR, appears to be (at least) a two-step process with an initial incision step followed by an elongation step (Symington & Gautier, 2011). The ATM damage dependent phosphorylation of CtIP has been shown to be indispensable for the initiation of resection as loss of this phosphorylation leads to complete loss of RPA foci following IR in G2 (Li *et al*, 2000; Shibata *et al*, 2011). Strikingly however, loss of ATM and/or CtIP allows unresected DSBs to be repaired by NHEJ with faster kinetics and without obvious deleterious consequences to the cells (Shibata *et al*, 2011). It should be noted however that ATMs function in facilitating HC relaxation is indispensable in G2 regardless of which repair pathway is used. ATM therefore has two distinct functions in G2. As in G1, it promotes HC relaxation via KAP1 phosphorylation but it also enables resection through CtIP phosphorylation. Given this I wanted to ask whether 53BP1 and

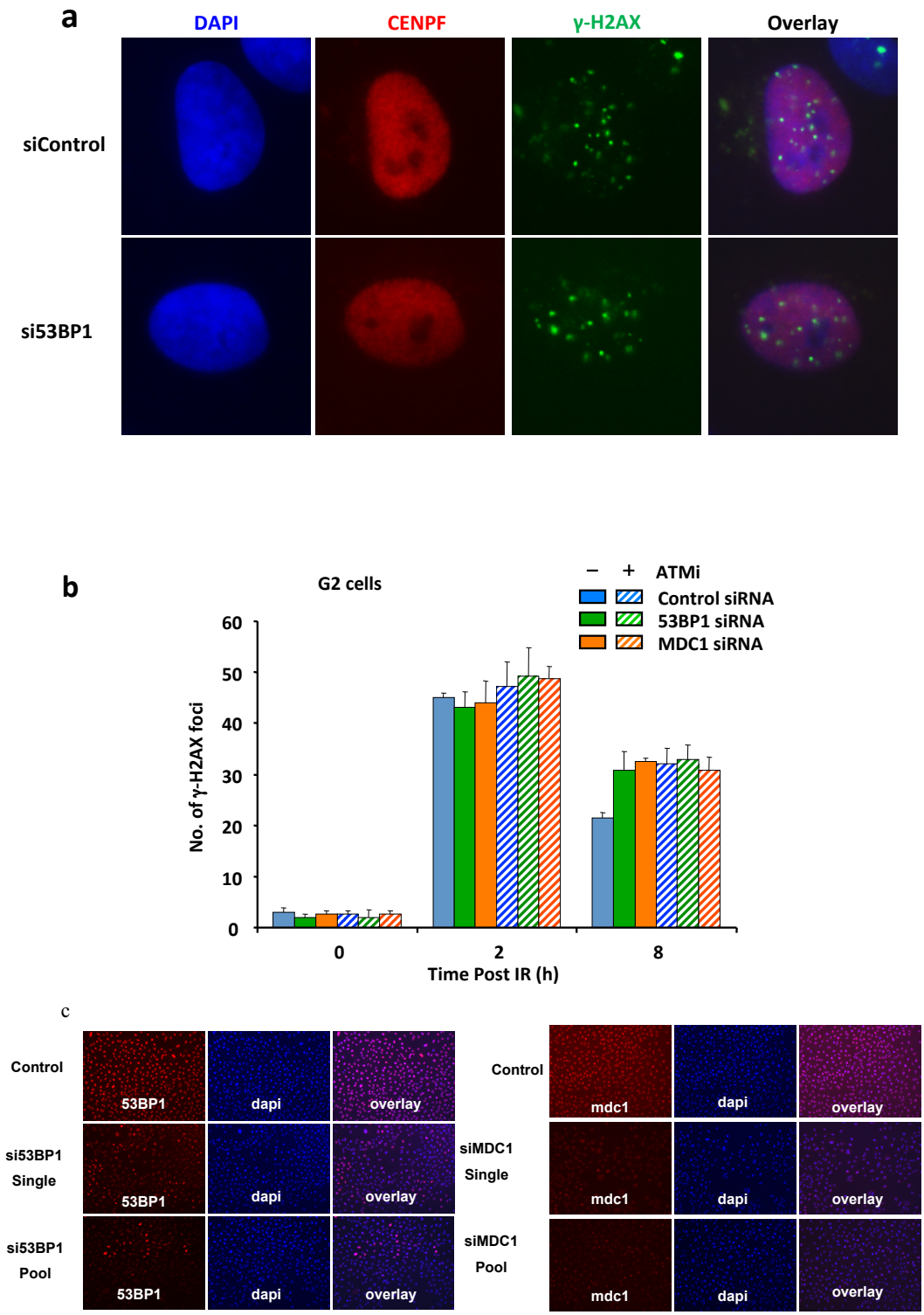

Figure 3.3: 53BP1 and MDC1 and required for IR induced DSB repair in G2.
a) A549 cells were treated with control, 53BP1 or MDC1 siRNA and were irradiated with 3Gy IR. Prior to irradiation aphidicolin was added to the cells to prevent S-phase cells from entering G2. The cells were then harvested at two and eight hours post IR and immunostained with CENP-F and γ-H2AX antibodies. G2 phase cells were identified by positive CENP-F staining and the cell nuclei were visualized by DAPI (a). γ-H2AX foci were enumerated specifically in CENP-F positive cells (b). Where indicated the ATMi was added 30 minutes prior to IR. (b) γ-H2AX foci were enumerated in 30 cells per time-point and the data represent the mean and standard deviation of three independent experiments. c) Knockdown efficiency in A549 cells following treatment with a pool or single siRNA oligonucleotides. Per knockdown, 100 pmol of siRNA duplexes per 2 x 10^5 logarithmically growing cells were used. Cells were then grown for 72 h prior to fixation and immunostaining with the indicated antibodies.

MDC1 mediate both of these functions and whether they themselves have distinct roles during HR.

First I decided to look at whether RPA foci formation in G2 cells was compromised following siRNA depletion of either 53BP1 or MDC1 (Figure 3.4b). As a positive control and to ask whether an epistatic relationship existed between these proteins and ATM, I also monitored cells in which ATMi was added. As observed previously, all cells (control, si53BP1,siMDC1) in which ATMi was added were completely impaired in RPA foci formation and no foci were visible two hours post 3Gy IR (Figure 3.4b). Surprisingly however, in the mediator depleted cells only a mild, but reproducible decrease in the level of RPA foci was observed (Figure 3.4b). This result strongly suggests that ATM dependent initiation of resection does not require 53BP1 and MDC1 function. The mild resection defect observed in mediator depleted cells could not explain the DSB repair defect which is identical to that observed in ATMi treated cells, so I considered whether these proteins function in HR downstream of resection. To ask this I monitored whether Rad51 loading was proficient in G2 cells following 53BP1 and MDC1 depletion (Figure 3.5). As for RPA foci, at two hours post 3Gy IR I observed no increase in Rad51 foci numbers when ATMi was added (Figure 3.5). Following 53BP1 or MDC1 siRNA, a two-fold reduction was observed in Rad51 foci, which was reproducibly greater than the reduction observed for RPA foci formation (Figure 3.5b). This result suggests that although not essential for the initiation of resection both 53BP1 and MDC1 are required for efficient progression through the HR pathway.

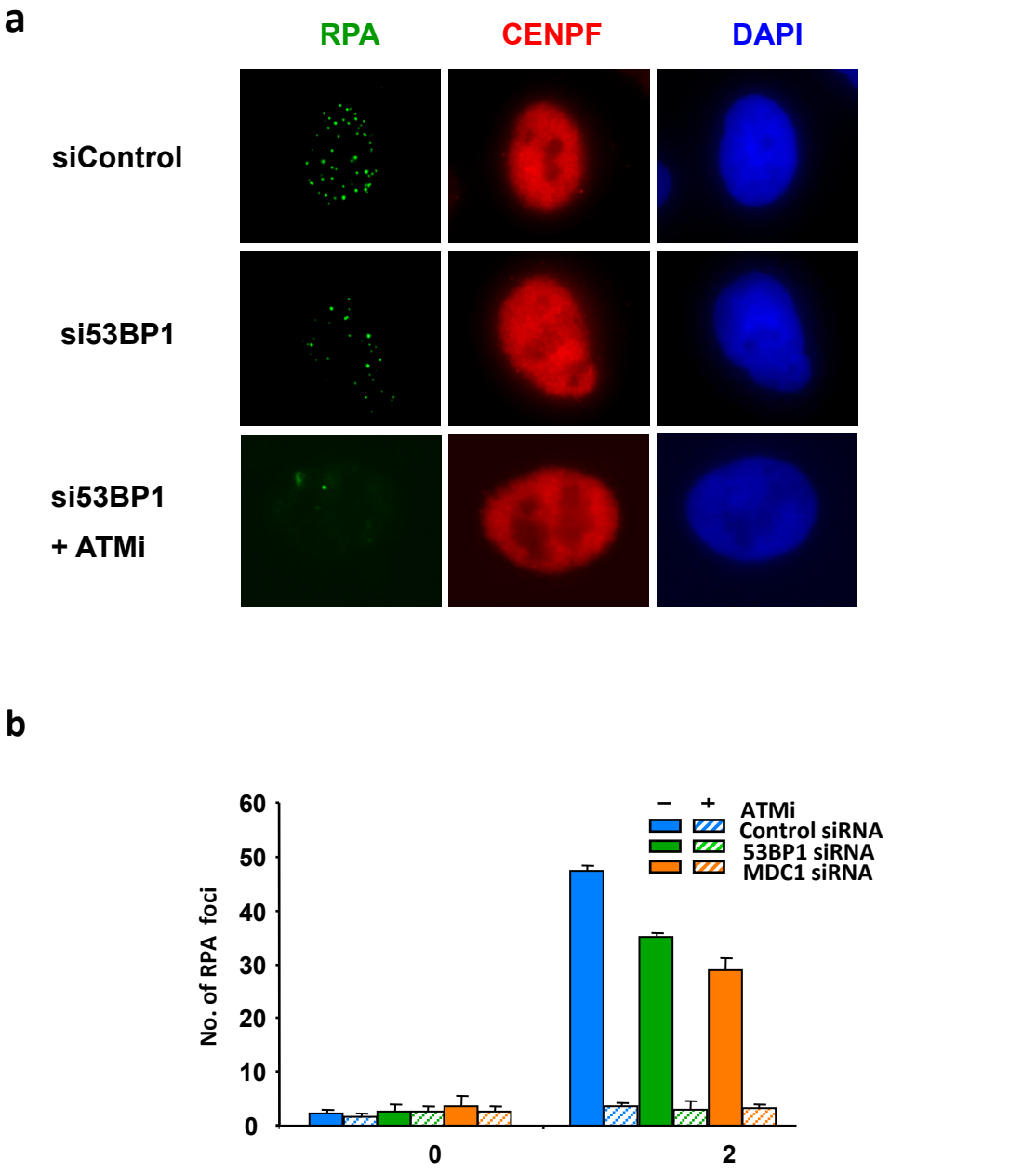

Figure 3.4: 53BP1 and MDC1 are partially required for RPA foci formation in G2.
a) A549 cells were treated with control, 53BP1 or MDC1 siRNA and were irradiated with 3Gy IR. Prior to irradiation aphidicolin was added to the cells to prevent S-phase cells from entering G2. The cells were then harvested at two hours post IR and immunostained with RPA and CENP-F antibodies. G2 phase cells were identified by positive CENP-F staining and the cell nuclei were visualized by DAPI (a). RPA foci were enumerated specifically in CENP-F positive cells (b). Where indicated the ATMi was added 30 minutes prior to IR. (b) RPA foci were enumerated in 30 cells per time-point and the data represent the mean and standard deviation of three independent experiments.

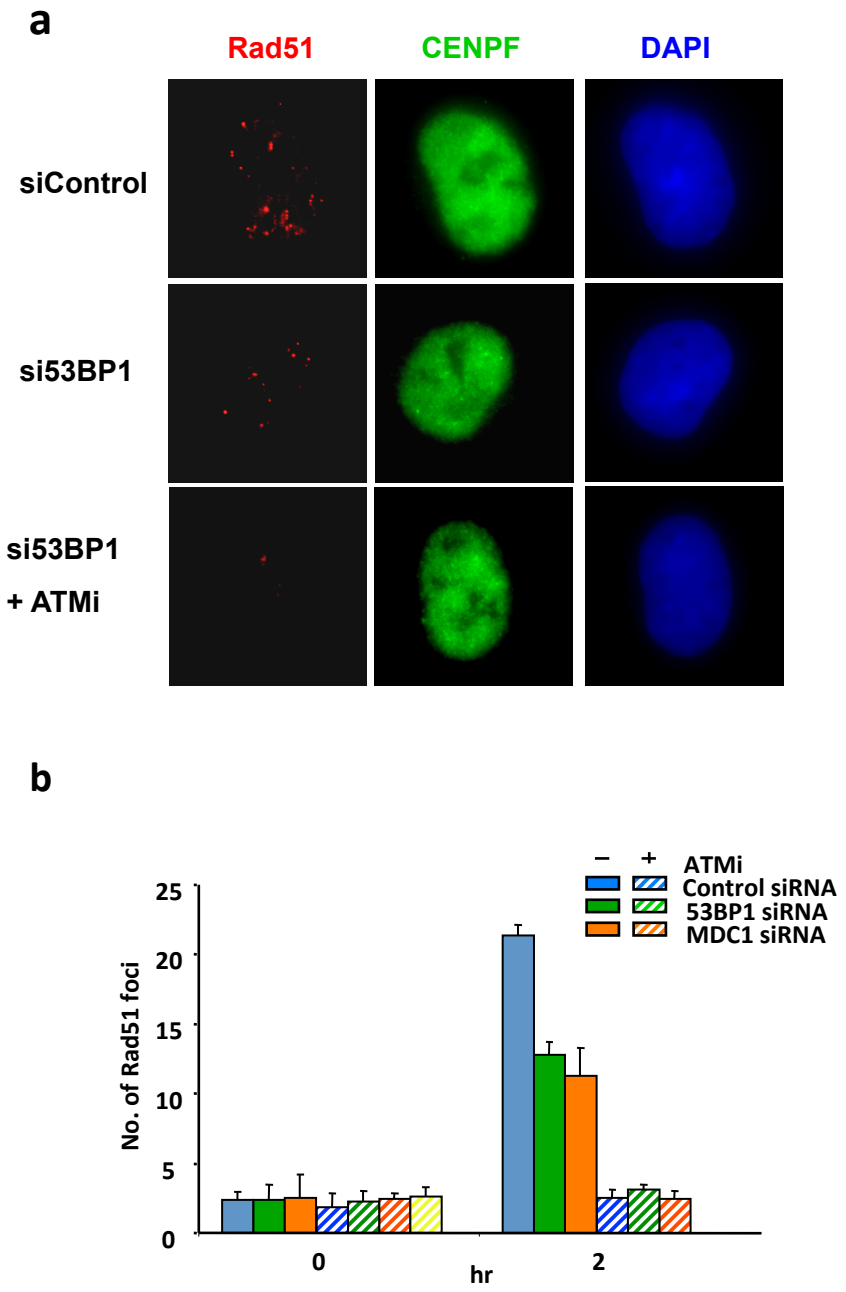

Figure 3.5: 53BP1 and MDC1 are partially required for Rad51 foci formation in G2.
a) A549 cells were treated with control, 53BP1 or MDC1 siRNA and were irradiated with 3Gy IR. Prior to irradiation aphidicolin was added to the cells to prevent S-phase cells from entering G2. The cells were then harvested at two hours post IR and immunostained with Rad51 and CENP-F antibodies. G2 phase cells were identified by positive CENP-F staining and the cell nuclei were visualized by DAPI (a). Rad51 foci were enumerated specifically in CENP-F positive cells (b). Where indicated the ATMi was added 30 minutes prior to IR. (b) Rad51 foci were enumerated in 30 cells per time-point and the data represent the mean and standard deviation of three independent experiments.

Next I wanted to know whether the cells attempting to repair DSBs by HR in the absence of 53BP1 and MDC1 were able to complete the process. To achieve this I utilised our modified assay in which SCEs are monitored as a read out of HR completion specifically in G2 phase cells (Conrad *et al*, 2011). BrdU labelled cells were irradiated with 2Gy and metaphase cells were collected 12h post IR so that all G2 phase cells at the time of IR are in mitosis. Aphidicolin was used to prevent S-phase cells from progressing into G2, caffeine was used to overcome the G2/M checkpoint and colcemid was used to arrest cells in mitosis. As expected, ATMi treated cells showed no IR induced increase in the number of SCEs (Figure 3.6b). Strikingly however, a complete loss of IR induced SCEs was also observed in 53BP1 and MDC1 depleted cells. This result indicates that although cells are able to initiate resection and form some Rad51 foci in the absence of 53BP1 and MDC1 this is not sufficient to complete HR resulting in a DSB repair defect.

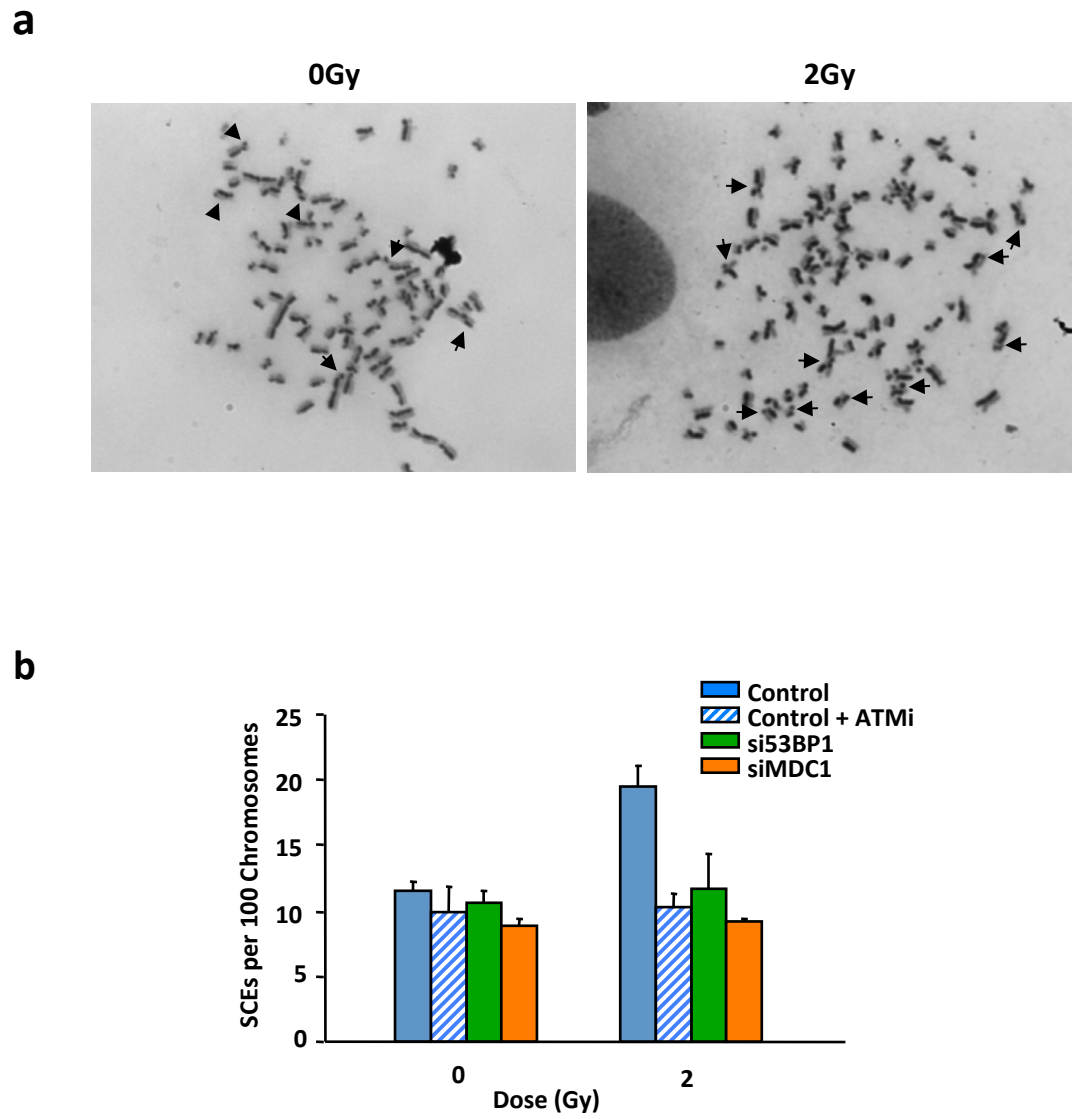

Figure 3.6: ATM, 53BP1 and MDC1 are required for IR induced SCEs in G2.
(a-b) A549 cells were treated with 53BP1 and MDC1 siRNA, grown for 48 hours in BrdU and irradiated with 2Gy IR. Prior to irradiation aphidicolin was added to the cells to prevent S-phase cells from entering G2. Eight hours after irradiation, colcemid was added to the cells to arrest them in mitosis and caffeine was added to overcome the G2/M checkpoint. Where indicated the ATMi was added 30 minutes prior to IR. SCEs were scored in at least 800 chromosomes from 3 independent experiments per data point and error bars represent the standard deviation amongst experiments.

3.2.3: Distinct functions of 53BP1 and MDC1 in G2 phase HR.

In previous work, our laboratory has demonstrated that 53BP1 and MDC1 function to promote 'concentrated' phosphorylation of KAP1 via the retention of active ATM at DSB sites (Noon *et al*, 2010). The requirement for ATM and the mediator proteins in G1 phase DSB repair can be alleviated via KAP1 depletion, which leads to sufficient relaxation of HC to bypass the need for ATM-dependent modifications. In G2 phase DSB repair, the requirement of ATM can also be overcome by KAP1 depletion but this leads to DSBs being repaired by NHEJ since resection cannot be initiated (Beucher *et al*, 2009; Shibata *et al*, 2011). Based on these findings I examined whether KAP1 depletion impacted on the outcome of DSBs repaired by HR in the absence of the mediator proteins 53BP1, MDC1 and H2AX (Figure 3.7).

Phosphorylation of histone H2AX is one of the earliest events in the DDR to DSBs and is required for the recruitment of downstream factors such as MDC1 (Bekker-Jensen & Mailand, 2010). I decided to monitor the requirement of H2AX in HR as an indirect method of assessing the importance of MDC1 focal accumulation on the process. As in G1, depletion of KAP1 had no effect on the repair kinetics of control cells and rescued the repair defect of 53BP1-depleted cells (Figure 3.7a). Strikingly however and distinct to repair in G1, KAP1 depletion did not rescue the repair defect of MDC1 depleted cells (Figure 3.7a). This result suggested that 53BP1 facilitates G2 phase HR via mediating KAP1 phosphorylation whilst MDC1 has an additional and distinct role. To try to elucidate at which step MDC1 functions I decided to look at the different HR intermediates.

KAP1 depletion in control cells has no effect on the number of RPA foci formed two hours post 3Gy IR in G2 (Figure 3.8b). However KAP1 depletion in 53BP1 knockdown cells restores the number of RPA foci to that of control cells (Figure 3.8b). Therefore the mild resection defect seen in 53BP1 knockdown cells likely results from inefficient HC remodelling and relaxation. Surprisingly however, the RPA foci numbers of H2AX and MDC1 knockdown cells also return to control levels following KAP1 co-depletion (Figure 3.8b). This result is not consistent with the DSB repair defect that persists in H2AX and MDC1 knockdown cells following KAP1 co-depletion (Figure 3.7a).

A possible explanation for this unexpected result is that MDC1 and H2AX may function in an HR step downstream of resection. I postulated that this might be a

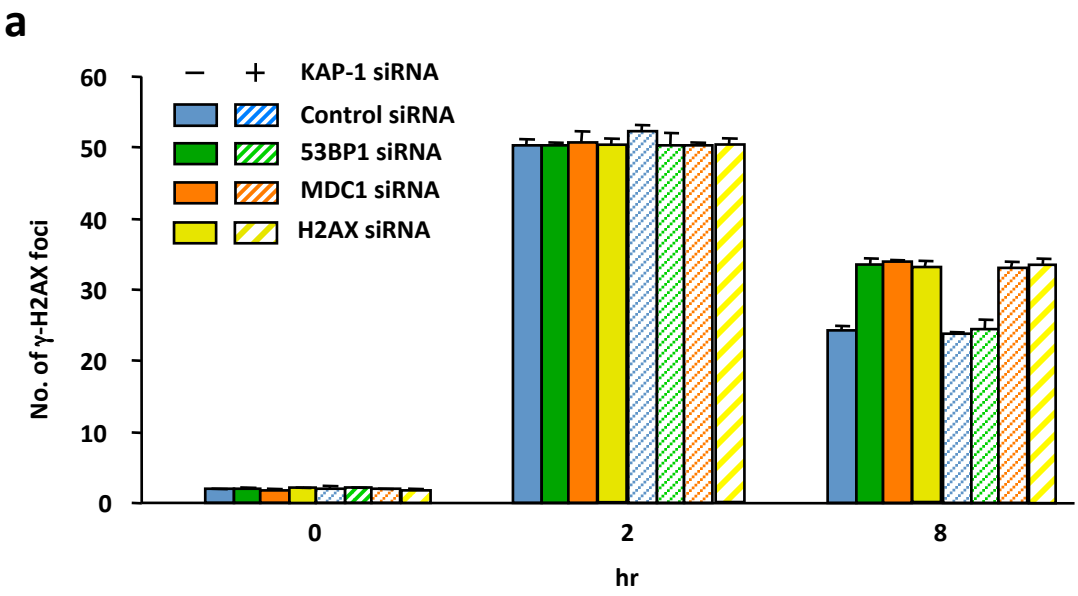

Figure 3.7: The role of 53BP1 in G2 phase DSB repair is overcome by KAP1 depletion but those of MDC1 and H2AX are not.

a) A549 cells were treated with control, 53BP1,MDC1 or H2AX siRNA and KAP-1 was co-depleted where indicated. The cells were treated with 3Gy IR and then harvested at two and eight hours post IR and immunostained with γ-H2AX and CENP-F antibodies. G2 phase cells were identified by positive CENP-F staining and the cell nuclei were visualized by DAPI. γ-H2AX foci were enumerated specifically in CENP-F positive cells. Where indicated KAP1 was co-depleted by siRNA. γ-H2AX foci were enumerated in 30 cells per time-point and the data represent the mean and standard deviation of three independent experiments.

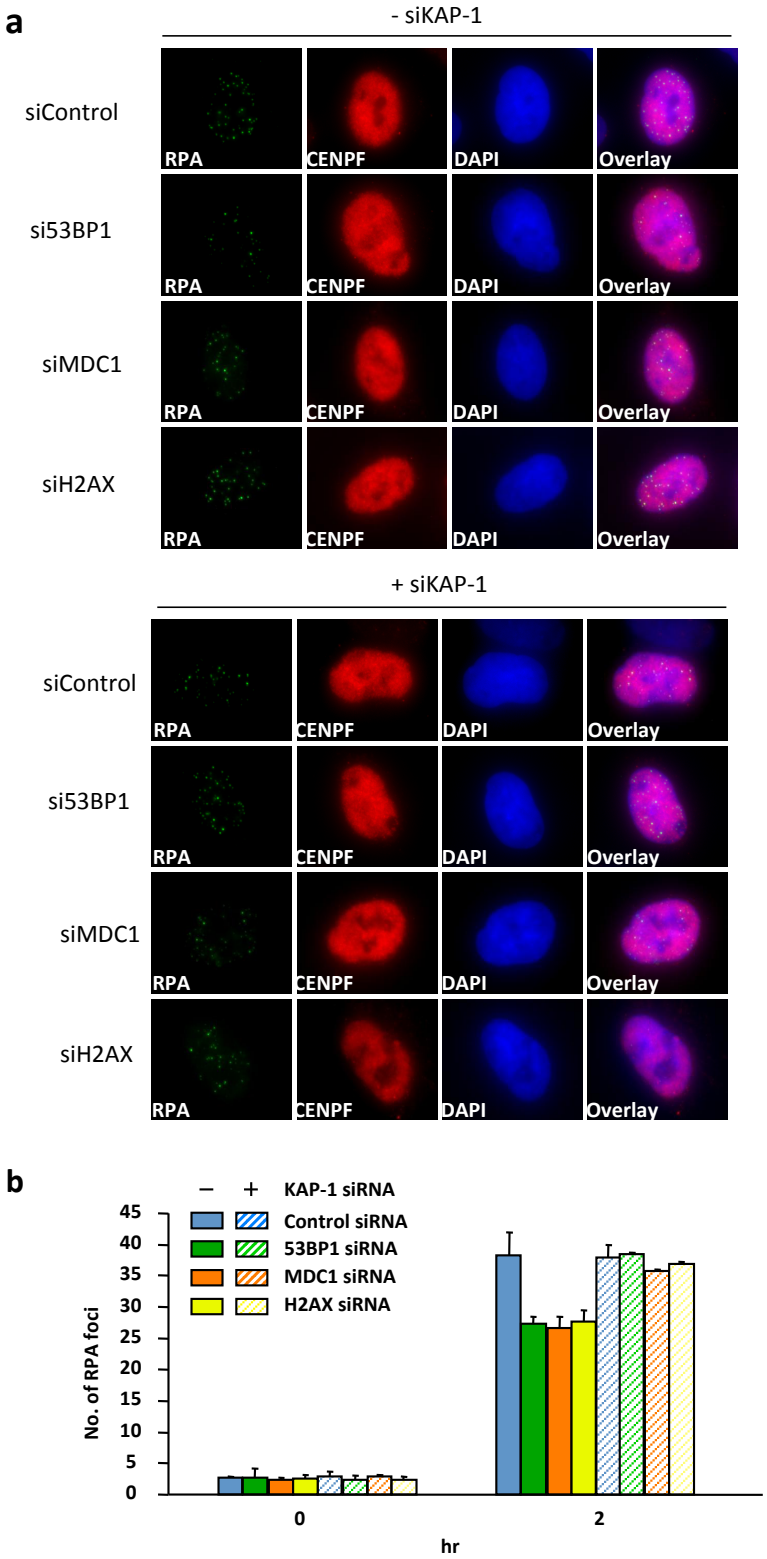

Figure 3.8: The requirement for 53BP1, MDC1 and H2AX in G2 phase RPA foci formation is overcome by KAP1 depletion.

a) A549 cells were treated with control, 53BP1,MDC1 or H2AX siRNA and KAP-1 was co-depleted where indicated. The cells were treated with 3Gy IR and then harvested at two hours post IR and immunostained with RPA and CENP-F antibodies. G2 phase cells were identified by positive CENP-F staining and the cell nuclei were visualized by DAPI. b) RPA foci were enumerated specifically in CENP-F positive cells. Where indicated KAP1 was co-depleted by siRNA. RPA foci were enumerated in 30 cells per time-point and the data represent the mean and standard deviation of three independent experiments.

requirement for Rad51 loading and set out to test this. As expected, KAP1 depletion had no effect on Rad51 foci numbers in control cells but was able to rescue the Rad51 foci defect seen in 53BP1 knockdown cells (Figure 3.9b). Again this is consistent with the notion that 53BP1 only facilitates this process via HC modification. Importantly however, the Rad51 foci defect seen in MDC1 and H2AX knockdown cells was not rescued following co-depletion of KAP1 (Figure 3.9b). This finding indicates that MDC1 has a role in Rad51 loading that is distinct to that of 53BP1 and that goes beyond its role in HC modification. To further verify this I decided to see whether MDC1 is required for HR repair of DSBs located in EU.

As described earlier, co-depletion of Ku80 and DNA-PKcs in G2 leads to an increase in the number of euchromatic DSBs repaired by HR. It also leads to slower repair kinetics with a significantly greater number of γ-H2AX foci persisting compared to control cells. This delay in repair corresponds to a greater proportion of remaining breaks (γ-H2AX foci) at four hours post IR undergoing resection (RPA foci) (Figure 3.10a). When Ku80/DNA-PKcs are co-depleted in either 53BP1 or MDC1 knockdown cells, more RPA foci are observed than in cells where Ku80/DNA-PKcs are present. This suggests that the increased resection seen following co-depletion of Ku80/DNA-PKcs is in EU and is mediator protein independent. Significantly however, the number of RPA foci in cells depleted for 53BP1 or MDC1 + Ku80/DNA-PKcs is less than in Ku80/DNA-PKcs knockdown cells (Figure 3.10a). This is due to the inability of mediator protein deficient cells to remodel HC into the relaxed confirmation needed for efficient resection. However when KAP1 is also depleted then the number of RPA foci increases to the level of Ku80/DNA-PKcs knockdown cells as the mediator proteins become redundant (Figure 3.10b). This data supports the model whereby 53BP1 and MDC1 facilitate resection via HC remodelling but have no direct role in the process per se.

Next I repeated these experiments but this time I analysed the Rad51 loading step of HR. As for RPA foci, the number of Rad51 foci seen four hours post IR in G2 increases following co- depletion of Ku80/DNA-PKcs (Figure 3.11a). This time however, when I co-depleted Ku80/DNA-PKcs in 53BP1 and MDC1 knockdown cells I only observed an increase in Rad51 foci in 53BP1 depleted cells (Figure 3.11a). This result indicates that the increased Rad51 foci seen following co-depletion of Ku80/DNA-PKcs are in EU and their formation is 53BP1 independent but MDC1 dependent. Furthermore, when KAP1 was also depleted, the number of Rad51 foci

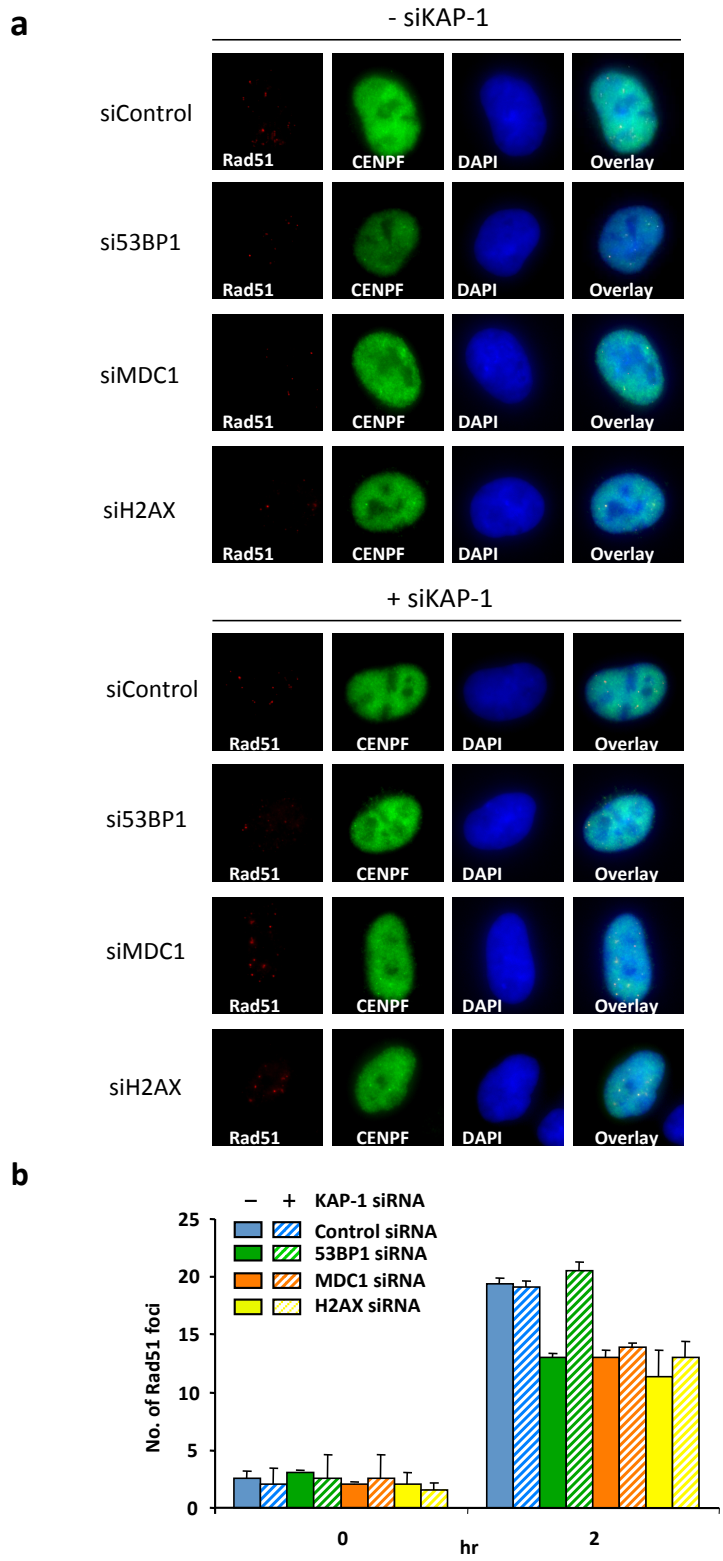

Figure 3.9: The requirement for 53BP1 in G2 phase Rad51 foci formation is overcome by KAP1 depletion but those of MDC1 and H2AX are not.

a) A549 cells were treated with control, 53BP1,MDC1 or H2AX siRNA and KAP-1 was co-depleted where indicated. The cells were treated with 3Gy IR and then harvested at two hours post IR and immunostained with Rad51 and CENP-F antibodies. G2 phase cells were identified by positive CENP-F staining and the cell nuclei were visualized by DAPI. b) Rad51 foci were enumerated specifically in CENP-F positive cells. Where indicated KAP1 was co-depleted by siRNA. Rad51 foci were enumerated in 30 cells per time-point and the data represent the mean and standard deviation of three independent experiments.

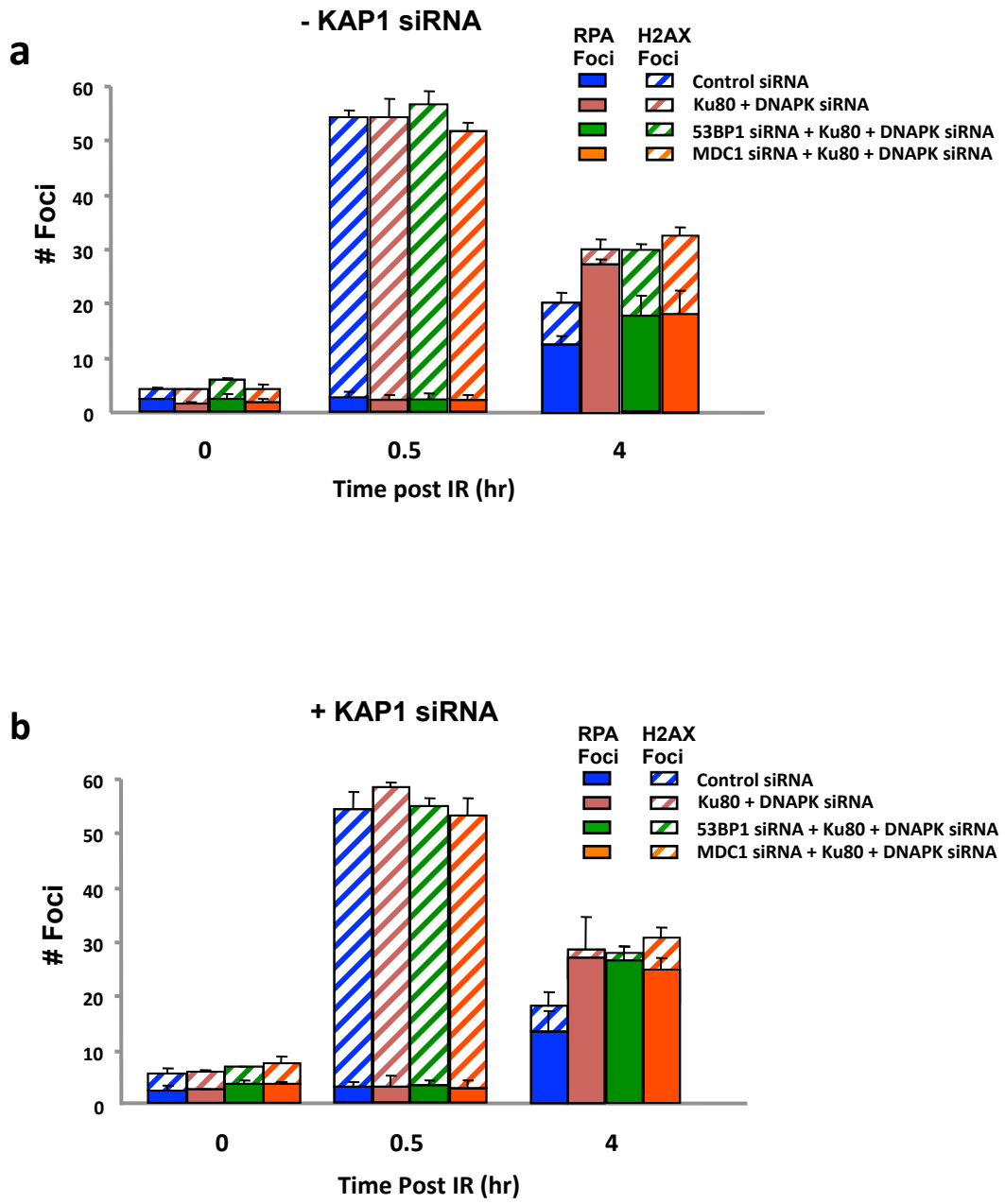

Figure 3.10: 53BP1 and MDC1 are dispensable for RPA foci formation in euchromatin.
a) A549 cells were treated with control, 53BP1 or MDC1 siRNA and Ku80 and DNA-PKcs were co-depleted where indicated. The cells were treated with 3Gy IR and then harvested at 0.5 and 4 hours post IR. Next one set of samples was immunostained with RPA and CENP-F and the other with γ-H2AX and CENP-F antibodies. G2 phase cells were identified by positive CENP-F staining and the cell nuclei were visualized by DAPI. RPA and γ-H2AX were enumerated and plotted on the same graph with hashed bars indicating γ-H2AX foci and solid bards indicating RPA foci.
b) As for a) but KAP-1 was co-depleted in all samples. Foci were enumerated in 30 cells per time-point and the data represent the mean and standard deviation of three independent experiments.

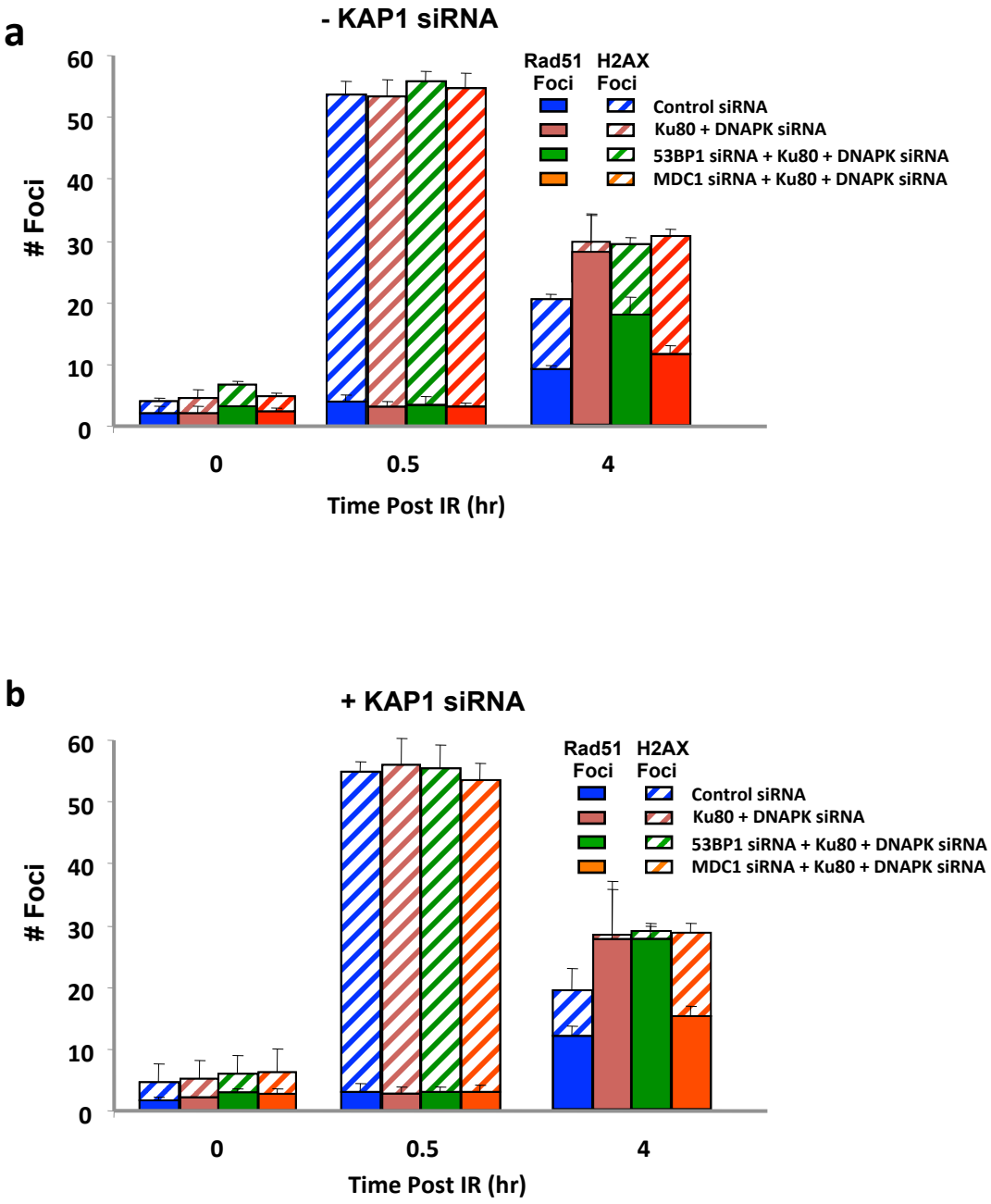

Figure 3.11: 53BP1 is dispensable for Rad51 foci formation in euchromatin but MDC1 is not.
a) A549 cells were treated with control, 53BP1 or MDC1 siRNA and Ku80 and DNA-PKcs were co-depleted where indicated. The cells were treated with 3Gy IR and then harvested at 0.5 and 4 hours post IR. Next one set of samples was immunostained with Ra51 and CENP-F and the other with γ-H2AX and CENP-F antibodies. G2 phase cells were identified by positive CENP-F staining and the cell nuclei were visualized by DAPI. Rad51 and γ-H2AX were enumerated and plotted on the same graph with hashed bars indicating γ-H2AX foci and solid bards indicating Rad51 foci. b) As for a) but KAP-1 was co-depleted in all samples. Foci were enumerated in 30 cells per time-point and the data represent the mean and standard deviation of three independent experiments.

observed in 53BP1 + Ku80/DNA-PKcs knockdown cells increased to that observed in Ku80/DNA-PKcs depleted cells (Figure 3.11b). In contrast, when KAP1 was depleted in MDC1 + Ku80/DNA-PKcs knockdown cells, no increase was observed in Rad51 foci numbers indicating an important role for MDC1 in Rad51 filament formation (Figure 3.11b).

Finally I looked at whether KAP1 depletion could alleviate the defect in IR induced SCEs following mediator protein depletion. Consistent with the above, KAP1 depletion did not affect the number of SCEs seen in control cells but increased the number of SCEs seen in 53BP1 knockdown cells to control levels (Figure 3.12). However the SCE formation defect of ATMi and MDC1 knockdown cells was not rescued by KAP1 knockdown. ATM inhibited cells are unable to initiate resection and therefore KAP1 depletion has no effect on their ability to carry out HR whilst MDC1 depleted cells are unable to efficiently form Rad51 filaments and are therefore unable to complete HR even after KAP1 depletion. Importantly however, ATMi cells show no repair defect in G2 following KAP1 depletion, whilst MDC1 and H2AX knockdown cells do (Figure 3.12). It appears that failure to initiate resection in ATMi treated cells allows these breaks to be repaired by NHEJ as long as chromatin structure is favourable. In contrast, MDC1 knockdown cells in which resection is initiated but Rad51 loading fails are unable to return to NHEJ and thus a DSB defect is observed even following KAP1 depletion (Figure 3.12).

a

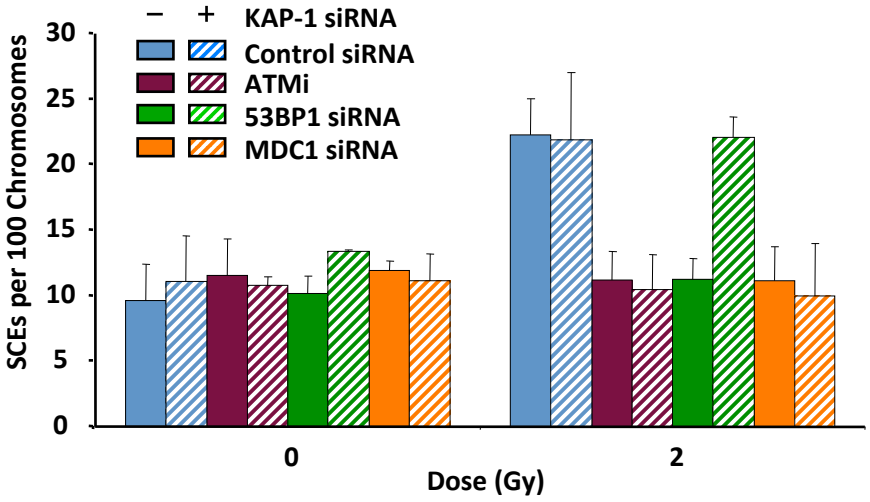

Figure 3.12: The requirement for 53BP1 in G2 phase IR induced SCE formation is overcome by KAP1 depletion but those of MDC1 and H2AX are not.
a) A549 cells were treated with control, 53BP1,MDC1 or H2AX siRNA and KAP-1 was co-depleted where indicated. The cells were grown for 48 hours in BrdU and irradiated with 2Gy IR. Prior to irradiation aphidicolin was added to the cells to prevent S-phase cells from entering G2. Eight hours after irradiation, colcemid was added to the cells to arrest them in mitosis and caffeine was added to overcome the G2/M checkpoint. SCEs were scored in at least 800 chromosomes from 3 independent experiments per data point and error bars represent the standard deviation amongst experiments.

3.2.4: The requirement of MDC1 for 53BP1 and FK2 IRIF formation cannot be relieved by siRNA KAP1.

The data so far indicates that the requirement for MDC1 in resection (RPA foci) but not in Rad51 foci formation can be relieved by KAP1 depletion in contrast to 53BP1 depleted cells where both processes are rescued. I postulated that a factor(s) acting downstream of MDC1 but upstream of 53BP1 may be required for efficient Rad51 filament formation. MDC1 is one of the earliest factors to be recruited to DSBs where it binds to γ-H2AX via its BRCT domain (Stucki *et al*, 2005). Once there it acts as a scaffold protein for the recruitment of downstream factors including the ubiquitin ligases RNF8 and RNF168 (Doil *et al*, 2009). Once at DSB sites, RNF8/RNF168 ubiquitylate downstream targets including the histone variant H2A (Mailand *et al*, 2007). Via its role in the recruitment of these ligases, MDC1 has also been shown to be required for these ubiquitylation events, detected via FK2 foci that mark polyubiquitin chains. I decided to test whether siRNA depletion of KAP1 had any impact on MDC1s ability to form ubiquitin chains or recruit 53BP1. As expected, 53BP1 depletion had no impact on FK2 foci formation at DSB sites whilst MDC1 depleted cells failed to form 53BP1 and FK2 foci irrespective of KAP1 status (Figure 3.13a-b).

These findings verify that KAP1 depletion does not impact upon ubiquitin chain formation or 53BP1 recruitment. It is therefore plausible that the inability of MDC1 knockdown cells to form Rad51 foci may result from their inability to recruit the ubiquitin ligases. In support of this model, the ubiquitin ligase Rad18 has previously been shown to be required for Rad51c and subsequently Rad51 foci formation (Huang *et al*, 2009). The role of the ubiquitin system and in particular the ubiquitin ligases RNF8/RNF168 is the focus of my work in chapter 4.

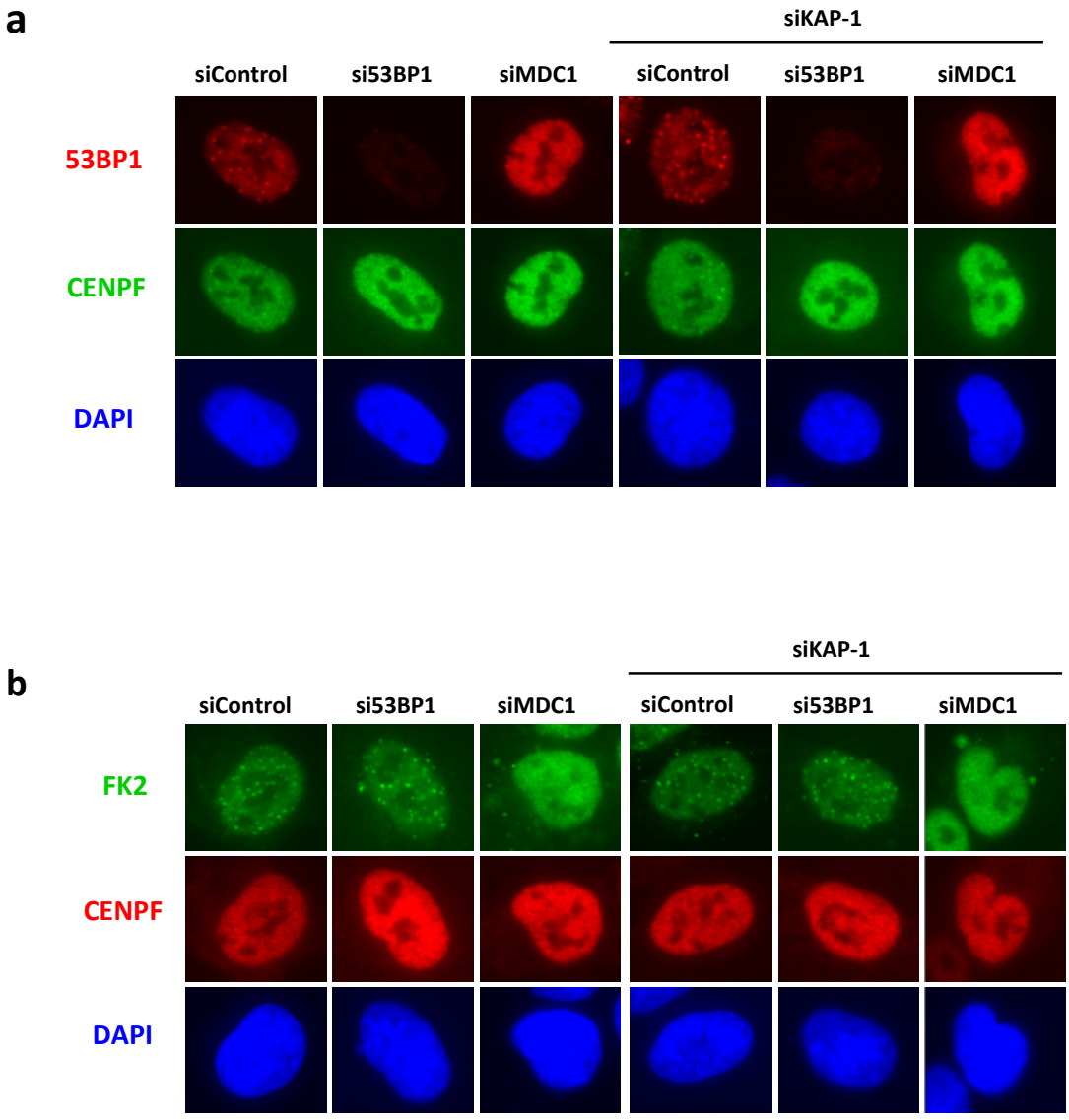

Figure 3.13: The requirement of MDC1 for 53BP1 and FK2 IRIF formation cannot be relieved by siRNA KAP1.
a-b) A549 cells were treated with control, 53BP1 or MDC1 siRNA and KAP-1 was co-depleted were indicated. Two hours post 3Gy IR the cells were harvested and immunostained with 53BP1 and CENP-F (a) or FK2 and CENP-F (b) antibodies. DAPI was used to visualize cell nuclei.

3.2.5: S-phase resection requires CtIP and the PIKK kinases.

Exposure to ionizing radiation leads to the formation of DSBs in all cell cycle phases. In the G1 and G2 phases of the cell cycle these lesions arise when a duplex DNA molecule is fractured into two parts. Such DSBs are two ended and are repaired by NHEJ or HR. In addition to the direct formation of two ended DSBs, exposure to ionizing radiation also leads to the formation of single stranded DNA breaks. Single stranded DNA breaks form at a twenty fold greater frequency than DSBs and are mainly repaired by the base excision repair pathway (Caldecott, 2007). If unrepaired, single strand DNA breaks can be converted into the more toxic DSBs during replication.

When a replication fork encounters a single strand break, it can collide with the lesion leading to replication fork collapse and the formation of a one-ended DSB (Helleday *et al*, 2007). These lesions are distinct to two ended DSBs and are normally repaired by homology directed repair leading to restoration of the replication fork (Figure 3.17a). Although distinct to G2 phase HR, homology directed repair at the replication fork requires the core HR components including Rad51 and BRCA2 (Helleday *et al*, 2007).

In addition to IR other cytotoxic agents can lead to replication fork collapse and the formation of one-ended DSBs. Camptothecin is a topoisomerase 1 poison that stabilizes the normally transient interaction between topoisomerase 1 and DNA (Shao *et al*, 1999). Topoisomerase 1 functions to relieve DNA tension during processes such as DNA replication, transcription and repair, and does this by introducing nicks that are re-ligated once reduction of DNA supercoiling is achieved (Pommier, 1996). Following camptothecin treatment, when an incoming replication fork encounters a topoisomerase-DNA complex, it leads to replication fork collapse and the formation of one-ended DSBs (Helleday *et al*, 2007). These lesions are sensed and activate a DDR that includes the activation of the PIKK kinases ATM, ATR and DNA-PK.

Following the finding that ATM has a direct role in G2 phase HR I postulated that this role might also be required during S-phase homology directed repair of one-ended DSBs. This hypothesis seemed plausible as homology directed repair involves 5'-3' resection which in G2 phase HR necessitates ATM function (Petermann & Helleday, 2010). DNA resection in S-phase also leads to extensive ssDNA regions that are coated by RPA and hence activation of ATR. To test this, I used a flow cytometry approach to measure RPA signal intensity in S-phase cells following exposure to different

concentrations of CPT (Figure 3.15). I decided to use this approach because, unlike the situation in G2 where distinct RPA foci can be seen and enumerated, CPT exposure in S-phase leads to pan-nuclear RPA staining. Flow cytometry thus allowed me to measure changes in overall RPA signal intensity whilst DNA content quantification by Propidium Iodide staining enabled me to distinguish cell cycle phases (Figure 3.15). Exposure to 4μM CPT for one hour, led to a reproducible increase in RPA signal intensity so this dose was selected. Propidium Iodide co-staining indicated that this increase was most pronounced in S-phase cells consistent with previous findings that CPT leads to DNA lesions in cells where DNA replication in on-going (Figure 3.15).

Next I used the ATMi inhibitor to test whether the increase in RPA signal intensity was dependent upon ATM. As a positive control and to ensure that the flow cytometry assay was working, I irradiated cycling cells with 15Gy and measured RPA signal intensity in the presence and absence of ATMi (Figure 3.14). In control cells, exposure to 15Gy IR led to an increase in RPA signal intensity, while PI staining indicated that this was primarily in G2 phase cells (Figure 3.14). Consistent with the data described earlier, addition of ATMi thirty minutes prior to irradiation led to no detectable changes in RPA signal intensity following 10Gy IR (Figure 3.14). Strikingly however, when the same experiment was repeated using CPT, addition of ATMi had no impact on RPA signal intensity in S-phase cells (Figure 3.15a). This result indicates that in S-phase, unlike the situation in G2, resection can proceed independently of ATM status. Since CtIP is required for resection in G2, I then decided to ask whether CtIP is required for S-phase resection following CPT treatment.

In G2 phase HR, CtIP undergoes regulatory phosphorylation by ATM at S664/S745 (Li *et al*, 2000). This phosphorylation in response to DNA damage is required for CtIP recruitment to damage sites and for the initiation of resection (Shibata *et al*, 2011). Consistently, when CtIP was depleted, no increase in RPA signal intensity was observed in G2 cells following 10Gy IR. Interestingly however and distinct to ATMi treated cells, no increase in RPA signal intensity was seen in S-phase CtIP knockdown cells following CPT treatment (Figure 3.16). This result suggests that CtIP is required for S-phase and G2 phase resection but that ATM regulates this only in G2. This finding raised the question of how S-phase resection is regulated and whether it requires DNA-PK or ATR.

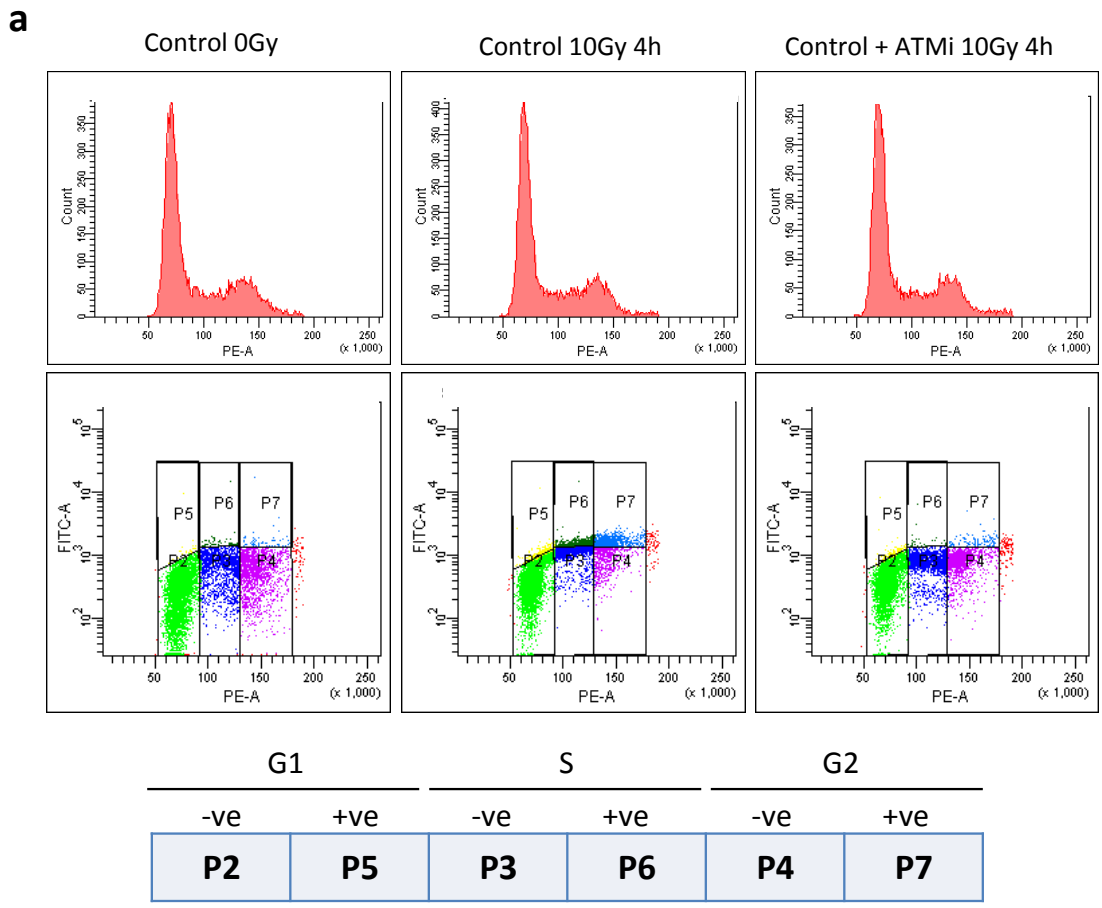

Figure 3.14: ATM is required for a G2 phase specific RPA intensity increase after IR.
a) Cycling A549 cells were treated with 10Gy IR. Irradiated and non-irradiated cells were harvested four hours post IR and immunostained with an RPA antibody and propidium iodide. In the lower panels populations p2, p3 and p4 correspond to G1,S and G2 phase cells respectively as determined by DNA content following propidium iodide staining. Populations p5,p6 and p7 represent cells of each cell cycle phase in which a radiation induced increase in RPA intensity was detected after IR treatment. The upper panels show the cell cycle profile for each condition as determined by propidium iodide staining.

a

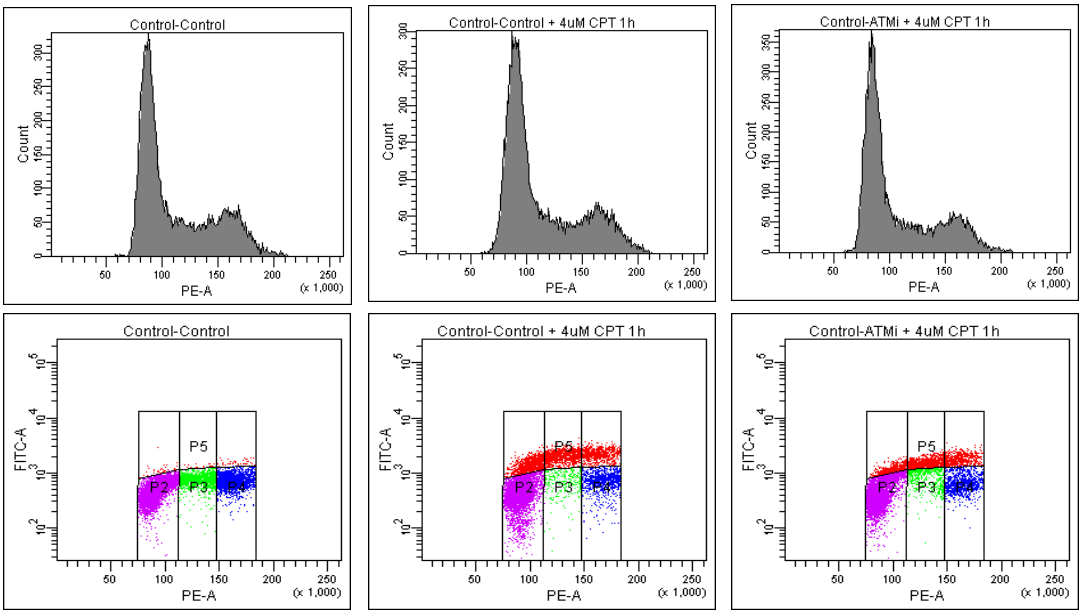

b

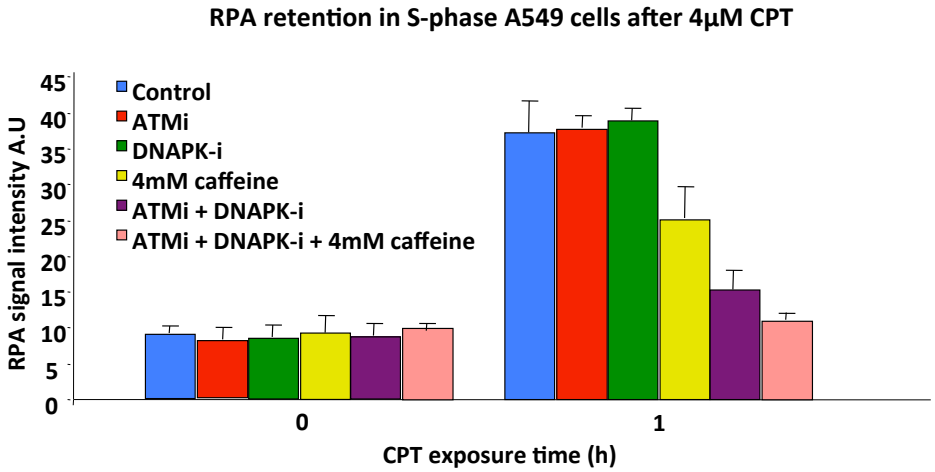

Figure 3.15: S-phase resection requires the PIKK kinases.
a) Cycling A549 cells were treated with 4µM CPT for one hour. Treated and non-treated cells were harvested and immunostained with an RPA antibody and propidium iodide. In the lower panels populations p2, p3 and p4 correspond to G1,S and G2 phase cells respectively as determined by DNA content by propidium iodide staining. Population p5 represents cells in which an increase in RPA intensity was observed. The far right panel indicate cells in which the ATMi was added thirty minutes prior to CPT treatment.
b) Quantification of RPA signal intensity after CPT treatment measured in A549 cells by flow cytometry. The cells were treated with ATMi, DNAPKi and caffeine where indicated. Results represent the average of three experiments and the standard deviation among these.

When a replication fork collapses as a result of colliding with a topoisomerase induced single strand nick, ssDNA is formed that is coated by RPA and leads to ATR activation (Shechter *et al*, 2004). In addition, DNA-PK is activated and phosphorylates RPA2 (Shao *et al*, 1999). To assess whether these kinases are required for single strand DNA formation at collapsed replication forks, I inhibited their function and monitored RPA signal intensity in response to CPT treatment. First I used ATM and DNA-PK inhibitors but in both cases I observed an increase in RPA intensity one-hour post CPT that was indistinguishable to control cells (Figure 3.15b). Next I used caffeine to inhibit ATR function. Interestingly, when caffeine was added at a 4mM concentration, a partial reduction in RPA signal intensity was observed relative to the control. It is important to note however that at this caffeine concentration, ATM function is also inhibited although DNA-PK is not (Sarkaria *et al*, 1999). This result indicates that there might be some redundancy amongst these kinases so I decided to inhibit them in conjunction. First I used both the ATM and DNA-PK inhibitors and monitored RPA signal intensity after CPT treatment. Although use of the inhibitors alone had no effect, when used together they led to a significant decrease in RPA intensity relative to control cells (Figure 3.15b). Finally I inhibited ATM, DNA-PK and ATR at the same time by using the two inhibitors and adding caffeine and observed an even greater reduction in RPA signal intensity (Figure 3.15b). This result indicates that the PIKK kinases are required for ssDNA formation and RPA loading at collapsed replication forks but that there is functional redundancy amongst them. Moreover the mechanism by which they regulate resection in S-phase is unclear but is unlikely to be via CtIP. This is because phosphorylation of CtIP in G2 is ATM specific and cannot be performed by DNA-PK or ATR. CtIP is also a CDK substrate and CtIP phosphorylation by CDK has been shown to be required for resection both in S and G2 cell cycle phases (Huertas & Jackson, 2009). It is possible that CtIP function at replication forks is regulated by CDK activity whilst ATM, ATR and DNA-PK enable this process indirectly via activation of intra S-phase checkpoint arrest.

3.2.6: The mediator proteins are dispensable for S-phase resection.

As discussed above, the mediator proteins MDC1, 53BP1 and H2AX are required for efficient resection at two ended DSBs in G2. However this is not due to a direct role of these proteins in the process but through ATM dependent chromatin remodelling. ATM dependent chromatin remodelling appears to be dispensable for resection in S-phase probably due to the de-condensed chromatin configuration during replication. Here I wanted to ask whether mediator protein function is required for ssDNA formation and RPA coating following CPT treatment. To achieve this I used the flow cytometry assay described above and monitored RPA signal intensity following one hour 4μM CPT treatment. siRNA knockdown of 53BP1, MDC1 or H2AX had no impact on the increase in RPA signal intensity seen after CPT treatment (Figure 3.16a). This result indicates that the mediator proteins are dispensable for ssDNA formation and RPA coating at stalled/collapsed replication forks.

a

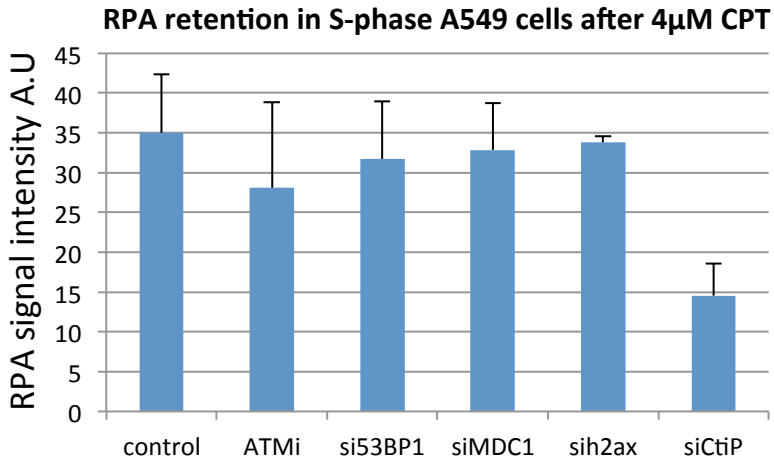

Figure 3.16: S-phase resection requires CtIP but not ATM or the mediator proteins.
a) Quantification of RPA signal intensity after CPT treatment measured in A549 cells by flow cytometry. Cycling A549 cells were treated with 4µM CPT for one hour. Treated and non-treated cells were harvested and immunostained with an RPA antibody and propidium iodide. Where indicated, cells were treated with ATMi or siRNA prior to CPT exposure.

3.2.7: Repair pathway choice of collapsed/stalled replication forks might affect genomic stability.

HR has an evolutionarily conserved role in the maintenance of genomic stability following replication stress. Whilst only functioning to repair a small subset of IR induced DSB breaks in G2, it has a critical role in preventing the genomic instability that can arise when a lesion is encountered at the replication fork (Lundin *et al*, 2003; Arnaudeau *et al*, 2001; Lundin *et al*, 2002). Consistent with this, cell lines deficient in HR display only modest radiation sensitivity but marked genomic instability and sensitivity to agents such as PARP inhibitors and MMS, which lead to enhanced replication fork stalling/collapse (Jasin, 2002; Kass *et al*, 2010).

It is unclear whether sites of DNA damage that are marked by γ-H2AX foci in S-phase are indeed DSBs or just stalled replication forks, but fork restoration is crucial for maintenance of chromosomal stability. BRCA1/2 and certain FA mutant cells are HR deficient and display sensitivity to replication stress and have increased chromosome breakage, radial chromosomes and other cytogenetic abnormalities (D'Andrea & Grompe, 2003). This cellular phenotype is a direct result of these cells failure to restore replication forks due to impaired HR. It is currently unclear why there is such a high dependence on HR in S-phase and why NHEJ can't repair these lesions as in G1 and G2. One explanation is that this is due to the difference in nature of DSBs in G1 and G2 versus S-phase. DSBs arising in G1 and G2 are two ended and can be accurately repaired by tethering the broken ends and re-joining them by NHEJ (Shibata *et al*, 2011). DSBs at the replication fork however are one ended and there is no adjacent DNA end for it to be ligated to (Helleday *et al*, 2007). If NHEJ is used to repair such a lesion, then DNA joining will occur between two distinct one-ended DSBs resulting in genomic rearrangements. It is plausible that repair of one ended DSBs by NHEJ in HR deficient cells results in the chromosomal abnormalities seen in BRCA and FA mutant cells following replication stress (Figure 3.17).

The mediator protein 53BP1 promotes ATM dependent DSB repair in G1 and G2 via HC remodelling (Noon *et al*, 2010). As discussed in the introductory chapter, 53BP1 also has ATM independent functions in V(D)J recombination, CSR, and telomere end fusions (Difilippantonio *et al*, 2008; Bothmer *et al*, 2011; Dimitrova *et al*, 2008). Intriguingly, in all three processes, 53BP1 functions to facilitate long-range re-joining events. In V(D)J recombination 53BP1 brings together recombination

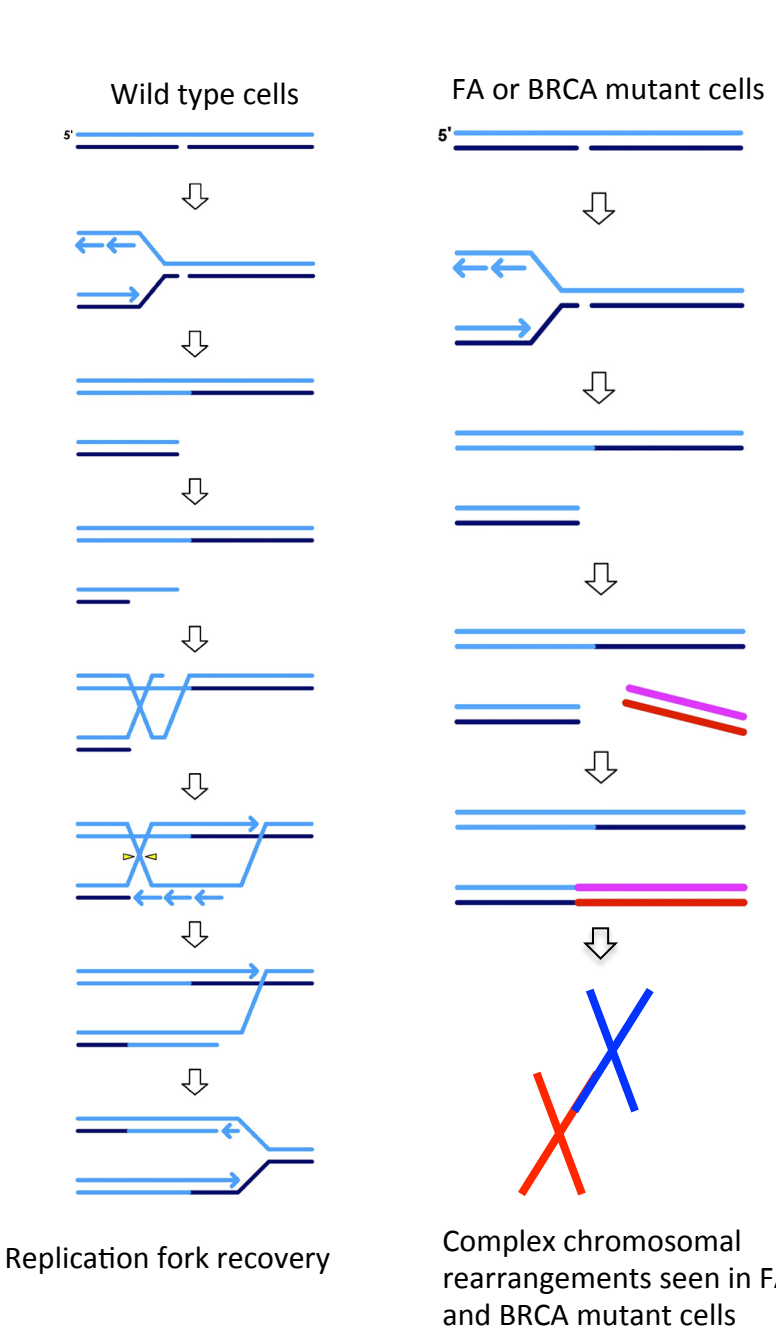

Adapted from: HELLEDAY et al. (2007). DNA double-strand break repair: From mechanistic understanding to cancer treatment.

Figure 3.17: Model for replication fork recovery.
a) Following replication fork collapse one-ended DSBs are created. In wild type cells homology directed repair is utilized to restore the collapsed replication fork and DNA replication can ensue. However in FA and BRCA mutant cells homology directed repair is defective. A model for the complex cytogenetic abnormalities seen in these cells is that one-ended DSBs arising following replication fork collapse are repaired erroneously by NHEJ. In this model two distinct and possibly distant one-ended DSBs are joined resulting in chromosomal re-arrangements.

signal sequences of distally separated V, D or J segments while in CSR it is required for the re-joining of AID cleavage sites when they are separated by more than 100kb. In uncapped telomere re-joining 53BP1 enables telomere fusions by bringing telomere ends close enough to each other so that re-joining by fusion takes place. The mechanism by which 53BP1 carries out these functions is unclear but 53BP1 accumulation and foci formation appear to be important as is its ability to oligomerise. From the above I reasoned that 53BP1 might enable the deleterious long range re-joining of one ended DSBs in HR deficient cells in S-phase. To test this I decided to monitor repair foci fusions by live cell imaging (LCI) following DNA damage in S-phase.

MMS treatment results in replication fork stalling/collapse in S-phase and restoration of these forks requires the HR pathway (Löbrich *et al*, 2010). Sites of MMS induced damage lead to the accumulation of γ-H2AX and intermediates of the HR pathway such as Rad51. To see whether 53BP1 may have a role in the processing of such lesions, I decided to look whether 53BP1 foci form following exposure to MMS. In order to detect 53BP1 foci and for later use in LCI experiments, I acquired the mCherry-BP1 construct used by the Titia de Lange group to study end fusions of uncapped telomeres (Dimitrova *et al*, 2008). In this construct, mCherry is fused to a truncated form of 53BP1 that lacks most functional domains of the protein but that maintains its TUDOR and γ-H2AX binding domains important for 53BP1 foci formation (Figure 3.18a).

Hela cells were transfected with the mCherry-BP1 construct and allowed to express it for twenty four hours prior to exposure to 1mM MMS for 30 minutes. Cells were then harvested and immunostained for γ-H2AX (Figure 3.18b). The twenty-four hour expression led to a panuclear distribution of the mCherry-BP1 protein, while cells that were treated with MMS formed distinct nuclear foci. These foci completely colocolised with γ-H2AX foci suggesting the fusion protein was able to accumulate at DNA damage sites (Figure 3.18b). Next I wanted to know whether or not the foci formed after MMS treatment were restricted to S-phase cells. To test this I exposed cells to the same concentration of MMS but this time stained with PCNA. In S-phase cells PCNA has a distinct, granular nuclear appearance with many small foci visible (Figure 3.18c) (van Dierendonck *et al*, 1991). Following MMS exposure mCherry-BP1 foci only formed in S-phase cells as determined by PCNA staining pattern (Figure 3.18c). I concluded that MMS was a suitable agent for inducing S-phase specific DNA damage

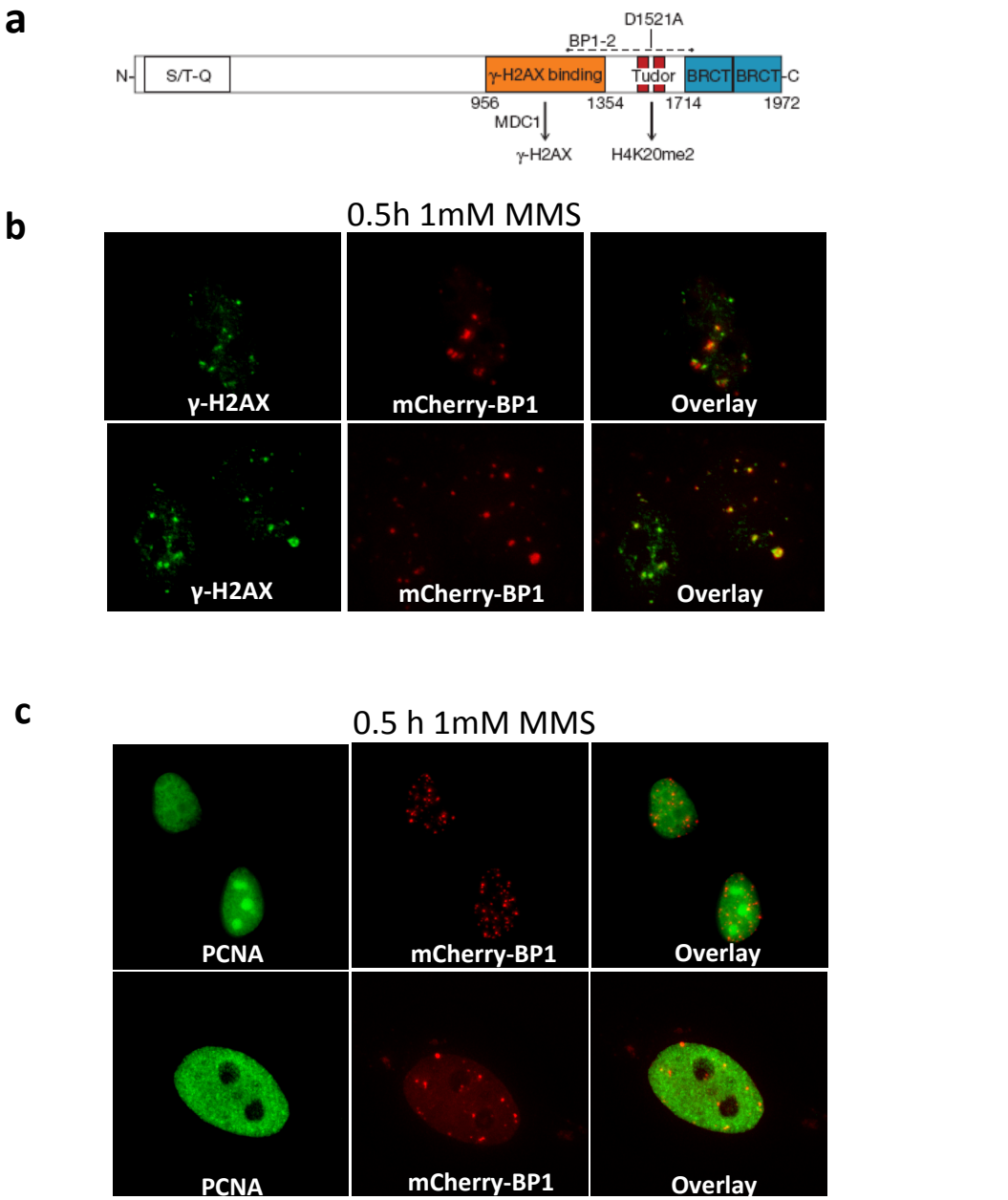

Figure 3.18: mCherry-BP1 construct forms foci that overlap with γ-H2AX foci specifically in S-phase.
a) Schematic representation of the mCherry-BP1 construct. The C-terminal BRCT domains are present, as are the TUDOR binding and γ-H2AX binding domains required for focal accumulation. The functional domains of 53BP1 are absent.
b) Hela cells were transfected with the mCherry-BP1 construct and allowed to express it for twenty-four hours. The cells were then exposed to 1mM MMS for one hour and then harvested and immunostained with a γ-H2AX antibody.
c) As for b), but this time the cells were immunostained with a PCNA antibody.

and that the mCherry-BP1 construct would allow me to test foci movement and fusions by LCI.

NHEJ repairs DSBs with fast kinetics with the majority of lesions repaired within two hours post damage induction (Riballo *et al*, 2004). I decided to monitor foci movement by LCI for three hours post MMS exposure, as this would allow ample time to detect any differences arising from 53BP1 status. Additionally, when monitoring telomere fusions by NHEJ in the presence or absence of 53BP1 a significant difference in telomere distance travelled was observed within twenty minutes of LCI (Dimitrova *et al*, 2008). Following transfection and transient expression of the mCherry-BP1 construct, I treated the cells with 1mM MMS and monitored foci movement by LCI. I also transfected the cells with a plasmid containing GFP tagged histone variant H2B and used this to visualize the cell nuclei (Figure 3.19a).

The experimental setup worked well and as predicted from IRIF foci behaviour in G1, MMS induced mCherry-BP1 foci expanded over time and were dynamic and mobile (Figure 3.19). Additionally, the number of foci that remained after three hours of LCI were significantly reduced indicating that repair was taking place (Figure 3.19b). The image processing software suite Imaris was used to quantify foci movement over the LCI period. When comparing the total distance travelled by individual foci a clear discrepancy became apparent (Figure 3.20b). If any given focus persisted for long, then it would likely travel further than one that disappeared in a shorter time. Therefore comparing the distance travelled over time i.e. the speed of each focus seemed a more appropriate parameter to compare. Control cells displayed uniform foci speed without substantial differences between the entire population (Figure 3.20c). Importantly, no obvious foci fusion events were observed in control cells. Next I repeated this experiment following BRCA1 depletion by siRNA. Following BRCA1 depletion I expected to see an increase in 53BP1 IRIF mobility since HR was compromised and repair would need to occur between distant one-ended DSBs. However following BRCA1 depletion, no significant changes in foci speed were observed and foci fusions were not detected (Figure 3.20b-c). This result was unexpected as HR defective cells were predicted to show an increase in foci speed or total distance travelled and increased foci fusions. Next I assessed the effect of 53BP1 on foci movement in an HR deficient background by co-depleting BRCA1 and 53BP1. However, co-depletion of BRCA1 and 53BP1 did not have a significant effect on foci speed compared to control

a

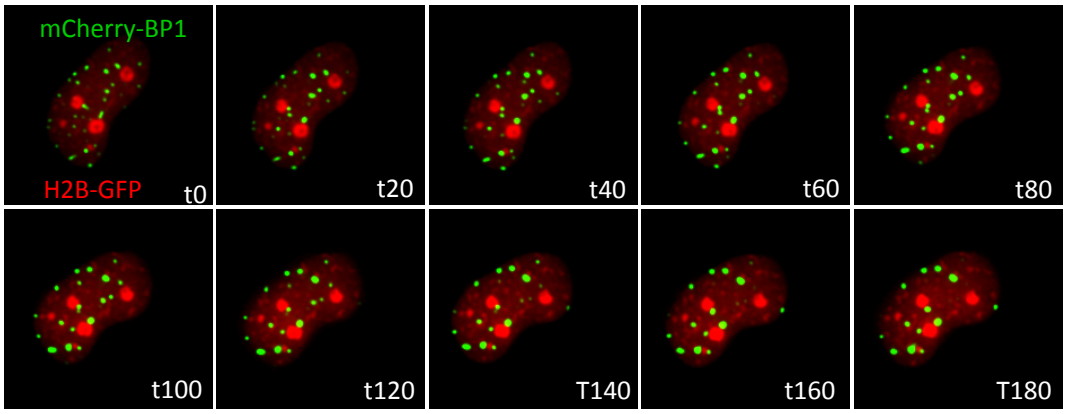

b

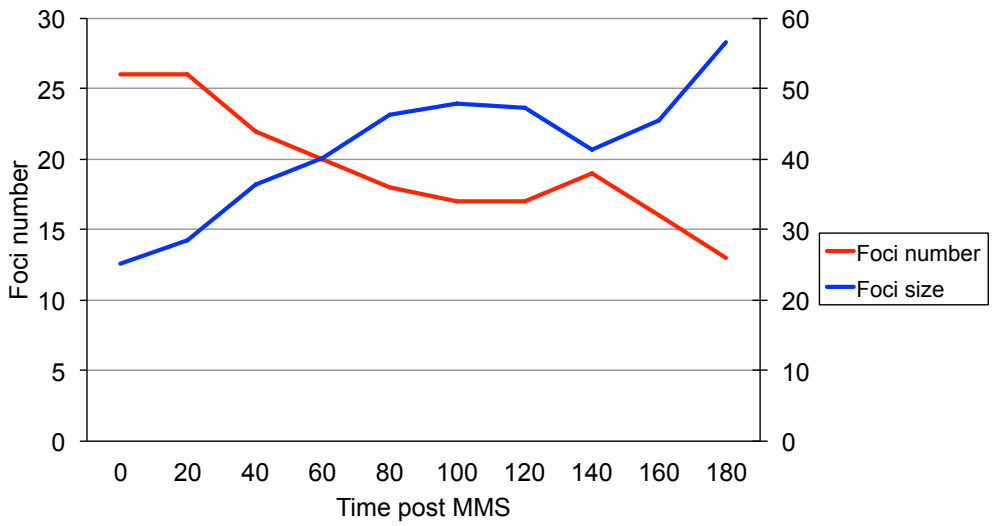

Figure 3.19: mCherry-BP1 construct foci that form after MMS treatment expand over time and decrease in number as repair ensues.
a) Hela cells were transfected with the mCherry-BP1 construct and with a plasmid expressing histone H2B-GPF. They were allowed to express these for twenty-four hours. The cells were then exposed to 1mM MMS for one hour and were then monitored for three hours by LCI. Images where take every 5 minutes but images here show twenty minute intervals.
b) Quantitative analysis of mCherry-BP1 foci size and number from LCI images. LCI images obtained using an Applied Precision® Delta Vision® RT Olympus IX70 deconvolution microscope were deconvolved by the Huygens Professional image processing software. The BitPlane Imaris image processing software suite was then used to quantify the foci number and size over time. The right Y-axes represents arbitrary units for foci size.

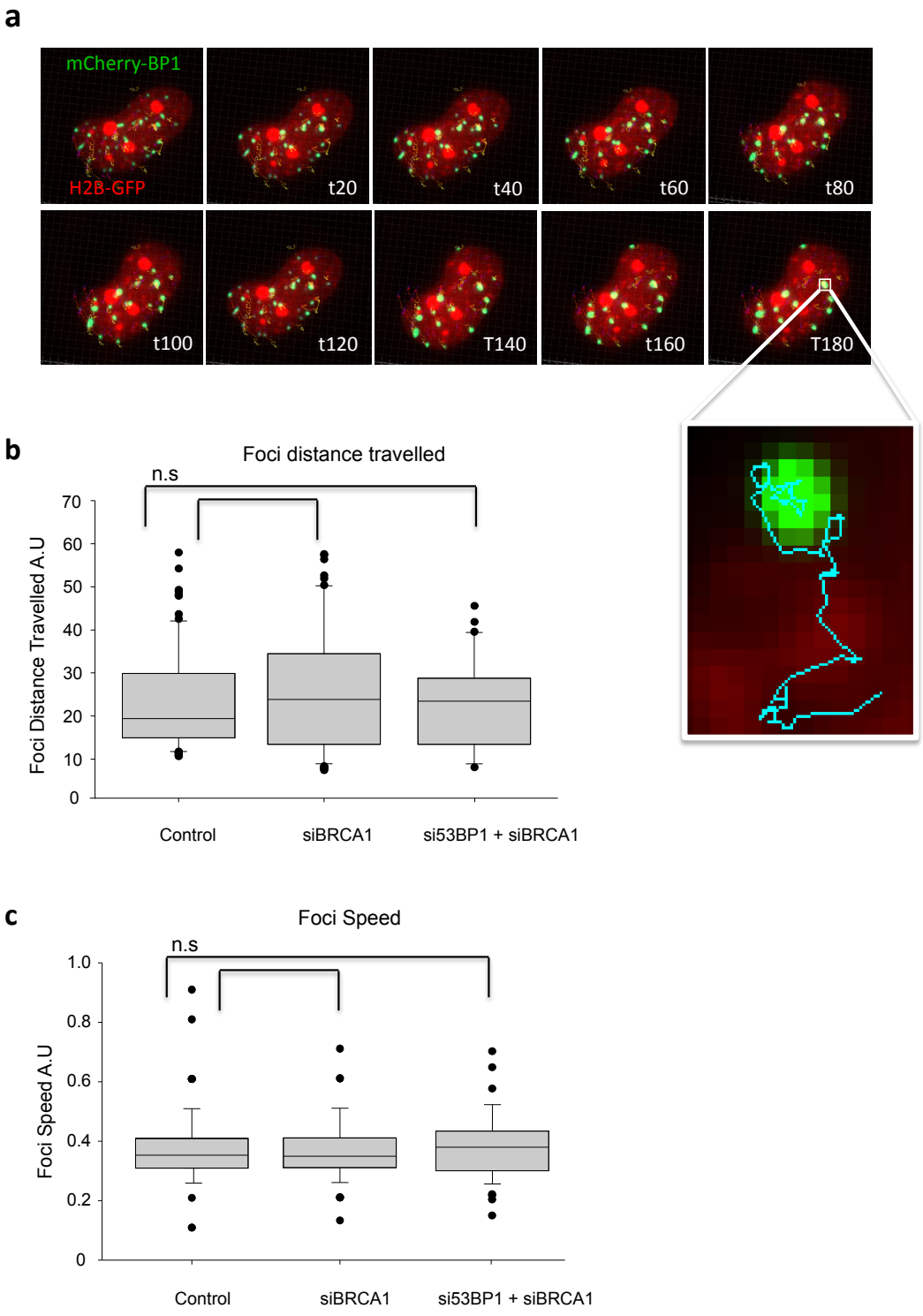

Figure 3.20: BRCA1 depletion does not affect the mobility of the mCherry-BP1 construct foci that form after MMS treatment.

a) Representative images of mCherry-BP1 foci detection and track measurement over time by the BitPlane Imaris image processing software suite. b) Quantification of the distance travelled by the mCherry-BP1 foci in control cells and in cells treated with BRCA1 and 53BP1 + BRCA1 siRNA. c) Quantification of the speed of the mCherry-BP1 foci in control cells and in cells treated with BRCA1 and 53BP1 + BRCA1 siRNA. In b) and c), the data represent the median and lower and upper quartiles from at least 10 nuclei from each of three experiments. Error bars represent the minimum and maximum valid values determined as the highest datum still within 1.5 the interquartile range of the upper quartile. These were used to eliminate abnormally large values (depicted as single points) arising from foci 'clumping' and resolution limitations. Statistical analysis was carried out using the Mann-Whitney rank sum test. Data were not deemed to be significant when a p value > 0.05 was obtained.

cells and neither did it increase the number of foci fusions formed (Figure 3.20b-c). Due technical difficulties in LCI experimental setup and data analysis, these studies were not taken further. Determining whether the increased sensitivity of HR and FA mutant cells to genotoxic exposure in S-phase results from aberrant re-joining of one-ended DSBs is an important future question.

3.3: Discussion

IR induced DSBs associated with HC are repaired via HR in G2

Traditionally, DSB repair has been separated into NHEJ and HR with one pathway repairing breaks in G1 and the other in G2. In recent years however this simplistic view has been overturned and the true complexity of DSB repair is becoming apparent. The regulation of repair pathway choice is still to be fully understood but appears to be influenced by cell cycle phase, chromatin structure and DNA damage complexity amongst other factors (Shibata *et al*, 2011; Symington & Gautier, 2011; Bothmer *et al*, 2010). In addition, an ever-growing number of proteins with a wide range of functional and interacting motifs are found to play a role in the DNA damage response (Mohammad & Yaffe, 2009). The tightly regulated orchestration of these factors by post-translational modification allows cells to perform the complex but vital task of repairing potentially lethal DSBs.

The influence of chromatin structure on DSB repair in G1 has been the subject of recent work from our laboratory. Chromatin structure at DSB sites was found to play a pivotal role in repair kinetics and the requirement, or not, of localized chromatin remodelling. Specifically breaks at HC were found to require localized chromatin relaxation that depended upon ATM and the mediator proteins and culminate in HC relaxation via KAP1 phosphorylation (Noon *et al*, 2010).

Subsequently, these experiments were extended to the G2 phase of the cell cycle that is distinct to G1 as HR is also functional. DSB repair in G2 was also found to be biphasic and there was a requirement for HC modification via ATM dependent KAP phosphorylation. Unexpectedly the slow component of repair in G2 was found to represent the DSBs undergoing repair by HR, with ATM and Artemis being required for the resection step (Beucher *et al*, 2009). The role of Artemis in resection is still unclear

but ATM was found to be required for the initiation of resection through phosphorylation of CtIP (Shibata *et al*, 2011). Consistent with the situation in G1, the DSBs that require ATM are located at HC regions. ATM dependent KAP1 phosphorylation is required for the repair of these breaks and the requirement for ATM can be overcome by KAP1 depletion. However, in such a scenario the HC DSBs are then repaired by NHEJ and we believe this is because resection cannot be initiated independently of ATM.

The major focus of this chapter lies in determining the requirement for the mediator proteins 53BP1, MDC1 and H2AX in G2 phase HR. 53BP1 has been described as a pro-NHEJ factor with an inhibitory role on HR (Xie *et al*, 2007). In stark contrast however, my experiments in G2 indicate that 53BP1 is required for HR that occurs at HC-DSBs. As in G1, 53BP1 enables the repair of HC DSBs by retaining activated ATM through its interaction with the MRN complex and leads to the localized robust KAP1 phosphorylation needed for HC relaxation. However, experiments in which KAP1 was depleted indicated that 53BP1 has no direct role in the HR process and is dispensable for all HR steps when chromatin configuration is favourable. Collectively, experiments in G1 and G2 indicate that 53BP1 does not appear to function in or regulate any given repair pathway but rather functions to promote the changes in HC superstructure that are a prerequisite for HC-DSB repair. Previous studies in which 53BP1 was described as a pro-NHEJ factor used I-Sce1 induced DSBs (Xie *et al*, 2007). However such systems may not monitor roles in chromatin modifications as the construct integration site is most likely not in HC regions. More recently an inhibitory role for 53BP1 in DNA end resection has been described and BRCA1 function is required to overcome this (Bunting *et al*, 2010; Bouwman *et al*, 2010). The interplay between 53BP1 and BRCA1 in DNA end resection will be the focus of chapter 5.

MDC1 and H2AX were also found to be required for G2 phase HR that occurs at HC-DSBs. Since H2AX functions upstream of MDC1 and is required for MDC1 recruitment I conclude that this is how H2AX mediates this process. As for 53BP1, MDC1 also has a role in HC-relaxation in G2 that is required for HR. However although the role of MDC1 in resection can be overcome by KAP1 depletion, its requirement for Rad51 foci formation and completion of HR (measured by SCEs) cannot. These findings indicate that MDC1 has two distinct roles in promoting G2 phase HR. Firstly, MDC1 is required to localize 53BP1, which is necessary for HC relaxation. Additionally MDC1 has a role in Rad51 loading although the precise

mechanism of how this occurs is currently unclear. One possibility is that MDC1 directly interacts with Rad51 and promotes filament formation while another possibility is that it facilitates the process via recruitment of downstream factors. There are currently data in the literature in support of both of these models (Zhang *et al*, 2005; Huang *et al*, 2009).

ATM is dispensable for MMS induced HR in S-phase.

In addition to its role in G2 phase DSB repair, HR is utilised in replication fork restoration following stalling or collapse in S-phase. In order to address the role of the ATM and mediator proteins in resection at the replication fork I monitored ssDNA formation following exposure to CPT. In S-phase chromatin is thought to be decondensed in preparation for replication and consistent with this, I found no effect on ssDNA formation by CPT in 53BP1, MDC1 and H2AX knockdown cells. This result indicates that HC modification in S-phase in not required for DNA end resection. Surprisingly however, the role of ATM was also found to be indispensable which is distinct to the situation in G2. It appears that the single stranded regions present at stalled/collapsed replication forks are a substrate for CtIP and therefore ATM function is no longer required. However as in G2, CtIP is required for resection in S-phase and CtIP depletion leads to a reduction in ssDNA formation after CPT.

MDC1 but not 53BP1 is required for HR following MMS treatment.

In collaboration with our work investigating the role of the mediator proteins in G2 phase HR, the laboratory of Markus Lobrich has monitored the role of the mediator proteins in HR in S-phase. They first showed that MMS induced lesions are repaired almost exclusively by HR in contrast to IR DSBs in G2, where the majority of breaks are repaired by NHEJ. By using MMS and IR doses that resulted in similar numbers of γ-H2AX foci and then monitoring SCEs, they found almost four times more SCEs after MMS treatment. They then went on to investigate the requirement of ATM and the mediator proteins, 53BP1 and MDC1, in HR repair of MMS induced damage.

Consistent with my data showing that ATM is dispensable for resection in S-phase, they observed normal Rad51 foci formation and SCEs in an A-T cell line after MMS treatment. This finding is also consistent with the notion that due to chromatin

restructuring in S-phase, ATM dependent chromatin decondensation is not a prerequisite for repair.

Next they monitored the requirement for 53BP1 and MDC1 in HR following MMS treatment. Consistent with the G2 phase data and the notion that 53BP1 has no direct role in HR, they observed normal repair (γ-H2AX) in 53BP1 knockdown cells after MMS treatment. Moreover they observed no impact on the formation of Rad51 foci or SCEs after MMS treatment. In contrast however, when they depleted MDC1, they observed persisting γ-H2AX foci, reduced Rad51 foci and reduced SCEs after MMS treatment. These observations indicate that following MDC1 depletion, HR cannot progress due to deficient Rad51 loading. This stalling of repair does not allow completion of HR (SCEs) and leads to a DSB repair defect (γ-H2AX). Taken together with the data in G2, these results strengthen the conclusions that MDC1 has a direct role in HR at the Rad51 filament formation stage while 53BP1 does not have a direct role in HR.

S-phase resection requires CtIP and the PIKK kinases.

The PIKK kinases ATM, ATR and DNA-PK have a prominent role in the DNA damage response to DSBs in all cell cycle phases. However elucidating the individual roles of these kinases can be difficult as there is often functional redundancy amongst them. Such an example is the phosphorylation of histone H2AX, where DNA-PK is able to substitute for ATM and carry out this modification after damage in the absence of ATM (Stiff *et al*, 2004). On the other hand, however, there are certain functions for each of these kinases that cannot be substituted.

In G2-phase HR, ATM phosphorylates CtIP and this phosphorylation is required for CtIP focal accumulation and the initiation of resection (Shibata *et al*, 2011). In the absence of ATM function, neither ATR nor DNA-PK is able to carry out this phosphorylation and a resection defect in observed. Paradoxically however, this phosphorylation appears to be dispensable in S-phase HR as RPA, Rad51 and SCEs form normally in the absence of ATM. One explanation for this is that CtIP is able to bind to ssDNA and initiate resection without modification by ATM. At stalled/collapsed replication forks there is single stranded DNA to which CtIP could bind whereas at Ku bound G2 phase DSBs there is not (Shechter *et al*, 2004; Langerak *et al*, 2011). It is important to note however that although the mechanism of CtIP regulation is S-phase is

unclear, as in G2, resection cannot proceed in the absence of CtIP. Consistently when CtIP is depleted in S-phase RPA signal intensity is reduced compared to control siRNA treated cells.

The extent of modifications to chromatin but also to target proteins that are required to facilitate resection are currently unclear. For example in G2 phase, chromatin relaxation via KAP1 phosphorylation is important for efficient resection and HR. In S-phase, the function of the PIKK kinases also appears to be required for S-phase resection. Although dispensable when inhibited individually, when inhibited in conjunction a reduction in RPA signal intensity is observed. The function of the PIKK kinases in facilitating resection in S-phase is unlikely to occur via CtIP modification but this has not been shown and their roles are currently unknown.

Repair pathway choice of collapsed/stalled replication forks can affect genomic stability.

The cause of the chromosome breakage, radial chromosomes and other cytogenetic abnormalities seen in BRCA and FA mutant cells is not understood. It is suggested however that these abnormalities result from an inability to properly respond to replication stress (D'Andrea & Grompe, 2003). As discussed previously, HR is a repair pathway that is frequently used to respond to replication fork stalling/collapse and is defective in both FA and BRCA mutant cells. One model for the cytogenetic abnormalities seen in these cells is the inappropriate repair of one-ended DSBs arising in S-phase by NHEJ (Helleday *et al*, 2007).

Since 53BP1 has been shown to function in long range re-joining events in V(D)J recombination, telomere fusions and CSR, I reasoned that it may play a role in NHEJ of distant one ended DSBs (Difilippantonio *et al*, 2008; Dimitrova *et al*, 2008; Bothmer *et al*, 2011). To test this, I depleted BRCA1 in Hela cells and monitored foci movement and re-joining in the presence and absence of 53BP1 by LCI.

However, following BRCA1 depletion I observed no increase in 53BP1 foci movement or increased re-joining compared to control cells. Additionally, co-depletion of 53BP1 and BRCA1 had no effect on foci movement and re-joining. These inconclusive results indicate that the experimental setup may need to be modified in order to detect any changes or that there is in fact no role for 53BP1 in the process. One

obvious difference between re-joining in V(D)J and CSR and the situation at one-ended DSBs in S-phase is the distance that separates the DSBs. In V(D)J and CSR there is a defined and measurable distance whereas in S-phase another one ended DSB could be relatively close or far.

Investigating the effect of 53BP1 on the cytogenetic abnormalities of FA and BRCA mutant cells may provide a clearer picture. Strikingly a recent study showed that the increased number of radial chromosomes observed in BRAC1 mutant cells return to normal when 53BP1 is co-depleted (Bunting *et al*, 2010). The authors propose a model whereby 53BP1 functions to block resection and promote NHEJ while BRCA1 functions to overcome the barrier posed by 53BP1 and enable HR. When the two are co-depleted, HR can ensue and the radial chromosomes are no longer observed. However, whether the repair of S-phase damage by NHEJ leads to radial chromosomes, whether these result from re-joining of distant one-ended DSBs and whether this requires 53BP1 function are all questions which need to be addressed.

CHAPTER 4

The role of ubiquitin signalling in Homologous Recombination

4 The role of ubiquitin signalling in Homologous recombination

4.1: Introduction

Following the induction of DSBs, a DDR is initiated that involves the function of multiple factors. The recruitment, interactions, and function(s) of these factors are highly regulated through PTMs that include phosphorylation and ubiquitylation. As discussed in the introductory chapter, the PIKKs ATM, ATR and DNA-PK are key regulatory components of the DDR, with important roles in cell cycle checkpoint initiation as well as in the DSB repair pathways (Lavin, 2008; Stiff *et al*, 2004). These kinases orchestrate the initial, rapid DDR via phosphorylation of downstream targets. Phosphorylation is a signalling PTM that can be carried out rapidly, and the first wave of DDR factor recruitment to DSBs is controlled by phosphorylation (Bekker-Jensen & Mailand, 2010). The recruitment and phosphorylation of these factors can activate their function, which might be required for repair, or might act as a binding platforms for downstream factors via phospho-specific interactions (Mohammad & Yaffe, 2009).

The second wave of DDR factor recruitment to DSBs involves ubiquitin signalling (Bekker-Jensen & Mailand, 2010). This signalling cascade is initiated by the recruitment of RNF8 to DSBs via the interaction of the FHA domain of RNF8 with phosphorylated MDC1 (Mailand *et al*, 2007). Once recruited to DSBs, RNF8 ubiquitylates downstream targets that include histones H2A, H2AX and H2B (Thomson & Guerra-Rebollo, 2010). The E3 ubiquitin ligase activity can lead to the formation of K48 and K63 linked ubiquitin chains, but HERC2 promotes the formation of K63 linked chains by catalysing the interaction between RNF8 and the E2 ligase UBC13 (Bekker-Jensen *et al*, 2010). RNF168 is subsequently recruited to DSBs via the interaction of its UIM with ubiquitylated histones, where it amplifies the ubiquitin response by interacting with UBC13 and carrying out further histone ubiquitylation (Doil *et al*, 2009; Stewart *et al*, 2009). The ubiquitin signalling pathway at DSBs is critical for the recruitment of 53BP1 and BRCA1.

As discussed in the previous chapter, 53BP1 functions in the repair of DSBs in G2 phase by mediating HR repair at HC. However, 53BP1 does not have a direct role in the HR pathway and is dispensable when HC is artificially relaxed via KAP-1 knockdown, or during HR in S-phase where chromatin is decondensed for DNA replication. In addition to 53BP1, ubiquitin signalling events at DSBs also lead to the recruitment of BRCA1 via the interaction of its binding partner RAP80 with ubiquitylated histones (Sobhian *et al*, 2007). Unlike 53BP1, BRCA1 is essential for DSB repair via HR although the details of BRCA1 function in this pathway have remained elusive (Baldeyron *et al*, 2002; Moynahan *et al*, 1999; Stark *et al*, 2004; Zhong *et al*, 2002; Huen *et al*, 2009). The position of BRCA1 in the HR pathway and its interplay with 53BP1 will be the focus of chapter 5 of this thesis. The requirement for RNF8, RNF168 and the ubiquitin signalling pathway in the recruitment of BRCA1, raise the possibility that these E3 enzymes might also function in the HR pathway. Moreover, a recent study demonstrated that RNF8/RNF168 catalysed histone ubiquitylation recruits RNF169 to DSBs, where it supresses 53BP1 recruitment and promotes repair by HR (Poulsen *et al*, 2012). In this chapter I examine whether ubiquitin signalling is required for HR in G2 phase following IR, and in S-phase following CPT treatment. In addition, I examine whether the E3 ubiquitin ligases RNF8 and RNF168 have distinct or overlapping roles in the formation of HR intermediates in G2 phase and also assess their requirement for resection in S-phase. Finally, since BRCA1 is itself an ubiquitin ligase, I test whether the ubiquitin ligase activity of BRCA1 is required for HR in G2 phase.

4.2: Results

4.2.1: RIDDLE patient cells are defective in G2 phase homologous recombination

RIDDLE (radiosensitivity, immunodeficiency, dysmorphic features and learning difficulties), is a recently discovered human disorder with a defective DDR due to mutated RNF168 resulting in defective 53BP1 focal recruitment (Stewart *et al*, 2007; 2009). Previous work from our laboratory investigated the role of RNF168 in G1 phase DSB repair by using cultured RIDDLE syndrome fibroblast cells (Noon *et al*, 2010). Following treatment with IR, ATM activation is normal in these cells however a DSB repair defect is observed that is identical to AT cells. This is because although RIDDLE

cells do not have defective ATM activation, they are unable to tether active ATM at DSB sites and do not form pKAP-1 foci (Noon *et al*, 2010). This results from their inability to form 53BP1 foci, which are important for ATM tethering via the MRN complex (Lee *et al*, 2010). Ultimately the radiosensitivity of RIDDLE patients appears to result from an inability to carry out the chromatin modifications necessary for efficient DSB repair.

As described in the previous chapter, HR in G2 preferentially repairs slowly repaired HC DSBs after IR. The process requires ATM and the mediators H2AX, MDC1 and 53BP1 that function to relax chromatin structure at DSB sites via KAP-1 phosphorylation. Additionally however, ATM is also required for the initiation of resection while MDC1 function is necessary for Rad51 foci formation. The role of 53BP1 in G2 phase HR is limited to chromatin relaxation.

In the choreographed recruitment of the DDR factors to DSB sites, the ubiquitin ligases RNF8 and RNF168 function downstream of MDC1 but upstream of 53BP1 (Huen *et al*, 2007; Mailand *et al*, 2007; Doil *et al*, 2009). Since MDC1 is required for all HR while 53BP1 is not, I reasoned that the ubiquitin ligases might have a direct role in DSB repair by HR and that the HR defect of MDC1 cells results from an inability to recruit the ubiquitin ligases. To test this I utilised cultured RIDDLE patient fibroblast cells and carried out the HR assays described in chapter 3. Additionally by using cells stably complemented with an empty HA vector or an HA vector with human wild type RNF168 (HA-RNF168) I could verify whether any effect observed was due to RNF168 function.

As in G1 phase, G2 phase RIDDLE fibroblasts stably expressing the empty HA vector display a repair defect specifically in slowly repaired DSBs (Noon *et al*, 2010) (Figure 4.1a). As a control, immortalised wild type human fibroblasts were used (1BrhTERT). At two hours post IR the number of γ-H2AX foci remaining in the RIDDLE fibroblasts was indistinguishable to that in wild type cells, but by eight hours a significant repair defect was observed (Figure 4.1a). Importantly, RIDDLE cells stably complemented with HA-RNF168 showed normal repair suggesting that the repair defect in RIDDLE cells results from mutated RNF168. Moreover the fact that RNF168 deficiency only affected slowly repaired DSBs indicated a role in HR.

To test whether RNF168 might indeed have a role in HR, I decided to monitor DNA end resection (RPA foci) and Rad51 filament formation (Rad51 foci) in RIDDLE patient cells (Figure 4.1b-c). Two hours following 3Gy IR, G2 phase RIDDLE cells had

a

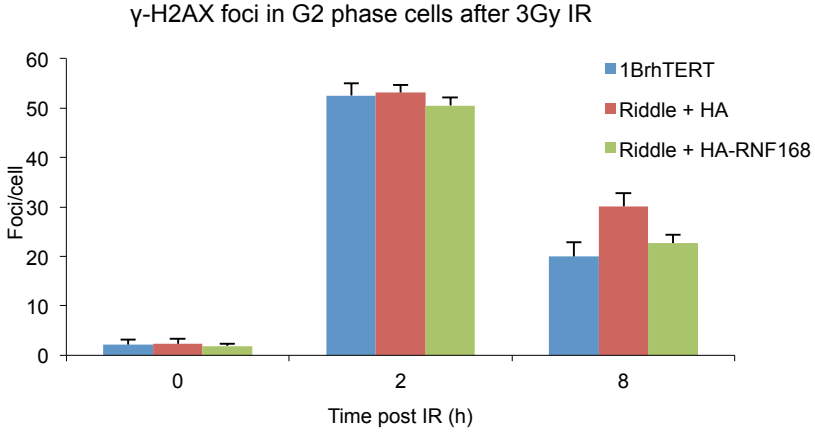

b

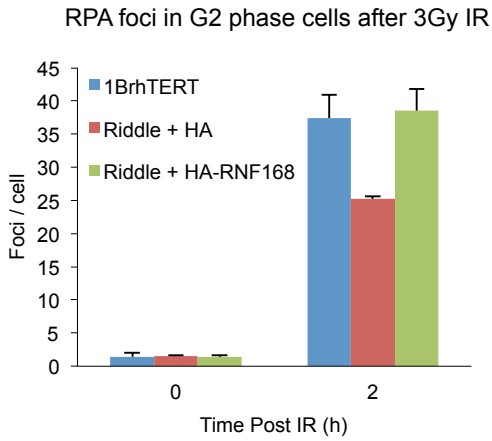

c

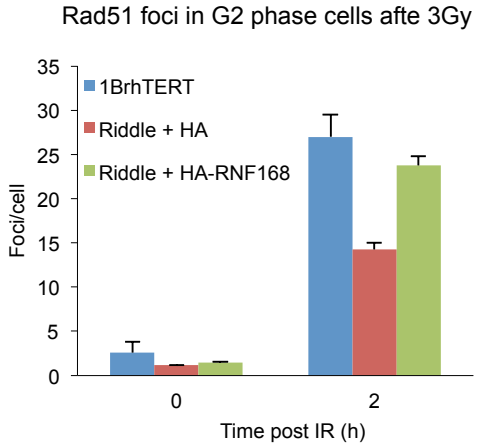

Figure 4.1: RIDDLE patient cells are deficient in G2 phase DSB repair by HR.
a) RIDDLE patient cells stably complemented with either HA or HA-RNF168 were irradiated with 3Gy IR. Prior to irradiation aphidicolin was added to the cells to prevent S-phase cells from entering G2. The cells were then harvested at two and eight hours post IR and immunostained with CENP-F and γ-H2AX antibodies. G2 phase cells were identified by positive CENP-F staining and the cell nuclei were visualized by DAPI. γ-H2AX foci were enumerated specifically in CENP-F positive cells. b) As for a) but here RPA foci were enumerated two hours post 3Gy IR. c) Enumeration of Rad51 foci two hours post 3Gy IR in G2 phase RIDDLE patient cells stably complemented with either HA or HA-RNF168. In a-c, foci were enumerated in 30 cells per time-point and the data represent the mean and standard deviation of three independent experiments.

a

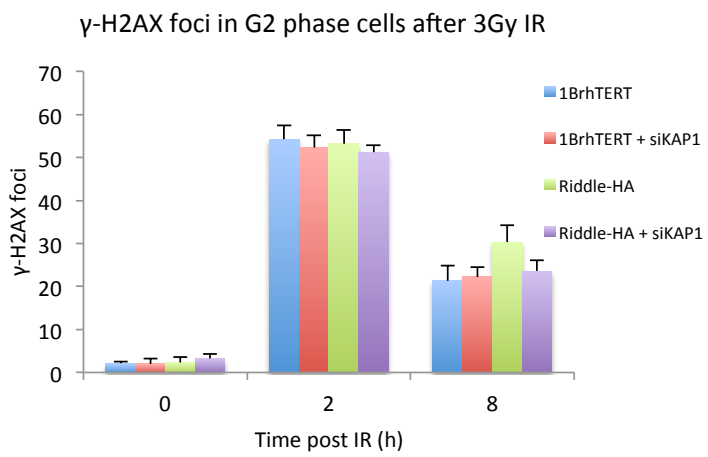

b

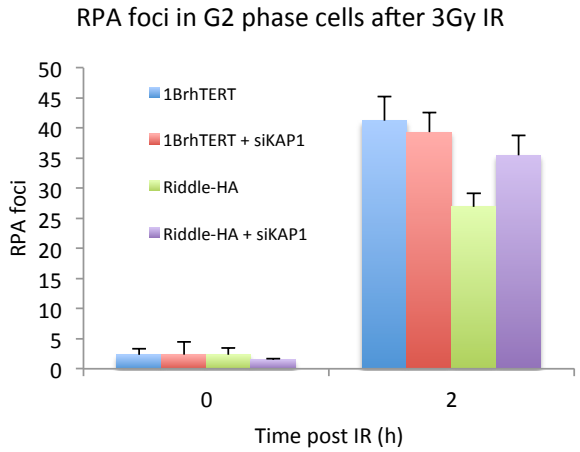

c

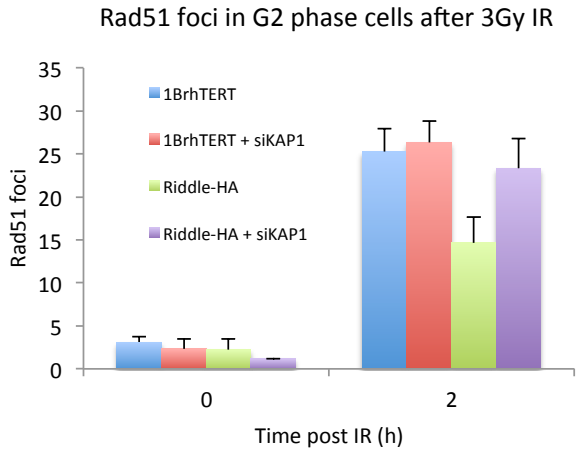

Figure 4.2: KAP-1 depletion alleviates the HR defect of RIDDLE patient cells.
a) RIDDLE patient cells stably complemented with either HA or HA-RNF168 were treated or not with KAP-1 siRNA and irradiated with 3Gy IR. Prior to irradiation aphidicolin was added to the cells to prevent S-phase cells from entering G2. The cells were then harvested at two and eight hours post IR and immunostained with CENP-F and γ-H2AX antibodies. G2 phase cells were identified by positive CENP-F staining and the cell nuclei were visualized by DAPI. γ-H2AX foci were enumerated specifically in CENP-F positive cells. b) As for a) but here RPA foci were enumerated two hours post 3Gy IR. c) Enumeration of Rad51 foci two hours post 3Gy IR in G2 phase RIDDLE patient cells stably complemented with either HA or HA-RNF168. In a-c, foci were enumerated in 30 cells per time-point and the data represent the mean and standard deviation of three independent experiments.

significantly fewer RPA foci than wild type cells although the defect was only partial. However, RIDDLE cells stably expressing HA-RNF168 had normal RPA foci numbers two hours post IR (Figure 4.1b). Similarly, a partial Rad51 foci formation defect was observed in RIDDLE cells but not in RNF168 complemented cells (Figure 4.1c). These results indicate that RNF168 function is required for resection and Rad51 loading and that the DSB repair defect observed in G2 phase RIDDLE cells results from defective HR repair.

In G1, RNF168 mediates DSB repair via HC relaxation however its role is overcome by KAP-1 depletion indicating that it is not a core repair component (Noon *et al*, 2010). To test whether RNF168 is a core HR component or whether it mediates repair via HC relaxation, I repeated the experiments outlined above with or without KAP-1 depletion. As predicted, KAP-1 depletion in 1BrhTERT cells had no effect on the speed or fidelity of DSB repair in G2 cells monitored by γ-H2AX foci (Figure 4.2a). However depletion of KAP-1 in G2 phase RIDDLE patient cells rescued the repair defect and the number of γ-H2AX foci remaining eight hours post IR was indistinguishable to control cells (Figure 4.2a). Similarly, KAP-1 depletion did not impact on control cells but rescued the RPA and Rad51 foci formation defect of RIDDLE patient cells (Figure 4.2b-c). These results indicate that RNF168 does not have a direct role in HR but like 53BP1 promotes the process by mediating the necessary localised chromatin relaxation. Importantly, the requirement of MDC1 for RNF168 recruitment cannot explain its role in HR as it is distinct to that of RNF168 and cannot be overcome by KAP-1 depletion.

4.2.2: RNF8 is required for IR induced HR in G2.

RNF8 is the second E3 ubiquitin ligase that is recruited to DSB sites in an MDC1 dependent manner. Previous work has shown that RNF8 functions together with RNF168 in the formation of the K63 polyubiquitin chains required for 53BP1 IRIF (Huen *et al*, 2007; Mailand *et al*, 2007; Kolas *et al*, 2007). To test whether the HR defect seen in MDC1 depleted cells results from an inability to recruit RNF8, I investigated the role of RNF8 in G2 phase HR.

As in G1, when γ-H2AX foci were monitored in G2 phase cells depleted for RNF8, a DSB repair defect affecting slow repairing DSBs was observed after IR (Figure 3a). Strikingly however and distinct to the situation in G1, when KAP-1 was co-depleted in these cells there was no rescue of the repair defect (Figure 4.3a). This finding indicates that RNF8 function in G2 phase DSB repair is distinct to that of RNF168 and goes beyond mediating the recruitment of 53BP1. To further investigate the involvement of RNF8 in HR repair I monitored RPA and Rad51 foci in G2 phase cells. Surprisingly, a severe RPA and Rad51 foci formation defect was observed in RNF8 knockdown cells and this was unaffected by KAP-1 depletion (Figure 4.3b-c). The magnitude of these defects are greater that those seen in MDC1 knockdown cells and suggest an important role for RNF8 in these processes. As discussed previously, ATM functions in the initiation of resection in G2 via phosphorylation of CtIP which is also required for resection (Shibata *et al*, 2011). As these two components are essential for resection, no repair by HR can take place in their absence. However, under these conditions, the DSB ends are still an end joining substrate and repair can ensue with faster kinetics by NHEJ and no repair defect is observed (Shibata *et al*, 2011). Distinct to the situation in ATM and CtIP depleted cells, RNF8 depleted cells display a persistent DSB repair defect in G2 even after KAP-1 depletion (Figure 4.3a). I interpret this as suggesting that resection is initiated but likely stalls at an early stage, thus not allowing HR progression or returning to repair by NHEJ.

a

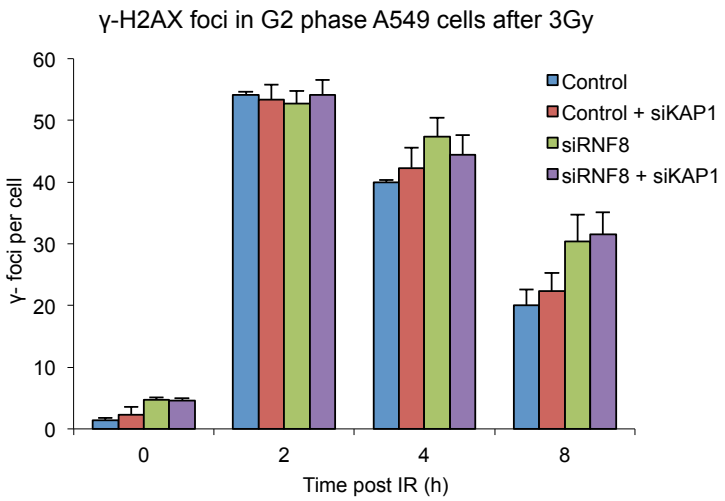

b

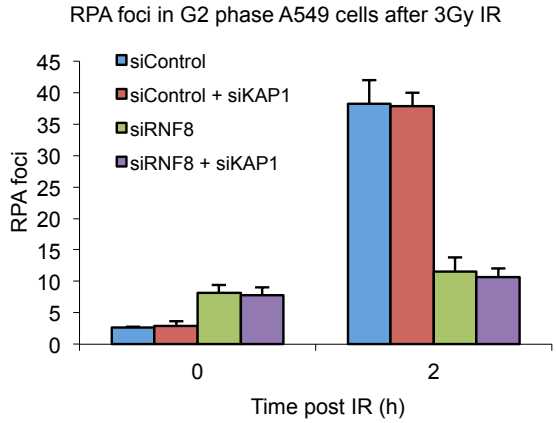

c

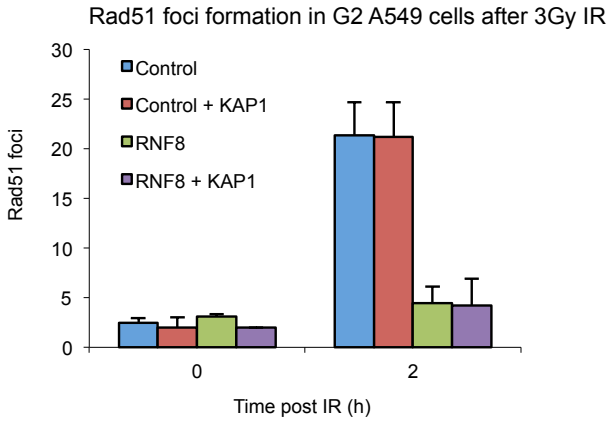

Figure 4.3:RNF8 is required for IR induced HR in G2 irrespective of KAP-1 status.
a) A549 cells were treated with control +/- KAP-1 and RNF8 +/- KAP-1 siRNA and were irradiated with 3Gy IR. Prior to irradiation aphidicolin was added to the cells to prevent S-phase cells from entering G2. The cells were then harvested at two and eight hours post IR and immunostained with CENP-F and γ-H2AX antibodies. G2 phase cells were identified by positive CENP-F staining and the cell nuclei were visualized by DAPI. b) As for a) but here RPA foci were enumerated two hours post 3Gy IR. c) Enumeration of Rad51 foci two hours post 3Gy IR in G2 phase A549 cells treated with control +/- KAP-1 and RNF8 +/- KAP-1 siRNA. In a-c, foci were enumerated in 30 cells per time-point and the data represent the mean and standard deviation of three independent experiments.

4.2.3: RNF8 and RNF168 have distinct roles in G2 phase HR.

The initial experiments carried out in RNF8 and RNF168 depleted/mutant cells indicated distinct roles for these E3 ubiquitin ligases in G2 phase HR. To gain further insight and in an attempt to verify that RNF8 is a core HR component I artificially increased the fraction of IR induced DSBs repaired by HR. As in chapter 3, I achieved this by inhibiting NHEJ through siRNA mediated depletion of Ku80 and DNA-PKcs. In control cells this led to an increase in the number of RPA foci observed four hours post IR treatment (Figure 4.4a). As expected, increased RPA foci numbers were also observed in RNF168 depleted cells although not to the level of control cells (Figure 4.4a). However, when KAP-1 was also depleted, the RPA foci in RNF168 depleted cells returned to control levels (Figure 4.4b). In summary, these results support the notion that RNF168 enables HR by mediating KAP-1 dependent HC relaxation but itself has no direct role in HR. In contrast, RNF8 depleted cells displayed an RPA foci defect that persisted even after KAP-1 depletion (Figure 4.4b). However, Ku80 and DNA-PK depletion did increase RPA foci numbers in RNF8 depleted cells (Figure 4.4a-b). This was surprising given the severe RPA foci defect seen in Figure 3b and suggests that RNF8 might be dispensable for resection in EU but not at HC. Another possibility is that the depletion of Ku80 and DNA-PK creates DSB ends that are favourable to resection even in the absence of RNF8.

Next I monitored Rad51 foci in RNF168 and RNF8 depleted cells following co-depletion of Ku80 and DNA-PKcs (Figure 4.5a-b). RNF168 knockdown cells showed only a partial reduction in Rad51 foci numbers compared to Ku80 + DNA-PKcs knockdown cells (Figure 4.5a). Moreover this defect was completely overcome by KAP-1 depletion again consistent with the notion that RNF168 is dispensable for HR when chromatin structure is relaxed (Figure 4.5b). In stark contrast, RNF8 depleted cells displayed a severe Rad51 foci formation defect even following Ku80 and DNA-PKcs knockdown (Figure 4.5a). KAP-1 depletion had no effect on the phenotype of RNF8 depleted cells and a severe Rad51 foci formation defect persisted (Figure 4.5a). These results indicate that some resection can take place at EU DSBs in the absence of RNF8, however Rad51 loading remains severely compromised and it is unlikely that repair by HR would be completed. It is plausible to suggest that the HR defect seen in MDC1 depleted cells in G2 phase, results from an inability to recruit RNF8.

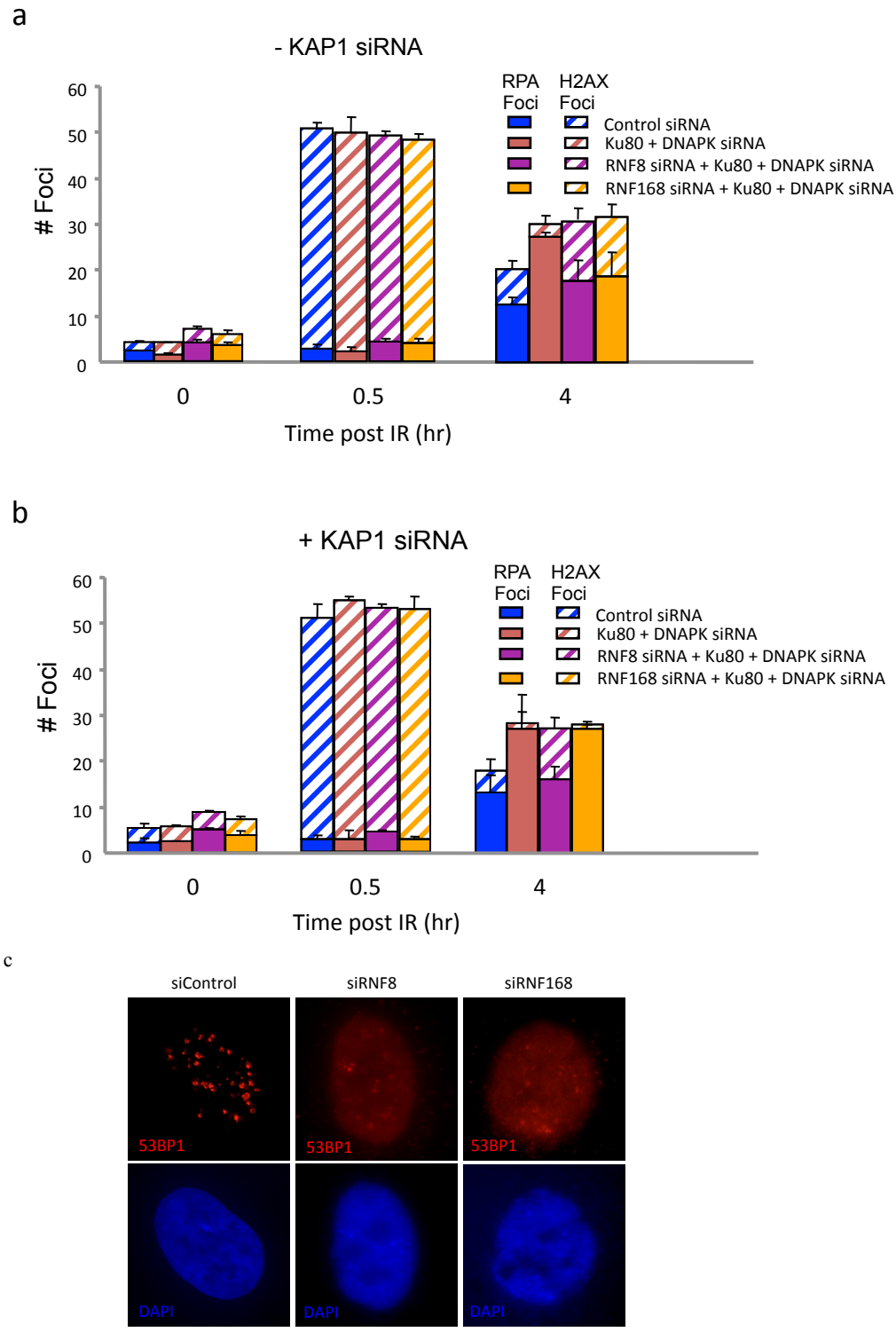

Figure 4.4: RNF168 is dispensable for RPA foci formation in euchromatin while RNF8 is partially required. a) A549 cells were treated with control, RNF8 or RNF168 siRNA and Ku80 and DNA-PKcs were co-depleted where indicated. The cells were treated with 3Gy IR and then harvested at 0.5 and 4 hours post IR. Next one set of samples was immunostained with RPA and CENP-F and the other with γ-H2AX and CENP-F antibodies. G2 phase cells were identified by positive CENP-F staining and the cell nuclei were visualized by DAPI. RPA and γ-H2AX were enumerated and plotted on the same graph with hashed bars indicating γ-H2AX foci and solid bards indicating RPA foci. b) As for a) but KAP-1 was co-depleted in all samples. Foci were enumerated in 30 cells per time-point and the data represent the mean and standard deviation of three independent experiments. c) A549 cells were treated RNF8 and RNF168 siRNA oligonucleotides. Per knockdown, 100 pmol of siRNA duplexes per 2 x 10^5 logarithmically growing cells were used. Cells were then grown for 72 h, irradiated with 3Gy IR and fixed 4h later. 53BP1 immunostaining revealed that RNF8 and RNF168 siRNA treated cells failed to form 53BP1 IRIF indicating efficient knockdown.

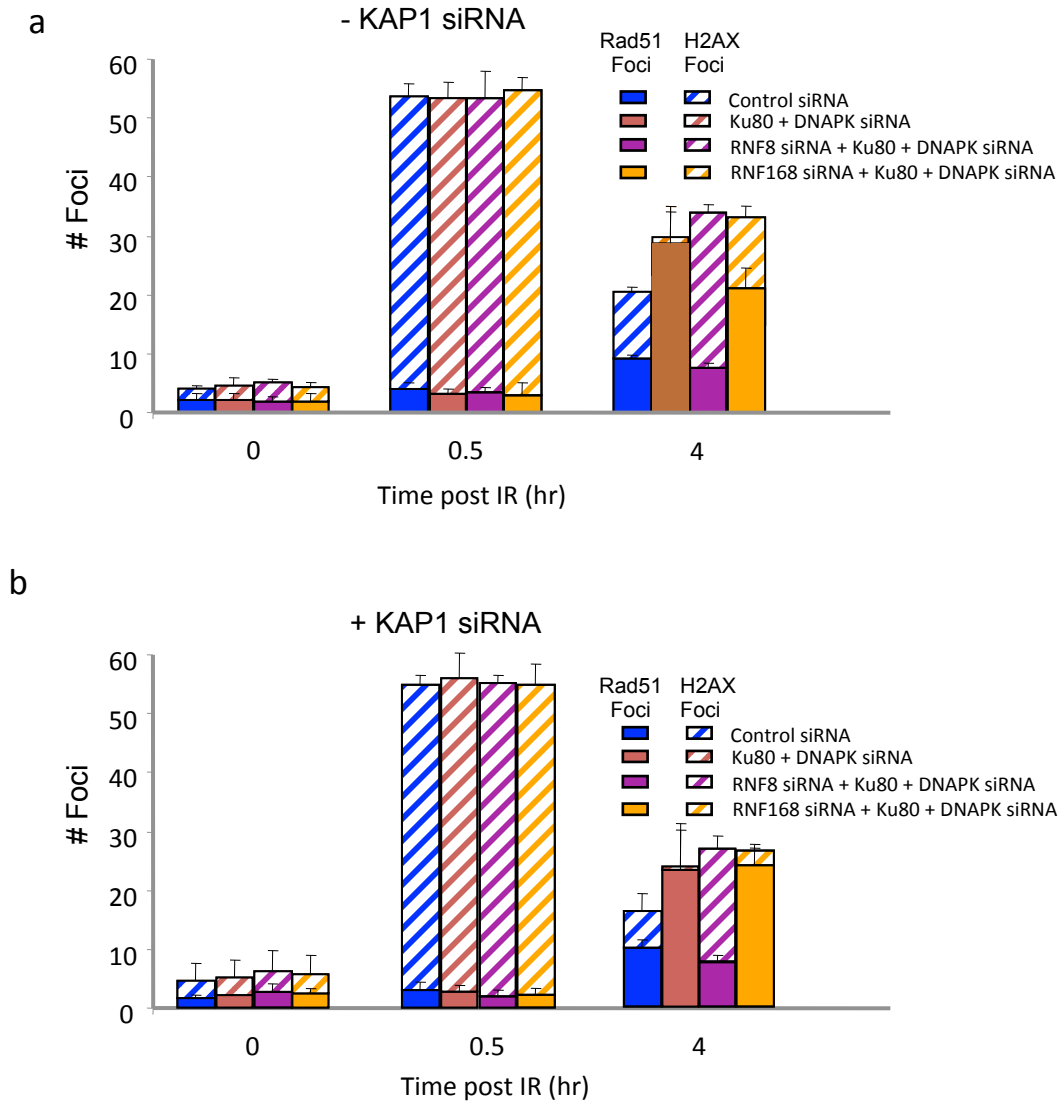

Figure 4.5: RNF168 is dispensable for RPA foci formation in euchromatin but RNF8 is not.
a) A549 cells were treated with control, RNF168 or RNF8 siRNA and Ku80 and DNA-PKcs were co-depleted where indicated. The cells were treated with 3Gy IR and then harvested at 0.5 and 4 hours post IR. Next one set of samples was immunostained with Ra51 and CENP-F and the other with γ-H2AX and CENP-F antibodies. G2 phase cells were identified by positive CENP-F staining and the cell nuclei were visualized by DAPI. Rad51 and γ-H2AX were enumerated and plotted on the same graph with hashed bars indicating γ-H2AX foci and solid bards indicating Rad51 foci. b) As for a) but KAP-1 was co-depleted in all samples. Foci were enumerated in 30 cells per time-point and the data represent the mean and standard deviation of three independent experiments.

4.2.4: Proteasome inhibition affects G2 phase DSB resection.

RNF8 and RNF168 are E3 ubiquitin ligases that are required for the formation of K63 polyubiquitin chains during the DDR (Doil *et al*, 2009). However to date not many targets for this modification have been identified and histone H2A is the best characterised (Panier & Durocher, 2009). Due to the large discrepancy in the requirement for RNF8 and RNF168 in RPA and Rad51 foci formation I decided to investigate the role of ubiquitin modifications in these processes. To achieve this I utilised the potent proteasome inhibitor epoxomicin (Meng *et al*, 1999). The post-translational modification of ubiquitylation is primarily used to target proteins for proteasomal degradation (Ramadan & Meerang, 2011). By treating cells with proteasome inhibitors, ubiquitylated proteins are not degraded leading to deficient ubiquitin turnover and a depletion of the ubiquitin pool.

To monitor the effect of epoxomicin on K63 polyubiquitin chain formation in response to IR I used an FK2 antibody to detect these chains. In control cells, a significant increase in FK2 nuclear signal was observed by thirty minutes after exposure to 3Gy IR (Figure 4.6a). This increase reached maximum levels by four hours after IR treatment and was still evident at eight hours after IR. Cell cycle stage, determined by CENPF staining, had no effect on the intensity of the FK2 signal (Figure 4.6a). In cells treated with 100μM epoxomicin for four hours prior to IR exposure, there was a clear reduction in nuclear FK2 signal compared to control cells (Figure 4.6b). Although there was an increase in cytoplasmic FK2 signal, nuclear signal was inhibited even at eight hours post IR (Figure 4.6b).

Next I monitored RPA foci in cells treated with 100μM epoxomicin for four hours prior to IR exposure. The number of RPA foci in epoxomicin treated cells was significantly reduced at two hours post IR compared to control cells (Figure 4.7a). In control cells, the number of RPA foci reached maximum numbers at two hours post IR and then gradually decreased over the eight-hour time course. In contrast, epoxomicin treated cells failed to efficiently form RPA foci by two hours and then displayed delayed RPA foci clearance during the eight hour time course (Figure 4.7a). These results indicate that epoxomicin is a potent proteasome inhibitor that prevents the formation of FK2 foci following IR exposure. Additionally ubiquitin modifications appear to be important for DNA resection as treatment with epoxomicin leads to decreased RPA foci numbers in response to IR. It is important to note that the

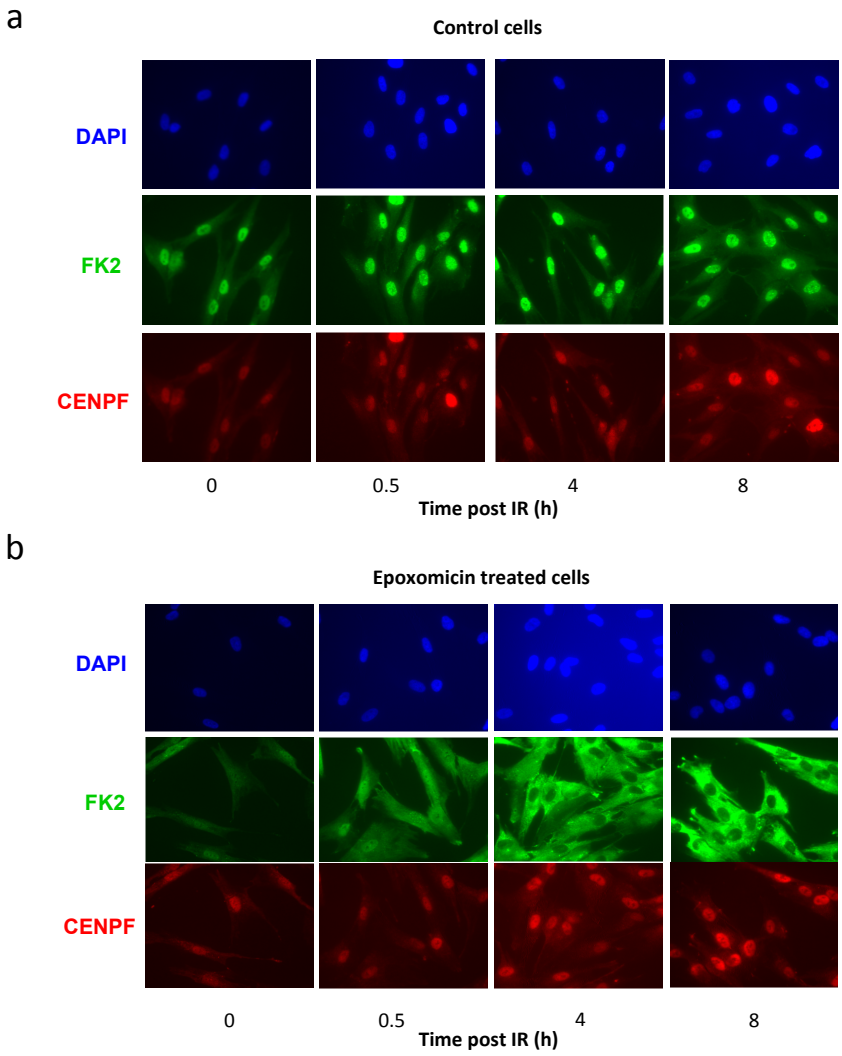

Figure 4.6: Epoxomicin treatment leads to reduced FK2 nuclear staining after IR.
a) A549 cells were treated with 3Gy and harvested 0.5, 4 and 8 hours after IR. The cells were then immunostained with FK2 and CENPF antibodies while DAPI stain was used to visualise cell nuclei. b) A549 cells were treated with 50μM epoxomicin for four hours prior to being irradiated with 3Gy. The cells were then harvested 0.5, 4 and 8 hours after IR and immunostained with FK2 and CENPF antibodies while DAPI stain was used to visualise cell nuclei.

a

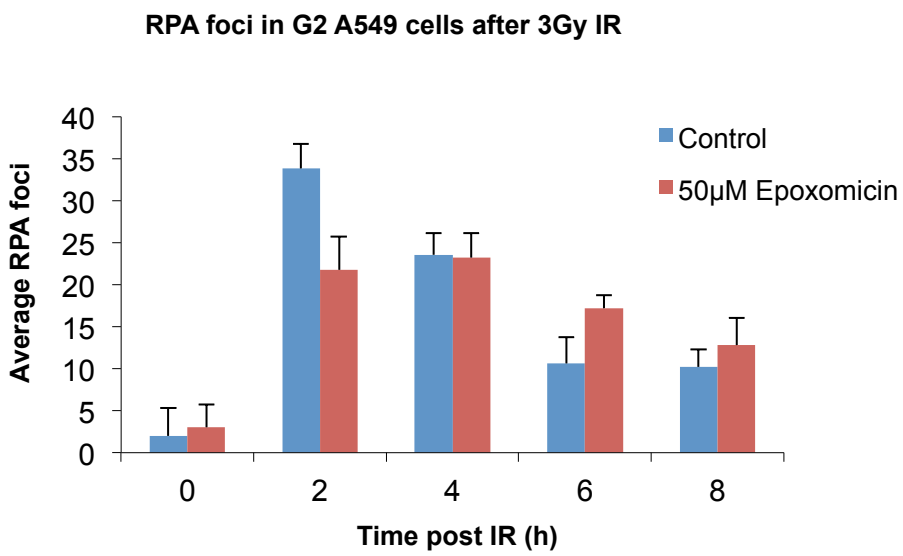

Figure 4.7: Proteasome inhibition effects G2 phase DSB resection.
A549 cells were treated or not with 50μM epoxomicin for four hours prior to being irradiated with 3Gy. The cells were then harvested 2, 4, 6 and 8 hours after IR and immunostained with RPA and CENPF antibodies while DAPI stain was used to visualise cell nuclei. Foci were enumerated in 30 cells per time-point and the data represent the mean and standard deviation of three independent experiments.

reduction in RPA foci number after epoxomicin treatment was similar in magnitude to RNF168 deficient/depleted cells but smaller than that observed in RNF8 depleted cells.

4.2.5: Neither proteasome inhibition nor RNF8 depletion affect S-phase resection.

The magnitude of the resection defect in RNF8 depleted cells and the fact that it could not be overcome by KAP-1 depletion indicated a role in the process that went beyond mediating the process via HC relaxation. In order to further assess the role of RNF8 in DNA resection I decided to use a flow cytometry approach to differentially assess resection in G2 versus S-phase. In S-phase chromatin structure is thought to be in a decondensed configuration and as discussed in chapter 3 resection can ensue in the absence of ATM, MDC1 or 53BP1.

First I assessed the effect of RNF8 depletion and epoxomicin treatment on RPA signal intensity in G2 cells four hours post 15 Gy (Figure 4.8a). Both epoxomicin treatment and RNF8 depletion led to a significant reduction in RPA signal intensity compared to control cells and was comparable to ATMi treated cells (Figure 4.8a). Surprisingly however when RPA signal intensity was monitored in S-phase cells following a one-hour exposure to 4μM camptothecin, no reduction in RPA intensity was observed compared to control cells (Figure 4.8b). This unexpected result indicated that RNF8 function and the formation of polyubiquitin chains are required for DNA resection in G2 phase but not in S-phase.

a

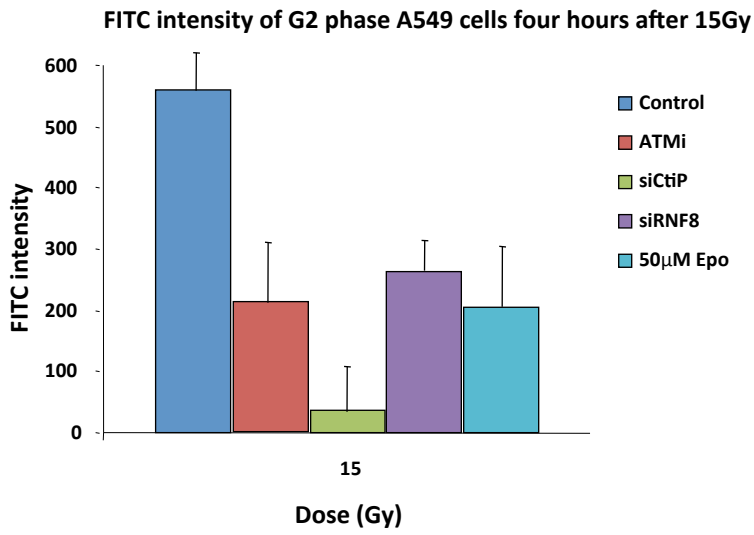

b

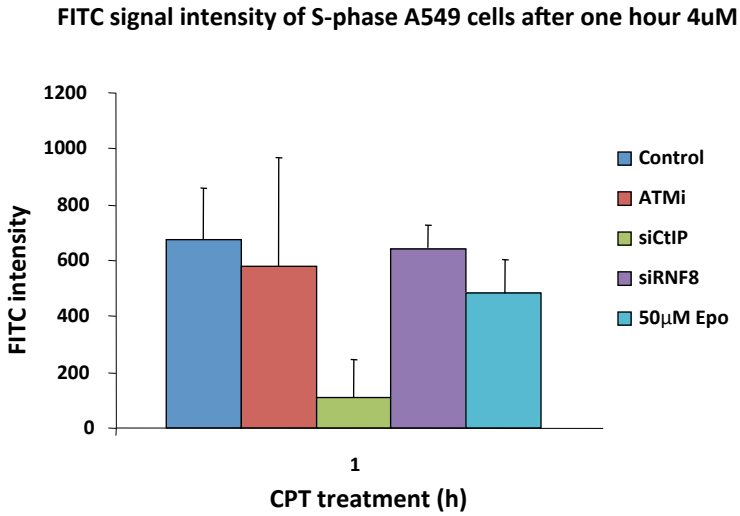

Figure 4.8: RNF8 depletion and proteasome inhibition effect RPA signal intensity after IR in G2 but not in S-phase.
a) Cycling A549 cells were treated with ATMi, epoxomicine, CtIP siRNA or RNF8 siRNA and irradiated with 15Gy IR. Irradiated cells were harvested four hours post IR and immunostained with an RPA antibody and propidium iodide. RPA signal intensity was measured by flow cytometry and the quantification is shown. Propidium iodide staining was used to detect G2 phase cells based on DNA content. b) As for a) but here RPA signal intensity was measured by flow cytometry after one hour exposure to 4μM camptothecin. Propidium iodide staining was used to detect S-phase cells based on DNA content. In a-b 10,000 cells were analysed per condition and the results represent the average of three experiments and the standard deviation among these.

4.2.6: BRCA1 is also required for G2 phase HR.

As discussed in chapter 3, CtIP phosphorylation by ATM is response to DNA damage is a pre-requisite for DNA resection in G2 (Shibata *et al*, 2011). However is S-phase, although CtIP is still required for resection, its function is ATM independent. I postulated that a similar scenario may be true for ubiquitylation i.e. it is required for resection in G2 but dispensable for resection in S-phase. CtIP has previously been reported to be ubiquitylated in response to DNA damage (Yu *et al*, 2006). This ubiquitylation does not target CtIP for degradation but rather promotes the association of CtIP with chromatin. BRCA1, another E3 ubiquitin ligase, is thought to directly ubiquitylate CtIP is response to DNA damage although the recruitment of BRCA1 depends on RNF8 function (Wang & Elledge, 2007). Interestingly, the ubiquitylation of CtIP by BRCA1 requires prior phosphorylation of CtIP and interaction with the BRCT domains of BRCA1. It therefore appears that at least in G2 phase, phosphorylation and ubiquitylation of CtIP cooperate to target CtIP to DSB sites so that resection can take place and repair by HR can ensue.

To test this hypothesis I decided to investigate the role of BRCA1 in the formation of HR intermediates in G2 following IR. BRCA1 has long been known as a vital component of homology directed repair (Moynahan *et al*, 1999; Schlegel *et al*, 2006; Huen *et al*, 2009). However, its role(s) in the process are not fully understood. First, I tested whether depletion of BRCA1 by siRNA affects DSB repair in G2 phase cells (Figure 4.9a). Indeed BRCA1 depletion led to a DSB repair defect that specifically affected the slow component of repair in G2 phase (Figure 4.9a). The number of γ-H2AX foci at two hours post 3Gy was similar to the control cells but by eight hours a significant repair defect was observed (Figure 4.9a). Importantly KAP-1 co-depletion did not rescue the BRCA1 repair defect suggesting that its role in HR is not due to a role in HC relaxation (Figure 4.9a).

Next I monitored RPA foci formation in G2 phase BRCA1 depleted cells following IR treatment. A substantial reduction in RPA foci number two hours post IR was observed and this could not be rescued by KAP-1 co-depletion (Figure 4.9b). This finding indicates that BRCA1 has a direct role in resection that is not dependent on chromatin compaction. Finally, I monitored Rad51 foci in G2 phase BRCA1 depleted cells following IR treatment. I observed a significant reduction in Rad51 foci number two hours post IR that could not be rescued by KAP-1 co-depletion (Figure 4.9c).

a

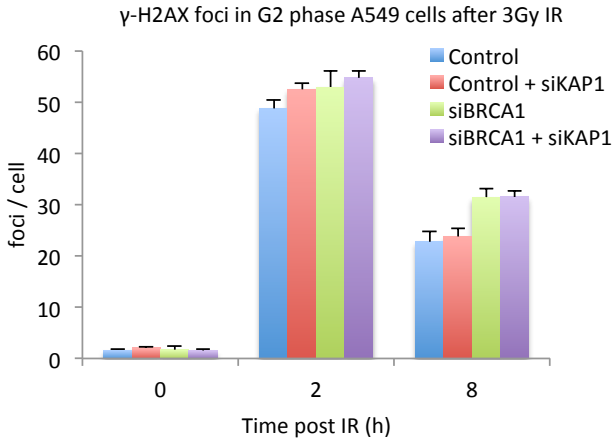

b

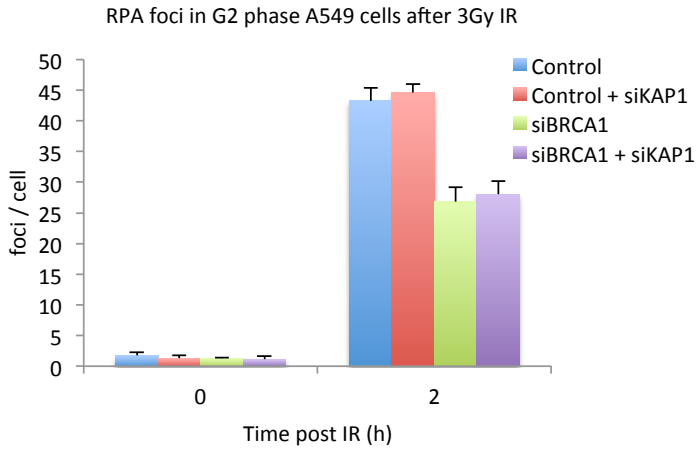

c

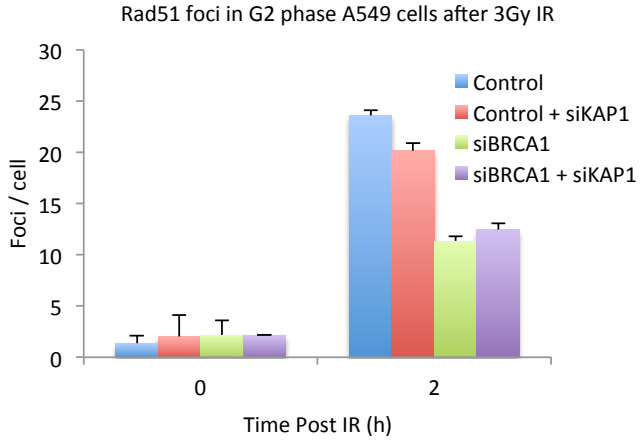

Figure 4.9: BRCA1 is required for IR induced HR in G2 irrespective of KAP-1 status.
a) A549 cells were treated with control +/- KAP-1 and BRCA1 +/- KAP-1 siRNA and were irradiated with 3Gy IR. Prior to irradiation aphidicolin was added to the cells to prevent S-phase cells from entering G2. The cells were then harvested at two and eight hours post IR and immunostained with CENP-F and γ-H2AX antibodies. G2 phase cells were identified by positive CENP-F staining and the cell nuclei were visualized by DAPI. b) As for a) but here RPA foci were enumerated two hours post 3Gy IR. c) Enumeration of Rad51 foci two hours post 3Gy IR in G2 phase A549 cells treated with control +/- KAP-1 and BRCA1 +/- KAP-1 siRNA. In a-c, foci were enumerated in 30 cells per time-point and the data represent the mean and standard deviation of three independent experiments.

These findings indicate a direct role for BRCA1 in G2 phase HR that is important for both RPA and Rad51 foci formation. Significantly this role(s) appear to be independent of chromatin compaction as KAP-1 co-depletion rescued neither the γ-H2AX, RPA nor Rad51 foci formation defects. All the above are consistent with a model whereby BRCA1 enables resection by ubiquitylating CtIP in response to DNA damage and targeting it to DSB sites. To test this model I acquired BRCA1 MEFs with a mutated RING finger domain, responsible for its ubiquitin ligase activity.

4.2.7: The BRCT domain but not the RING domain of BRCA1 is required for G2 phase HR.

When amino acid twenty-six of BRCA1 is mutated from an isoleucine to an alanine (I26A), it results in a ubiquitin ligase dead version of the protein (Sankaran *et al*, 2006). However, this mutation does not affect the ability of BRCA1 to interact with its binding partners or its ability to localise to DNA damage sites. I used MEFs isolated from mice carrying this mutation to test whether BRCA1 ubiquitin ligase activity is required for resection in G2 phase (Figure 4.10a) (Shakya *et al*, 2011). Surprisingly and contrary to the model suggested above, G2 phase BRCA1-I26A MEFs formed RPA foci to the same level as wild-type MEFs. Additionally, Rad51 foci formation in these cells was also normal and indistinguishable to wild-type cells (Figure 4.10b). In contrast, when these experiments were carried out using BRCA1 MEFs in which the BRCT domain is mutated (S1598F), a two-fold reduction in both RPA and Rad51 foci was observed (Figure 4.10 a-b). In summary, these results indicate that BRCA1 has a direct role in resection and Rad51 loading which is independent of chromatin compaction. Furthermore, the role of BRCA1 in HR appears to depend on the BRCT domain of the protein while its RING domain and ubiquitin ligase activity are dispensable.

a

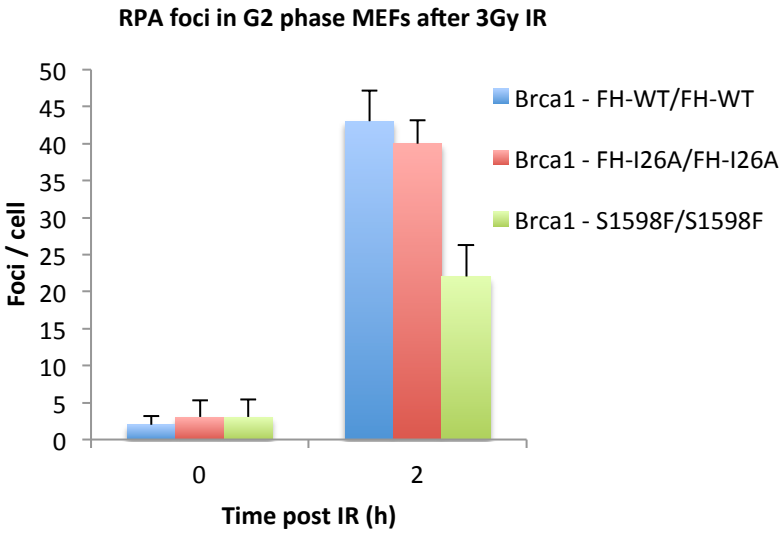

b

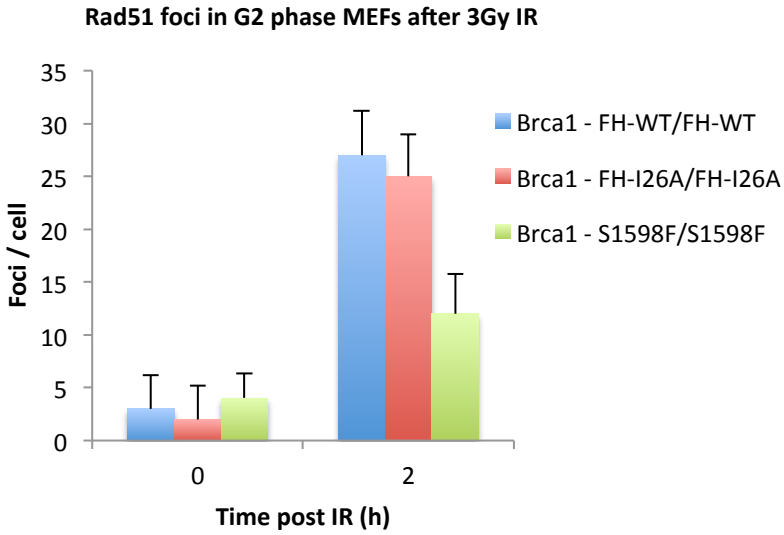

Figure 4.10: The BRCT domain but not the RING domain of BRCA1 is required for G2 phase HR.
a) BRCA1 $^{FH\text{-}WT/FH\text{-}WT}$, BRCA1 $^{FH\text{-}I26A/FH\text{-}I26A}$ and BRCA1 $^{S1598F/S1598F}$ MEF cells were irradiated with 3Gy IR. Prior to irradiation aphidicolin was added to the cells to prevent S-phase cells from entering G2. The cells were then harvested at two and eight hours post IR and immunostained with CENP-F and RPA antibodies. G2 phase cells were identified by positive CENP-F staining and the cell nuclei were visualized by DAPI. RPA foci were enumerated specifically in CENP-F positive cells. b) As for a) but here Rad51 foci were enumerated two hours post 3Gy IR. In a-b), foci were enumerated in 30 cells per time-point and the data represent the mean and standard deviation of three independent experiments.

4.3: Discussion.

RIDDLE patient cells are defective in G2 phase HR.

RIDDLE patient cells have previously been described as radiosensitive and deficient in DNA DSB repair due to mutated RNF168 (Stewart *et al*, 2007; 2009). Work from our laboratory using confluence arrested G1 RIDDLE patient cells, identified a defect in ATM dependent robust and localised KAP-1 phosphorylation, resulting in deficient DSB repair of HC DSBs (Noon *et al*, 2010). RNF168 is an ubiquitin ligase that is able to form the K63 polyubiquitin chains that are required for 53BP1 IRIF. In the absence of RNF168, 53BP1 foci do not form which in turn in a failure of activated ATM to be tethered at DSB sites (Doil *et al*, 2009; Lee *et al*, 2010). Since RNF168 deficient cells are unable to form 53BP1 foci in all cell cycle phases and given the role of 53BP1 in mediating HR (described in chapter 3), I predicted that RNF168 deficient cells would be impaired in DSB repair by HR. Indeed this was the case as RIDDLE patient cells displayed a mild γ-H2AX, RPA and Rad51 foci defect in G2 that was similar to that seen in 53BP1 depleted cells.

To consolidate the notion that RNF168 mediates HC DSB repair by HR in G2 by enabling 53BP1 IRIF, I depleted KAP-1 in RIDDLE cells and monitored the same endpoints. Following KAP-1 depletion, γ-H2AX, RPA and Rad51 foci numbers returned to control levels. These results strongly suggest that RNF168 also enables HR by mediating KAP-1 dependent HC relaxation but does not have a direct role in the process per se.

RNF8 is required for IR induced HR in G2.

As demonstrated in chapter 3, the mediator protein MDC1 has a role during Rad51 loading that is independent of its ability to mediate HR via KAP-1 HC relaxation. Consequently, the requirement for MDC1 in Rad51 loading cannot be bypassed by KAP-1 depletion where as that of 53BP1 can. The ubiquitin ligases RNF8 and RNF168 fall between MDC1 and 53BP1 in the DSB repair signalling cascade and this led me to investigate their role in HR. However, the results from this chapter indicate that the Rad51 phenotype of MDC1 depleted cells cannot be explained by their failure to recruit

RNF168. This is because unlike MDC1 depleted cells, RNF168 depleted cells have a defect in γ-H2AX, RPA and Rad51 foci that can be rescued by KAP-1 depletion.

Next I looked at the role of RNF8 in G2 phase DSB repair by HR. I was surprised to find that the phenotype of RNF8 depleted cells was distinct to that of RNF168 depletion and much greater in magnitude. RNF8 depleted cells had a severe RPA and Rad51 foci formation defect that could not be overcome by KAP-1 depletion. This phenotype was also distinct to that of MDC1 depleted cells in which the RPA foci defect can be overcome by KAP-1 depletion. This finding suggested that RNF8 mediated ubiquitylation may be critical for G2 phase HR while RNF168 mediated poly-ubiquitylation is dispensable when HC is relaxed. Consistent with this possibility, a recent study looking at replication fork recovery by homology directed repair found a direct role for RNF8 in Rad51 recruitment (Sy *et al*, 2011). RNF168 function, however, was not required, further indicating that the roles of these E3 ubiquitin ligases in HR are distinct. The role of RNF8 in resection appears to be less critical than its role in Rad51 loading. Consistent with this, when I inhibited NHEJ and increased the fraction of DSBs repaired by HR, there was a partial increase in RPA foci in RNF8 depleted cells. On the other hand, the number of Rad51 foci that formed in RNF8 depleted cells under the same conditions remained severely impaired.

The function of RNF8 and RNF168 is important for the recruitment of a 'second wave' of factors important for accurate completion of the DNA repair pathways. The mediator 53BP1 and the E3 ubiquitin ligases Rad18 and BRCA1 are all recruited with slower kinetics downstream of RNF8 and RNF168. Interestingly however, Rad18 focal accumulation was recently shown to depend on RNF8 function but not on RNF168 (Sy *et al*, 2011). Rad18 is recruited to DNA damage sites where it directly interacts with Rad51c and is required for Rad51 loading and completion of DSB repair by HR (Huang *et al*, 2009). One explanation therefore is that the severe Rad51 foci formation defect of RNF8 depleted cells results from an inability to recruit Rad18. In the case of RNF168 depleted cells, Rad18 recruitment and Rad51 loading take place normally but an HR defect is observed resulting from an inability to recruit 53BP1. Finally, since MDC1 is required for RNF8 recruitment, the Rad51 foci formation defect seen in MDC1 depleted cells likely results from loss of the RNF8-Rad18-Rad51c pathway. It must be noted however that RNF8 depleted cells also display an RPA foci formation defect that indicates a role for RNF8 in resection.

The role of the non-proteolytic ubiquitin signalling pathway that is regulated by K63 linked ubiquitin chains is well established in the DDR, but recent evidence indicates that the formation of K48 linked ubiquitin chains also function in the DDR (Meerang *et al*, 2011; Mallette *et al*, 2012; Feng & Chen, 2012). The formation of K48 linked ubiquitin chains on a target substrate target it for degradation by the 26S proteasome. The proteasome has previously been implicated in the DDR, but these recent findings have begun to decipher distinct requirements for the ubiquitin ligases involved in the DDR for the formation of proteasomal and non-proteasomal ubiquitin conjugates. Two independent studies have demonstrated that RNF8 but not RNF168 is required for the formation of K48 linked ubiquitin chain IRIF at DSB sites and for accumulation of these ubiquitin conjugates at laser induced DNA damage tracks (Feng & Chen, 2012; Meerang *et al*, 2011). The removal of factors modified by K48 linked ubiquitin chains from DSB sites by the proteasome appears to be important for 53BP1, BRCA1 and Rad51 recruitment (Meerang *et al*, 2011; Mallette & Richard, 2012). Strikingly, the depletion of RNF8 but not RNF168 supressed HR as measured by a GFP-reporter assay, supporting the data from this chapter depicting distinct roles for RNF8 and RNF168 in HR (Ramadan & Meerang, 2011). RNF8 was recently shown to target Ku80 for proteasomal degradation through K48 ubiquitylation (Feng & Chen, 2012). As demonstrated in this chapter and in chapter 3, the removal of the Ku heterodimer from DSB ends is an important step in the initiation of resection. Consistent with this, depletion of Ku leads to increased resection as measured by RPA foci. It is therefore possible that during G2 phase HR, RNF8 function promotes resection through Ku80 K48 ubiquitylation, which triggers its removal and degradation, while RNF168 is dispensable for this process. Moreover, the requirement of RNF8 for resection is at least partially overcome by Ku80 depletion. These findings highlight that ubiquitin signalling plays an important role in the regulation of HR through the timely recruitment of 53BP1, BRCA1 and Rad51. Moreover, RNF8 appears to have an additional role in the regulation of resection by promoting the removal of Ku80 from DNA ends.

Proteasome inhibition effects G2 phase DSB resection.

The ubiquitin ligases RNF8, RNF168, Rad18, BRCA1 and HERC2 have all been implicated in the cellular response to DNA DSBs (Doil *et al*, 2009; Huang *et al*, 2009; Huen *et al*, 2009; Bekker-Jensen *et al*, 2010). However, the mechanism of their function is still to be elucidated. It is likely that there is some functional redundancy amongst these ligases resulting from common ubiquitylation targets. In addition, it is likely that there are distinct functions for each of the above as demonstrated by the distinct and overlapping functions of RNF8 and RNF168 in HR.

I wanted to gain insight into the overall requirement of the ubiquitin pathway in HR and in particular its requirement for the initial resection step, as this seems to be the process that determines which repair pathway is used. If resection is not initiated then repair can ensue by NHEJ, while following the initiation of resection repair must take place by HR as NHEJ can no longer repair the DSB. To investigate the role of the ubiquitin pathway in resection I used the proteasome inhibitor epoxomicin. Epoxomicin inhibits ubiquitylated protein degradation by covalently binding to the catalytic subunits of the proteasome. This inhibition leads to a depletion of the ubiquitin pool resulting in inhibition of further ubiquitylation events (Meng *et al*, 1999). When 1BrhTERT cells were treated with 50μM epoxomicin for four hours prior to exposure to IR, they stained negatively for nuclear FK2 up to eight hours after IR (Figure 6b). The FK2 antibody detects K63 monoubiquitylated proteins and polyubiquitin chains that form following DSB induction (Fujimuro *et al*, 1994) . Consistent to this, control cells treated with IR showed an increase in nuclear FK2 signal intensity (Figure 6a). Since there was no increase in nuclear FK2 signal following IR in cells treated for four hours with 50μM epoxomicin, I reasoned that ubiquitylation events were efficiently inhibited (Figure 6a).

Treatment of cells with the proteasome inhibitor epoxomicin prior to exposure to IR, led to a significant reduction in the formation of RPA foci in G2 phase cells (Figure 7). However the reduction was partial and smaller in magnitude that that seen in RNF8 depleted cells (Figure 3). One possibility is that the smaller effect on resection seen in epoxomicin treated cells compared to RNF8 depleted cells results from inefficient proteasomal inhibition. Another possibility is that the role of RNF8 in G2 phase resection is independent of its ubiquitin ligase activity however this seems unlikely.

Proteasome inhibition and RNF8 depletion do not affect S-phase resection.

The role of RNF8 in G2 phase resection cannot be overcome by KAP-1 depletion (Figure 4.3). This indicates a role for RNF8 in this process that goes beyond chromatin structure and is likely to be required in all HR events. To test this, I investigated the role of RNF8 in replication fork recovery following CPT treatment. As discussed in chapter 3, HR is utilised for replication fork restoration and CtIP function is required for this process. As in G2, CtIP is also required for resection in S-phase and CtIP depletion leads to deficient resection after CPT (Figure 4.8a). However, unlike in G2 where CtIP needs to be phosphorylated by ATM in order to be recruited to DSB sites, in S-phase, CtIP function is ATM independent (Figure 4.8b). Consequently ATMi treated S-phase cells show a normal increase in RPA signal intensity following CPT treatment (Figure 4.8b).

When RNF8 is depleted, G2 phase cells treated with IR show reduced RPA signal intensity compared to control cells indicating deficient resection (Figure 4.8a). Strikingly however, when RNF8 depleted cells are treated with CPT, there is no reduction in the RPA signal intensity in S-phase cells compared to the control (Figure 4.8b). This finding indicates that as for ATM, RNF8 function is required for resection in G2 phase but dispensable for resection in S-phase. The most plausible explanation for this is that ATM and RNF8, function to recruit CtIP to DSB sites in G2 but that this is dispensable in S-phase. This model is consistent with data showing that CtIP is ubiquitylated in response to DNA damage and that this modification is required for its association with chromatin. I propose a model whereby DSB induction in G2 leads to CtIP phosphorylation by ATM that in turn leads to its association with its binding partner BRCA1 via the BRCA1 BRCT domains. BRCA1 then targets CtIP to chromatin where it functions in the resection step of HR. BRCA1 directly ubiquitylates CtIP in response to DNA damage however this event could be dispensable for resection since the ubiquitin ligase activity of BRCA1 is not required for HR (Yu *et al*, 2006; Greenberg, 2011). However, although BRCA1 ubiquitin ligase activity is dispensable for HR, there might be redundancy amongst the E3 ubiquitin ligases and another member of this family could carry out CtIP ubiquitylation when BRCA1 is mutated. RNF8 might also directly ubiquitylate CtIP or may promote CtIP ubiquitylation by recruiting BRCA1. In S-phase however, CtIP is recruited to sites of stalled replication forks independently of ATM and RNF8 function. The most likely explanation for this is

the difference between stalled replication forks and two ended DSBs in G2. Stalled replication forks have some ssDNA which may act as a substrate for direct CtIP binding thus making ATM and RNF8 function redundant.

RNF8 function may be dispensable for resection in S-phase, but experiments in G2 indicated that RNF8 function is critical for Rad51 filament formation (Figure 4.3-4.5). It is highly probable that RNF8 function is required for Rad51 loading also in S-phase and for replication fork recovery by HR. The mechanism whereby RNF8 leads to Rad51 loading likely involves its role in recruiting Rad18 which has been shown to interact with Rad51c and is required for HR. In support of this model, there is evidence showing that RNF8 depletion compromises Rad18 and Rad51 recruitment to damage sites following hydroxyurea treatment. In addition replication fork recovery after hydroxyurea, which has been shown to depend on HR, is severely compromised in RNF8 depleted cells. In summary, the role of RNF8 in S-phase and G2 phase DNA repair goes far beyond its role in G1 repair as a result of its involvement in HR. In contrast RNF168 functions in G2 as in G1 and promotes efficient DSB repair by mediating KAP-1 dependent chromatin relaxation.

The BRCT domain but not the RING domain of BRCA1 is required for G2 phase HR.

BRCA1 is the ubiquitin ligase thought to ubiquitylate CtIP in response to DNA damage. As discussed previously, CtIP function is required for DNA resection during HR in G2 and in S-phase. However experiments in this chapter using the proteasome inhibitor epoxomicin indicate that ubiquitylation events are required for resection in G2 phase but dispensable in S-phase (Figures 4.7-4.8). I decided to investigate whether BRCA1 function is required for resection in G2 phase and whether this depends on its function as a ubiquitin ligase. Consistent with its well-characterised role in HR, BRCA1 depleted cells displayed a defect in RPA and Rad51 foci in G2 after IR resulting in a DSB repair defect (Figure 4.9). This defect could not be overcome by KAP-1 depletion indicating that BRCA1 function in G2 phase HR is not dependent on chromatin status.

Next I used MEFs isolated from mice with mutated or wild type BRCA1 to test the role of BRCA1 as ubiquitin ligase in resection. One set of MEFs carried a mutation that leads to a ubiquitin ligase dead version of the protein (I26A), while the other had a

deletion in the BRCT region (S1598F). Strikingly, the I26A MEFs showed normal RPA and Rad51 foci numbers indicating that BRCA1 function as a ubiquitin ligase is dispensable for G2 phase HR. This is a highly surprising result given its function in CtIP ubiquitylation following DNA damage. One possible explanation is that there is functional redundancy amongst the ubiquitin ligases in G2 and that another ligase can ubiquitylate CtIP in MEFs carrying the I26A mutation. In contrast, the MEFs in which the BRCA1 BRCT domains are deleted showed a significant defect in both RPA and Rad51 foci formation compared to the wild type cells. The BRCT domains of BRCA1 are important for its interaction with its binding partners CtIP, BACH1, Abraxas and RAP80. BRCA1 interacts with phosphorylated Abraxas via its BRCT domain and forms a complex with Abraxas and RAP80. The ubiquitin interacting motif of RAP80 binds to RNF8-RNF168 ubiquitylated sites and targets the complex to DNA damage sites. The BRCT domains of BRCA1 are therefore important for its recruitment to DSB sites although its function when it gets there does not require its ubiquitin ligase activity. Moreover, the overall role of BRCA1 as a tumour suppressor and its function in maintenance of genomic stability was recently shown to depend on the BRCT but not the RING domain of the protein.

The results from this chapter indicate that BRCA1 function is required for efficient resection and Rad51 filament formation during DSB repair by HR in G2. In the next chapter the role of BRCA1 in G2 phase HR will be studied in more detail.

CHAPTER 5

BRCA1 repositions 53BP1 during Homologous Recombination in G2 to enable resection at heterochromatin

5 BRCA1 repositions 53BP1 during Homologous Recombination in G2 to enable resection at heterochromatin

5.1: Introduction.

DSB repair pathway choice is a highly regulated process, the details of which are not fully understood. As discussed in the introductory chapter, the initiation of DNA resection appears to be the key event that determines whether NHEJ or HR repairs a DSB. The removal of Ku from DSB ends is a pre-requisite for the initiation of resection as is the recruitment of Mre11 and CtIP (Fattah *et al*, 2010; Shao *et al*, 2012; Sun *et al*, 2012; Langerak *et al*, 2011; Shibata *et al*, 2011). In addition, the mediator proteins MDC1, 53BP1, RNF8, and BRCA1 have all been demonstrated as having an impact on DSB repair pathway choice (Xie *et al*, 2007; Feng & Chen, 2012; Yu *et al*, 2006; Schlegel *et al*, 2006).

Previous findings and my results from chapter 4 indicate that MDC1 is an important mediator of HR (Xie *et al*, 2007). In addition to its role in recruiting important downstream factors such as RNF8 and BRCA1, MDC1 also appears to have a direct role in Rad51 loading (Zhang *et al*, 2005). Conversely, 53BP1 has been described as a factor that promotes repair by NHEJ (Xie *et al*, 2007). More recently, the interplay between 53BP1 and BRCA1, both factors that are recruited by the MDC1, RNF8, RNF168 pathway, has been shown to determine DSB repair pathway choice by regulating DNA resection (Bouwman *et al*, 2010; Bunting *et al*, 2010). Loss of BRCA1 is embryonic lethal, however MEFs and ES cells harbouring the hypomorphic $BRCA1^{\Delta 11/\Delta 11}$ mutation are viable. This mutation does not impact on the BRCT or RING finger domains of BRCA1 but disrupts its phosphorylation and interaction with Rad50, and leads to impaired HR (Huber *et al*, 2001). Moreover, 98% of $BRCA1^{\Delta 11/\Delta 11}$ embryos die between days 12 and 18 of development indicating that BRCA1 function is critical in these stages of embryonic development (Xu *et al*, 2001). Interestingly, the embryonic lethality of $BRCA1^{\Delta 11/\Delta 11}$ can be rescued by loss of ATM, Chk2 or p53 (Cao *et al*, 2006). However, $BRCA1^{\Delta 11/\Delta 11}$ animals lacking p53 display cancer susceptibility and premature aging, while $BRCA1^{\Delta 11/\Delta 11}$ animals lacking Chk2 or ATM have a greater lifespan but also develop tumours (Cao *et al*, 2006). More recently, the senescence and cell death seen in $BRCA1^{\Delta 11/\Delta 11}$ MEFs was shown to also be rescued by deleting 53BP1 (Cao *et al*, 2009). Moreover, 53BP1 deletion also rescued the embryonic lethality of the

BRCA1$^{\Delta 11/\Delta 11}$ mutation, and the BRCA1$^{\Delta 11/\Delta 11}$ 53BP1$^{-/-}$ mice have a normal lifespan and do not display elevated tumour formation (Cao *et al*, 2009). These findings suggested that 53BP1 function antagonises the tumour suppressor function of BRCA1.

Two independent studies reported that 53BP1 antagonises BRCA1's function in HR by promoting XRCC4/LigIV dependent NHEJ (Bunting *et al*, 2010; Bouwman *et al*, 2010). Bunting et al, demonstrated that increased cytogenetic abnormalities are observed in BRCA1$^{\Delta 11/\Delta 11}$ cells but that these are rescued by deleting 53BP1. Moreover, they demonstrated that 53BP1 deletion leads to increased ATM/CtIP dependent DNA resection and rescues the HR defect of BRCA1$^{\Delta 11/\Delta 11}$ cells (Bunting *et al*, 2010). Consistently, 53BP1 deletion rescued the sensitivity of BRCA1$^{\Delta 11/\Delta 11}$ cells to PARPi and CPT treatment. The authors concluded that in S-phase, where HR is the primary DSB repair pathway, BRCA1 functions to overcome the inhibitory function of 53BP1 on resection. However, when BRCA1 function is compromised, 53BP1 blocks resection and promotes erroneous XRCC4/LigIV dependent NHEJ leading to the cytogenetic abnormalities seen in BRCA1 mutant cells (Bunting *et al*, 2010). Bouwman et al, demonstrated that 53BP1 loss rescues the hypersensitivity of BRCA1 null ES cells to DNA damaging agents such as cisplatin and mitomycin C and partially restores the HR defect of these cells (Bouwman *et al*, 2010). Importantly, the authors also demonstrated that 53BP1 is more frequently lost or aberrantly expressed in BRCA1/2 associated breast cancers and in triple negative sporadic breast cancers compared to sporadic tumours (Bouwman *et al*, 2010). This finding indicates that 53BP1 could serve as a biomarker for the effectiveness of PARPi and platinum drugs for the treatment of BRCA associated cancers (Bouwman *et al*, 2010).

These studies demonstrating that 53BP1 is inhibitory to repair by HR are contradictory to my findings in chapter 3, where 53BP1 was shown to be required for G2 phase HR by mediating HC relaxation via KAP-1 phosphorylation. A possible explanation for this discrepancy is that the studies showing that 53BP1 depletion overcomes the requirement for BRCA1 in HR, monitored HR is S-phase where chromatin is decondensed in preparation for DNA replication. In this chapter I assess whether 53BP1 and BRCA1 co-depletion can restore HR also in the G2 phase of the cell cycle.

Currently little is known about where BRCA1 functions in the HR pathway and how it mechanistically overcomes the inhibitory function of 53BP1 on resection. As discussed earlier, the removal of Ku from DNA ends requires CtIP and Mre11 but also

ubiquitylation by RNF8 which leads to the degradation of Ku by the proteasome (Feng & Chen, 2012). One possibility is that BRCA1 promotes 53BP1 disassociation from chromatin via ubiquitylation. However, this seems unlikely since the ubiquitin ligase activity of BRCA1 is dispensable for HR, while my data from chapter 4 demonstrated that it is also dispensable for resection (Reid *et al*, 2008). Moreover, the tumour suppressor function of BRCA1 also does not appear to dependent on its function as a ubiquitin ligase (Shakya *et al*, 2011). Recently, the E3 ubiquitin ligase activity of BRCA1 was shown to be required for heterochromatin-mediated silencing (Zhu *et al*, 2011). Work from the Jeggo laboratory has previously observed normal DSB repair rates in other human syndromes having disordered heterochromatin (e.g. Rett Syndrome) but such cells display a diminished requirement for ATM for HC-DSB repair (Brunton *et al*, 2011; Goodarzi *et al*, 2008). However, unlike Rett syndrome cells, BRCA1-depleted cells display the anticipated DSB repair defect following ATMi addition in G1 and G2**.** Thus, any change in HC structure caused by BRCA1 depletion does not impact upon the need for ATM for HC-DSB repair.

Interestingly, the tumour suppressor function of BRCA1 is dependent on its BRCT domain, while this domain is also required for resection (chapter 4) and HR (Shakya *et al*, 2011). However, unlike the depletion of CtIP, which leads to complete loss of RPA foci formation, the BRCT domain mutant MEFs used in chapter 4 only displayed a partial RPA foci formation defect. This finding suggests that BRCA1 functions downstream of CtIP and that the disassociation of Ku from DSB ends might precede that of 53BP1.

The tandem BRCT domains on the C-terminus of BRCA1 enable it to bind to phosphorylated proteins with which it forms three distinct complexes, all of which function in the DDR (Huen *et al*, 2009) (Diagram 5.1). BRCA1 exists in all three complexes as a stable heterodimer with BARD1, which regulates the ubiquitin ligase activity of BRCA1 (Wu *et al*, 1996). The BRCA1c complex contains CtIP and the MRN complex, and it is through this complex that BRCA1 is thought to be involved in the regulation of resection. The BRCT domains of BRCA1 interact with

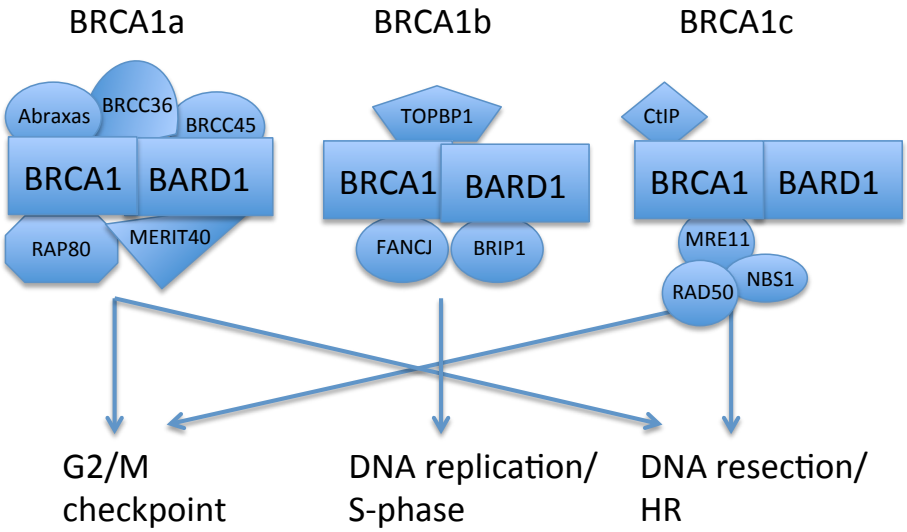

Diagram 5.1: Schematic of the three BRCA1 complexes and the cellular processes in which they function. BRCA1 exists in all three complexes as a stable heterodimer with BARD1, which regulates the ubiquitin ligase activity of BRCA1 (Wu *et al*, 1996). The BRCA1a complex consists of RAP80, Abraxas, BRCC36, BRCC45 and MERIT40. This complex is important for the localisation of BRCA1 to DNA damage sites via the binding of RAP80 to ubiquitylated histones flanking DSBs (Sobhian *et al*, 2007). The BRCA1a complex is also involved in the G2/M checkpoint response. The BRCA1b complex consists of BACH1 and TOPBP1 and the formation of the complex involves the interaction between phosphorylated BACH1 and the BRCT domains of BRCA1 (Huen *et al*, 2009). This complex has been implicated in DNA replication but also in the intra-S-phase and G2/M checkpoint responses (Huen *et al*, 2009). The BRCA1c complex contains CtIP and the MRN complex, and it is through this complex that BRCA1 is thought to be involved in the regulation of resection. The BRCT domains of BRCA1 interact with phosphorylated CtIP, a modification that is carried out by both ATM and CDK in response to DNA damage (Huertas & Jackson, 2009; Shibata *et al*, 2011). This interaction promotes CtIP dependent resection specifically in the S and G2 phases of the cell cycle

phosphorylated CtIP, a modification that is carried out by both ATM and CDK in response to DNA damage (Huertas & Jackson, 2009; Shibata *et al*, 2011). This interaction promotes CtIP dependent resection specifically in the S and G2 phases of the cell cycle, but how BRCA1 modulates this process is not clear although the ubiquitin ligase function of BRCA1appears to be dispensable (Yun & Hiom, 2009).

The BRCA1b complex consists of BACH1 and TOPBP1 and the formation of the complex involves the interaction between phosphorylated BACH1 and the BRCT domains of BRCA1 (Huen *et al*, 2009). This complex has been implicated in DNA replication but also in the intra-S-phase and G2/M checkpoint responses (Huen *et al*, 2009). Finally, the BRCA1a complex consists of RAP80, Abraxas, BRCC36, BRCC45 and MERIT40. This complex is important for the localisation of BRCA1 to DNA damage sites via the binding of RAP80 to ubiquitylated histones flanking DSBs (Sobhian *et al*, 2007). The BRCA1a complex is involved in the G2/M checkpoint response where BRCA1 is thought to impact on the checkpoint proficiency by regulating CHK1 kinase phosphorylation and activation (Yarden *et al*, 2002). More recently, the BRCA1a complex has also been described as a negative regulator of resection (Coleman & Greenberg, 2011; Hu *et al*, 2011). It is thought that by binding to ubiquitylated histones via its UIM domain, RAP80 forms an inhibitory barrier to resection and prevents excessive nucleolyitc processing. Consistent with this, depletion of RAP80 or any of the other BRCA1a complex components, leads to increased resection (Hu *et al*, 2011).

It is becoming evident that DNA end resection is regulated by the simultaneous action of factors that either promote or inhibit the process. There appear to be at least three negative regulators that need to be overcome for the process to progress. Firstly, Ku needs to be removed from DNA ends so nucleases can access the DSB and so that resection can be initiated. Secondly, the inhibitory barrier posed to the process by 53BP1 needs to be overcome, and thirdly, the elongation step of resection requires the disassociation of RAP80 from ubiquitylated histones. In this chapter I address where BRCA1 functions in the series of events that regulate resection, with particular emphasis on its interplay with CtIP and MRE11. Moreover, I assess how BRCA1 together with the DUB POH-1 overcome the barriers posed by 53BP1 and RAP80 respectively.

5.2: Results

5.2.1: BRCA1 is required for HR at HC-DSBs in G2 but is dispensable for HC relaxation.

The function of BRCA1 in DSB repair is distinct to that of ATM and the mediator proteins (H2AX, 53BP1, MDC1, RNF8, RNF168) as it is specifically required for repair in G2 but not in G1 (Figure 5.1). When I monitored γ-H2AX foci loss post IR in G1 and G2, a characteristic repair defect specifically affected the slow repair component of G2 phase cells was observed (Figure 5.1). Furthermore the repair defect seen in G2 phase cells could not be alleviated by KAP-1 knockdown. BRCA1 depletion does not affect pKAP-1 foci formation in G2, in contrast to the defect observed following 53BP1 siRNA (Figure 5.2). Taken together these results support the notion that BRCA1 functions specifically in HR in a way that is not affected by KAP-1 status.

5.2.2: BRCA1 functions in HR downstream of CtIP/MRE11.

Previous studies and my data from chapter 4 have shown that CtIP is required for resection in both the S and G2 cell cycle phases. Consist with this, CtIP depletion leads to a complete loss of RPA foci following IR exposure in G2 phase (Figure 5.5a). Importantly however, CtIP depletion does not lead to a DSB repair defect in G2, as when resection is not initiated repair can take place by NHEJ. This notion is consolidated by previous work from our laboratory where CtIP and XLF co-depletion led to an additive defect since under these conditions both HR and NHEJ are compromised (Shibata *et al*, 2011). In contrast, BRCA1 loss leads to a DSB repair defect in G2 indicating that NHEJ cannot repair DSBs in G2 that have reached the HR stage where BRCA1 function is needed (Figure 5.1). This circumstantial evidence indicates that BRCA1 functions in an HR step that is downstream of CtIP and post commitment to repair by HR. To verify in which order BRCA1 and CtIP function during G2 phase HR, I examined whether CtIP depletion could rescue the repair defect of BRCA1 knockdown cells. As observed previously, CtIP depletion did not lead to a DSB repair defect in G2 cells but rather led to faster repair kinetics indicating that repair was taking place by NHEJ (Figure 5.3a). On the other hand, BRCA1 depletion led to a repair defect that affected the slow component of repair (Figure 5.3a). Strikingly, cells

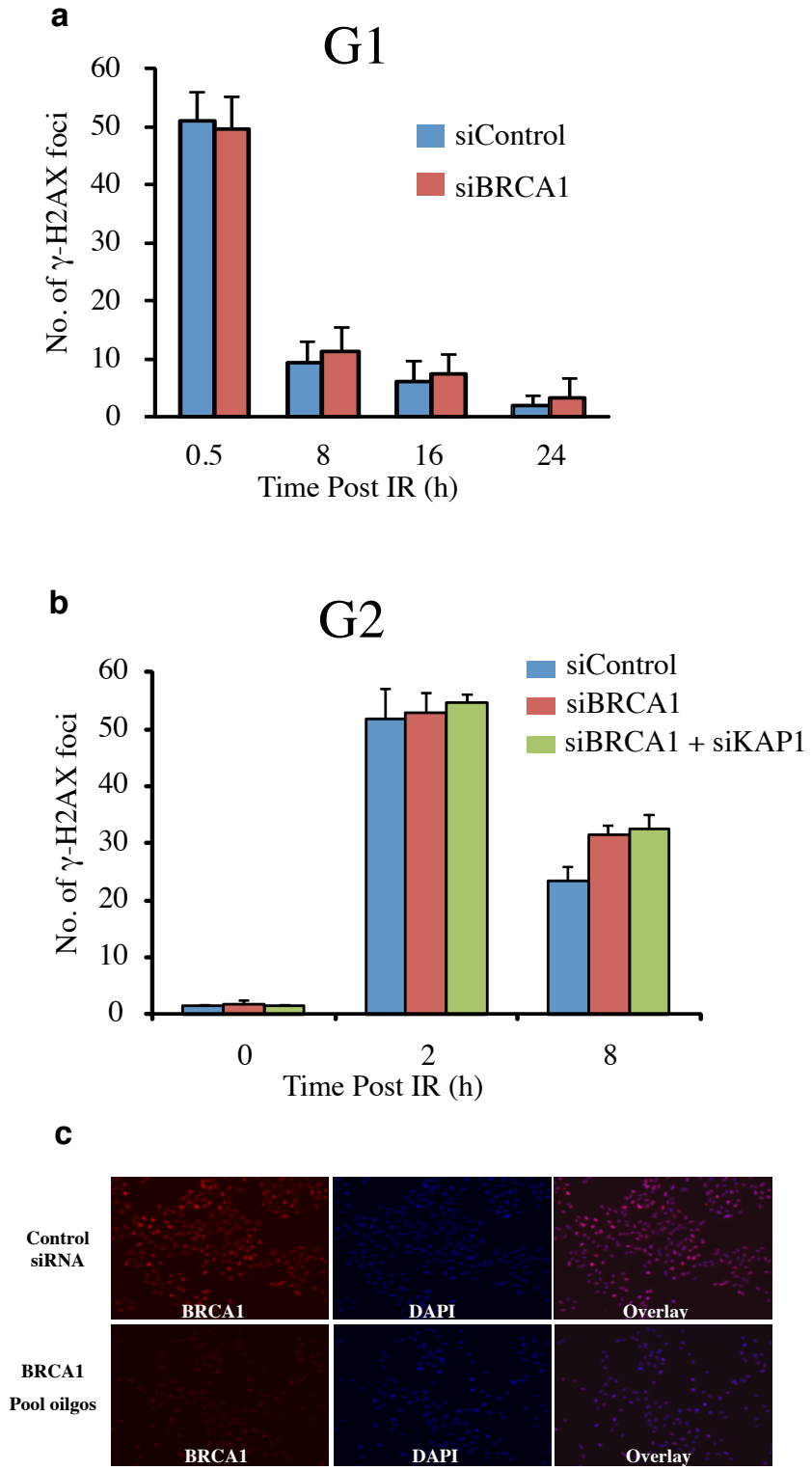

Figure 5.1. BRCA1 is specifically required for DSB repair in G2 and its role cannot be overcome by KAP-1 knockdown.

a-b) A549 cells were exposed to 3 Gy IR in G1 and G2 with or without BRCA1 and KAP-1 siRNA. The cells were then harvested at two and eight hours post IR and immunostained with CENP-F and γ-H2AX antibodies. G2 phase cells were identified by positive CENP-F staining and the cell nuclei were visualized by DAPI. γ-H2AX foci were enumerated in 30 cells per time-point and the data represent the mean and standard deviation of three independent experiments.

c) Knockdown efficiency in A549 cells following treatment with a pool of BRCA1 siRNA oligonucleotides. Per knockdown, 100 pmol of siRNA duplexes per 2 x 10^5 logarithmically growing cells were used. Cells were then grown for 72 h prior to fixation and immunostaining with the indicated antibodies.

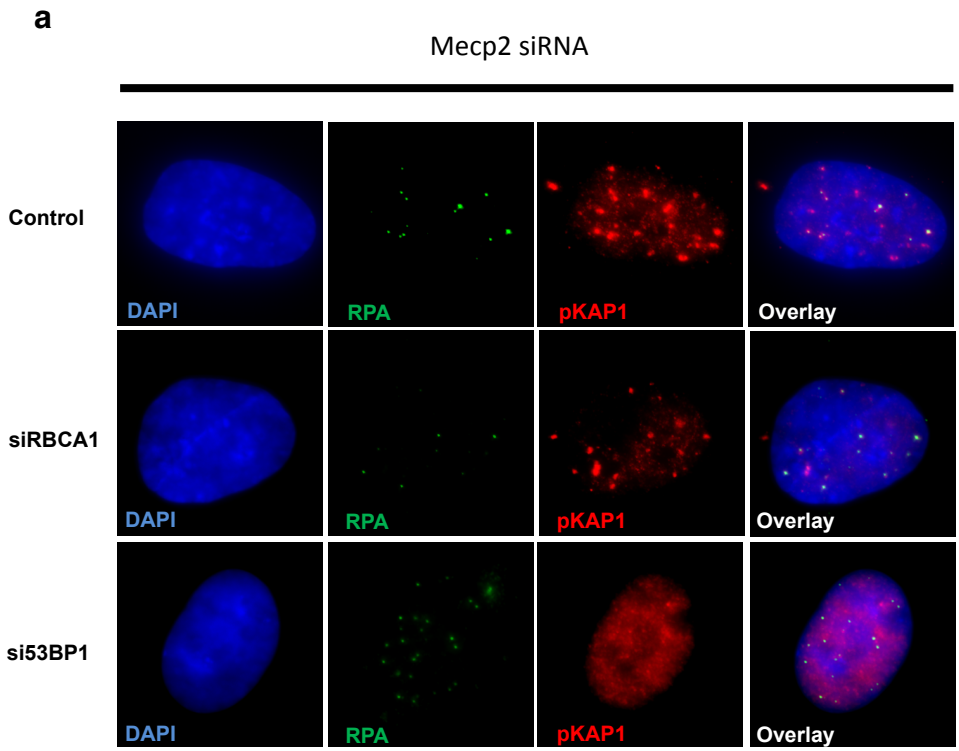

Figure 5 2: pKAP1 IRIF analysis in G2 phase 1BRhTERT cells after 53BP1 or BRCA1 knockdown. 1BRhTERT cells were treated with the indicated siRNA for 72h. Next they were irradiated with 3 Gy IR, harvested 8 h post exposure and immunostained with the indicated antibodies. Aphidicolin was added to prevent S phase cells progressing into G2 during analysis. Analysis was undertaken in G2 phase cells. S phase cells were excluded from analysis by their pan-nuclear RPA staining that arises as a consequence of aphidicolin addition. 53BP1 knockdown cells are unable to form pKAP-1 IRIF leading to an HR defect in G2 due to defective HC relaxation. BRCA1 knockdown cells form normal pKAP-1 IRIF indicating that their HR defect in G2 is not due to defective HC relaxation.

in which CtIP and BRCA1 were co-depleted showed normal repair (Figure 5.3a). This finding indicates that CtIP functions upstream of BRCA1 to initiate resection, committing to repair by HR. BRCA1 seems to function downstream of CtIP and is required for the efficient completion of resection. Importantly, if resection is not initiated then BRCA1 function is dispensable since repair ensues by NHEJ.

To substantiate this model further, I tested whether CtIP or BRCA1 knockdown could overcome the DSB repair defect seen in BRCA2 depleted cells. BRCA2 functions downstream of resection and is required for Rad51 loading. BRCA2 knockdown cells show normal resection but fail to load Rad51. I expected that if BRCA1 functions downstream of the CtIP-dependent initiation of resection then BRCA1 depletion would not rescue the repair defect of BRCA2 knockdown cells. On the other hand CtIP depletion should rescue the repair defect of BRCA2 knockdown cells since under these conditions repair would ensue by NHEJ and therefore be independent of BRCA2. As previously reported, when I depleted BRCA2 and monitored γ-H2AX foci loss after IR in G2 cells I observed a repair defect at late times post IR (Figure 3c) (Beucher *et al*, 2009). Importantly and consistent with the proposed model, CtIP depletion rescued the repair defect caused by BRCA2 siRNA, while joint BRCA1 and BRCA2 knockdown resulted in defective DSB repair (Figure 5.3c).

The regulation of resection and DSB repair pathway choice are highly complex processes involving many factors including MRE11.MRE11 is a nuclease that is required for the initiation of resection (Mimitou & Symington, 2011). However, MRE11 is part of the MRN complex that has previously been shown to be required for efficient HC-DSB repair via KAP-1 phosphorylation. As discussed previously, Rad50 bridges the interaction between 53BP1 and pATM resulting in pATM retention at DSB sites and the robust localised KAP-1 phosphorylation needed for HC-DSB repair (Lee *et al*, 2010). When I depleted MRE11 by siRNA, I observed a repair defect in the slow repair component of G2 phase cells that was similar in magnitude to that seen in BRCA1 or BRCA2 depleted cells (Figure 5.4). However when MRE11 and KAP-1 were co-depleted normal repair ensues (Figure 5.4). This finding indicates that either MRE11 is dispensable for HR when chromatin structure is relaxed, or that it also functions in the initiation of resection and repair can ensue by NHEJ in MRE11- KAP-1 co-depleted cells. To test which of the above is correct I carried out triple knockdown of BRCA1, MRE11 and KAP-1 (Figure 5.4). Under these conditions the repair defect

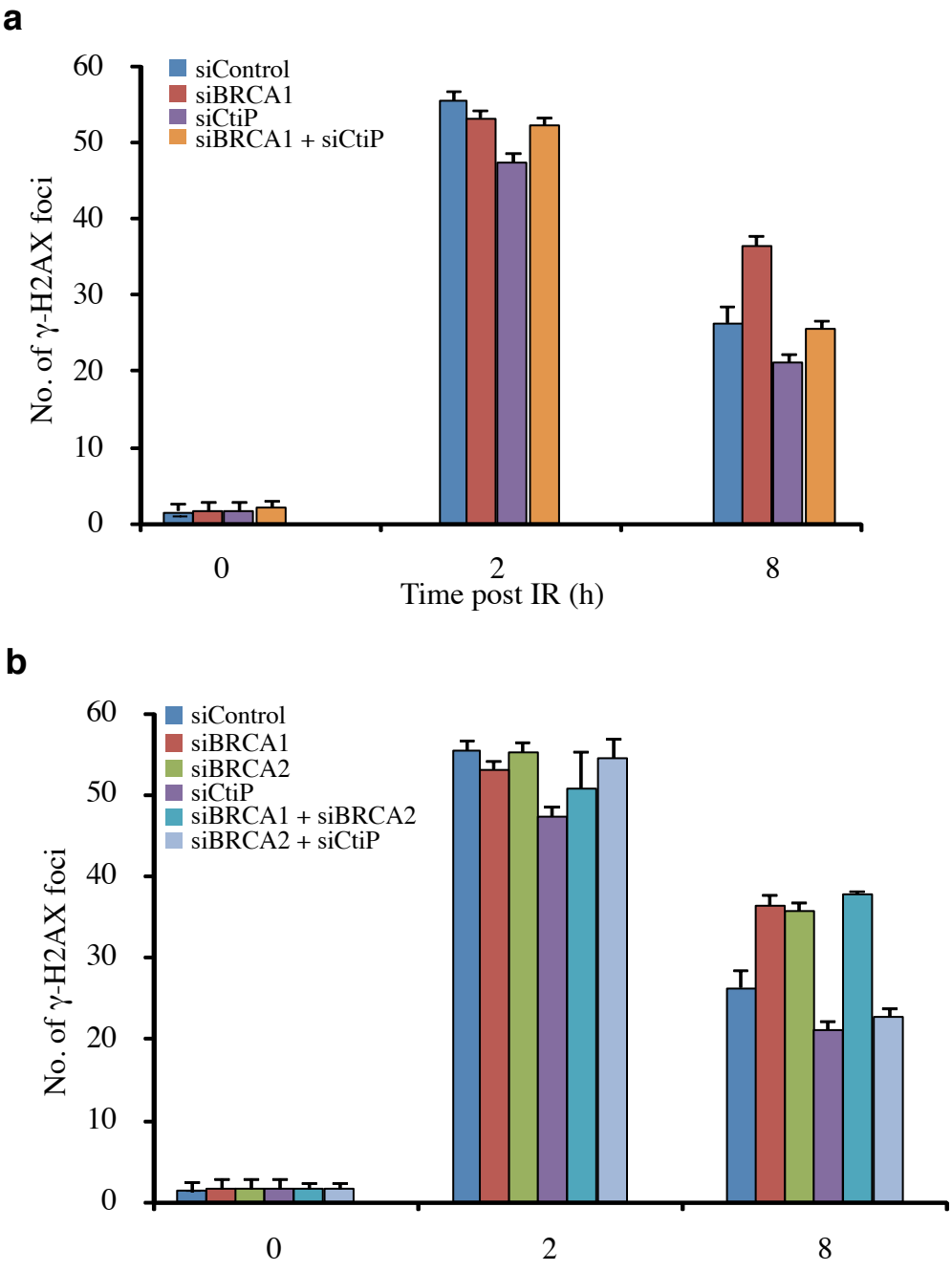

Figure 5.3. CtIP depletion rescues the G2 phase repair defect of BRCA1 and BRCA2 deficient cells by channelling DSBs into NHEJ.
a-b) A549 cells were treated with the indicated siRNA and then exposed to 3 Gy IR in G2. The cells were then harvested at two and eight hours post IR and immunostained with CENP-F and γ-H2AX antibodies. γ-H2AX foci were enumerated in 30 cells per time-point and the data represent the mean and standard deviation of three independent experiments.

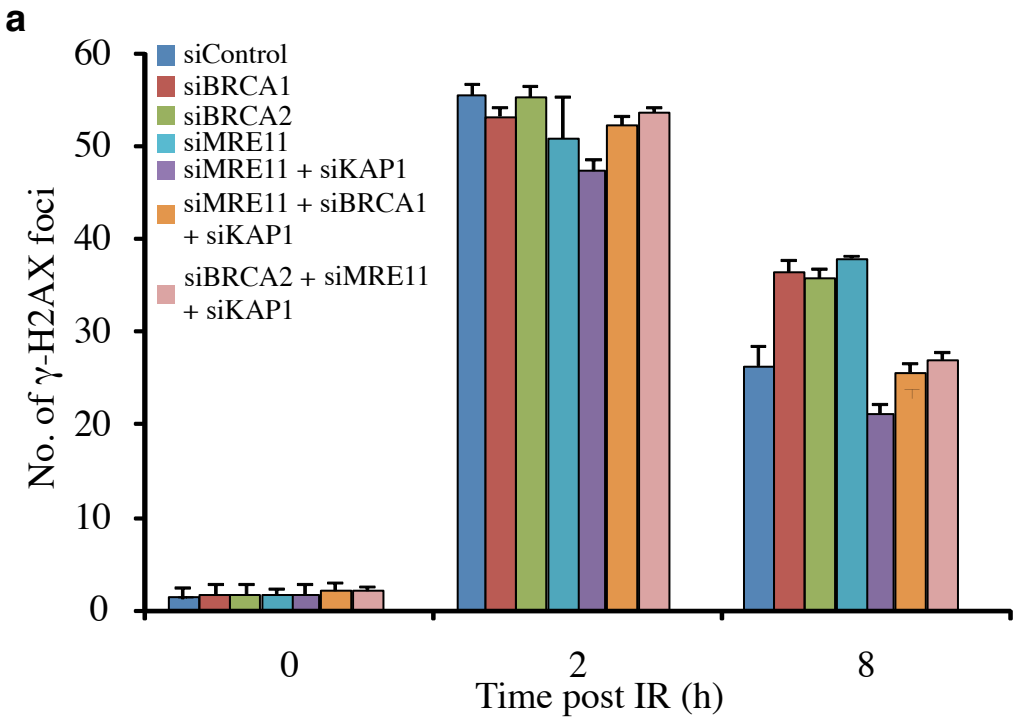

Figure 5.4. MRE11 + KAP-1 depletion also rescues the G2 phase repair defect of BRCA1 and BRCA2 deficient cells by channelling DSBs into NHEJ.
a) A549 cells were treated with the indicated siRNA and then exposed to 3 Gy IR in G2. The cells were then harvested at two and eight hours post IR and immunostained with CENP-F and γ-H2AX antibodies. γ-H2AX foci were enumerated in 30 cells per time-point and the data represent the mean and standard deviation of three independent experiments.

of BRCA1 depleted cells was rescued and γ-H2AX foci returned to control levels. These findings strongly suggest that MRE11, like CtIP, functions upstream of BRCA1 and is required for the initiation of resection. MRE11 and CtIP function commits to repair by HR whereas BRCA1 has a downstream role promoting resection post the initiation step.

To gain further insight into the position at which BRCA1 functions in the different steps of HR, I monitored RPA and RAD51 foci formation. As predicted, G2 phase cells in which BRCA1 was depleted showed a significant reduction in RPA foci number two hours following IR treatment compared to control cells (Figure 5.5b). Importantly, BRCA1 depleted cells were also severely compromised in Rad51 foci formation indicating that inefficient or incomplete resection in the absence of BRCA1 impacts on downstream Rad51 loading (Figure 5.5b). In contrast to BRCA1 and consistent with previous findings, BRCA2 depleted cells showed normal RPA foci formation after IR treatment but showed a complete loss of Rad51 foci (Figure 5.5a-b). When BRCA1 and BRCA2 where co-depleted, a two-fold reduction in RPA foci number and a complete loss of Rad51 foci was observed (Figure 5.5a-b). These findings strongly indicate that BRCA1 functions upstream of BRCA2 in resection while BRCA2 functions during Rad51 loading.

Next, I tested the impact of CtIP depletion on these two endpoints. As expected, CtIP depletion completely abrogated the formation of both RPA and Rad51 foci formation indicating that resection was not initiated and HR did not take place (Figure 5.5a-b). In addition, CtIP + BRCA1 and CtIP + BRCA2 again led to a complete loss of RPA and Rad51 foci indicating that CtIP functions upstream of these HR factors (Figure 5.5a-b). Under these conditions BRCA1 and BRCA2 are dispensable for repair, since DSBs are repaired by NHEJ.

Finally, I tested the impact of MRE11 depletion on RPA and Rad51 foci formation in G2 phase cells. Depletion of MRE11 leads to a reduction in RPA foci consistent with the notion that its exonuclease activity plays a role in resection (Figure 5.5a). Surprisingly however, the magnitude of the resection defect was smaller than that of CtIP depleted cells. One interpretation is that MRE11 functions downstream of CtIP in resection, but inefficient siRNA is also possible. The MRE11 resection defect was not rescued by KAP-1 knockdown unlike the situation in 53BP1 and MDC1 knockdown cells (Figure 5.5a). This suggests that MRE11 has a direct role in resection and does not facilitate the process via KAP-1 mediated HC relaxation.

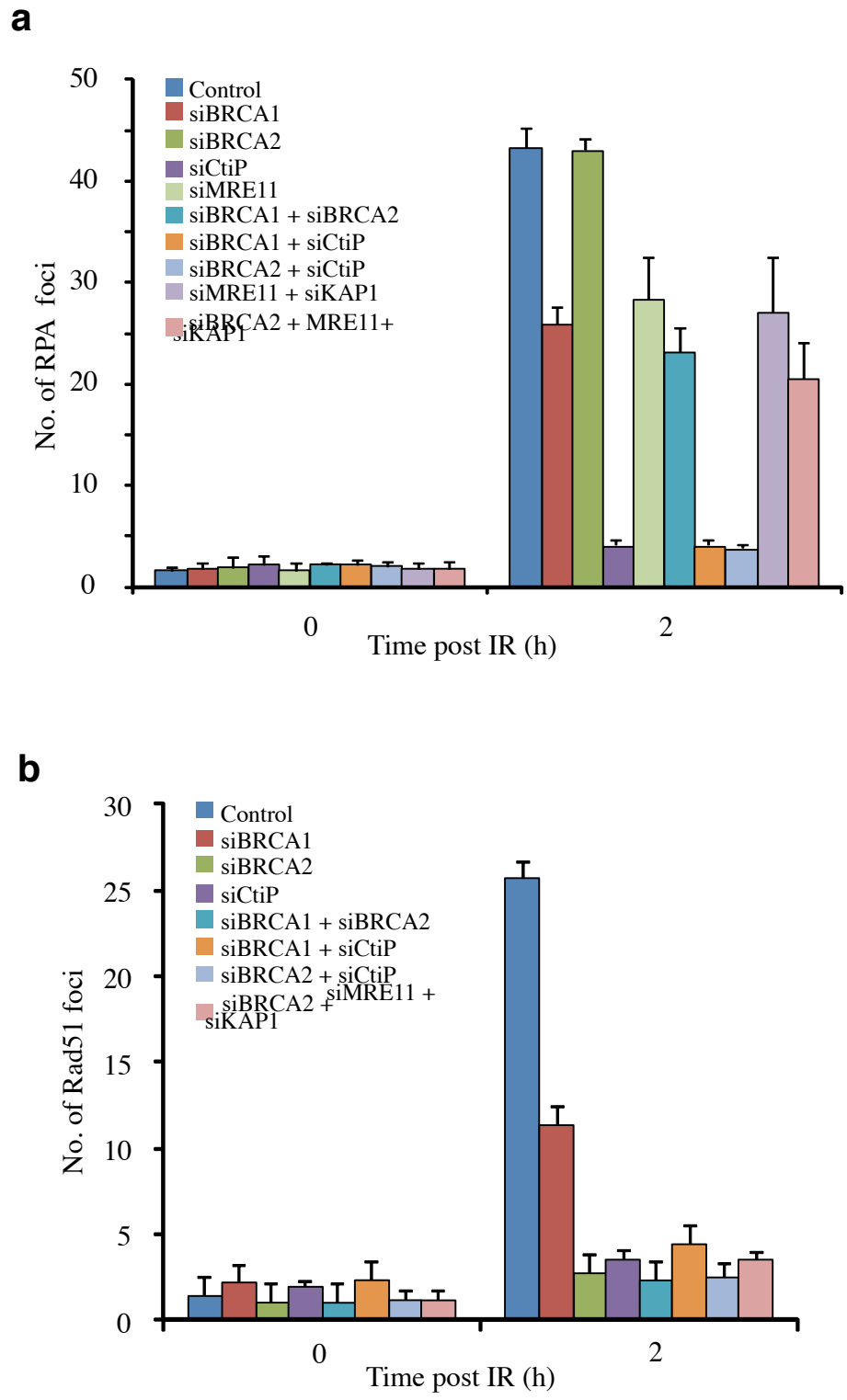

Figure 5.5. BRCA1 functions downstream of CtIP/MRN in G2 to promote resection and Rad51 loading during HR repair of HC-DSBs.
a-b) A549 cells were treated with the indicated siRNA and then exposed to 3 Gy IR in G2. Prior to irradiation aphidicolin was added to the cells to prevent S-phase cells from entering G2. The cells were then harvested at two hours post IR and immunostained with RPA (a) ,Rad51 (b) and CENP-F antibodies. G2 phase cells were identified by positive CENP-F staining and the cell nuclei were visualized by DAPI. Foci were enumerated specifically in CENP-F positive cells. RPA and Rad51 foci were enumerated in 30 cells per time-point and the data represent the mean and standard deviation of three independent experiments.

Importantly however, KAP-1 knockdown does rescue the repair defect of MRE11 depleted cells (Figure 5.4). This result strongly indicates that in MRE11 + KAP-1 co-depleted cells repair takes place by NHEJ since RPA and Rad51 foci formation is compromised. This result is somewhat surprising since the presence of some RPA foci following MRE11 siRNA suggests that resection has been initiated at least at a fraction of DSBs. Although normally the initiation of resection commits to repair by HR and does not allow repair by NHEJ, under these conditions (MRE11 + KAP1) repair takes place since no DSB repair defect is observed (Figure 5.4). It is highly likely that these DSBs are repair by NHEJ since RPA and Rad51 foci are compromised, but another HR endpoint such as SCEs is needed to confirm this. Triple siRNA knockdown of MRE11, BRCA2 and KAP-1 led to reduced RPA and Rad51 numbers (Figure 5.5 a-b) consistent with the notion that the DSB repair observed in Figure 4 occurs by NHEJ not HR. The fact that repair can take place by NHEJ implies that MRE11 functions in the initiation of resection or at a stage prior to commitment to repair by HR.

Collectively these findings show that CtIP/MRE11 function early in HR, with a role in the initiation of resection that commits to repair by HR. If the initiation of resection is prevented then DSBs that would normally be repaired by HR undergo repair by NHEJ. In contrast BRCA1 functions in a downstream step of resection possibly in the elongation or completion of the CtIP/MRE11 initiation. The HR phase in which BRCA1 functions is post commitment to HR which is consistent with the severe HR defect seen in BRCA1 depleted/mutant cells.

5.2.3: 53BP1 depletion rescues the HR defect of BRCA1 knockdown cells in G2.

In chapter 3 I described a novel function for 53BP1 in mediating G2 phase HR via KAP-1 dependent HC relaxation. This was an unexpected finding as the general consensus in the literature is that MDC1 functions to promote HR while 53BP1 promotes NHEJ (Xie *et al*, 2007; Minter-Dykhouse *et al*, 2008). Subsequently, two independent studies monitoring HR in S-phase reported that 53BP1 not only promotes NHEJ but actively supresses HR by inhibiting resection (Bunting *et al*, 2010; Bouwman *et al*, 2010). The authors went on to show that BRCA1 function is required to overcome the inhibitory function of 53BP1 on resection and that HR could be restored in BRCA1 mutant cells by depleting 53BP1. As these findings were contradictory to my findings, I set out to investigate the interplay between 53BP1 and BRCA1 during HR repair of two ended DSBs in G2 phase.

As indicated previously in this chapter and in chapter 3, depletion of either 53BP1 or BRCA1 leads to a repair defect in G2 phase cells that is similar in magnitude and effects slowly repaired DSBs (Figure 5.5a). However the repair defect of 53BP1 knockdown cells but not that of BRCA1 knockdown cells can be overcome with KAP-1 depletion (Figure 5.6a). This is consistent with the notion that 53BP1 is dispensable for HR but mediates the process via HC relaxation while BRCA1 has a direct role in HR. When 53BP1 and BRCA1 were co-depleted and repair was monitored in G2 phase cells a repair defect persisted at later time points (Figure 5.6a). This was contradictory to the studies showing that 53BP1 depletion could overcome the need for BRCA1 in HR. Strikingly however, triple knockdown of 53BP1, BRCA1 and KAP-1 lead to normal repair in G2 phase cells (Figure 5.6a). This unexpected finding showed that 53BP1 depletion could overcome the BRCA1 repair defect but that 53BP1's function in relaxing the HC structure is a requisite for repair.

Next I decided to investigate whether repair ensued by NHEJ or HR following 53BP1 and BRCA1 co-depletion in G2. As shown previously in this chapter and in chapter 3, depletion of either 53BP1 or BRCA1 leads to a defect in RPA and Rad51 foci formation (Figure 5.6b-c). However, the resection and Rad51 loading defect of 53BP1 knockdown cells but not that of BRCA1 knockdown cells can be overcome by KAP-1 depletion (Figure 5.6b-c). As was the case when monitoring γ-H2AX foci, the RPA and Rad51 foci defect of G2 phase BRCA1 knockdown cells could not be overcome by 53BP1 depletion (Figure 5.6b-c). Importantly however, triple knockdown of 53BP1,

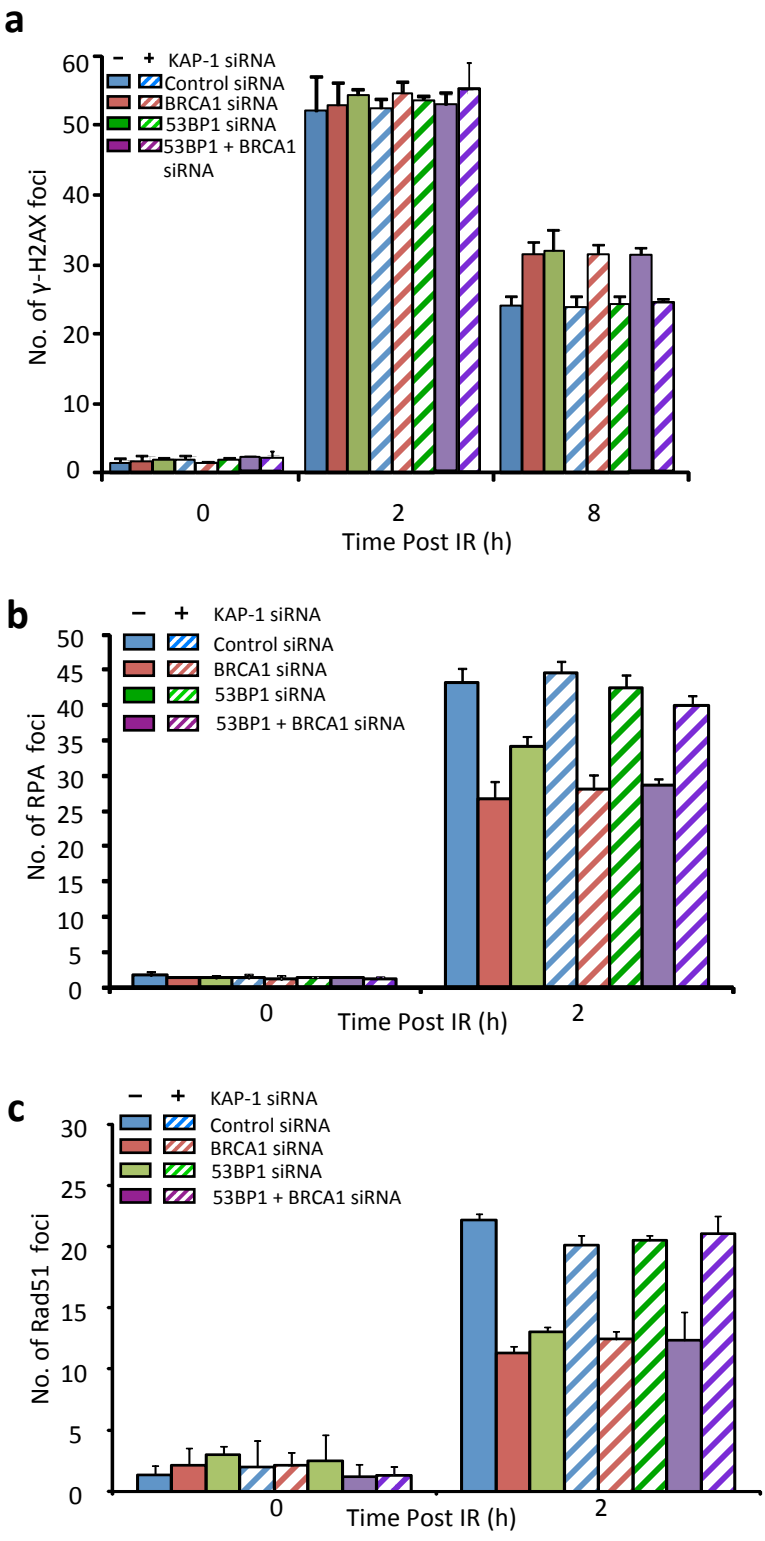

Figure 5.6. Combined loss of BRCA1, 53BP1 and KAP1 allows DSB repair by HR.
A549 cells were treated with the indicated siRNAs, exposed to 3 Gy IR and examined for RPA (a), RAD51 (b) or g-H2AX (c) foci at the indicated times. Prior to irradiation aphidicolin was added to the cells to prevent S-phase cells from entering G2. G2 phase cells were identified by positive CENP-F staining and the cell nuclei were visualized by DAPI. Results are shown in samples with or without siRNA KAP1 to expose the necessity to have relaxed HC to observe HR in G2 phase. In all panels results represent the mean of 3 experiments and error bars are the s.d.

BRCA1 and KAP-1 lead to normal RPA and Rad51 foci formation suggesting that under these conditions repair ensues by HR (Figure 5.6b-c).

There are several important conclusions that can be drawn from these findings. Firstly, 53BP1 appears to have two contrasting roles during DSB repair by HR in G2 phase. On one hand it inhibits HR by blocking resection while on the other hand it enables the accurate completion of HR by mediating KAP-1 dependent HC relaxation. Secondly, the function of BRCA1 in HR appears to be the removal of the barrier caused to resection by 53BP1. It seems that 53BP1 forms a barrier to resection downstream of the initiation step which is where BRAC1 function is required. Overcoming the barrier that 53BP1 poses to the completion of resection is very important, as repair can no longer ensue by NHEJ. The significance of this is demonstrated in BRCA1 depleted/mutated cells where a severe HR defect exists.

5.2.4: 53BP1 undergoes repositioning at IRIF during HR.

The unexpected finding that 53BP1 depletion can overcome the HR defect of BRCA1 depleted/mutant cells suggests that this is the only role for BRCA1 during HR. In order to elucidate the role of BRCA1 in HR I wanted to investigate how 53BP1 poses a barrier to resection and how BRCA1 overcomes this.

While examining the effect of 53BP1 and BRCA1 on the formation of HR intermediates, I also used immunofluorescence to test the knockdown efficiencies of the different siRNA oligos. Interestingly, when staining with a 53BP1 antibody in order to test 53BP1 siRNA efficiency, I observed that in control cells 53BP1 IRIF expanded over time. Previous studies have shown that the expansion of γ-H2AX signal can spread over megabases of DNA away from a DSB (Rogakou *et al*, 1999). I reasoned that the same could be true for the 53BP1 signal. However when monitoring 53BP1 IRIF expansion at later times (eight hours) after IR treatment, I observed that 53BP1 foci size was not uniform amongst all cells. Strikingly, when using CENP-F staining as a cell cycle marker I observed that the increase in 53BP1 foci size seemed to be restricted to G2 phase cells.

To examine this further I used enhanced-resolution imaging and 3D processing software to measure the volume of 53BP1 IRIF at different times after IR in G1 and G2. By taking Z-stacked images I was able to use the image processing software Imaris to reconstruct a 3D model of the 53BP1 IRIF and quantitatively measure their volume. Importantly, the 3D model of the foci accurately represented the Z-stacked immunofluorescence images acquired on the high-resolution microscope (Figure 5.7). Using these conditions, no substantial increase in 53BP1 foci volume in G1 cells over an eight-hour time course was observed (Figure 5.8a). In contrast, a doubling in 53BP1 IRIF volume was observed in G2 phase cells over an eight-hour time course (Figure 5.8a and Figure 5.14). What struck me about this result is that 53BP1 IRIF did not expand in G1 where BRCA1 function is dispensable, whereas they expanded in G2 where BRCA1 is required for efficient DSB repair. I reasoned that BRCA1 function may be required for 53BP1 IRIF expansion and that this may be important for repair by HR. Strikingly, when BRCA1 was depleted 53BP1 IRIF expansion was impeded resulting in foci that resembled those of G1 phase cells (Figure 5.7, 5.8b and 5.15).

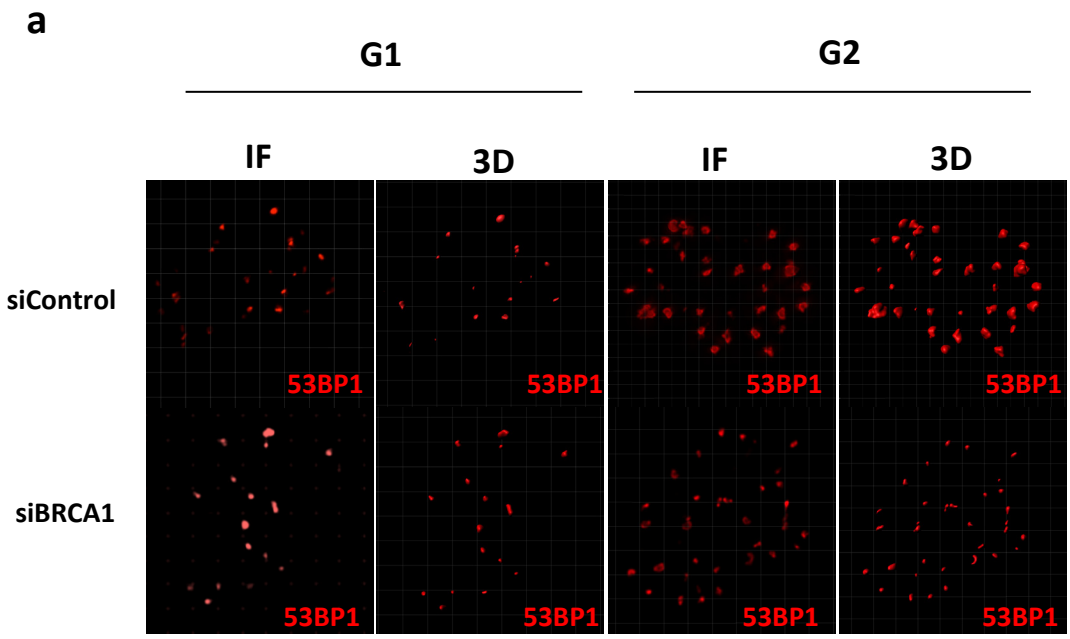

Figure 5.7. 3D modelling of 53BP1 IRIF accurately depicts the BRCA1 dependent G2 phase specific increase of 53BP1 IRIF volume as seen by IF.
a) A549 cells were treated with the indicated siRNA and then exposed to 3 Gy IR in G2. The cells were then harvested at eight hours post IR and immunostained with CENP-F and 53BP1 antibodies. G2 phase cells were identified by positive CENP-F staining and the cell nuclei were visualized by DAPI. 53BP1 foci were imaged using an Applied Precision® Delta Vision® RT Olympus IX70 deconvolution microscope and softWoRx® Suite software at eight hours post IR in G1 and G2 phase cells. The immunofluorescence images (IF) indicate a two dimensional projection of the acquired Z-stacked images while the 3D panels show a snapshot of the 3D model constructed from the Z-stacks. Please see the materials and methods section for a detailed description of the image acquisition and processing parameters.

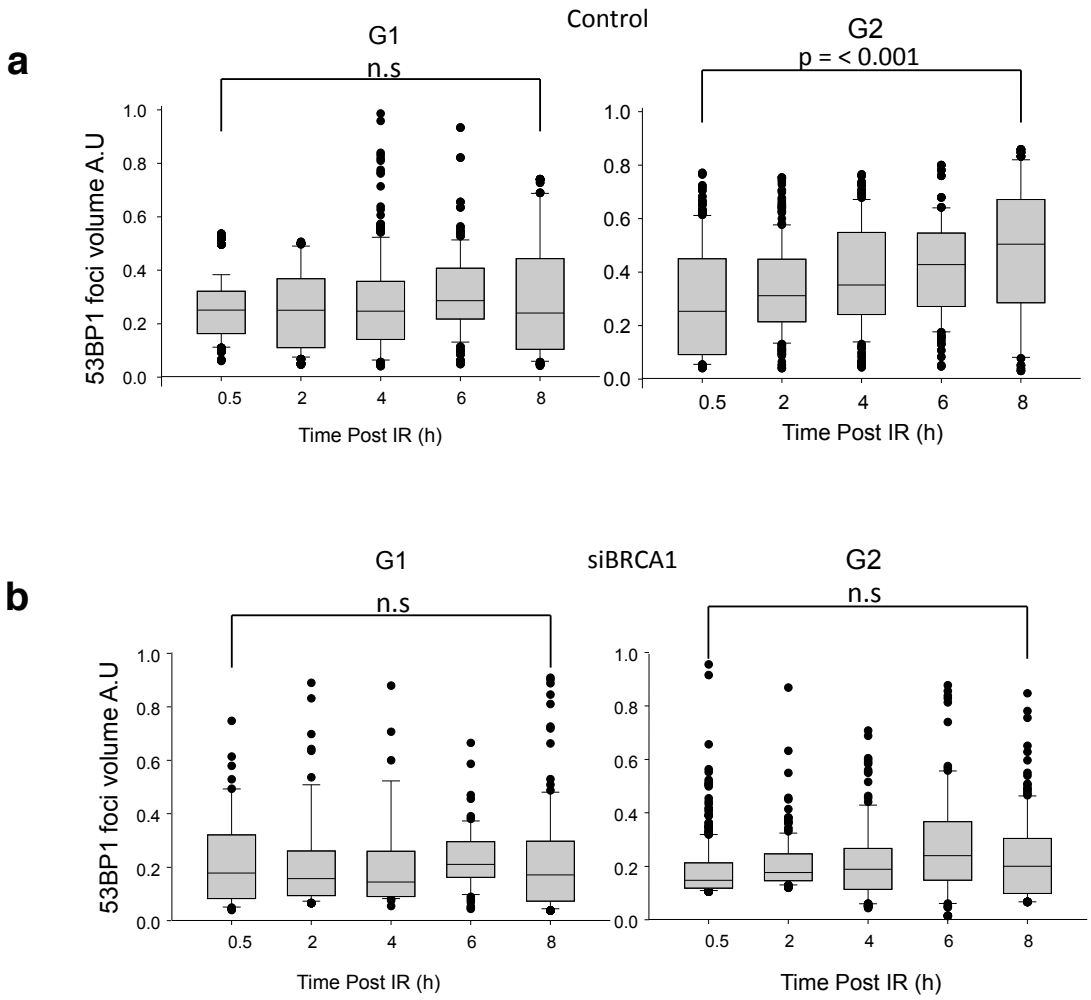

Figure 5.8. Analysis of 53BP1 IRIF in G1 and G2 phase cells using enhanced resolution microscopy.
a-b) Analysis of the volume of 53BP1 foci in A549 cells following exposure to 3 Gy IR. The volume of 53BP1 foci was assessed by 3 dimensional imaging using an Applied Precision® Delta Vision® RT Olympus IX70 deconvolution microscope and softWoRx® Suite software at the indicated times in G1 and G2 phase cells (see materials and methods for details of image processing). G2 phase cells were identified by CENPF staining. Analysis was carried out in untreated cells (a) and following treatment with siRNA BRCA1 (b). The data represent the median and lower and upper quartiles from at least 10 nuclei from each of three experiments. Error bars represent the minimum and maximum valid values determined as the highest datum still within 1.5 the interquartile range of the upper quartile. These were used to eliminate abnormally large values (depicted as single points) arising from foci 'clumping' and resolution limitations. Statistical analysis was carried out using the Mann-Whitney rank sum test. Data were not deemed to be significant when a p value > 0.05 was obtained.

Following the observation that 53BP1 IRIF expansion in G2 was BRCA1 dependent, I postulated that this might be related to BRCA1's function in overcoming the barrier 53BP1 poses to resection. I examined the behaviour of 53BP1, RPA and BRCA1 IRIF at different time-points by high-resolution microscopy to gain insight into the BRCA1-53BP1 interplay during HR. When a 3D model of 53BP1 foci was made from a 0.5 and 8-hour time-point there was a significant difference in volume due to 53BP1 foci expansion (Figure 5.9a). In addition however, when the 3D model of an individual 53BP1 focus was visualised as a wireframe structure I observed that by 8 hours post IR, they had become hollow structures (Figure 5.9a and Figure 5.15). This interesting result made me question whether the 53BP1 IRIF expansion as well as the central core devoid of 53BP1 could be important for resection. To test this I repeated the high resolution and 3D modelling experiments but this time co-stained with 53BP1 and RPA. When both 53BP1 and RPA were visualised together, only the 53BP1 signal was apparent (Figure 5.9b). Strikingly however, when the 53BP1 IRIF was visualised as a wireframe structure, the RPA foci became visible. Intriguingly, the RPA foci had formed in the central core of the 53BP1 IRIF, in the area devoid of 53BP1 signal (Figure 5.9b). This finding strongly indicated that 53BP1 IRIF expansion is a pre-requisite to RPA foci formation and that BRCA1 function is required to drive this repositioning of 53BP1.

To test this further I repeated the high resolution and 3D modelling experiments using 53BP1, BRCA1 and RPA triple staining. At four hours post 3Gy, the immunofluorescence signal of RPA, 53BP1 and BRCA1 all overlapped (Figure 5.10a). However the size of the 53BP1 foci appeared greater than that of BRCA1 foci. Strikingly, when the IRIF were visualised as a 3D model of the Z-stacked images the 53BP1 signal appeared on the periphery (Figure 5.10b). Visualising the 53BP1 IRIF as a wireframe structure revealed that BRCA1 foci form internally to 53BP1. Finally by visualising the BRCA1 IRIF as a wireframe structure revealed that RPA foci form internally to BRCA1 (Figure 5.10b and Figure 5.15).

In summary these findings indicate that 53BP1 becomes relocated as DSB repair by HR ensues. This relocation is dependent upon BRCA1 function and is required for resection and the formation of RPA foci. BRCA1 foci form internally to 53BP1 and RPA foci form in the centre. Next, I tested whether the reduced expansion of 53BP1 IRIF observed in BRCA1 depleted cells resulted from the reduced resection in these cells. To do this, I monitored 53BP1 IRIF expansion in Artemis depleted

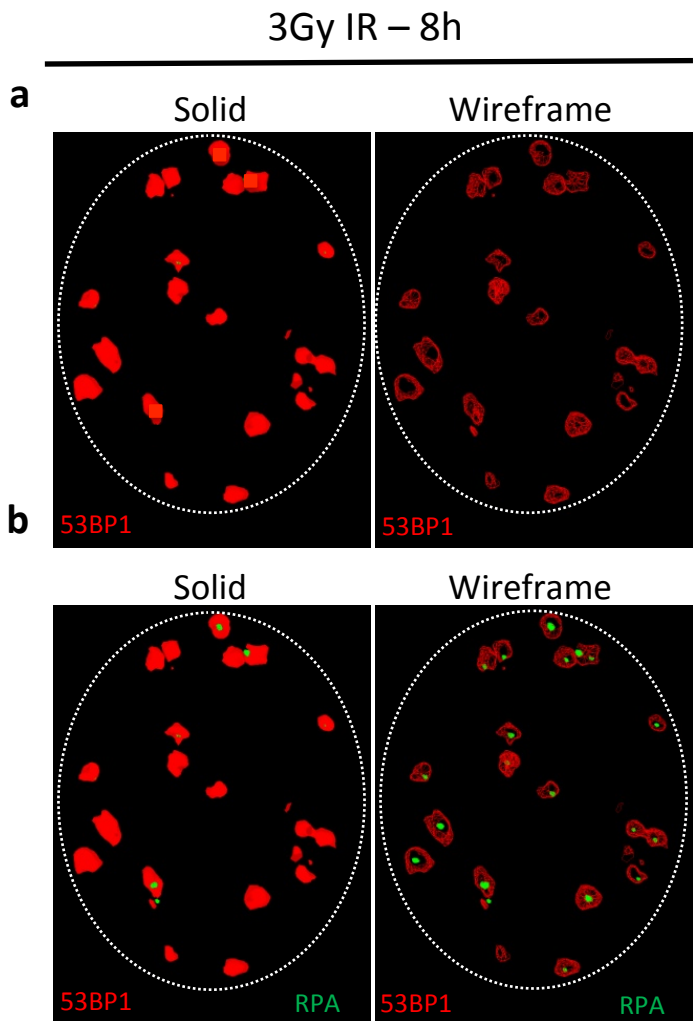

Figure5. 9. 53BP1 is relocalised during G2 phase HR creating a core devoid of 53BP1 where RPA foci form. a) A549 cells were exposed to 3 Gy IR in G2, harvested at eight hours post IR and immunostained with 53BP1 (a) or 53BP1 + RPA antibodies (b). Z-stacked images were acquired using an Applied Precision® Delta Vision® RT Olympus IX70 deconvolution microscope and softWoRx® Suite software. A 3D model of the Z-stacked images was then produced and visualised as either 'solid' or 'wireframe' to reveal the internal space of the IRIF.

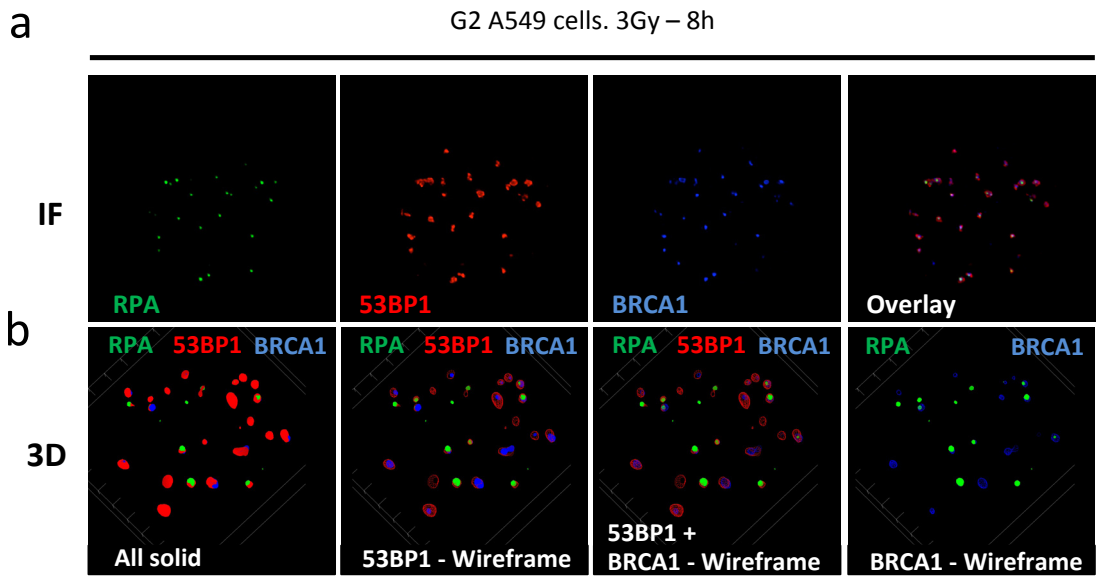

Figure 5.10. BRCA1 foci form internally to 53BP1 and RPA foci form in the core devoid of 53BP1.
a-b) A549 cells were exposed to 3 Gy IR in G2, harvested at eight hours post IR and immunostained with 53BP1, BRCA1 and RPA antibodies. Z-stacked images were acquired using an Applied Precision® Delta Vision® RT Olympus IX70 deconvolution microscope and softWoRx® Suite software. a) The immunofluorescence images (IF) indicate a two dimensional projection of the acquired Z-stacked images while the 3D panels (b) show a snapshot of the 3D model constructed from the Z-stacks. The 3D model is displayed as either 'solid' or 'wireframe' to reveal the internal space of the IRIF. BRCA1 foci form internally to 53BP1 and RPA foci form in the core devoid of 53BP1.

cells. Artemis is an endonuclease that is required for resection in G2 phase HR (Beucher *et al*, 2009). Importantly, depletion of Artemis results in a resection defect in G2 that is similar in magnitude to that of BRCA1 knockdown cells. However when I used high-resolution imaging and 3D modelling to assess 53BP1 IRIF volume in Artemis depleted cells, I observed normal IRIF expansion (Figure 5.11a). Therefore despite the resection defect seen in Artemis depleted cells (Figure 11b) normal 53BP1 IRIF expansion was observed. Furthermore, and distinct to BRCA1 depletion, co-depletion of 53BP1 and KAP-1 in Artemis knockdown cells failed to restore the resection and repair defects in these cells (Figure 5.11b-c). Taken together these findings indicate that the role of Artemis in G2 phase HR is distinct to that of BRCA1 and does not affect 53BP1 IRIF relocation. More importantly, however, these results indicate that BRCA1 actively promotes the relocation of 53BP1 to enable resection and HR and that the loss of this in BRCA1 depleted cells is not a consequence of reduced resection.

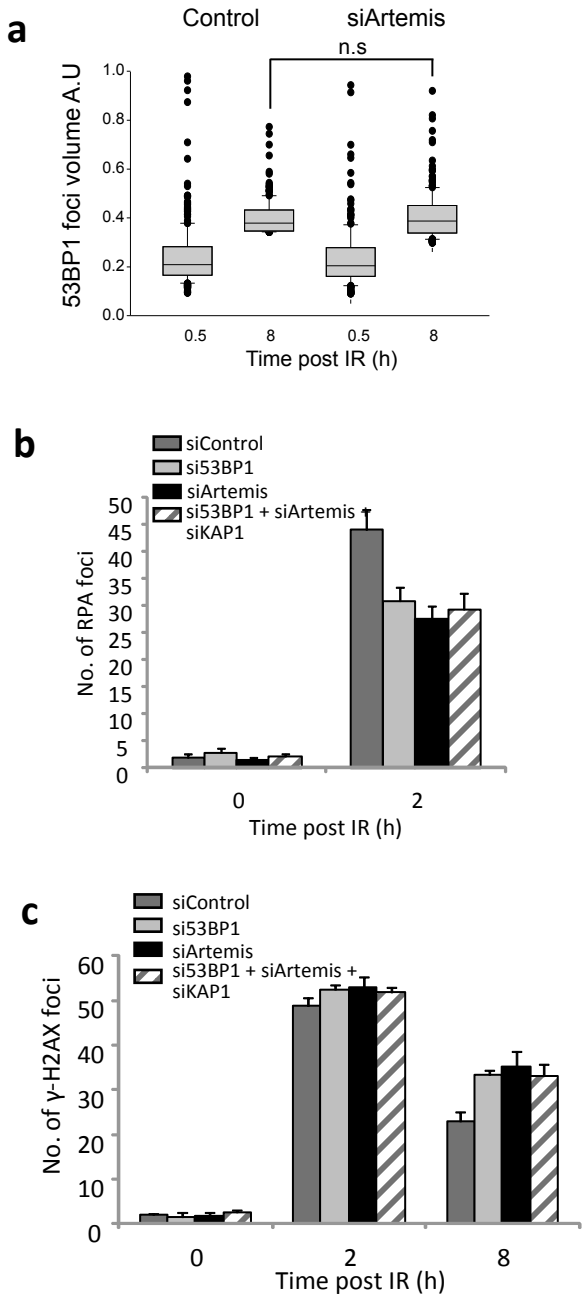

Figure 5.11. 53BP1 repositioning is not driven by resection while 53BP1 depletion does not alleviate the requirement of Artemis

A549 cells were treated with the indicated siRNA and then exposed to 3 Gy IR in G2 and analysed for (a) 53BP1 foci volume, (b) RPA foci and (c) γ-H2AX foci. In a) , 53BP1 foci volume quantification following Artemis siRNA was carried out as in Figure 8. Statistical analysis was carried out using the Mann-Whitney rank sum test. Data were not deemed to be significant when a p value > 0.05 was obtained. In b) and c), G2 phase cells were identified by positive CENP-F staining and the cell nuclei were visualized by DAPI. RPA and γ-H2AX foci were enumerated in 30 cells per time-point and the data represent the mean and standard deviation of three independent experiments.

5.2.5: 53BP1 repositioning during HR is distinct to regular foci expansion.

The IRIF that form during the DDR are dynamic in nature and tend to move and change in shape before eventually disappearing once repair is completed. As mentioned above, studies monitoring the expansion of the γ-H2AX signal reported spreading over megabases of DNA (Rogakou *et al*, 1999). I wanted to verify that the 53BP1 repositioning that I observed in G2 phase cells was distinct to the regular IRIF expansion seen with other DDR factors. I suspected that this was the case, as in my experiments I observed a G2 phase specific increase in 53BP1 IRIF volume that I had not observed for IRIF of other factors.

To test whether 53BP1 was specifically relocated during HR, I decided to compare 53BP1 IRIF to γ-H2AX IRIF during G2 phase HR. At early time points (0.5h) following exposure to IR in G2, 53BP1 and γ-H2AX foci where similar in size and strongly co-localised although γ-H2AX IRIF appeared external to 53BP1 IRIF at these time points (Figure 5.12). Strikingly, from two hours onwards, a time that coincides with the appearance of RPA foci, 53BP1 IRIF continued to enlarge while the size of γ-H2AX foci remained unchanged. By eight hours following IR treatment, the 53BP1 foci were on the periphery of the IRIF and enclosed the γ-H2AX and RPA foci (Figure 5.12). By producing a 3D model of the IRIF and viewing the 53BP1 signal as a wireframe structure, I was able to confirm that 53BP1 is specifically relocated and forms a hollow structure that surrounds γ-H2AX and RPA. Using the same method I observed that γ-H2AX also expands but to a lesser extent and that RPA foci form in the centre. These results indicate that the relocation of 53BP1 is a BRCA1 dependent process that is required for resection and that is distinct to normal signal expansion seen for other IRIF.

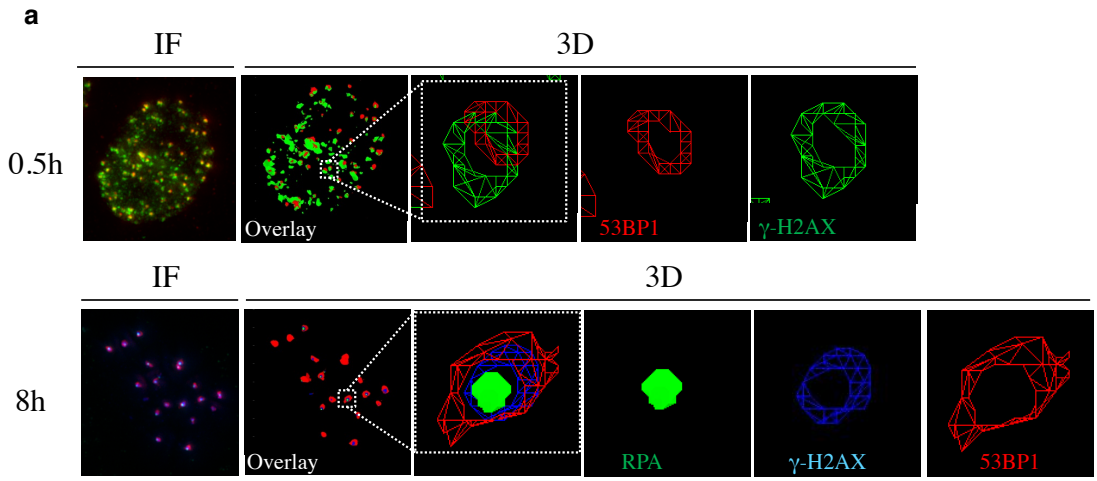

Figure 5.12. γ-H2AX foci form internally to 53BP1 and RPA foci form in the core devoid of 53BP1 and γ-H2AX .

As for Figure 9 but this time γ-H2AX foci were visualised instead of BRCA1. At these time points (8h), 53BP1 IRIF have expanded significantly more that γ-H2AX IRIF and are located on the IRIF periphery. γ-H2AX foci form internally to 53BP1 and RPA foci form in the core devoid of 53BP1 and γ-H2AX.

5.2.6: pATM and ubiquitin chains re-localise with 53BP1 in G2.

The formation of 53BP1 IRIF requires RNF8-RNF168- dependent ubiquitylation at DSBs(Huen *et al*, 2007; Mailand *et al*, 2007; Doil *et al*, 2009). I predicted that 53BP1 relocation to the periphery of IRIF might necessitate the repositioning of the polyubiquitin chains required for 53BP1 IRIF formation. To test this, I used an FK2 antibody to detect ubiquitylation events and polyubiquitin chains and repeated the high resolution and 3D modelling experiments described above. I observed that in G2 cells the FK2 IRIF expand over time and like 53BP1 vacate the central core and strongly co-localise with 53BP1 (Figure 5.13 and Figure 5.14a). Similarly to 53BP1 IRIF, the RPA foci formed internally to FK2 in the vacated central core.

As discussed previously, 53BP1 functions during HC DSB repair in G1 and G2 by tethering activated ATM at DSB sites and therefore mediating the robust localised KAP-1 phosphorylation needed for repair (Noon *et al*, 2010). Using the high resolution and 3D imaging assay I tested whether pATM IRIF also become relocated during HR. Strikingly, pATM signal also expanded over time and relocated to the periphery of IRIF and strongly co-localised with 53BP1 (Figure 5.14b and 5.15b). siRNA mediated knockdown of BRCA1 ablated the expansion and repositioning of 53BP1, FK2 and pATM (Figure 5.15c).

Previous studies have suggested that during HR there is a handover from ATM to ATR since ATM is not efficiently activated at resected DSBs (Shiotani & Zou, 2009). However, other studies have demonstrated that in G1 53BP1 tethers pATM at DSB sites via interactions between 53BP1-RAD50 and NBS1-ATM (Noon *et al*, 2010; Lee *et al*, 2010). Importantly, the high resolution imaging in this chapter specifically looking at G2 phase HR indicates that pATM is tethered at DSBs even up to 8 hours post IR. However, the specificity of pATM antibodies has been questioned so as an alternative way of assessing the requirement of pATM, I decided to test whether its retention at later times (4-8h) post IR is important for the completion of the HR pathway. To achieve this, I irradiated cells with 3Gy and then added the ATMi at different times post IR to test whether ATMi function was still required. Significantly, addition of the ATMi at two or even four hours post IR led to a similar repair defect at eight hours to that seen in cells where ATMi was added prior to IR (Figure 5.15d). When ATMi was added 6 hours post IR the effect was not substantial but this may have resulted from the time needed for the drug to diffuse and take effect.

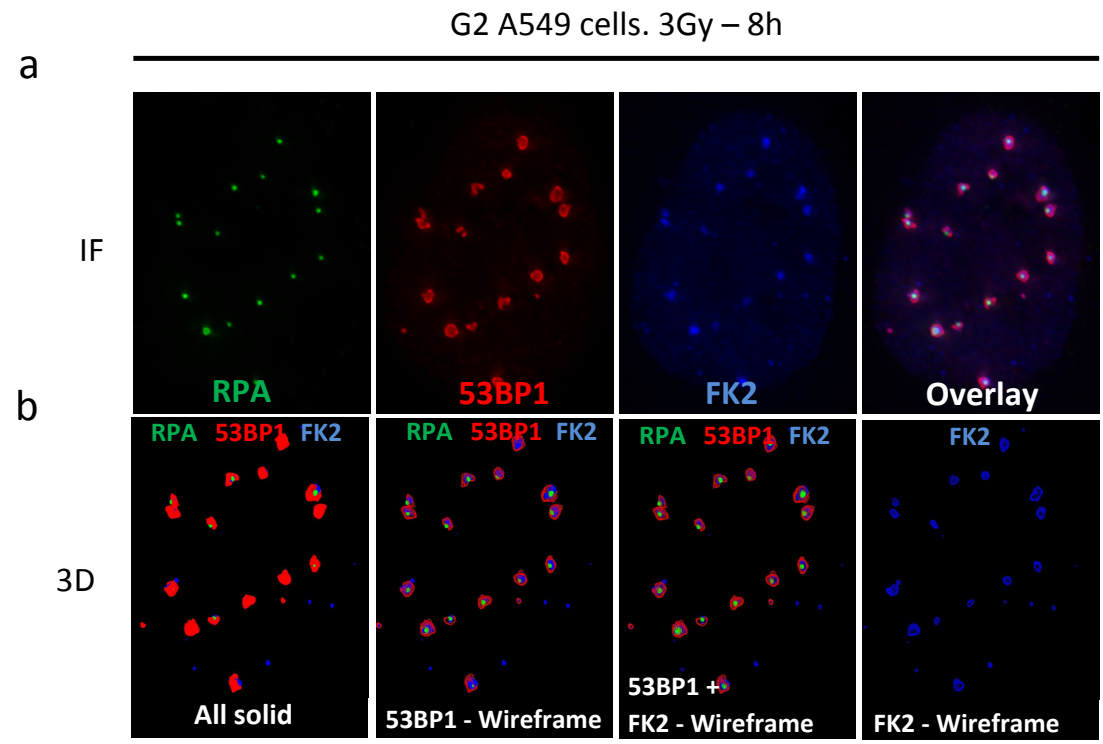

Figure 5.13. FK2 IRIF are also relocalised during G2 phase HR creating a core devoid of 53BP1 and FK2 where RPA foci form.
a-b) A549 cells were exposed to 3 Gy IR in G2, harvested at eight hours post IR and immunostained with 53BP1, FK2 and RPA antibodies. Z-stacked images were acquired using an Applied Precision® Delta Vision® RT Olympus IX70 deconvolution microscope and softWoRx® Suite software. a) The immunofluorescence images (IF) indicate a two dimensional projection of the acquired Z-stacked images while the 3D panels (b) show a snapshot of the 3D model constructed from the Z-stacks. The 3D model is displayed as either 'solid' or 'wireframe' to reveal the internal space of the IRIF. FK2 foci form internally to 53BP1 and RPA foci form in the core devoid of 53BP1 and FK2.

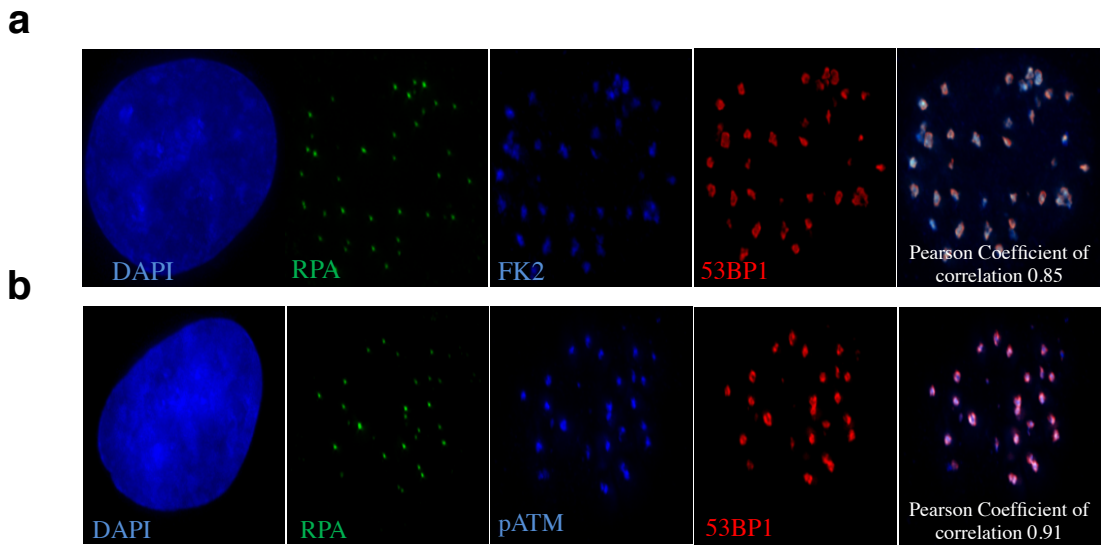

Figure 5.14. 53BP1, FK2 and pATM all become relocalised during G2 phase HR and strongly colocolise
a-b) A549 cells were immunostained with the indicated antibodies 8 h post 3Gy IR and colocalisation between 53BP1 and pATM (b) and FK2 (a) was carried out using softWoRx® Suite software. The Pearson Coefficient of Correlation indicates how closely the two intensities are colocolised on a pixel-by-pixel basis (full colocalisation is 1.0)

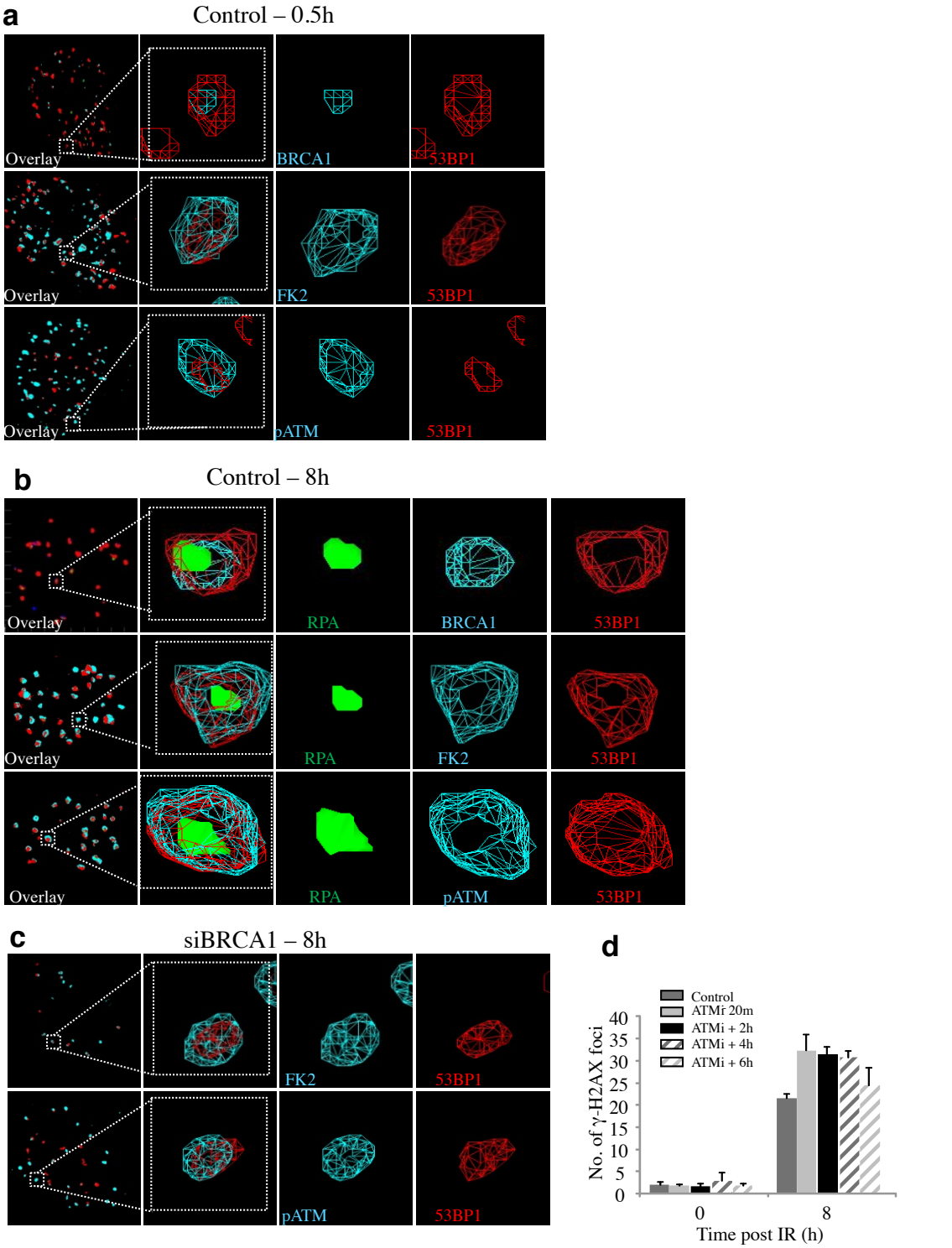

Figure 5.15: **BRCA1 promotes relocalisation of 53BP1 in G2 phase creating a core devoid of 53BP1, ubiquitin chains and pATM.**
a-b) Analysis of G2 A549 cells at 0.5 (a) and 8 (b) hours post 3 Gy IR. Following immunostaining with the indicated antibodies (53BP1, BRCA1, RPA, FK2 and p1981-ATM), 3D IRIF analysis was undertaken using softWoRx® Suite. The red and green signals represent 53BP1 and RPA, respectively; the blue signal is as indicated. 'Wireframe' images are displayed allowing 3D visualization. Foci volume enlarges from 0.5- 8 h post IR generating an expanded core lacking 53BP1. BRCA1 localizes internally to 53BP1 and RPA lies within the core. c) Images following siRNA BRCA1 8 h post IR where no significant expansion in 53BP1, FK2 or pATM IRIF is observed. d) Addition of ATMi at varying times post IR. Cells were exposed to 3 Gy IR and γ-H2AX foci enumerated 8 h later. ATMi was added 15 min before IR or 2, 4 and 6 h post IR, as indicated. ATMi addition at 2 and 4 h caused a repair defect similar to that observed when ATMi was added prior to IR (which is similar to that observed in cells lacking ATM). Thus, ATM activity is required for HC-DSB repair for at least 4 h post IR.

These findings show that as in G1, the retention of pATM during DSB repair in G2 is also required for at least four hours post IR, a time when RPA foci numbers have become maximal.

5.2.7: The BRCT but not the RING domain of BRCA1 is required for 53BP1 repositioning during HR.

Following the observation that BRCA1 function is required for 53BP1 IRIF repositioning during G2 phase HR, I wanted to gain some insight into the mechanism of this function. There is a multitude of studies in the literature investigating the role of BRCA1 in the DDR and this is discussed in the introductory chapter. What makes BRCA1 particularly versatile are its interacting domains that result in a plethora of complexes with wide ranging functions (Huen *et al*, 2009). In addition, BRCA1 also possesses enzymatic activity and acts as an ubiquitin ligase. The above characteristics of BRCA1 made the identification of a mechanism by which it promotes the relocation of 53BP1 during HR challenging.

First I tested whether the ubiquitin ligase activity of BRCA1 was required for 53BP1 relocation. I reasoned that this was a good place to start since the ubiquitin chains detected by the FK2 antibody where also repositioned as HR progressed. However, published evidence in the literature has suggested that the enzymatic activity of BRCA1 is dispensable for HR (Shakya *et al*, 2011; Greenberg, 2011; Reid *et al*, 2008). Nevertheless I decided to pursue these experiments, as the finding that BRCA1 E3 ligase activity was dispensable for HR was not widely accepted and the model suggesting that 53BP1 repositioning depends on BRCA1 E3 ligase activity was appealing. Concurrently I also tested whether the BRCT domains of BRCA1 were required for its function in 53BP1 relocation. This would provide insight as to whether the interaction of BRCA1 with its phosphobinding partners is important for this function.

Initially, I developed a strategy involving BRCA1 depletion by siRNA and complementation using BRCA1 cDNA. I acquired full length human BRCA1 and mutant BRCA1 in a plasmid that also contained an HA tag. The mutant versions of BRCA1 included the I26A mutation that leads to a ligase dead version of the protein and a BRCT domain delete. Next I designed primers and used site directed mutagenesis to introduce silent mutations in the region that was targeted by the siRNA oligo thus

creating siRNA resistant constructs. Following verification of the site directed mutagenesis by sequencing, I transfected and transiently expressed the constructs in cells treated with BRCA1 siRNA. I aimed to specifically pick out the transfected cells by an HA antibody and then measure 53BP1 IRIF volume in these cells. Complementation using the different BRCA1 mutants would provide insight into the requirement of the BRCA1 domains for 53BP1 IRIF expansion and relocation. However, these experiments proved technically challenging and were ultimately unsuccessful. Treatment with BRCA1 siRNA is highly toxic in mammalian cells since BRCA1 function is essential and BRCA1 loss is embryonic lethal (Gowen *et al*, 1996). In these experiments, in addition to the BRCA1 siRNA treatment I also carried out an additional transfection with BRCA1 cDNA followed by a 24-hour overexpression. This additional step is also not well tolerated by cells. The end result of these combined treatments was high levels of cell death and not sufficient cells to carry out the 53BP1 imaging analysis.

While optimising these experiments, a study was published from the Ludwig and Baer laboratories, investigating the role of BRCA1 E3 ubiquitin ligase activity on BRCA1's function as a tumour suppressor (Shakya *et al*, 2011). This work involved the generation of homozygous mice expressing $BRCA1^{FH\text{-}I26A}$ resulting in ligase dead BRCA1. Intriguingly, the BRCA1 mutated mice prevented tumour formation to the same degree as wild-type mice in three different mouse models of cancer. This was an unexpected finding that suggested that BRCA1 function as an ubiquitin ligase is dispensable for its role as a tumour suppressor. In addition the authors also showed that MEFs isolated from these animals had no evidence for an abnormal response to genotoxic damage. Next, the authors investigated the requirement of the BRCT motifs of BRCA1in its function as a tumour suppressor. They generated homozygous $BRCA1^{FH\text{-}S1598F}$ mice that express mutant BRCA1 that is unable to interact via its BRCT domain with its binding partners, Abraxas, BACH1 and CtIP. Importantly, tumours were observed in all three of the mouse cancer models whilst isolated MEFs displayed hypersensitivity to genotoxic stress and defective homology directed repair (Shakya *et al*, 2011).

I contacted the authors and requested MEFs isolated from the mice expressing mutated BRCA1 so that I could carry out my 53BP1 IRIF analysis in these cells. The advantage of using these cells was that it did not necessitate doing knockdown of BRCA1 nor selection for transfected cells. Importantly, following irradiation of cultured

wild-type MEFs, an enlargement in 53BP1 IRIF volume was observed over time (Figure 16). Strikingly however, the MEFs expressing BRCA1$^{FH\text{-}I26A}$ also showed an increase in 53BP1 IRIF volume over time that was indistinguishable from that seen in wild type cells. On the other hand the MEF's expressing BRCA1$^{FH\text{-}S1598F}$ were compromised in their ability to reposition 53BP1 IRIF and a significant difference in IRIF volume was observed at eight hours post IR compared to wild-type cells (Figure 5.16). These results are consistent with the findings from Shakeya et al showing that BRCA1 phosphoprotein recognition via its BRCT domains is important for its role in homology directed repair. More specifically here I demonstrate that the phosphoprotein interactions are required for 53BP1 IRIF relocation thus overcoming its inhibitory effect on resection. However, although BRCA1 is required to facilitate this relocation, it does not appear to drive this process via its ubiquitin ligase activity.

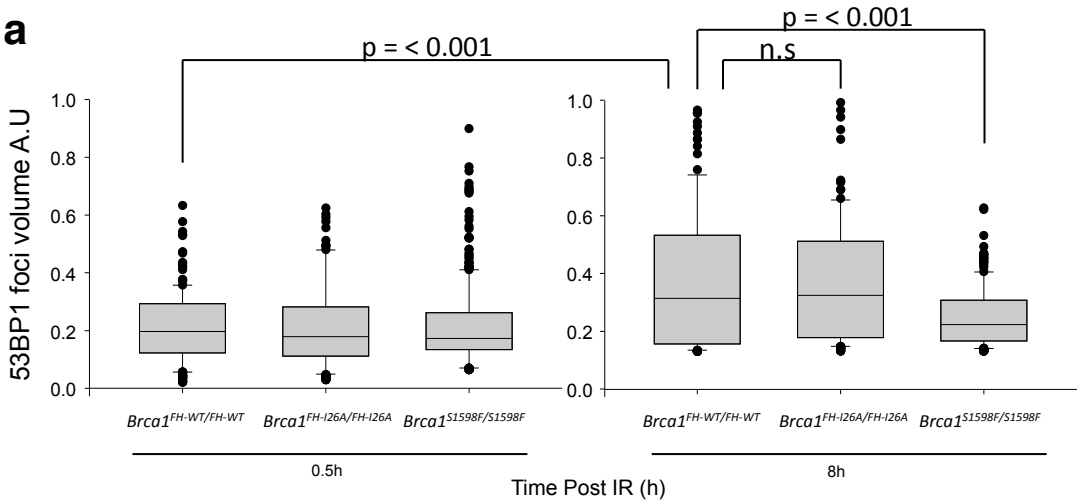

Figure 5.16. The BRCT but not the RING domain of BRCA1 is required for 53BP1 repositioning during HR. a) Analysis of 53BP1 foci volume in G2 phase Brca1$^{FH\text{-}WT/FH\text{-}WT}$, BRCA1$^{FH\text{-}I26A}$ and BRCA1$^{FH\text{-}S1598F}$ MEFs following 3Gy IR. 53BP1 foci analysis was carried out as in Figure 8. Statistical analysis was carried out using the Mann-Whitney rank sum test. Data were not deemed to be significant when a p value > 0.05 was obtained.

5.2.8: The BRCA1 interacting proteins BACH1, RAP80 and BRCC36 are not required for 53BP1 repositioning during HR.

As discussed earlier, BRCA1 forms distinct complexes that function in different aspects of the DDR (Huen *et al*, 2009). The BRCA1a complex consists of Abraxas, RAP80, BRCC36, BRCC45 and MERIT40. The BRCA1b complex comprises BACH1 and TOPBP1. Finally, the BRCA1c complex encompasses CtIP and the MRN complex. The finding that ablation of these interactions in the BRCA1$^{FH\text{-}S1598F}$ MEFs resulted in abnormal 53BP1 volume expansion indicated a possible role for these factors in this process. To examine, I depleted components of the different BRCA1 complexes and monitored their effect on 53BP1 IRIF volume.

First I monitored the impact of RAP80 and BRCC36 depletion on 53BP1 IRIF expansion. I reasoned that this complex might play a part in this process as it has previously been implicated in targeting BRCA1 to DSB sites (Sobhian *et al*, 2007). Additionally RAP80 and BRCC36 have been reported to play a role in 'tuning' BRCA1 dependent resection (Hu *et al*, 2011). Finally since BRCC36 is a DUB, I postulated that it might play a role in the formation of the hollow core of 53BP1 IRIF by promoting 53BP1 disassociation through histone de-ubiquitylation. However depletion of either of these factors had no impact on 53BP1 IRIF volume, since at eight hours post IR 53BP1 IRIF volume was indistinguishable to that in control cells (Figure 5.17).

Next I investigated the role of BACH1 in 53BP1 repositioning during HR. BACH1 is a helicase that has a role in DNA replication and also functions to unravel DNA during resection. Consequently, depletion of BACH1 leads to a resection defect in G2 phase. However when I depleted BACH1, I again observed no impact on 53BP1 IRIF volume, as at eight hours post IR they were indistinguishable to those in control cells.

The third complex that BRCA1 forms is with CtIP and the MRN complex. However the 53BP1 IRIF repositioning defect seen in the BRCA1$^{FH\text{-}S1598F}$ MEFs could not be attributed to loss of interaction with these factors as earlier in this chapter I demonstrated that they function upstream of BRCA1. CtIP/MRN dependent initiation of resection occurs independently of BRCA1 which functions in the later elongation/completion step. In addition 53BP1 repositioning during HR cannot be monitored in the absence of CtIP/MRN as when these factors are depleted repair ensues by NHEJ.

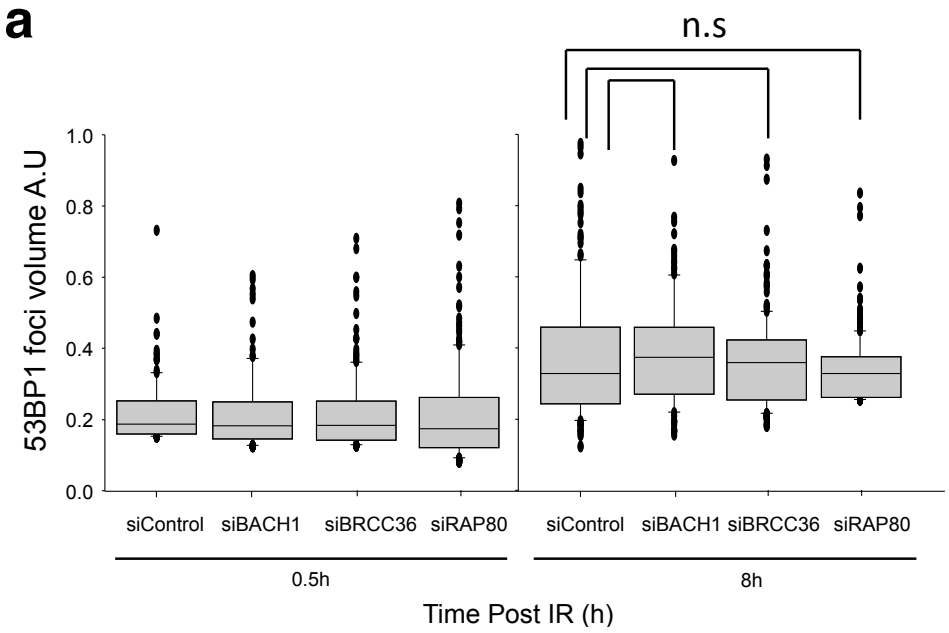

Figure 5.17. The BRCA1 interacting proteins BACH1, RAP80 and BRCC36 are not required for 53BP1 repositioning during HR.

a) Analysis of 53BP1 foci volume in A549 cells treated with the indicated siRNA, following 3Gy IR. 53BP1 foci analysis was carried out as in Figure 8. Statistical analysis was carried out using the Mann-Whitney rank sum test. Data were not deemed to be significant when a p value > 0.05 was obtained.

5.2.9: The deubiquitinating enzyme POH1 is required for resection and 53BP1 repositioning in G2.

The observations made so far in this chapter suggest that BRCA1 repositions 53BP1 is G2 to enable resection and DSB repair by HR. In addition to 53BP1 repositioning, a hollow core devoid of 53BP1 forms in the IRIF where RPA subsequently form. This hollow core also forms in FK2 and γ-H2AX IRIF and is also likely to be important for resection. An attractive model is that on-going ubiquitylation away from the DSB drives 53BP1 repositioning while histone deubiquitination in the IRIF core leads to 53BP1 disassociation and possibly histone eviction/degradation to allow resection. Such a mechanism would necessitate the function of a deubiquitinating enzyme (DUB) for the formation of the hollow core, but depletion of the DUB BRCC36 led normal 53BP1 volume expansion and resection (Figure 5.17). Indeed depletion of BRCC36 has been shown to lead to increased, not reduced resection (Hu *et al*, 2011).

Unpublished data from the Jo Morris laboratory indicates that the POH1 DUB enzyme also functions in the DDR. POH1, like BRCC36, is a JAMM domain containing protein that shows K63-Ub specific DUB activity (Cooper *et al*, 2009). POH1 is a member of the 19S portion of the 26S proteasome and like BRCC36; its DUB activity requires interaction with an MPN- domain-containing factor (Patterson-Fortin *et al*, 2010; Cooper *et al*, 2009). As part of the BRCA1a complex responding to DNA damage, BRCC36 interacts with Abraxas, which contains an MPN- domain and this interaction is required for its DUB activity. (Patterson-Fortin *et al*, 2010). On the other hand, POH1 interacts with the MPN- domain of RPN8 as part of the proteasome and appears to be important for HR (Morris et al unpublished). I decided to test whether POH1 DUB activity is required for disassociation of 53BP1 from the IRIF core and therefore for RPA foci formation. POH1 depletion by siRNA did not prevent 53BP1 foci from expanding in G2 from 0.5h to 8h after IR treatment. In addition, at 8h post IR in G2, the volume of 53BP1 IRIF in POH1 knockdown cells was indistinguishable from that in control cells (Figure 5.18a). As a control for redundancy among K63-Ub DUBs in this process I also co-depleted POH1 and BRCC36. Under these conditions 53BP1 foci expansion was also normal and 53BP1 IRIF volume at 8h post IR was indistinguishable to control cells (Figure 5.18a). In addition, when I co-depleted POH1 with either RAP80 or Abraxas I also observed normal 53BP1 foci expansion (Figure 5.18a).

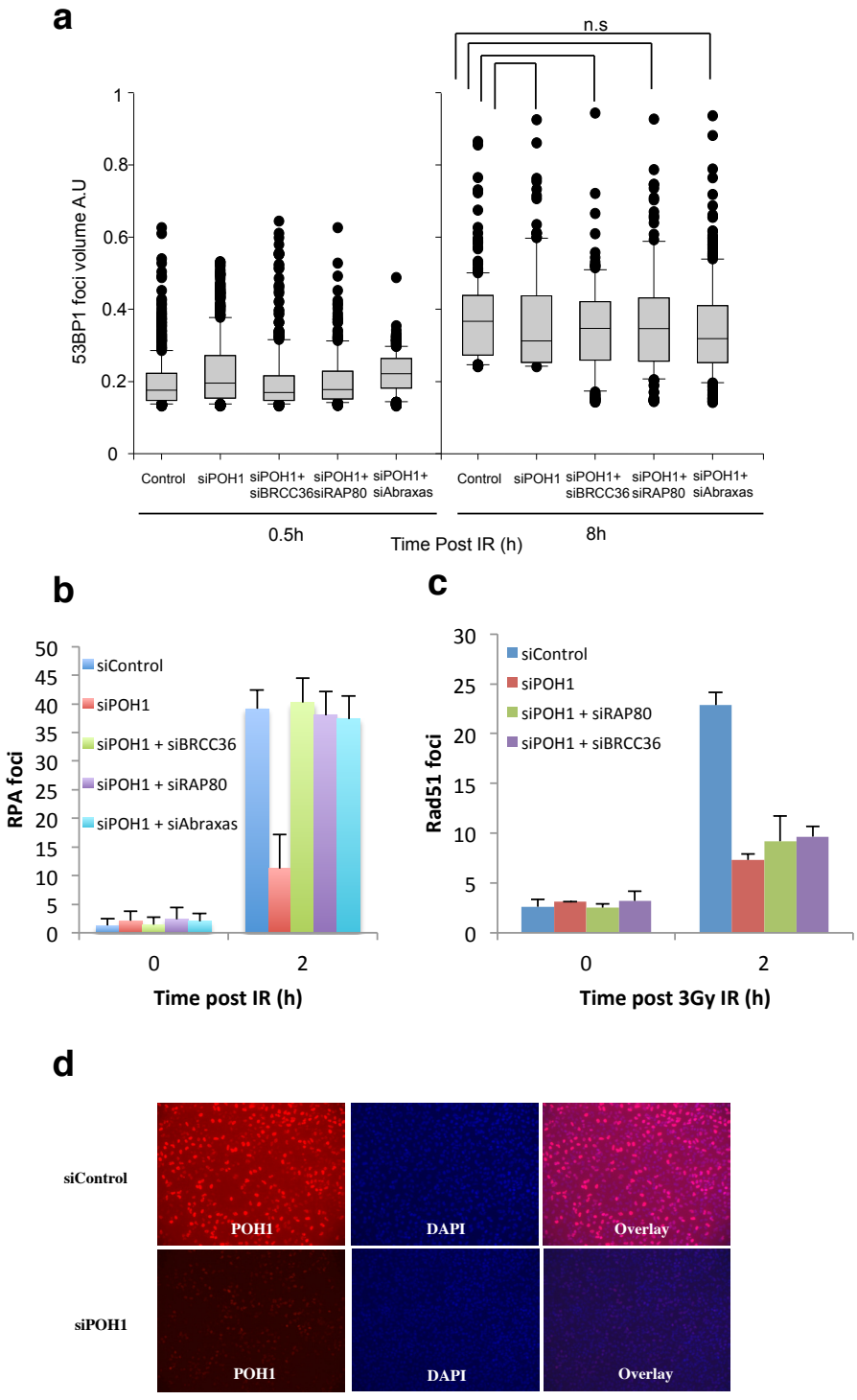

Figure 5.18. POH1 is dispensable for 53BP1 IRIF expansion in G2 but is required for RPA and Rad51 foci formation. Co-depletion of BRCC36, RAP80 or Abraxas alleviates the requirement of POH1 for RPA but for Rad51 foci formation.

a) Analysis of 53BP1 foci volume in A549 cells treated with the indicated siRNA, following 3Gy IR. 53BP1 foci analysis was carried out as in Figure 8. Statistical analysis was carried out using the Mann-Whitney rank sum test. Data were not deemed to be significant when a p value > 0.05 was obtained. b-c) A549 cells were treated with the indicated siRNA and then exposed to 3 Gy IR in G2. The cells were then harvested at two hours post IR and immunostained with RPA/Rad51 and CENP-F antibodies. G2 phase cells were identified by positive CENP-F staining and the cell nuclei were visualized by DAPI. Foci were enumerated specifically in CENP-F positive cells. RPA/Rad51 foci were enumerated in 30 cells per time-point and the data represent the mean and standard deviation of three independent experiments. c) Knockdown efficiency in A549 cells following treatment with a pool of POH1 siRNA oligonucleotides. Per knockdown, 100 pmol of siRNA duplexes per 2 x 10^5 logarithmically growing cells were used.

This is consistent with other studies showing that loss of these proteins does not impair but enhances HR (Hu *et al*, 2011; Coleman & Greenberg, 2011). When carrying out these experiments, I also immunostained the cells with an RPA antibody to assess resection under these conditions. Strikingly, at 2h post IR, the number of RPA foci that formed in POH1 depleted cells were significantly reduced compared to control cells (Figure 5.18b). This is distinct to loss of BRCC36 where an increase in resection is observed (Hu *et al*, 2011). Importantly, cells in which POH1 and BRCC36, RAP80 or Abraxas were co-depleted showed normal levels of RPA foci indicating that POH1 function in resection is redundant when these factors are depleted (Figure 5.18b). Binding of the BRCA1a complex to ubiquitylated histones at DSB sites via the UIM of RAP80, is inhibitory to resection (Coleman & Greenberg, 2011). I therefore interpret these findings to suggest that POH1 is required to overcome the inhibitory function of RAP80/BRCC36/Abraxas on resection. Importantly, POH1 depletion also led to a defect in Rad51 foci formation (Figure 5.18c). However, the Rad51 foci formation defect of POH1 depleted cells could not be rescued by RAP80 or BRCC36 co-depletion indicating that POH1 might also have a direct downstream role in Rad51 loading (Figure 5.18c). Consistent with this, unpublished work from the Morris laboratory has shown that POH1 is required for the recruitment of the BRCA2-co-factor DSS1 to DSB sites. Moreover, POH1 was shown to form a complex with BRCA2 and BRC1 following HU treatment. These findings suggest that the 19S proteasome, which contains POH1, interacts with factors that promote Rad51 loading.

Next, I used the 3D imaging assay described earlier to assess whether the IRIF core devoid of 53BP1 that is required for RPA foci can form when POH1 is depleted. At 8h post 3Gy in G2, the hollow core where RPA foci form is clearly visible in control cells in both immunofluorescence and 3D model images (Figure 5.19a). Remarkably, following POH1 depletion, the severe RPA foci formation defect seen in these cells coincides with a failure to form a hollow core in 53BP1 IRIF (Figure 5.19a). However, when BRCC36 is also depleted the resection defect of POH1 cells as well as their ability to form a hollow core in 53BP1 IRIF is rescued (Figure 5.19a).

Finally, I tested whether POH1 function is required for the formation of a hollow core in FK2 IRIF since in control cells this occurs at DSBs that undergo resection and repair by HR (Figure 5.15). Following POH1 depletion, G2 phase cells failed to form a hollow core in FK2 IRIF and this coincided with a severe RPA foci formation defect (Figure 5.19b). However, following POH1 and BRCC36 co-depletion,

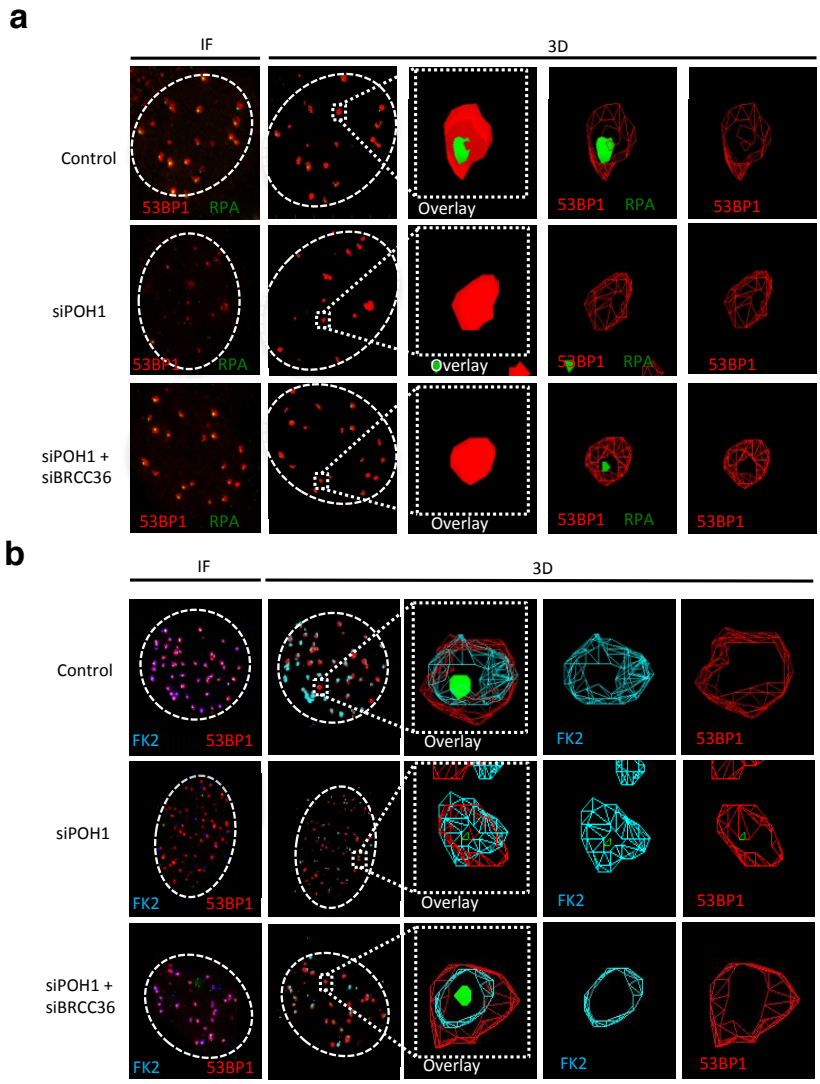

Figure 5.19. POH1 promotes resection in G2 by overcoming the inhibitory barriers of 53BP1 and RAP80. A549 cells were immunostained with the indicated antibodies 8 h post 3Gy IR. G2 cells were selected by CENPF^{+} staining. The far left panels are a projection of the immunofluorescence (IF) Z-stacked images acquired on an Applied Precision® Delta Vision® RT Olympus IX70 deconvolution microscope. These images were converted into a 3D model using the softWoRx® Suite and are shown in the subsequent panels. Individual foci from cells treated with the indicated siRNA were magnified and displayed either as solid or wireframe structures. Wireframe images allow visualisation of the hollow core in 53BP1 and FK2 IRIF where RPA foci form. A devoid core does not form following siRNA POH1 in neither 53BP1 or FK2 IRIF but does form following siRNA BRCC36+POH1.

the RPA foci formation defect was rescued and the FK2 foci contained a hollow core where the RPA foci formed (Figure 5.19b). These findings indicate that the DUB enzyme POH1 is required for the formation of the hollow core in 53BP1 and FK2 IRIF that is required for RPA foci formation. The formation of the hollow core in FK2 IRIF likely represents the disassociation of the RAP80/Abraxas/BRCC36 complex, which is inhibitory to resection.

5.3.1: Discussion

BRCA1 functions in HR downstream of CtIP/MRE11.

In this chapter I have investigated the role of BRCA1 in HR with particular emphasis on the process of resection. Following the contrasting findings that 53BP1 both mediates resection and HR as well as actively inhibiting the process, I aimed to gain insight into the interplay of BRCA1 and 53BP1 during G2 phase HR.

The requirement of BRCA1 for HR has long been established. However, the exact mechanism of its function has remained elusive. Here I initially show that the requirement of BRCA1 for DSB repair is dispensable in G1 where HR is inactive (Figure 5.1). In contrast, BRCA1 function is required for DSB repair in G2 where loss of BRCA1 leads to defective repair of slowly repaired DSBs (Figure 5.1). Importantly in chapter 3, I provide evidence showing that HR repairs DSBs in G2 that arise at HC regions. This is consistent with the widely accepted notion that BRCA1 specifically functions in DSB repair by HR. Moreover, the requirement of BRCA1 cannot be overcome by KAP-1 depletion indicating that its function in the process is distinct to that of 53BP1 (figure 5.1). Whereas 53BP1 depletion impacts upon pKAP-1 IRIF formation and HC relaxation, depletion of BRCA1 is dispensable for pKAP-1 IRIF. In conclusion the role of BRCA1 in G2 phase repair by HR is distinct to the mediator proteins 53BP1, and MDC1 and is not involved in ATM mediated HC relaxation.

To gain insight into the role of BRCA1 in HR, I first used the assays described in chapter 3 for monitoring the formation of HR intermediates to determine which step(s) of the process BRCA1 functions in. Interestingly, BRCA1 depletion leads to a modest defect in resection visualised as reduced RPA foci numbers in G2 cells following IR exposure (Figure 5.4). Additionally, BRCA1 knockdown cells also display

defective Rad51 loading with a marked reduction in foci numbers two hours post 3Gy IR in G2 (Figure 5.4). However, BRCA1 depletion only leads to a twofold reduction in RPA and Rad51 foci unlike the complete loss observed following CtIP depletion (figure 5.4). Moreover unlike CtIP depleted cells where repair can take place by NHEJ since resection is not initiated, BRCA1 depleted cells display a repair defect that likely results from stalled HR (Figure 5.3). This suggests that BRCA1 functions downstream of CtIP in HR.

To try to place BRCA1 function in the HR process, I investigated the impact of CtIP or MRE11 depletion on BRCA1 depleted cells. When CtIP is depleted no repair defect is observed. However MRE11 depletion leads to a repair defect since MRE11 has two functions during G2 phase repair by HR (Figure 5.3). An upstream role in the initiation of resection, and a downstream role as a mediator protein where it bridges the interaction between 53BP1 and pATM and enables pKAP-1 and HC relaxation (Lee *et al*, 2010). Consequently, when MRE11 and KAP-1 are co-depleted no repair defect is observed and repair ensues by NHEJ as resection is not initiated (Figures 5.3 and 5.4). Importantly, CtIP or MRE11/KAP-1 knockdown overcomes the requirement of BRCA1 in G2 phase DSB repair (Figure 5.3). However under these conditions no RPA or Rad51 foci were observed indicating that repair takes place by NHEJ (Figure 5.4). These findings strongly suggest that CtIP/MRN initiate resection and commit the cells to repair by HR. BRCA1 is not required for this initiation step but rather functions downstream to complete resection. A recent study has demonstrated that the E3 ubiquitin ligase RNF169 is recruited to DSBs downstream of RNF8/RNF168 but upstream of 53BP1 and BRCA1. RNF169 inhibits the recruitment of 53BP1 and BRCA1 by binding to ubiquitylated histones and is thought to promote repair by HR (Poulsen *et al*, 2012). One possibility is that by delaying the recruitment of 53BP1, RNF169 enables the CtIP/MRE11 initiation of resection, while BRCA1 functions downstream in the elongation step of the process.

53BP1 depletion rescues the HR defect of BRCA1 knockdown cells in G2.

It was recently proposed that BRCA1 function in HR is to promote efficient resection by overcoming the inhibitory barrier that 53BP1 poses on this process (Bunting *et al*, 2010; Bouwman *et al*, 2010). In these studies monitoring HR in S-phase, 53BP1 depletion restored the HR defect of BRCA1 deficient cells. The notion that 53BP1

actively inhibits resection was surprising as my data from chapter 3 indicates that 53BP1 mediates efficient HR by promoting pKAP-1 foci and HC relaxation. I tested whether in G2 depletion of 53BP1 could overcome the requirement for BRCA1 in HR (Figure 5.5). However, I also had to deplete KAP-1 since in G2, HC structure poses a barrier to HR unlike the situation in S-phase. Strikingly, under these conditions, the γ-H2AX, RPA and Rad51 foci formation defect of BRCA1 depleted cells were rescued indicating that proficient HR repair ensued (Figure 5.5). 53BP1 therefore has two opposing roles in G2 phase HR. On one hand, it inhibits HR by blocking resection while it also enables the accurate completion of HR by mediating KAP-1 dependent HC loosening. Perhaps more importantly, these findings indicate that the function of BRCA1 in HR is the removal of the barrier caused to resection by 53BP1. It seems that 53BP1 forms a barrier to resection downstream of the initiation step which is where BRAC1 function is required. The barrier that 53BP1 poses is not complete since some RPA foci are observed in BRCA1 depleted cells. However the significance of overcoming the partial barrier that 53BP1 poses to resection is demonstrated in BRCA1 depleted/mutated cells where a severe HR defect exists.

BRCA1 promotes relocalisation of 53BP1 in G2 creating a core devoid of 53BP1.

Using high resolution imaging and 3D image processing software I was able to gain insight into the role of BRCA1 in overcoming the inhibitory barrier posed by 53BP1 on resection. It appears that BRCA1 promotes a G2 phase specific relocalisation of 53BP1 to the periphery of IRIF during HR, creating an internal core devoid of 53BP1 (Figure 5.14). Similar results were recently obtained using super-resolution microscopy (Chapman *et al*, 2012). 53BP1 IRIF enlargement and relocalisation is specific to DSBs repaired by HR and is not observed in G1 phase (Figure 5.7). Significantly the formation of an internal core devoid of 53BP1 appears to be important for resection as this is where RPA foci form (Figure 5.14).

In addition to 53BP1, pATM signal is also repositioned and localises externally to 53BP1 on the IRIF periphery. It appears that the retention of activated ATM at DSB sites is important for the completion of resection as addition of the ATMi even up to four hours after damage induction leads to a repair defect in G2 (Figure 5.14). One explanation is that on-going ATM dependent HC relaxation is required until the

completion of HR. In BRCA1 depleted cells pATM IRIF also fail to relocalise although this likely results from deficient 53BP1 relocalisation.

The BRCT but not the RING domain of BRCA1 is required for 53BP1 repositioning during HR.

An important question from the data described above is how BRCA1 mechanistically overcomes the barrier that 53BP1 poses to resection. I suspected that the ubiquitin ligase activity of BRCA1 might be important as FK2 IRIF depicting polyubiquitin chains also become relocalised as HR ensues in a BRCA1 dependent manner (Figure 5.14). I postulated that BRCA1 might drive 53BP1 repositioning away from the DSBs ends by on-going ubiquitylation. Moreover, a recent study reported that BRCA1 can ubiquitylate H2A and carries out this modification during its role in HC maintenance (Zhu *et al*, 2011). To gain insight into this, I tested whether the BRCT or RING domains of BRCA1 are required for this function. The RING domain of BRCA1 is the catalytic domain of its ubiquitin ligase activity whereas the BRCT domains are responsible for its phosphoprotein interactions. I tested 53BP1 IRIF volume in MEFs expressing either RING or BRCT mutant BRCA1 and compared it to WT MEFs. Surprisingly, the ubiquitin ligase activity of BRCA1 was dispensable for this process whereas the BRCT mutant MEFs failed to relocalise 53BP1 to the same extent as the WT cells (Figure 5.15). These findings strongly suggest that BRCA1 does not directly promote 53BP1 relocalisation via its ubiquitin ligase activity but rather promotes the process via its interaction with one or more of its interacting factors.

To determine whether any of the BRCA1 interacting factors is required for 53BP1 relocalisation, I depleted several of these factors. First I investigated the impact of BRCC36 or RAP80 depletion on 53BP1 IRIF foci volume (Figure 5.16). However BRCC36 depletion had no effect on 53BP1 IRIF relocalisation in G2 and the foci in these cells were indistinguishable to those in control cells (Figure 5.16). RAP80 is another factor that interacts with BRCA1 and targets it to ubiquitylated histones flanking DSBs via its ubiquitin interacting motif (UIM) (Sobhian *et al*, 2007). Since RAP80 impacts on BRCA1 recruitment and BRCA1 dependent resection I reasoned that it might also impact on BRCA1's ability to relocalise 53BP1. However, depletion of RAP80 did not impact on 53BP1 IRIF volume in G2 and the foci in these cells were indistinguishable to those in control cells (Figure 5.16).

Next I tested the effect of BACH1 knockdown on BRCA1's ability to relocalise 53BP1. BACH1 is a helicase that interacts with BRCA1 so it is plausible that BACH1 mediated DNA unwinding might be necessary for resection and consequently 53BP1 IRIF expansion (Huen *et al*, 2009). However BACH1 depletion by siRNA also did not impact on 53BP1 IRIF relocalisation in response to IR in G2 (Figure 5.16).

The deubiquitinating enzyme POH1 is required for resection and 53BP1 repositioning in G2.

The BRCA1a complex is comprised of BRCA1, RAP80, Abraxas, BRCC36, NBA1 and BRCC45 (Huen *et al*, 2009). The complex is targeted to DSBs by RAP80 binding to ubiquitylated histones via its UIM (Sobhian *et al*, 2007). Previous studies have indicated that RAP80 binding to ubiquitylated histones is inhibitory to resection and functions to counteract BRCA1 function and prevent excessive resection (Hu *et al*, 2011). Consistent with this, depletion of RAP80 leads to elevated levels of BRCA1 mediated resection. Moreover, disruption of the BRCA1a complex by depletion of either Abraxas or BRCC36 also leads increased resection thought to result from loss of RAP80 from ubiquitylated histones. The inhibitory function of RAP80 on resection needs to be overcome for the process to ensue however how this is achieved is currently unclear. From my data in this chapter I propose a model whereby the DUB enzyme POH1 promotes RAP80 disassociation from ubiquitylated histones thereby enabling resection. Consistent with this model, siRNA depletion of POH1 leads to a marked defect in RPA foci formation following IR in G2 (Figure 5.18). Moreover, I propose that POH1 DUB activity is required to form the hollow core observed in 53BP1 and FK2 IRIF, which is required for RPA foci formation. POH1 deubiquitylation of histone H2A likely leads to disassociation of RAP80 and 53BP1 from these regions thus overcoming their inhibitory role on resection. Once RAP80 disassociation is achieved, then histone eviction/degradation or sliding can take place so resection can ensue. Interestingly, when RAP80 is depleted or when the BRCA1a complex is disrupted by Abraxas of BRCC36 depletion, POH1 function becomes redundant for RPA foci formation. This finding suggests that when ubiquitylated histones are not protected by RAP80 binding to them, they can be evicted/degraded and resection can take place. However, although RAP80/Abraxas/BRCC36 can overcome the requirement for POH1

in RPA foci formation, this is not the case for Rad51 foci. This suggests that POH1 has a direct role in Rad51 loading, possibly by recruiting the BRCA2-co-factor DSS1.

In addition to being disassociated from the IRIF core, 53BP1 also needs to be repositioned away from DSB ends in order for resection and HR to ensue. My data from this chapter indicate that 53BP1 repositioning requires BRCA1 function, consistent with published data showing that BRCA1 overcomes the 53BP1 inhibition of resection (Bunting *et al*, 2010; Bouwman *et al*, 2010). More specifically, my data reveal that 53BP1 repositioning requires the BRCT domain of BRCA1 but that the ubiquitin ligase activity of BRCA1 is dispensable for this process (Figure 5.16). However, despite the ubiquitin ligase activity of BRCA1 not being required for 53BP1 repositioning, in the absence of BRCA1, FK2 IRIF also fail to reposition. I interpret this finding to suggest that 53BP1 repositioning away from DSB ends is driven by on-going ubiquitylation that is driven by BRCA1 although it might not be the E3 ligase carrying out this modification. There are several ubiquitin ligases that function in the DDR including RNF8/RNF168, Rad18 and HERC2. One, or more, of these ligases might be involved in 53BP1 repositioning but testing this is difficult since depletion of some of these ligases leads to loss of 53BP1 foci formation. It is currently unclear how the BRCT domain of BRCA1 functions to overcome the barrier posed by 53BP1, although an interaction with POH1 and an E3 ligase is likely. In support of this model, co-immunoprecipitation experiments carried out by the Morris laboratory revealed that POH1 and BRCA1 interact following DSB induction (Morris et al unpublished).

Deciphering the mechanism behind BRCA1 dependent 53BP1 repositioning during HR is a difficult task. There are many factors that contribute to this. First it is highly likely that there are currently unidentified BRCA1 interacting factors that might play a role in this process. Secondly, even if these factors were to be identified there might be functional redundancy amongst them, which means that the requirement of one might be overcome by the function of another. Indeed this could well be the case for some of the BRCA1 interacting factors tested in this chapter. However, concurrent depletion of multiple factors especially in BRCA1 depleted cells makes analysis extremely difficult due to toxicity and a small G2 population. Recently, processes in the DDR that are regulated by multiple and simultaneous post-translational modifications including ubiquitylation and sumoylation have been described. Indeed both BRCA1 and 53BP1 have been shown to be sumo-modified in response to DSB induction so it is possible that the factors responsible for these modifications are required to help

overcome the barrier that 53BP1 poses to resection (Galanty *et al*, 2009; Morris *et al*, 2009). Given the central role that BRCA1 plays in HR it is unlikely that its sole function is to relocalise 53BP1. However, it is now clear that this is a necessary step and consolidating how BRCA1 achieves this is an important future question.

Model for the roles of 53BP1, BRCA1 and POH1 in HR.

The question of how 53BP1 becomes repositioned during HR is an important one, but equally important is understanding why the retention of 53BP1 on the IRIF periphery is required for efficient HR. Our findings indicate that following exposure to γ-radiation in G2, DSBs at HC regions are predominantly repaired by HR with slow kinetics. ATM dependent pKAP-1 formation is required for HR repair of such DSBs as it leads to the HC relaxation required to make the chromatin region accessible. In HR, the undamaged template on the sister chromatid is used to fill in the resected regions and to accurately repair the break (Diagram 5.2a). However if a DSB is in an HC region it is likely that the homologous region on the sister chromatid will also be heterochromatic and access will necessitate chromatin relaxation. I propose that the G2 phase specific enlargement of 53BP1 and pATM during HR represents chromatin modifications on the undamaged template. The repositioning of the ubiquitin modifications likely drives the 53BP1 repositioning although this process doesn't require BRCA1's RING domain. The ability of 53BP1 to oligomerise is likely important for its ability to encompass the damaged and undamaged templates and its BRCT domain is important for pATM retention and HC relaxation. In the core of the IRIF, the creation of a 53BP1 devoid region is BRCA1 and POH1 dependent and necessary for the completion of resection (Diagram 5.2b). BRCA1 and 53BP1 therefore cooperate in G2 phase HR to ensure that resection is efficiently completed and to carry out the necessary chromatin modifications.

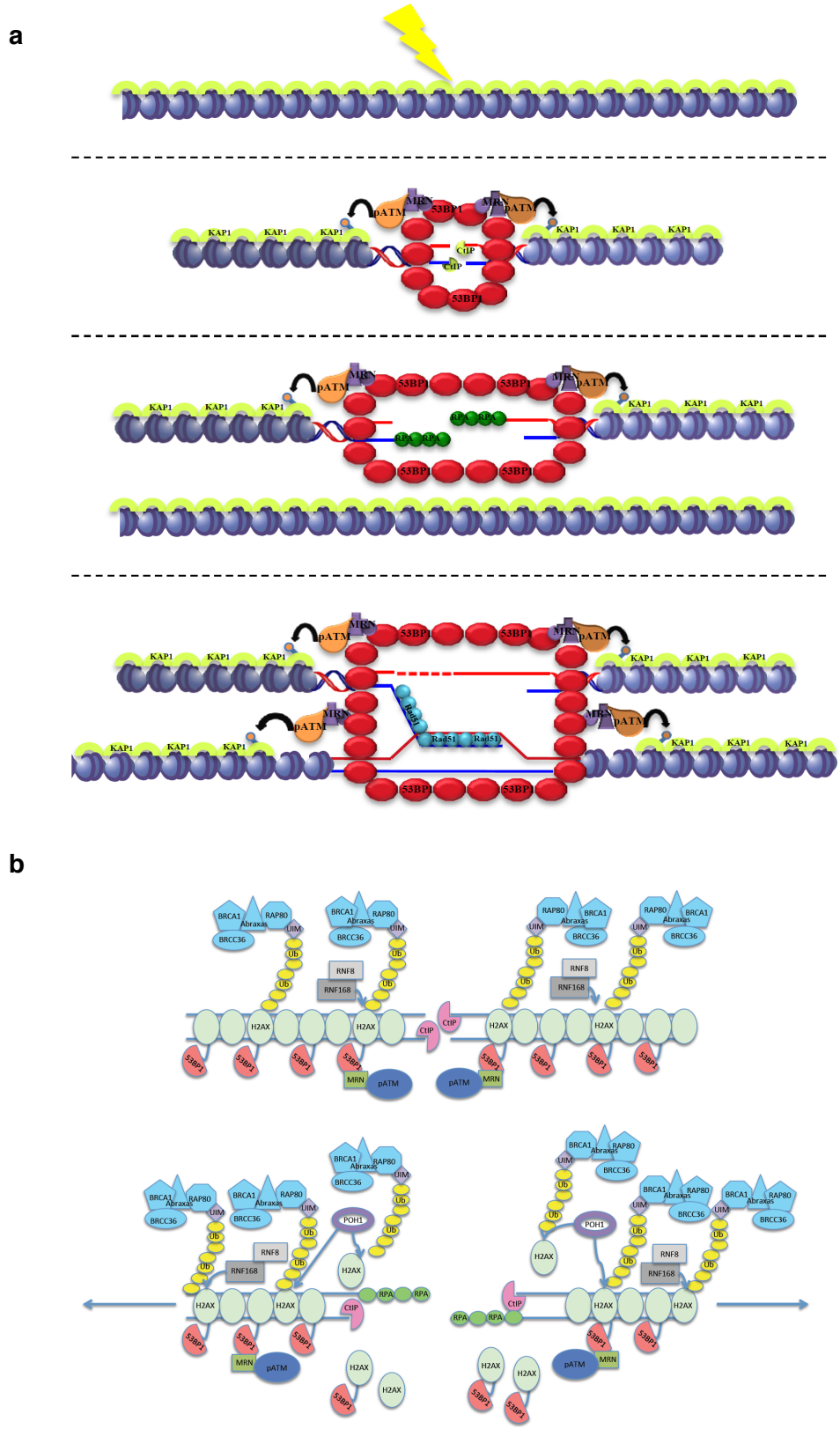

Diagram 5.2: **Model showing the expansion of 53BP1 foci in G2 phase and the formation of an IRIF core devoid of 53BP1 and FK2 where RPA foci form.**
a) Model showing the requirement for 53BP1 to affect HC changes on the undamaged sister chromatid. The slowly repaired DSBs that arise within regions of heterochromatin (HC) undergo resection and repair by HR (HC is depicted in green). In early G2 phase (30 min post IR), 53BP1 foci form around the DSB on a single DNA molecule similar to the situation in G1 phase. 53BP1 is likely not located at the extreme DNA end. 53BP1 interacts with RAD50 of the

MRN complex; NBS1 of the MRN complex interacts with ATM. Thus, ATM tethering at the DSB is enhanced by the presence of 53BP1 foci (interactions between MRN and MDC1 or H2AX also enhance ATM tethering but 53BP1 appears to be critical for the presence of pATM foci at DSBs). ATM phosphorylates KAP-1 located at HC-DSBs in a concentrated manner producing pKAP-1 foci (note that pan-nuclear pKAP-1 also occurs at early times post IR but this is not 53BP1-dependent; in contrast the formation of pKAP-1 foci, which only form at HC-DSBs is 53BP1-dependent). This causes HC-relaxation in the vicinity of the DSB (not depicted in the figure). HC forms a partial barrier to resection that is overcome by 53BP1-ATM pKAP-1 foci formation. The presence of 53BP1 on the DNA molecule also forms a partial barrier to the completion of resection and a bigger barrier to RAD51 loading. However, neither 53BP1 nor KAP1 prevent the initiation of resection by CtIP-MRN, since they function downstream of CtIP-MRN dependent commitment to HR and since RPA foci numbers are only partially reduced. Later in G2 (evident at 2 h), further resection ensues followed by the single stranded DNA overhang with bound RPA and/or RAD51 invading the undamaged sister template. 53BP1 foci formation expands to allow further resection and to encompass the undamaged DNA molecule, resulting in a two fold expansion in foci volume. The expansion of 53BP1 foci requires the BRCT but not the RING finger domain of BRCA1 and involves repositioning of ubiquitin modifications on histones. Thus, we propose that BRCA1 promotes deubiquitination and/or proteasome mediated protein degradation in the core region and new ubiquitin events on the damaged and, we propose, the undamaged molecule. For simplicity this has not been depicted in the figure. The presence of 53BP1 on the undamaged strand allows pKAP1 formation and hence HC relaxation on this strand, which promotes the completion of resection and/or RAD51 loading. We have depicted 53BP1 as entirely encircling the DNA molecule although its initial tethering involves interactions with methylated H4. This is consistent with evidence that 53BP1 undergoes oligomerisation and has a role in synapsis during long range V(D)J recombination (Adams et al, 2005; Difilippantonio et al, 2008). In G2 phase, 53BP1 may also enhance synapsis but this does not appear to be essential since HR can ensue in the absence of 53BP1+BRCA1. We suggest that the close association of sister chromatids in G2 phase via cohesin interactions can function redundantly to 53BP1-dependent synapsis in G2 phase. Thus, 53BP1-dependent synapsis is only essential for long-range translocation events in G1 phase.

b) Model showing the role of POH1 in removing 53BP1 from the foci core region.

Previous studies have demonstrated that 53BP1 and RAP80 form a restrictive barrier to resection by binding to methylated and ubiquitylated histones at DSBs. The BRCT domain of BRCA1 is required for 53BP1 repositioning away from the DSB ends as well as for the formation of an IRIF core devoid of 53BP1 where resection occurs. Similarly, the BRCT domain of BRCA1 is also required for the formation of an IRIF central core devoid of ubiquitin modifications. We propose that BRCA1 achieves this via the recruitment of the deubiquitinating enzyme POH1which functions to promote the removal of 53BP1 and ubiquitin chains but is dispensable for 53BP1 repositioning to the foci periphery. POH1 DUBing might lead to histone degradation thus exposing DNA to the nucleases which carry out the elongation step in resection.

CHAPTER 6

Transcriptional silencing at DSBs requires ATM and RNF8 as well as the chromatin remodellers BAF180 and CHD7

6 Transcriptional silencing at DSBs requires ATM and RNF8 as well as the chromatin remodellers BAF180 and CHD7

6.1: Introduction

Repair of DNA damage occurs within the context of chromatin and it is becoming increasingly evident that the ability to modify chromatin can greatly impact on repair efficiency. As discussed in previous chapters, post translational modification of chromatin components (γ-H2AX, uH2A, pKAP-1) are particularly important in dense HC regions where chromatin compaction poses a barrier to repair. Conversely, in EU regions, posttranslational modifications are also required for efficient DSB repair and for interfacing repair with other DNA metabolic processes such as transcription (Zhu *et al*, 2007; Zhou *et al*, 2009). The process of transcription, like other process where access to DNA is required, is associated with chromatin decondensation (Müller *et al*, 2001). It has been suggested that chromatin decondensation at transcriptionally active EU regions needs to be inhibited in the presence of DNA damage but until recently no evidence existed for this model. In support of such a model, post-translational modifications such as histone H2A ubiquitylation have been shown to be important in both DNA repair and transcriptional repression(Ulrich & Walden, 2010; Wang *et al*, 2004). This model suggests that transcription associated chromatin decondensation in the presence of DNA damage might lead to erroneous repair and is therefore inhibited.

The idea that transcription is inhibited in the presence of DNA damage is conceptually appeasing. However, how this inhibition is regulated is not clear. Until recently it was also not clear whether transcription is globally inhibited in the presence of DNA damage or whether this is restricted to DNA damage sites (Shanbhag *et al*, 2010). Recently, the Greenberg laboratory developed an elegant reporter system that they used to gain insight into the regulation of transcription in *cis* to DSBs. The authors hypothesised that there might be a link between the ubiquitylation events at DSB sites and the ubiquitylation events leading to the inhibition of transcription. They reasoned that since posttranslational modifications spread megabases from DSBs that these may lead to the inhibition of transcription within these regions (Rogakou *et al*, 1999). To address these questions they integrated a reporter system at a single site in the U2OS cell line.

The reporter system provided concomitant read outs for DSB induction as well as active transcription. It consists of a lac operator array that is bound by the lac repressor protein following its expression. The lac repressor protein was tagged with the fluorescent protein mCherry thus allowing visualisation of the reporter site. A CMV promoter drives the expression of a CFP-tagged peroxisomal targeting peptide that accumulates in the cytoplasm and provides a read out for protein production. The expression of this protein can be controlled via a 4kb region of tandem tetracycline response elements located between the promoter and the operator sequences that bind a doxycycline-inducible transactivator. Following doxycycline treatment, the tetracycline-controlled transcactivator binds to the tetracycline response elements and activates transcription. In addition to monitoring protein production, nascent transcript can also be visualised by YFP tagged MS2 viral coat protein. The reporter transcript contains 24 repeats of stem loop structures that are bound to by YFP-MS2 thus allowing visualisation of the nascent transcript.

In order to assess the impact of DSB induction on transcription, the authors fused the nuclease domain of the FOK1 endonuclease to the mCherry-LacI construct. Following expression of this construct, DSBs are produced in the lac operator sequence thus at a distance of 4-13 kb from the promoter. By simultaneous expression of the mCherry-LacI-FOK1 construct and the tetracycline-controlled transactivator, the impact of DSBs on transcription within a 4-13 kb distance from the DSB sites could be assessed. Strikingly, a 4 to 10 fold reduction in nascent transcript levels was observed following DSB induction, compared to cells where transcription was induced but no DSBs were created. Importantly, enrichment of γ-H2AX was observed across the reporter locus by ChIP, indicating that DSB induced chromatin modifications spread across the region separating the DSBs and the transcription sites.

Next the authors used radiation exposure and laser micro-irradiation to assess whether the inhibition of transcription following DSB induction is a global phenomenon or restricted to DSB sites. Perhaps surprisingly, they observed that nascent transcript levels from their reporter system were not affected by exposure to IR or micro-irradiation strongly suggesting that transcriptional silencing only occurs in *cis* to DSBs. These results indicate that the expansion of chromatin posttranslational modifications away from DSBs lead to transcriptional silencing within these regions. By quantifying the FOK1 locus area following doxycycline induced transcription, the authors also demonstrated that chromatin is decondensed at transcription sites. However upon

induction of DSBs chromatin decondensation as well as well as transcription is inhibited.

6.1.2: Histone H2A ubiquitylation and ATM are required for DSB associated transcriptional silencing.

The ubiquitylation of histone H2A has previously been linked to transcriptional silencing (Wang *et al*, 2004). As mentioned above, using their reporter system Shanbhag et al observed γ-H2AX spreading across the reporter locus located between 4-13 kb from the sites of DSB induction (Shanbhag *et al*, 2010). To test whether DSB induced histone ubiquitylation also spreads over the same region, they used ubiquitin specific antibodies and observed an enrichment of ubiquitin modified H2A as well as K48 and K63 conjugate polyubiquitin chains at the reporter site. This finding indicates that the transcriptional repression observed in *cis* to DSB sites may be regulated via the spreading of ubiquitin modifications away from the DSB sites.

ATM has many roles in the DDR to DSBs that include the modification of chromatin topography to facilitate efficient repair (Lavin, 2008). Work from our laboratory has demonstrated that ATM plays a central role in regulating the chromatin decondensation that needs to occur for the repair of DSBs located within HC regions (Goodarzi *et al*, 2008). Following the observation that transcription associated chromatin decondensation in *cis* to DSB sites is inhibited, Shanbhag et al questioned whether ATM is required for this process. Remarkably, ATMi treatment led to defective inhibition of transcription following the induction of DSBs. In addition, the inhibition of transcription associated chromatin decondensation also failed following ATMi treatment. Although ATM activity is not directly required for histone H2A ubiquitylation, the maintenance of this modification was greatly defective in ATMi treated cells. The mechanism of ATM dependent transcriptional repression is not clear from these findings but ATM activity and histone H2A ubiquitylation appear to play a central role.

As discussed in chapter 4, RNF8 and RNF168 are two of the E3 ubiquitin ligases that carry out the ubiquitylation modifications at DSB sites (Mailand *et al*, 2007; Huen *et al*, 2007; Doil *et al*, 2009). Since histone H2A is a well-characterised target of these ligases, Shanbhag et al tested the effect of RNF8 and/or RNF168 depletion on transcriptional silencing using their reporter system. When they depleted each ligase

alone they did not a great effect, but joint depletion led to a significant defect in transcriptional silencing. Interestingly, the reversal of histone H2A ubiquitylation by the DUB USP16 led to the restoration of transcription.

Overall, Shanbhag et al demonstrated that transcription and chromatin decondensation are inhibited in *cis* to DSBs through histone H2A ubiquitylation. Moreover, ATM function is required to inhibit chromatin decondensation and to maintain the RNF8/RNF168 mediated H2A ubiquitylation until repair is completed. However, although great insight into the roles of these factors has been gained, many future questions remain. Firstly, it is not clear how ATM maintains histone H2A ubiquitylation or how it inhibits transcription associated chromatin decondensation. ATM might manipulate chromatin structure directly as in HC repair via KAP-1 phosphorylation or indirectly via chromatin remodellers. Secondly, it is not clear whether there is an impact on the ability to repair DSBs when transcription is not efficiently inhibited. By using the reporter system acquired from the Greenberg laboratory, and other functional assays, I attempted to gain insight into the roles of ATM, RNF8 and chromatin remodellers in the inhibition of transcription in *cis* to DSBs and the repair of these lesions.

6.1.3: Chromatin remodelling at DSBs

The efficient formation of pKAP-1 foci following IR exposure is dependent upon ATM function and is a prerequisite for repair at HC regions. However until recently the mechanism by which pKAP-1 foci formation leads to HC relaxation was unclear. As discussed in the introductory chapter, chromatin structure impacts upon DNA metabolic processes and there are several lines of evidence indicating that facultative HC offers a level of control over gene expression (Dillon & Festenstein, 2002). This dense structure is assembled and maintained by the concomitant function of enzymes that remove transcription associated chromatin modifications and by chromatin remodellers that densely pack nucleosomes. Histone acetylation is associated with transcription while histone methylation is predominately associated with the repression of transcription. Consistently, HC regions are enriched for methylation associated posttranslational modifications (Dillon & Festenstein, 2002).

Recent work from our laboratory investigated the changes in the histone posttranslational modification landscape specifically at HC DSBs (Goodarzi *et al*,

2011). Perhaps surprisingly; no changes in HC acetylation or methylation were detected following exposure to IR. This does not necessarily indicate that these changes do not take place as the high stoicheometric background of these modifications rendered the detection of IR induced changes by immunofluorescence difficult. In the same study the impact of pKAP-1 formation on chromatin remodellers leading to HC compaction was also investigated. The nucleosome remodelling and deacetylase complex (NuRD) is a well-characterised ATP-dependent complex that promotes heterochromatinisation via nucleosome compaction (Denslow & Wade, 2007). This function is achieved via the direct interaction of the NuRD complex with KAP-1 (Schultz *et al*, 2001). Specifically, the CHD3 component of the NuRD complex binds to autosumoylated KAP-1 via its SUMO interaction motif. Following exposure to IR, ATM phosphorylation of KAP-1 leads to the generation of a motif that abolishes the CHD3 KAP-1 SIM-SUMO interaction and CHD3 becomes disassociated from HC (Goodarzi *et al*, 2011). This leads to a loss of HC compaction, which allows repair to take place and is only re-established following the completion of repair and KAP-1 de-phosphorylation.

Following the observation that ATM is required for transcriptional silencing and the inhibition of the associated chromatin decondensation, I reasoned that this process might also be achieved via chromatin remodelling complexes.

The SWI/SNF chromatin remodelling complexes have been implicated in both the DDR and transcriptional regulation (Tang *et al*, 2010). These complexes alter chromatin structure by manipulating nucleosomes via their ATP-dependent nucleosome remodelling activity (Xu & Price, 2011). They are involved in a diverse set of processes by sliding and ejecting nucleosomes, but do not appear to function in chromatin assembly. The RSC complex is a yeast chromatin-remodelling complex that is homologous to mammalian SWI/SNF-b or PBAF (Diagram 6.1) (Table 6.1) (Clapier & Cairns, 2009). RSC has an important role in transcriptional regulation but also functions in several DDR pathways (Kent *et al*, 2007). RSC exists as two isoforms that differ on whether Rsc1 or Rsc2 are present (Diagram 6.1). Mutant strains of both rsc1 and rsc2 display defective NHEJ activity, while Rsc1 but not Rsc2 is required for nucleosome sliding at DSBs sites, a process that seems to require its bromo-adjacent homology (BAH) domain (Chambers *et al*, 2012). RSC utilises its ATPase activity to modify nucleosomes at DSBs but until recently little was known about the functional

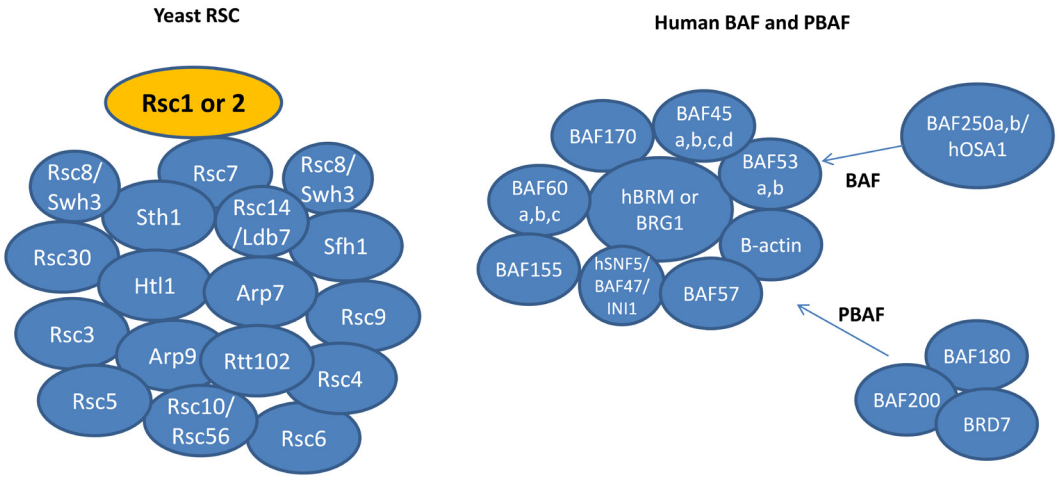

Diagram 6.1: Schematic representation of the yeast RSC and human BAF/PBAF chromatin remodelling complexes.
Yeast RSC comprises of 17 subunits and functions in DNA repair pathways as well as in transcriptional regulation. There are two isoforms of the RSC complex, one that contains Rsc1 and the other Rsc2. The homologous complex in humans is PBAF. PBAF contains BAF180, which is a fusion of yeast Rsc1, Rsc2 and Rsc4. The PBAF complex functions in transcriptional regulation but a role in DNA repair has not been described. Adapted from (Kasten *et al*, 2011).

Family and composition		Organisms								
		Yeast			Fly			Human		
SWI/SNF	**Complex**	**SWI/SNF**		**RSC**	**BAP**		**PBAP**	**BAF**		**PBAF**
	ATPase	Swi2/Snf2		Sth1	BRM/Brahma			hBRM or BRG1		BRG1
	Noncatalytic homologous subunits	Swi1/Adr6			OSA/eyelid			BAF250/hOSA1		
							Polybromo BAP170			BAF180 BAF200
		Swi3		Rsc8/Swh3	MOR/BAP155			BAF155, BAF170		
		Swp73		Rsc6	BAP60			BAF60a or b or c		
		Snf5		Sfh1	SNR1/BAP45			hSNF5/BAF47/INI1		
					BAP111/dalao			BAF57		
		Arp7, Arp9			BAP55 or BAP47			BAF53a or b		
					Actin			β-actin		
	Unique	[a]		[b]						
ISWI	**Complex**	**ISW1a**	**ISW1b**	**ISW2**	**NURF**	**CHRAC**	**ACF**	**NURF**	**CHRAC**	**ACF**
	ATPase	Isw1		Isw2	ISWI			SNF2L	SNF2H[c]	
	Noncatalytic homologous subunits			Itc1	NURF301	ACF1		BPTF	hACF1/WCRF180	
						CHRAC14			hCHRAC17	
						CHRAC16			hCHRAC15	
					NURF55/p55			RbAp46 or 48		
	Unique	Ioc3	Ioc2, Ioc4		NURF38					
CHD	**Complex**	**CHD1**			**CHD1**	**Mi-2/NuRD**		**CHD1**	**NuRD**	
	ATPase	Chd1			dCHD1	dMi-2		CHD1	Mi-2α/CHD3, Mi-2β/CHD4	
	Noncatalytic homologous subunits					dMBD2/3			MBD3	
						dMTA			MTA1,2,3	
						dRPD3			HDAC1,2	
						p55			RbAp46 or 48	
						p66/68			p66α,β	
	Unique								DOC-1?	
INO80	**Complex**	**INO80**		**SWR1**	**Pho-dINO80**	**Tip60**		**INO80**	**SRCAP**	**TRRAP/Tip60**
	ATPase	Ino80		Swr1	dIno80	Domino		hIno80	SRCAP	p400
	Noncatalytic homologous subunits	Rvb1,2			Reptin, Pontin			RUVBL1,2/Tip49a,b		
		Arp5,8		Arp6	dArp5,8	BAP55		BAF53a		
		Arp4, Actin1			dActin1	Actin87E		Arp5,8	Arp6	Actin
		Taf14		Yaf9		dGAS41			GAS41	
		Ies2,6						hIes2,6		
				Swc4/Eaf2		dDMAP1			DMAP1	
				Swc2/Vps72		dYL-1			YL-1	
				Bdf1		dBrd8				Brd8/TRC/p120
				H2AZ,H2B		H2Av,H2B			H2AZ,H2B	
				Swc6/Vps71					ZnF-HIT1	
						dTra1				TRRAP
						dTip60				Tip60
						dMRG15				MRG15 MRGX
						dEaf6				FLJ11730
						dMRGBP				MRGBP
						E(Pc)				EPC1, EPC-like
						dING3				ING3
	Unique	Ies1,Ies3-5,Nhp10		Swc3,5,7	Pho			[d]		

[a]Swp82, Taf14, Snf6, Snf11.
[b]Rsc1 or Rsc2, Rsc3-5, 7, 9, 10, 30, Htl1, Ldb7, Rtt102.
[c]In addition, SNF2H associates respectively with Tip5, RSF1, and WSTF to form **NoRC**, **RSF,** and **WICH** remodelers.
[d]Amida, NFRKB, MCRS1, UCH37, FLJ90652, FLJ20309.

Table 6.1: Remodeller composition and orthologous subunits (Clapier & Cairns, 2009)**.**

importance of its BAH domain. Work form the Downs laboratory recently described a mechanism whereby the RSC complex binds to chromatin (histone H3) via the (BAH) domain in the Rsc2 subunit. Importantly, site directed mutations in the BAH domain led to impaired Rsc2 chromatin association and compromised the function of RSC in rDNA silencing, transcriptional regulation and the DDR (Chambers et al unpublished).

The BAH domains of the yeast RSC complex are conserved in the mammalian PBAF homologue. However, the BAH domains of Rsc1, and Rsc2 exist on a single protein called BAF180, which appears to be a fusion of Rsc1, Rsc2 and Rsc4 (Goodwin & Nicolas, 2001; Mohrmann & Verrijzer, 2005). Site directed mutations in the conserved BAH domains of BAF180 also lead to a reduction in chromatin binding affinity (Chambers et al unpublished). It is not clear whether the roles of Rsc1, 2 and 4 in transcriptional regulation and the DDR are functionally conserved in BAF180 and whether these require the BAH domains. Interestingly, BAF180 was previously identified as an ATM phosphorylation target in a large proteomics study (Matsuoka *et al*, 2007). However, the role of this modification in the DDR has not been characterised.

Functional studies examining the role of BAF180 in maintaining genomic stability are clinically significant as it is frequently mutated in cancer (Xia *et al*, 2008; Varela *et al*, 2011). It is currently unclear exactly how BAF180 functions to prevent carcinogenesis. BAF180 is thought to bind to promoter regions of genes involved in genome maintenance via its bromodomains, where, as part of the PBAF complex it regulates the expression of these genes (Brownlee *et al*, 2012). Consistent with this notion, disruption of the BAF180 or BRD7 subunits of the PBAF complex, lead to defective replicative senescence and checkpoint activation due to impaired p53 transcriptional activity (Xia *et al*, 2008; Burrows *et al*, 2010). To date no published studies have addressed whether BAF180 has a direct role in DNA repair. Given the established role of RSC in the DDR and the fact that ATM phosphorylates BAF180 in response to DNA damage, I decided to investigate the role of BAF180 in DSB repair and in transcriptional repression in *cis* to DSBs.

6.2: Results

6.2.1: RNF8 is required is for efficient DSB repair in euchromatin.

In chapter 4, I investigated the role of RNF8 in the repair of HC DSBs by HR in G2. Previous work from our laboratory has also investigated the requirement for RNF8 in DSB repair in G1 (Noon *et al*, 2010). In both G1 and G2, RNF8 functions in the slow component of DSB repair that corresponds to DSBs located at HC regions. In G1 phase, RNF8 promotes the repair of these breaks by mediating ATM dependent HC loosening while in G2 it has an additional role in promoting RPA and Rad51 foci formation. Paradoxically, the work from Shanbhag et al suggests that RNF8 ubiquitin ligase activity also functions to silence transcription in *cis* to DSBs via a pathway that also involves ATM. However, DSBs in *cis* to transcriptionally active regions are likely to be located in EU not in HC. Following exposure to γ-radiation, approximately 20% of induced DSBs are located at HC regions, which corresponds with approximately 20% of mammalian genomes being heterochromatic (Goodarzi *et al*, 2008). MEFs form distinct chromocenters in G1 that can be visualised by DAPI staining and are understood to represent dense HC regions (Guenatri *et al*, 2004). Using chromocenters as an HC marker we can visualise whether a break is in HC or EU by analysing the position of γ-H2AX foci relative to the chromocenters (Figure 6.1a). Using this system, previous work from our laboratory has demonstrated that loss of ATM or any of the mediator proteins in G1 phase leads to a DSB repair defect in the slow component of repair and that these remaining foci co-localise with HC regions (Figure 6.1b) (Goodarzi *et al*, 2008). However, no requirement for the repair of EU breaks that are repaired with fast kinetics has been observed for ATM or the mediator proteins. Particularly in the first hour post DSB induction, no significant change in the number of breaks located at HC regions is observed, indicating that repair of DSBs at these early times only represent repair in EU (Figure 6.1c).

In the past, attempts were made to assess whether ATM is required for the repair of DSBs at very early times post irradiation. However, this was not possible by using γ-H2AX foci as a surrogate marker for DSBs. ATM directly phosphorylates histone H2AX at DSB sites and although DNA-PK can carry out this modification in ATM deficient cells, the foci that form are smaller and can not be accurately compared to those in ATM proficient cells (Stiff *et al*, 2004). Since RNF8 does not affect histone

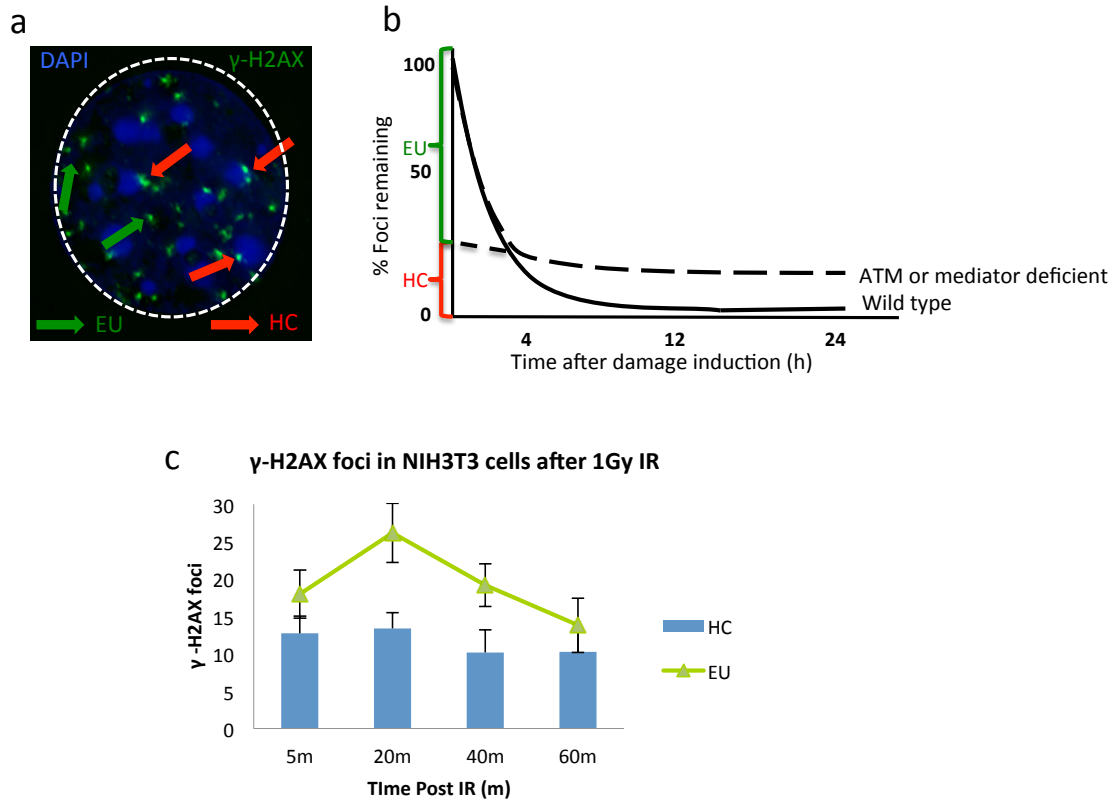

Figure 6.1: DSB repair in EU and HC following IR exposure.
NIH3T3 cells were seeded and allowed to enter G0 by contact inhibition. The cells were then irradiated with 1Gy IR and harvested at the indicated time points. Fixed cells were then immunostained with a γ-H2AX antibody and DAPI and imaged on a fluorescent microscope. a) Representative immunofluorescence image of a cell harvested at 30m post 1Gy IR. Red arrows indicate γ-H2AX foci associated with DAPI chromocenters depicting HC, while green arrows indicate γ-H2AX in EU. b) Schematic of DSB repair over time after IR exposure. At early times post IR, EU DSBs are repaired with fast kinetics and their repair is completed by 4h post 3Gy IR. DSBs associated with HC are repaired with slower kinetics and require ATM and the mediators for efficient repair. c) During the first 60m post 1Gy IR, predominantly DSBs in EU are repaired. γ-H2AX foci were enumerated in 30 cells per time-point and the data represent the mean and standard deviation of three independent experiments.

H2AX phosphorylation but appears to function in the ATM pathway leading to transcriptional silencing at DSB sites, I decided to investigate the requirement of RNF8 for repair of DSBs at very early time points post the induction of damage (Figure 6.2). Strikingly, RNF8 knockdown led to a repair defect at early times post 1.5Gy IR treatment with the biggest difference being observed at the 20 and 40-minute time points. However, by 60 minutes post IR treatment, the number of γ-H2AX foci in RNF8 knockdown cells were almost at the same level as that observed in control cells consistent with previous findings whereby no repair defect was observed in the fast component of repair. The repair defect/delay at the very early time points in RNF8 knockdown cells was not previously observed and we considered might result from an inability to efficiently silence transcription in EU.

a

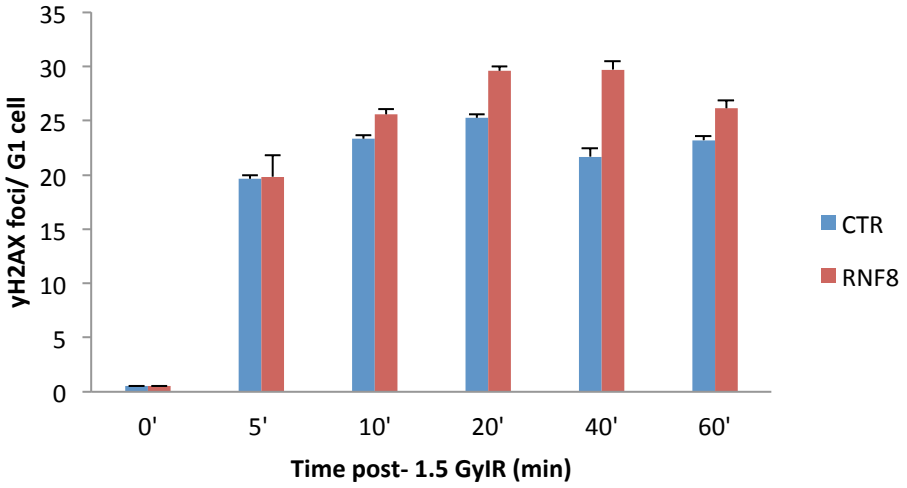

Figure 6.2: RNF8 is required for DSB repair at early times post IR.
1BrhTERT cells were treated with control or RNF8 siRNA and were irradiated with 1.5Gy IR. The cells were then harvested at the indicated time points and immunostained with CENP-F and γ-H2AX antibodies. G1 phase cells were identified by negative CENP-F staining and the cell nuclei were visualized by DAPI. γ-H2AX foci were enumerated specifically in CENP-F negative cells. γ-H2AX foci were enumerated in 30 cells per time-point and the data represent the mean and standard deviation of three independent experiments.

6.2.2: RNF8 functions in the same pathway as ATM leading to transcriptional silencing in *cis* to DSBs.

Once I acquired the reporter system from the Greenberg laboratory, I first tested whether I could reproduce their transcriptional silencing defect following ATMi inhibition (Figure 6.3). As expected, doxycycline treatment drove the expression of the CFP-tagged peroxisomal targeting peptide and nascent transcripts were detected by YFP in 80 – 90 % of cells (Figure 6.3). However, when the FOK1 endonuclease was activated by transfection, the resulting DSBs led to transcriptional silencing across the reporter region and an almost complete loss of nascent transcripts was observed (Figure 6.3).

Next I assessed the effect of ATMi inhibition and/or RNF8 depletion on transcriptional silencing following DSB induction. Consistent with the data from Shanbhag et al, following ATMi treatment there was no significant reduction in the number of cells with nascent transcripts following DSB induction indicating deficient transcriptional silencing. Additionally, when RNF8 was depleted I observed a significant defect in the inhibition of transcription following DSB induction although this was not as severe as that of ATMi treated cells. The defect observed in RNF8 depleted cells was greater however than that observed by Shanbhag et al where they only observed a significant defect after RNF8/RNF168 double knockdown. This difference can be attributed to greater knockdown efficiency as in my experiments a pool of RNF8 siRNA oligos were used. When the ATMi was added to RNF8 knockdown cells, the transcriptional silencing defect increased to the level of ATMi treated cells (Figure 6.3).

6.2.3: The PBAF chromatin-remodelling complex is required for transcriptional repression in *cis* to DNA DSBs.

Depletion of BAF180 by siRNA was carried out in the U20S cells carrying the transcriptional reporter. The level of transcriptional read out after doxycycline treatment was not affected by the depletion of BAF180 indicating that BAF180 function is not required for the activation of transcription in this system. Remarkably however, depletion of BAF180 led to a significant defect in transcriptional silencing following FOK1 induced DSBs (Figure 6.4). This result indicates that BAF180

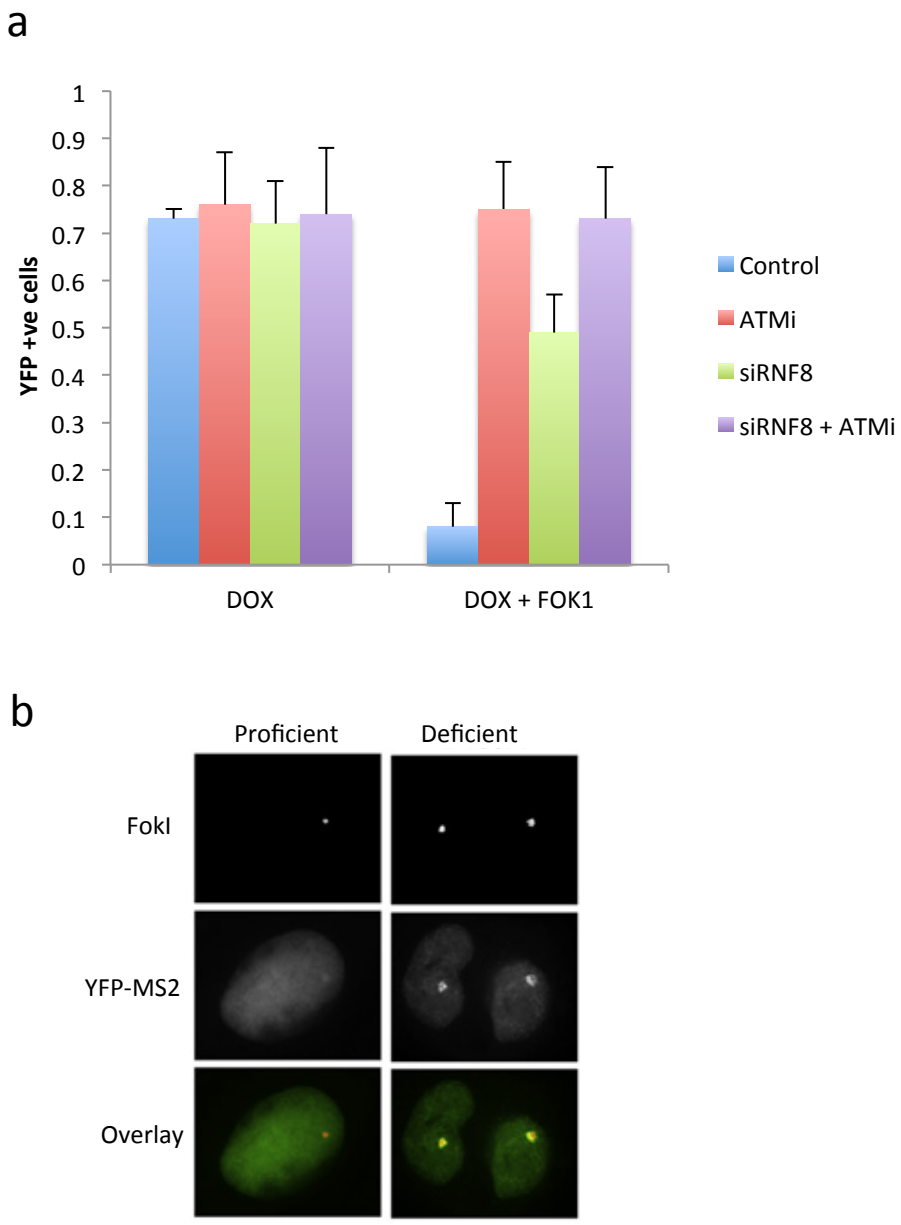

Figure 6.3: RNF8 is required for transcriptional silencing is *cis* to DSBs
Transcription reporter U2OS cells were treated with control or RNF8 siRNA. 48h later, the cells were transfected, or not, with the mCherry-FOK1 endonuclease. 24h later, doxycycline was added to the cells to drive transcription and the cells were harvested 4h later. The cells were then visualized on a fluorescent microscope. Doxycycline driven transcription was visualized as YFP-MS2 protein binding to MS2 nascent transcript. In cells expressing FOK1, DSBs were visualized by FOK1 focal accumulation and transcription in these cells was monitored by YPF-MS2. Where indicated, ATMi was added 30m prior to doxycycline treatment. Y-axis indicates the fraction of YFP positive cells where 1=100%. The presence or absence of nascent transcripts was analysed in a minimum of 30 cells per condition and the data represent the mean and standard deviation of three independent experiments. b) Representative images of cells proficient and deficient in transcriptional silencing (determined by YFP-MS2 signal) is *cis* to DSBs (determined by FOKI signal) (adapted from (Shanbhag *et al*, 2010)).

a

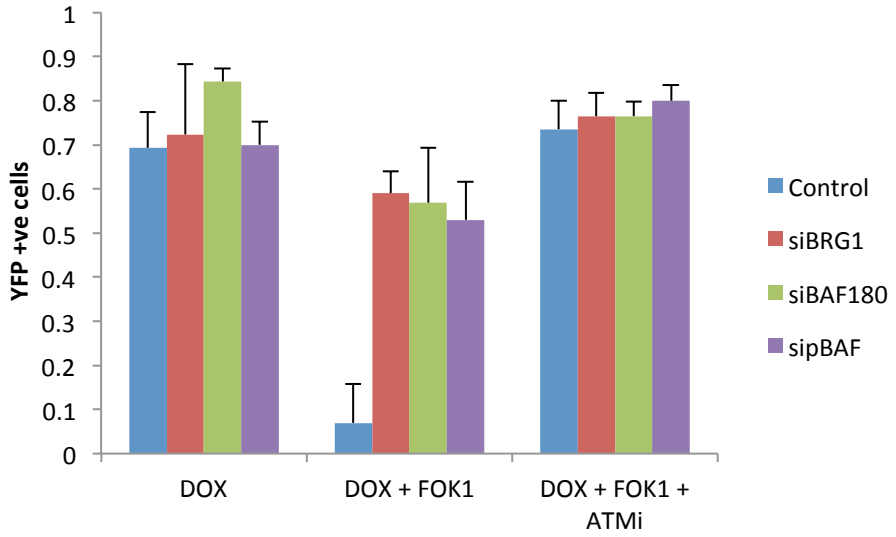

Figure 6.4: The PBAF complex and its subunits are required for transcriptional silencing in *cis* to DSBs. Transcription reporter U2OS cells were treated with control, BRG1, BAF180 or combined BRG1 and BAF180 (PBAF) siRNA. 48h later, the cells were transfected, or not, with the mCherry-FOK1 endonuclease. 24h later, doxycycline was added to the cells to drive transcription and the cells were harvested 4h later. The cells were then visualized on a fluorescent microscope. Doxycycline driven transcription was visualized as YFP-MS2 protein binding to MS2 nascent transcript. In cells expressing FOK1, DSBs were visualized by FOK1 focal accumulation and transcription in these cells was monitored by YPF-MS2. Where indicated, ATMi was added 30m prior to doxycycline treatment. Y-axis indicates the fraction of YFP positive cells where 1=100%. The presence or absence of nascent transcripts was analysed in a minimum of 30 cells per condition and the data represent the mean and standard deviation of three independent experiments.

function is required to silence transcription in *cis* to DSBs possibly by mediating chromatin compaction. Importantly, addition of ATMi to BAF180 depleted cells leads to a defect similar in magnitude to ATMi treated cells (Figure 6.4).

BAF180 contains two BAH domains that appear to be important for the association of the PBAF complex with chromatin (Downs et al unpublished). However BAF180 is not the ATPase catalytic subunit of the complex. The ATPase catalytic subunits of the SWI/SNF complexes are either BRM or BRG1, but in SWI/SNF-b (PBAF) only BRG1 exists (Clapier & Cairns, 2009). To examine whether the ATP-dependent chromatin remodelling activity of the PBAF complex is required for transcriptional silencing in *cis* to DSBs, I depleted BRG1 in the U20S reporter cells. As for BAF180, depletion of BRG1 did not lead to a reduction in doxycycline induced transcription of the reporter gene (Figure 6.4). However, following FOK1 induced DSBs there was impairment in transcriptional silencing in BRG1 depleted cells (Figure 4). The observed defect was similar in magnitude to BAF180 depleted cells indicating that they function in the same pathway/complex (Figure 6.4). To confirm this I carried out joint BAF180, BRG1 depletion (PBAF) and monitored transcription after FOK1 induced DSBs. As expected, the joint depletion of BAF180 and BRG1 did not lead to an additive defect indicating that they function in the same complex (Figure 6.4). Finally, addition of the ATMi to BAF180 depleted cells led to a defect similar in magnitude to ATMi treated cells (Figure 6.4). These results and the previous findings from the Downs and Jeggo laboratories, indicate that RSC – PBAF are important chromatin remodelling complexes in transcriptional regulation and the DDR. In the case of DSB associated transcriptional silencing, PBAF appears to play a pivotal role. The BAH domains of BAF180 appear to be important for the association of the complex with chromatin, while the ATPase activity of BRG1 is required for the chromatin remodelling leading to chromatin compaction.

6.2.4: The PBAF complex is required for efficient DSB repair in euchromatin.

The results from figures 2-3 show that RNF8 is an important player in the cascade of events leading to transcriptional silencing is *cis* to DSBs via histone H2A ubiquitylation. In addition, loss of RNF8 leads to a DSB repair defect/delay at very early time points after IR specifically in transcriptionally active EU. I decided to test whether depletion of BAF180, BRG1 or both (PBAF) would also affect DSB repair at these early time points (Figure 6.5). Depletion of PBAF or either BAF180 or BRG1 led to a DSB repair defect at very early times post IR (Figure 6.5). This defect was observed as early as 10 minutes port IR and was most evident 20-40 minutes post IR. Importantly, the repair defect was identical in magnitude to that observed in RNF8 depleted cells, consistent with the possibility that these factors function in the same pathway responding to DSBs at early times post IR (Figure 6.5).

6.2.5: BAF180 is recruited to DSB containing laser tracks.

Following the observation that depletion of BAF180 leads to a DSB repair defect/delay at very early times post IR, I decided to investigate whether BAF180 accumulates at DSBs and to test the kinetics of its focal accumulation. However, following treatment with IR and immunostaining with BAF180 antibodies no distinct foci were observed at DSB sites marked by γ-H2AX. This is not uncommon, as other members of the DDR do not form IRIF. In the case of BAF180, the failure to form IRIF may be because not enough protein accumulates at DSBs or because it does not accumulate at all DSBs. Another method routinely used to assess the accumulation of a given factor tagged with a fluorescent protein to damaged chromatin is via laser induced chromatin damage (Kong *et al*, 2009).

The intact BAF180 cDNA was cloned into a GFP vector by a postdoc in the Jeggo laboratory (E. Riballo). I subsequently obtained the construct and transfected it into HEK293 cells. Following a 48h expression, the cells were incubated with Hoescht dye for 30 minutes before being micro irradiated with a 351 nm UVA laser. The laser was targeted so that a dose of 4.36 J/m^2 was administered in a 0.1 μM wide track across the width of the nucleus. These conditions have previously been shown to generate DNA damage that includes DSBs along the laser track (Rulten *et al*, 2011). Only GFP-

a

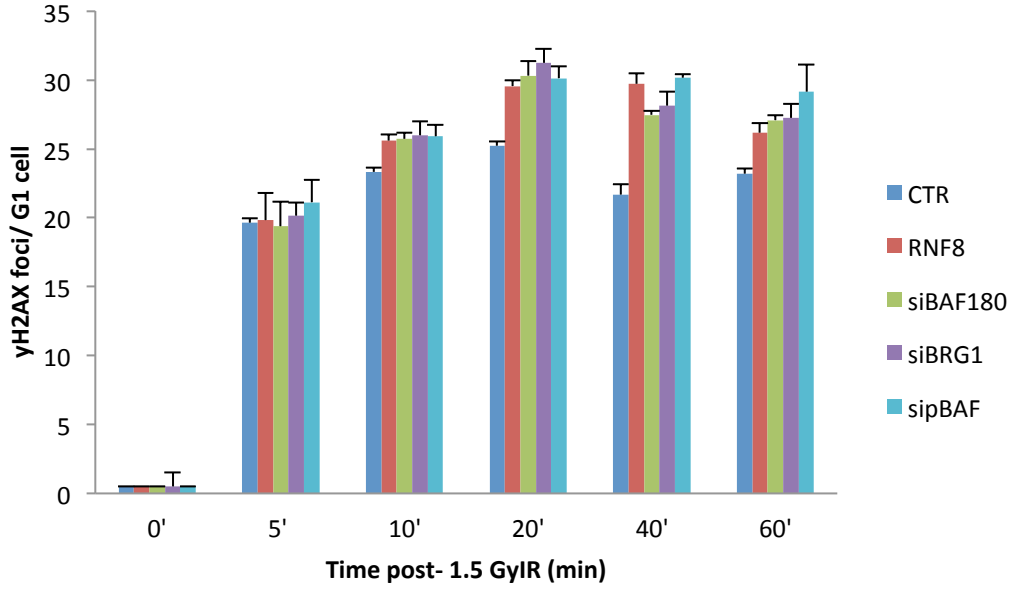

Figure 6.5: The PBAF complex and its subunits are required for DSB repair at early times post IR. 1BrhTERT cells were treated with control, BRG1, BAF180 or combined BRG1 and BAF180 (PBAF) siRNA and were irradiated with 1.5Gy IR. The cells were then harvested at the indicated time points and immunostained with CENP-F and γ-H2AX antibodies. G1 phase cells were identified by negative CENP-F staining and the cell nuclei were visualized by DAPI. γ-H2AX foci were enumerated specifically in CENP-F negative cells. γ-H2AX foci were enumerated in 30 cells per time-point and the data represent the mean and standard deviation of three independent experiments.

expressing cells were micro irradiated. The cells were then imaged at 15-second intervals for a total of three minutes. Strikingly, BAF180 was initially dispersed from the track but was then rapidly relocalised and concentrated along the path of the laser micro irradiation (Figure 6.6). BAF180-GFP was recruited to the laser track with very fast kinetics and a track was visible within a minute post damage induction in GFP expressing cells. Previous studies looking at DDR factor accumulation following DSB inducing laser micro irradiation have demonstrated that not all factors are accumulated with identical kinetics. There is an initial wave of recruitment that is initiated by the phosphorylation of H2AX and involves the recruitment of MDC1 and the MRN complex. This initial wave is very fast and the focal intensity of these factors peaks within a couple of minutes post damage induction. The second wave of recruitment depends upon the UBC13, RNF8 and RNF168 mediated ubiquitylation events at DSB sites (Strauss & Goldberg, 2011; Bekker-Jensen & Mailand, 2010). These modifications lead to the recruitment of BRCA1 and its phosphobinding partners as well as that of 53BP1. There is a lag of approximately 1-2 minutes between the recruitment of the first and second wave of DDR factors at DSBs. The data in Figure 6.6 indicate that BAF180 is recruited to DSB sites with fast kinetics and is likely recruited upstream of the ubiquitylation events at DSBs. Consistent with this, the signal intensity of BAF180-GFP along the laser induced damaged chromatin track peaked within 60s of damage induction (Figure 6.7).

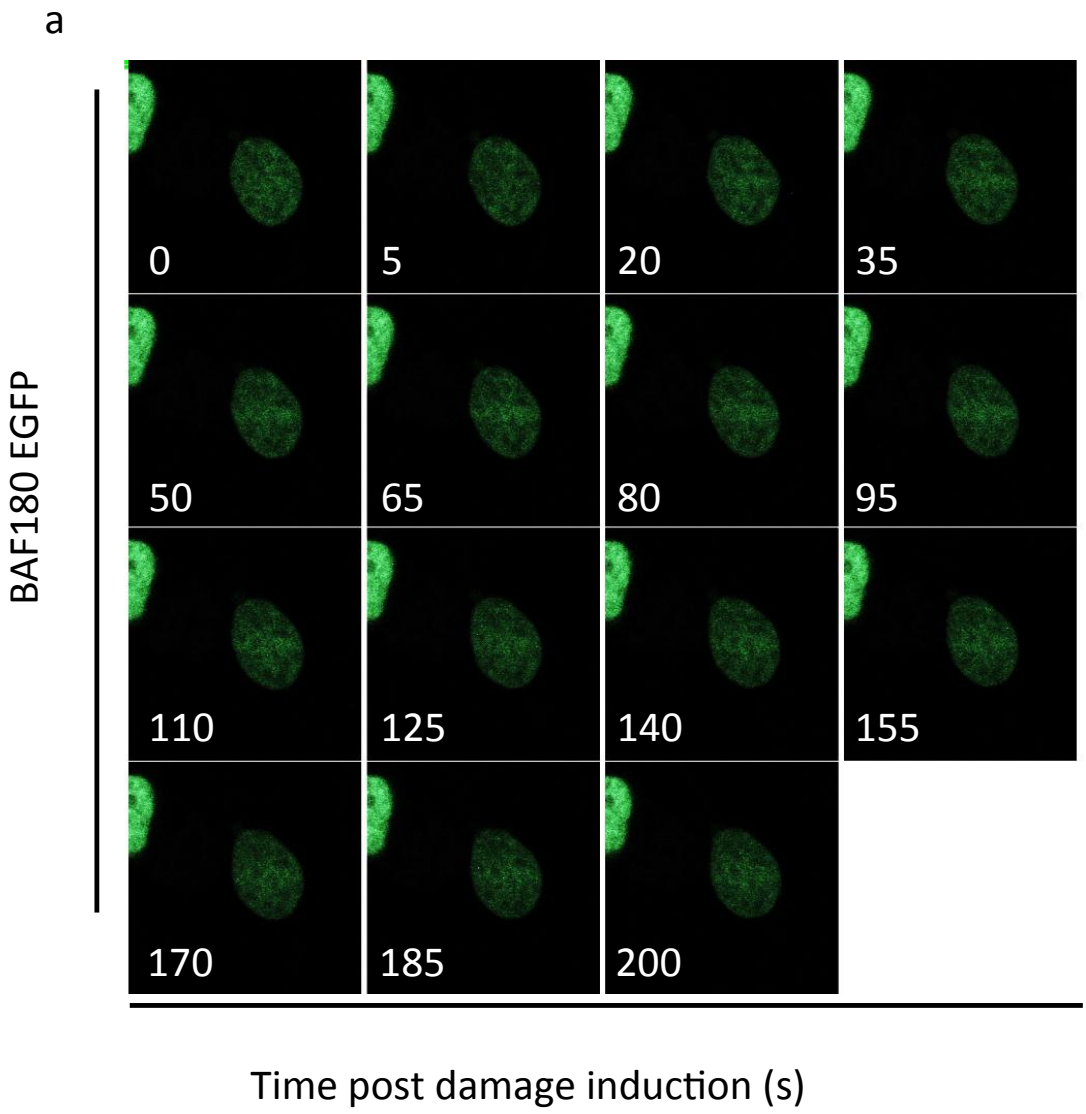

Figure 6.6: BAF180 localises to UVA laser induced DNA damage regions.
HEK293 cells were transfected with 1µg BAF180-GFP. 24h later the cells were preincubated with 10 µg/ml Hoechst 33258 at 37°C for 30m. Selected cells were then irradiated with a 351-nm UVA laser focused through a 40x/ 1.2-W objective using an LSM 510 Meta Zeiss Axiovert microscope. UVA (10.47 µJ) was targeted to a track of 2µm diameter that ran through the cell nucleus (approximately 0.35 µJ/µm^2). Images of irradiated cells were taken at the indicated time points.

a

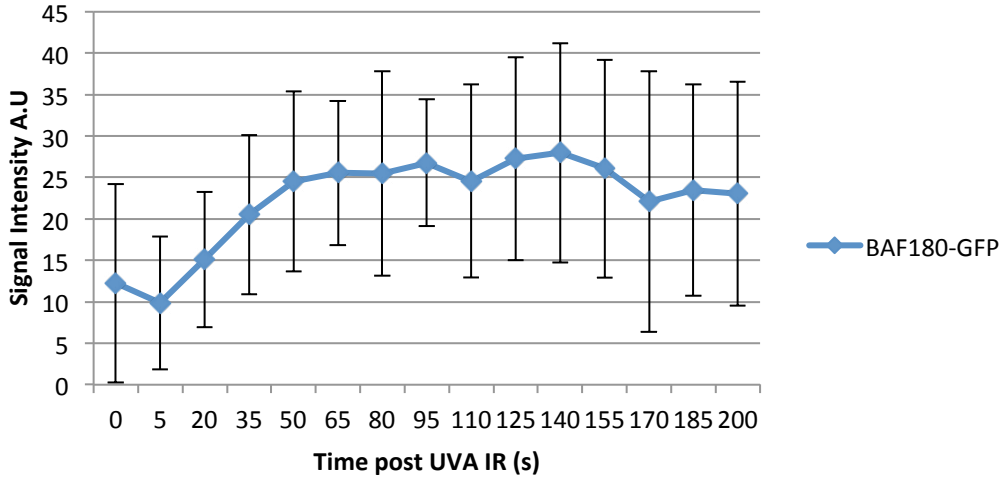

Figure 6.7: BAF180 localisation to UVA laser induced DNA damage regions reaches maximum intensity by 60s post irradiation.
HEK293 cells expressing BAF180-GFP were preincubated with 10 µg/ml Hoechst 33258 at 37°C for 30m and irradiated with a 351-nm UVA laser. Images of the irradiated cells were taken at 15s intervals up to 200s post irradiation. The Zeiss AIM software was then used to measure the signal intensity of BAF180-GFP along the laser track as well as in an unirradiated area. The background fluorescence level was subtracted from the measurement along the irradiated track. The increase in BAF180-GFP intensity along the laser track over time is shown here. Results indicate the mean and standard deviation of BAF180 signal intensity from a minimum of 30 cells imaged over three independent experiments.

6.2.6: BAF180 recruitment to DSB containing laser tracks does not depend on phosphorylation by ATM.

Following the induction of DNA damage, ATM and ATR phosphorylate a myriad of factors thereby playing a key role in the coordination of the DDR (Matsuoka *et al*, 2007). A single damage dependent phosphorylation site has been identified on BAF180 (Matsuoka *et al*, 2007). However the function of phosphorylation of BAF180 on serine 948 is currently unknown. In order to gain insight into the function of this modification, I performed site directed mutagenesis and mutated this site to either an Alanine (A) or a Glutamic acid (E). Mutation to Alanine leads to a non-phosphorylatable form of the protein while mutation to Glutamic acid acts as a phospho-mimic since phospho-Serine is structurally similar to Glutamic acid. In Figure 6.8 the base pair and amino acid sequence in proximity to the BAF180 SQ phosphorylation site is shown. Additionally the mutational changes leading to the phospho-mutant and phosphor-mimic versions of BAF180 are shown.

The successful introduction of the described mutations was confirmed by sequencing and the constructs were then used in the UVA laser tracking experiments. The recruitment of BAF180 to the damaged DNA tracks was not affected by the mutation of S948 to either an Alanine or a Glutamic acid (Figure 6.9). These results indicate that the ATM dependent phosphorylation of BAF180 on S948 after DNA damage is dispensable for its accumulation at damage sites. The accumulation of BAF180 and subsequently PBAF to DNA damage sites might depend on the BAH domains of BAF180 which were recently shown to be required for BAF180 chromatin binding (Downs et al unpublished). Phosphorylation of BAF180 by ATM appears to be dispensable for its recruitment but this could be a result of currently unidentified phosphorylation sites on BAF180. In this case mutation of S948 would not be enough as phosphorylation of other sites could still target BAF180 to chromatin. Using ATMi treated cells would indicate whether the BAF180 phosphorylation is dispensable for its recruitment to DNA damage sites but possible redundancy between ATM and ATR would not allow for definitive conclusions. On the other hand, ATM function might be required for BAF180 function downstream of its recruitment to DNA damage sites. This phosphorylation could lead to conformational changes that regulate the nucleosome remodelling activity of the PBAF complex leading to chromatin compaction and the inhibition of transcription.

a

2821 AAAAGAGAAGCTGAAAAGAGTGAAGATTCCTCTGGTGCTGCAGGCCTCTCAGGCTTACAT
2881 CGCACATAC***AGC***CAGGACTGTAGCTTTAAAAACAGCATGTACCATGTTGGAGATTACGTC

2885 cat cgc aca tac **agc** cag gac tgt agc ttt — WT BAF180
944 H R T Y **S** Q D C S F

2885 cat cgc aca tac gcc cag gac tgt agc ttt — S ➔A BAF180
944 H R T Y A Q D C S F

2885 cat cgc aca tac gag cag gac tgt agc ttt — S ➔E BAF180
944 H R T Y E Q D C S F

Figure 6.8: Production of BAF180 phosphomutant and phosphomimic constructs by site directed mutagenesis. The QuikChange® Multi Site-Directed Mutagenesis Kit was used to introduce the indicated mutations in the BAF180-GFP construct. Mutagenic primers were used to introduce these mutations and thus create BAF180-GFP phosphomutant (S to A) and phosphomimic (S to E) constructs following the manufacturers instructions. The successful introduction of the mutations was verified by sequencing.

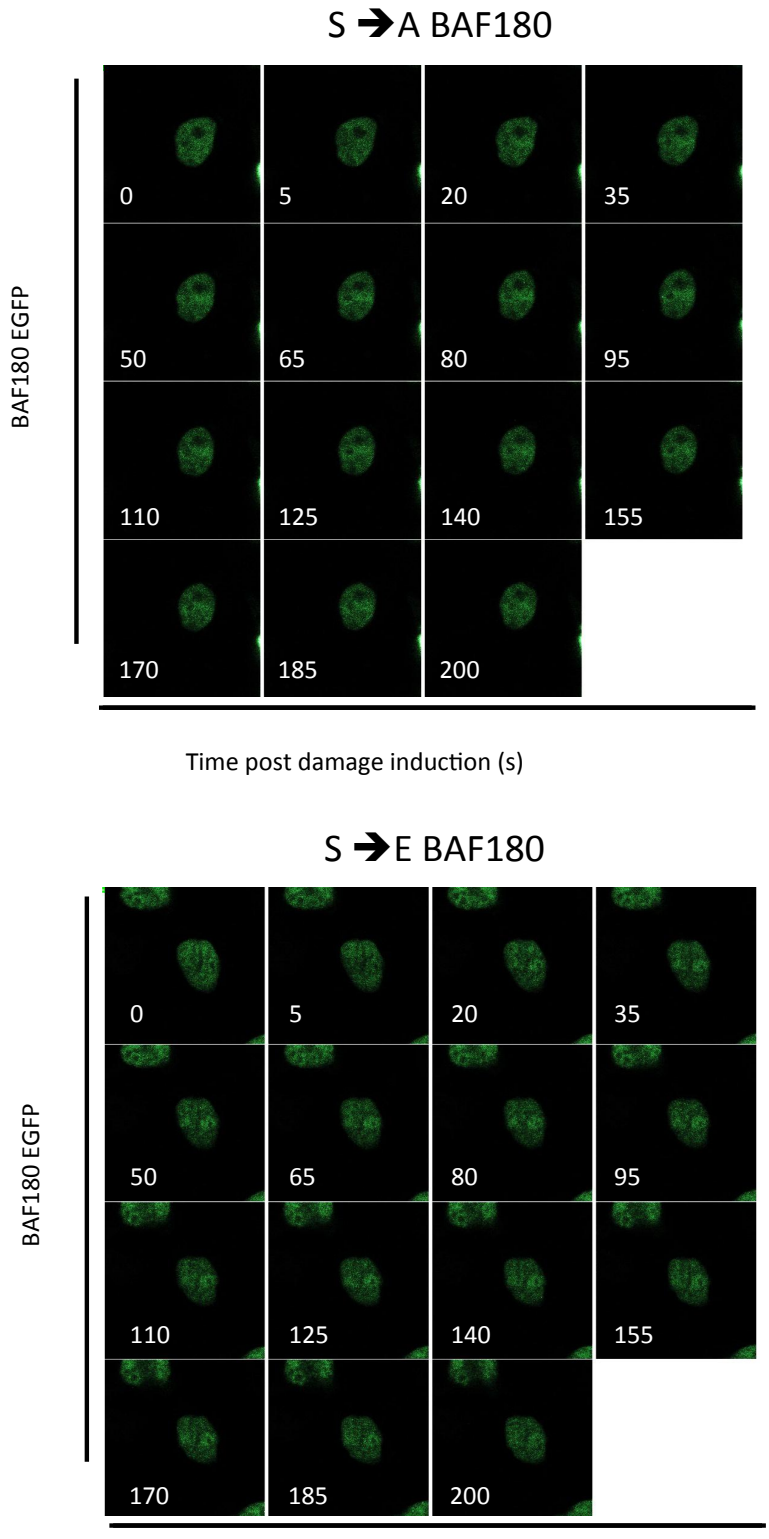

Figure 6.9: BAF180 localisation to UVA laser induced DNA damage regions is not affected by mutating S948. HEK293 cells expressing phosphomutant (SèA) and phosphomimic (SèE) BAF180-GFP were preincubated with 10 µg/ml Hoechst 33258 at 37°C for 30m and irradiated with a 351-nm UVA laser. Images of the irradiated cells were taken at 15s intervals up to 200s post irradiation. Neither mutation abrogated the ability of BAF180 to localize to laser irradiated tracks.

6.2.7: CHD7 is required is for efficient DSB repair in euchromatin.

The proteomics study that identified BAF180 as an ATM phosphorylation target, also identified other chromatin remodelling factors. Amongst these was CHD7, a component of the 9 member CHD family of ATP-dependent chromatin remodelling enzymes (Matsuoka *et al*, 2007). The CHD family of chromatin remodellers are involved in transcriptional regulation and can both activate and repress the process via their chromodomains and their SNF-like ATPase domain (Marfella & Imbalzano, 2007). Recent studies have indicated that CHD7 plays an important role in embryonic development by controlling gene expression in embryonic stem cells (Bajpai *et al*, 2010). Loss of CHD7 in mice is embryonic lethal, further demonstrating its importance in embryonic development (Janssen *et al*, 2012). On the other hand, heterozygous mutations in CHD7 lead to CHARGE (coloboma of the eye, heart defects, atresia of the choanae, retardation of growth and/or development, genital and/or urinary abnormalities and ear abnormalities and deafness) syndrome (Vissers *et al*, 2004).

As discussed previously, members of the CHD family of chromatin remodellers have been shown to function in the DDR (Polo *et al*, 2010; Larsen *et al*, 2010; Smeenk *et al*, 2010; Luijsterburg *et al*, 2012; Goodarzi *et al*, 2011). Interestingly, CHD3 has been shown to promote HC formation and is therefore inhibitory to repair of DSBs at HC regions, whereas CHD4 function was recently identified as a factor that enables DSB repair via chromatin decondensation (Goodarzi *et al*, 2011; Luijsterburg *et al*, 2012). Since transcriptional silencing at DSB sites seems to require chromatin compaction, it is likely that these chromatin alterations necessitate the function of multiple chromatin remodelling factors. Interestingly, CHD7 has been shown to interact with PBAF in embryonic development where they control gene expression during neuronal crest formation (Bajpai *et al*, 2010). Given that PBAF is required for transcriptional silencing in *cis* to DSBs and given that CHD7 is phosphorylated by ATM on S2255 in response to DNA damage, I decided to investigate whether CHD7 is also required for DSB repair at early times post IR.

Following depletion of CHD7 by siRNA treatment, γ-H2AX foci were enumerated in murine NIH3T3 cells at early and late times post IR. Strikingly, depletion of CHD7 led to elevated numbers of γ-H2AX foci at early times post IR with the most significant difference being observed at 30 minutes post IR (Figure 6.10). However, by one hour post IR the number of γ-H2AX foci in CHD7 knockdown cells

was indistinguishable to that in control cells and no repair defect was observed at late time points (Figure 6.10). This phenotype mirrors that of BAF180 and RNF8 depleted cells at early time points indicating that CHD7 may also function in the same pathway. Distinct to the situation in RNF8 depleted cells however, no repair defect was observed at late time points indicating that CHD7 is dispensable for chromatin remodelling at HC DSBs.

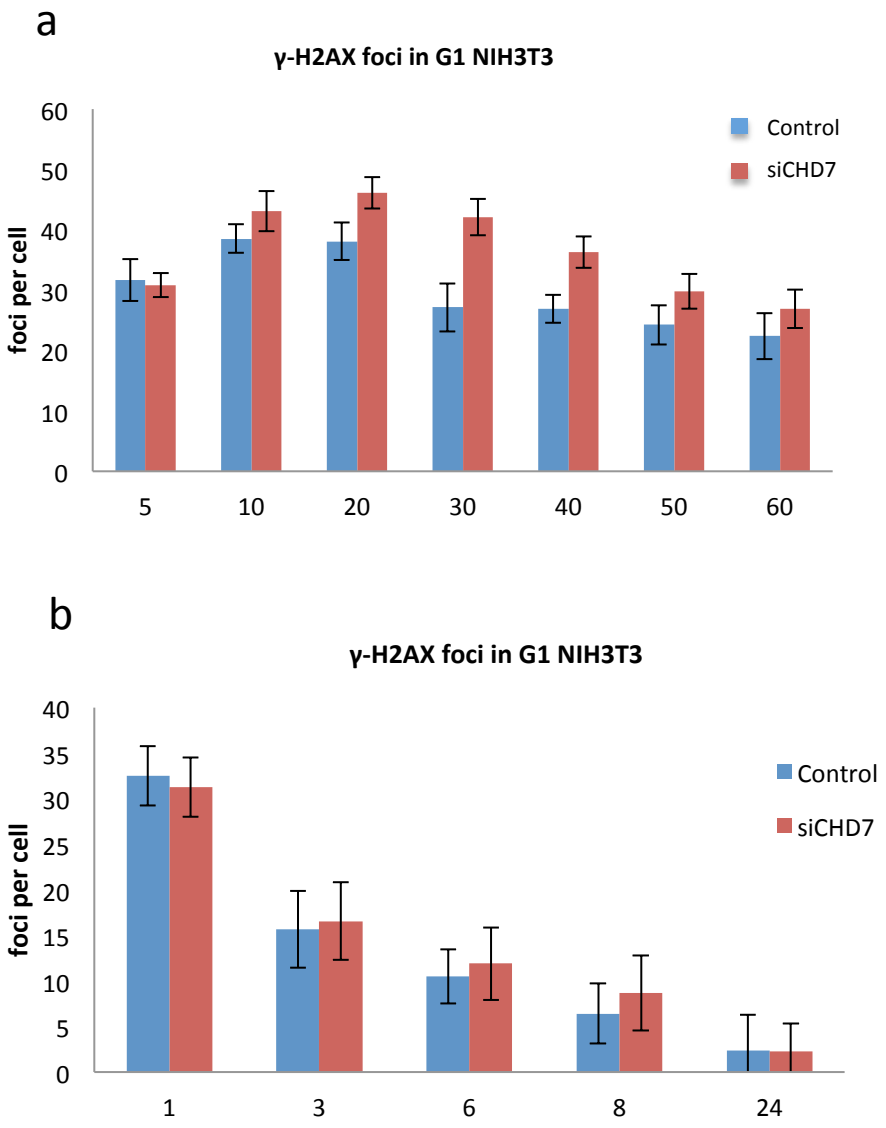

Figure 6.10: The chromatin remodeller CHD7 is required for DSB repair at early times post IR.
NIH3T3 cells were transfected with control and CHD7 siRNA and then allowed to enter G0 by contact inhibition (48h). The cells were then irradiated with 1.5Gy IR and harvested at the indicated time points. Fixed cells were then immunostained with a γ-H2AX antibody and DAPI and imaged on a fluorescent microscope. γ-H2AX foci were enumerated in 30 cells per time-point and the data represent the mean and standard deviation of three independent experiments.

6.2.8: CHD7 is required for transcriptional repression in *cis* to DNA DSBs.

Following the finding that CHD7 knockdown leads to a DSB repair defect at early times post IR, I investigated whether this coincides with a defect in transcriptional silencing after DSB induction. To test this, I used the U2OS transcription reporter system and monitored nascent transcript formation in the presence and absence of FOK1 induced DSBs. The level of doxycycline driven transcription was not affected by CHD7 knockdown as no reduction in nascent transcript levels compared to control cells was observed (Figure 6.11). Remarkably however, CHD7 knockdown lead to a defect in transcriptional silencing in *cis* to the FOK1 induced DSBs and nascent transcripts were observed in the majority of FOK1 transfected cells.

The defect in transcriptional silencing at DSB sites following CHD7 knockdown is identical in magnitude to that observed after PBAF knockdown (or either of its subunits). This finding raises the possibility that these chromatin remodellers function in the same pathway leading to transcriptional silencing following DSB induction. There are several lines of evidence supporting the notion that these factors are involved in the regulation of gene transcription via their chromatin remodelling activities (Murawska, 2011; Morrison & Shen, 2009; Clapier & Cairns, 2009). Moreover, a direct interaction between CHD7 and the PBAF complex has been demonstrated in neural crest cells. During the formation of the neural crest, CHD7 and PBAF function together to promote neural crest gene expression (Bajpai *et al*, 2010). Both these chromatin remodellers have been implicated in both the activation and repression of transcription but how this occurs mechanistically is currently unclear.

a

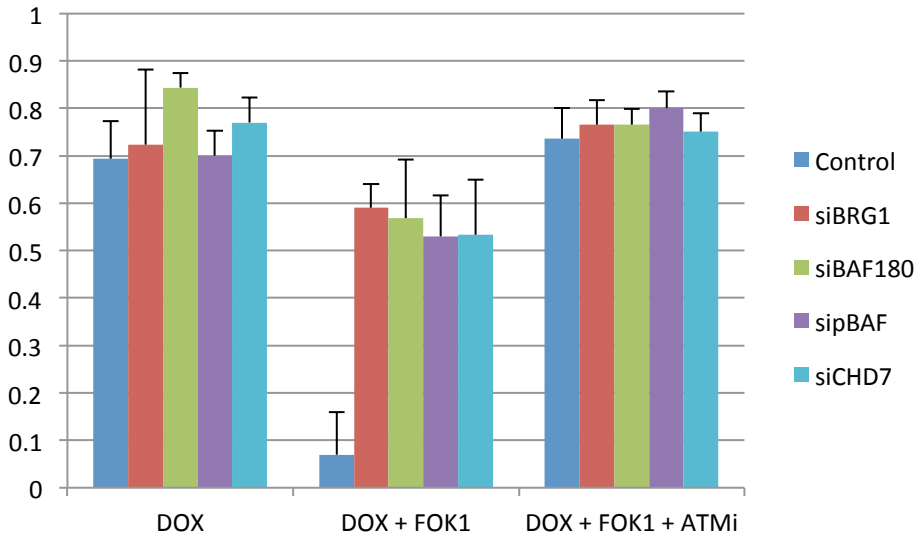

Figure 6.11: CHD7 as well as the PBAF complex are required for transcriptional silencing in *cis* to DSBs. Transcription reporter U2OS cells were treated with control, CHD7, BRG1, BAF180 or combined BRG1 and BAF180 (PBAF) siRNA. 48h later, the cells were transfected, or not, with the mCherry-FOK1 endonuclease. 24h later, doxycycline was added to the cells to drive transcription and the cells were harvested 4h later. The cells were then visualized on a fluorescent microscope. Doxycycline driven transcription was visualized as YFP-MS2 protein binding to MS2 nascent transcript. In cells expressing FOK1, DSBs were visualized by FOK1 focal accumulation and transcription in these cells was monitored by YPF-MS2. Where indicated, ATMi was added 30m prior to doxycycline treatment. Y-axis indicates the fraction of YFP positive cells where 1=100%. The presence or absence of nascent transcripts was analysed in a minimum of 30 cells per condition and the data represent the mean and standard deviation of three independent experiments.

6.3: Discussion

In recent years, an ever-expanding body of evidence has emerged indicating that chromatin remodelling plays an important role in the DDR (Misteli & Soutoglou, 2009). Work from our laboratory has primarily focused on DSB repair of lesions at HC regions. Published work and data presented in chapter 3 of this thesis demonstrate that DSBs that are repaired with slow kinetics following exposure to X or γ- rays correspond to DSBs at HC. The accurate repair of these lesions requires ATM and the mediator proteins, which function in a pathway that culminates with the phosphorylation of KAP-1. This modification leads to localised chromatin relaxation, which is essential for access to damaged chromatin. More recently prolonged KAP-1 phosphorylation was found to be required to maintain a relaxed chromatin state by inhibiting the heterochromatin building function of the chromatin remodeller, CHD3. The phosphorylation of KAP-1 is dispensable for DSB repair in EU and this is thought to be because the relatively relaxed conformation of EU does not pose a barrier to repair.

As part of the DDR, cells have evolved cell cycle checkpoints that delay the progression from one cell cycle to the next while repair is on-going. This is vital, as attempts to carry out processes such as DNA replication or cell division in presence of DNA damage could have devastating consequences for genomic integrity (Ulrich & Walden, 2010). However, there are also inter-phase metabolic processes that require access to DNA and chromatin remodelling that cannot be inhibited by cell cycle checkpoints. The process of transcription requires localised chromatin decondensation in order for the transcription machinery to access the required region of DNA. One model is that if a DSB arises in a transcriptionally active region, then transcription is inhibited in order to prevent erroneous repair. Recent work from the Greenberg laboratory demonstrated that this indeed the case (Shanbhag *et al*, 2010). They found that transcription is silenced at least up to 13kb from a DSB site and that histone H2A ubiquitylation is necessary for this process. Strikingly, they demonstrated that ATM kinase activity is also required. However how ATM achieves this mechanistically is still unclear.

In this chapter I aimed to build on these findings and investigate how ATM kinase activity leads to transcriptional silencing in *cis* to DSBs. In addition, I assessed the role of the chromatin remodellers BAF180 and CHD7 since they are both ATM

substrates. Finally, I investigated the impact of deficient transcriptional silencing on the overall fidelity of DSB repair.

The original publication investigating transcriptional silencing in *cis* to DSBs demonstrated that H2A ubiquitylation is required for this process (Shanbhag *et al*, 2010). This modification is carried out by the ubiquitin ligases RNF8 and RNF168 and loss of these leads to deficient transcriptional silencing. In addition, ATM kinase activity is required for the maintenance of ubiquitin chains on histone H2A and for the inhibition of transcription associated chromatin decondensation. Here I wanted to ask whether loss of ATM activity leads to deficient DSB repair as a result of deficient transcriptional silencing. Previous work from our laboratory has demonstrated that loss of ATM leads to a DSB repair defect at late repairing DSBs that repair at early time points is normal. However, due to ATMs role in γ-H2AX phosphorylation IRIF are smaller in ATMi treated cells at early times and comparison to control cells is difficult. To overcome this limitation, I tested the impact of RNF8 knockdown on DSB repair at very early time points. I reasoned that since RNF8 functions in the same pathway as ATM in transcriptional silencing, depletion of RNF8 would have the same impact on repair as the inhibition of ATM. RNF8 status does not impact on γ-H2AX IRIF, thus allowing direct comparison to control cells. Interestingly, I observed that RNF8 knockdown leads to a defect/delay in the repair of DSBs within the first hour post IR when only EU DSBs undergo repair (Figure 6.1-6.2). One interpretation of this result is that the defect in transcriptional silencing in *cis* to DSBs following RNF8 depletion (Figure 6.3) has a direct impact on DSB repair in EU. However, in light of recent findings indicating that RNF8 promotes chromatin decondensation at DSBs via its interaction with CHD4, it is also possible that the repair defect observed at early times post IR results from a failure to carry out this process (Luijsterburg *et al*, 2012). An interesting future experiment will be to use a transcription marker such as antibodies towards the 7- methylguanosine (m7G) cap structure present on nascent transcripts, to investigate whether the γ-H2AX foci in RNF8 depleted cells colocalise with transcription sites.

Chromatin remodellers carry out changes in the organisation of chromatin to facilitate important cellular processes. In the case of transcription, chromatin decondensation is required to allow access to the transcription machinery. However in the presence of DNA damage, chromatin decondensation must be prevented so that transcription is not initiated in the presence of damage. ATM and RNF8 are clearly

required for this process but as neither protein is an ATP-dependent chromatin remodeller they cannot directly manipulate nucleosomes. Here I have identified the PBAF chromatin-remodelling complex as a key component of the transcriptional silencing response in *cis* to DSBs. I investigated the role of this complex since the homologous complex in yeast (RSC) has a direct role in both transcription and DSB repair. Moreover, RSC is able to manipulate the position of nucleosomes in the vicinity of DSBs via its chromatin remodelling activity. Finally, the PBAF complex seemed a good candidate since the BAF180 subunit had previously been identified as an ATM DNA damage dependent phosphorylation substrate.

Depletion of PBAF or either of its subunits (BRG1, BAF180), led to deficient transcriptional silencing following DSB induction (Figure 6.4). This result strongly suggests that PBAF is the chromatin-remodelling complex, or one of them, carrying out the chromatin changes leading to transcriptional repression after DSB induction. Moreover, depletion of BRG1 or BAF180 also led to a DSB repair defect in early repairing DSBs supporting the notion that DSBs at transcriptionally active regions are rapidly repaired (Figure 6.5). Importantly, the repair defect of PBAF knockdown cells at early time points was similar in magnitude to RNF8 knockdown cells. These results indicate that PBAF functions in the same pathway as ATM and RNF8 leading to transcriptional repression in *cis* to DSBs.

Several studies have investigated the recruitment of DDR factors to DNA damage sites as the recruitment kinetics of a particular factor can provide clues as to its position in the cascade of events. For example the recruitment of MDC1 and RNF8/RNF168 to DSBs are dependent on ATM phosphorylation events and are recruited with faster kinetics than 53BP1 and BRCA1 which are recruited by ubiquitylation events (Bekker-Jensen & Mailand, 2010). In order to gain insight into where PBAF functions in the cascade of events leading to transcriptional silencing, I monitored its recruitment to laser damaged chromatin (Figures 6.6-6.7). When BAF180-GFP was expressed in cells that were exposed to laser micro irradiation, it initially dispersed from the irradiated region but then quickly returned and accumulated along the DNA damaged track (Figures 6.6-6.7). Interestingly, BAF180-GFP was recruited with fast kinetics and reached maximum intensity along the damaged region within 60s. This result is consistent with the notion that BAF180 might be remodelling chromatin into a configuration favourable for the RNF8/RNF168 ubiquitylation events leading to transcriptional silencing.

ATM phosphorylates BAF180 on S948 in a DNA damage dependent manner. To assess the significance of this phosphorylation event on the recruitment of BAF180 to DNA damage sites, I mutated this residue to either and Alanine or a Glutamic acid thus creating a phosphomutant and phosphomimic version of the protein. However these mutations did not effect the recruitment of BAF180 and normal recruitment was seen in both cases (Figure 6.9). This result indicates that this modification is dispensable for BAF180 recruitment to damaged chromatin. Treating BAF180-GFP expressing cells with ATMi and repeating these tracking experiments might be informative but redundancy amongst ATM, ATR and DNA-PK in phosphorylating downstream targets can make interpretation difficult. A recent study from the Downs laboratory demonstrated that BAF180 chromatin binding is compromised in vivo when its two BAH domains are mutated. It will be interesting to see whether these mutations will also abrogate the ability of BAF180 to accumulate at DNA damage tracks.

If the phosphorylation of BAF180 by ATM proves to be dispensable for its recruitment to DNA damage sites, then this modification might regulate its function downstream of its recruitment. Future experiments using the phosphomimic and phosphomutant BAF180 constructs will address these questions by monitoring transcriptional silencing and DSB repair. These experiments entail depleting endogenous BAF180 by siRNA treatment and then reconstituting with siRNA resistant versions of the BAF180 phosphomimic and phosphomutant constructs. If these endpoints are affected by these mutations then the phosphorylation of BAF180 might be required to regulate its function downstream of its recruitment to DSBs. These endpoints must also be investigated in cells expressing the mutated BAH domain version of BAF810.

Overall, these findings support the notion that RNF8 and PBAF function in the ATM pathway leading to transcriptional silencing in *cis* to DSBs. Moreover, I provide evidence showing that defective inhibition of transcription via RNF8 or PBAF depletion leads to a DSB repair defect affecting breaks in EU. However it is not yet clear how these factors co-operate in this process and where they are positioned in the cascade of events. A recent study looking at the role the SWI/SNF complexes in DSB repair, described a role for p400 in promoting RNF8 dependent histone ubiquitylation (Xu *et al*, 2010). Interestingly, in this study the authors demonstrated that p400 functions upstream of RNF8 in the DDR and destabilises nucleosomes (Xu *et al*, 2010). This destabilisation was shown to be a pre-requisite for RNF8 dependent histone H2A

ubiquitylation and the subsequent recruitment of 53BP1 and BRCA1. Similarly, a separate study demonstrated that CHD4 directly interacts with RNF8 and via its ATPase activity promotes RNF8 catalysed histone ubiquitylation leading to chromatin decondensation (Luijsterburg *et al*, 2012). BRG1, like p400 and CHD4 is a chromatin remodeller with ATPase activity. It is therefore possible that BRG1 like p400 and CHD4, acts upstream of RNF8 to remodel nucleosomes into a confirmation that is favourable for histone H2A ubiquitylation and the associated transcriptional silencing. Conversely, PBAF might function downstream of RNF8 to directly mediate transcriptional silencing via nucleosome compaction. Deciphering how RNF8 and PBAF co-operate in the ATM dependent transcriptional silencing pathway in response to DSBs is an important future question.

CHD7 is a member of the CHD family of chromatin remodellers that are involved in transcriptional regulation (Murawska, 2011). In addition, CHD7 has been shown to interact with PBAF during neural crest development where they control gene expression. CHD7 has not been reported to play a role in the DDR but ATM phosphorylates it on S2255 in response to DNA damage. Given this, I investigated the role of CHD7 in transcriptional silencing in *cis* to DSBs but also in DSB repair. Surprisingly, depletion of CHD7 led to a delay in the repair of DSBs at very early times post IR and similar to the situation following PBAF or RNF8 depletion this could only be detected up to 60m post IR (Figure 6.10). This result indicates that CHD7 might play a role in transcriptional silencing following DNA damage. Importantly, no repair defect was observed at late time points indicating that CHD7 is dispensable for HC DBS repair.

CHD7 siRNA treatment led to defective transcriptional silencing in *cis* to DSBs (Figure 6.11). This defect was similar in magnitude to that seen following PBAF depletion indicating that these chromatin remodellers function in the same pathway. CHD7 localises to genomic regions enriched for H3K4me3 that are associated with the up-regulation of transcription (Schnetz *et al*, 2009). Interestingly in yeast, H3K4me3 has been demonstrated to be required for a proficient response to DSBs (Faucher & Wellinger, 2010). Moreover, RSC was shown to be required for this modification via its role in the recruitment of Set1p, the H3 specific mehtyltransferase responsible for H3K4me3 (Faucher & Wellinger, 2010). Genomic regions with high levels of H3K4me3 are described as transcriptionally active where as regions that are permanently silenced, such as HC, are enriched for H3K9 (Seiler *et al*, 2011).

Surprisingly in yeast, the 'pro-transcriptional' modification of H3K4me3 is enriched at DSBs and required for efficient repair by NHEJ. On the other hand, the 'anti-transcriptional modification' of H2B ubiquitylation is also enriched at DSBs indicating that a balancing act takes place. Consistent with this notion, RNF8 has been shown to promote both chromatin decondensation and compaction via histone ubiquitylation (Shanbhag *et al*, 2010; Luijsterburg *et al*, 2012). It appears that a delicate equilibrium needs to be achieved whereby chromatin is sufficiently relaxed to facilitate repair and sufficiently compact to inhibit transcription.

It is thought that CHD7 functions in transcriptional regulation although how this is achieved is unclear. CHD7 is able to bind to H3K4me2/3 in vitro via its chromodomains (Schnetz *et al*, 2009). This histone modification is frequently found at enhancer sequences that regulate the expression of specific genes. CHD7 was found to directly bind to these enhancer regions via its interaction with H3K4 and this directly impacted on the transcription of the associated genes (Schnetz *et al*, 2009). There is therefore ample evidence indicating that CHD7 is required for transcriptional regulation and this appears to be important also in regions in *cis* to DSBs.

The data showing that CHD7 directly interacts with enhancers via H3K4 binding suggest that CHD7 is a 'pro-transcriptional' factor. Following the observation that transcription in not efficiently silenced in the absence of CHD7, I postulated that this might be a result of defective loss of pro-transcriptional histone modifications. Indeed, a recent study demonstrated that DSB induced transcriptional silencing is associated with loss of H3K4me3. This group used a microscopy based approach and reported that H3K4me3 is lost from γ-H2AX sites and that this loss depends on the function of the JARID1A demethylase (Seiler *et al*, 2011). An important future question is whether ATM and CHD7 are also required for these histone modifications in *cis* to DSBs and whether ATM regulates CHD7 function. It is becoming evident that post-translational modifications such as ubiquitylation and methylation play a key role in the regulation of transcription in *cis* to DSBs. ATM and the chromatin remodellers CHD7 and BAF180 play an important role in this process but their detailed functions are yet to be determined.

CHAPTER 7

Discussion

7 Discussion

7.1: Chapter 3: Investigating the role of the mediator proteins in HR

7.1.1: Major conclusions from Chapter 3

- DSBs induced by γ-radiation G2 phase co-localise with pKAP1 foci and are repaired by HR.
- The mediator proteins 53BP1, MDC1 and H2AX promote the repair of these DSBs by enabling chromatin relaxation through KAP1 phosphorylation.
- In addition to mediating pKAP1 formation, MDC1 function is required for Rad51 foci formation in G2 phase.
- The role of 53BP1 in G2 phase HR, but not that of MDC1, can be overcome via KAP1 depletion.
- CtIP is required for resection in S-phase following CPT treatment but the mediator proteins are dispensable.

Previous work from our laboratory, demonstrated that in G1 phase cells, DSBs repaired with slow kinetics following exposure to X or γ-radiation are those located at HC regions (Noon *et al*, 2010). In order for such lesions to be repaired, ATM, Artemis and the mediator proteins are required to remodel chromatin into a relaxed configuration through robust localised KAP1 phosphorylation (Noon *et al*, 2010). Subsequent experiments revealed that the slow component of repair in G2 phase cells also requires ATM and Artemis for efficient repair but that these DBSs are repaired by HR (Beucher *et al*, 2009).

In chapter 3, I demonstrated that DSBs that are repaired with slow kinetics in G2 phase, undergo resection and co-localise with pKAP1 IRIF (Figure 3.1). Moreover, I showed

that pATM and 53BP1 IRIF overlap with pKAP1 IRIF suggesting that as in G1, they are required for pKAP1 IRIF also in G2 phase (Figure 3.1). Since pKAP1 IRIF are thought to depict HC regions, I propose that slowly repaired DSBs in G2 are located at HC regions and are repaired by HR (Noon *et al*, 2010). In support of this model, when I inhibited NHEJ by depleting Ku80 and DNA-PKcs, I observed more RPA and Rad51 foci as well as more SCEs compared to control cells indicating that HR was repairing a greater fraction of DSBs (Figure 3.2). Importantly, under these conditions there was a reduction in the fraction of RPA foci that co-localised with pKAP1 foci indicating that resection of DSBs in EU was taking place in contrast to control cells where resection is limited to pKAP1 enriched regions.

Following the observation that 53BP1 foci co-localise with pATM, pKAP1, and RPA IRIF in G2 phase, I investigated whether the mediator proteins are required for G2 phase DSB repair (Figure 3.3). I observed a requirement for 53BP1, MDC1 and H2AX in the repair of a subset of induced DSBs in G2 phase cells (Figure 3.3). The repair defect following the depletion of these proteins affected the slow component of repair and was epistatic to ATMi treated cells indicating that these proteins are required for efficient HR repair in G2 phase (Figure 3.3). I verified this by showing that RPA and Rad51 foci formation are partially defective following depletion of these proteins, while IR induced SCEs are completely abolished indicating deficient HR in the absence of these factors (Figures 3.4-3.6).

The requirement of 53BP1 in G2 phase DSB repair was overcome by KAP1 depletion as was its requirement for RPA IRIF, Rad51 IRIF and SCEs. This finding indicates that in G2 phase, 53BP1 promotes HR via pKAP1 mediated HC relaxation but does not have a direct role in the HR process. In support of this conclusion, 53BP1 is dispensable for resection in EU as well as for resection in S-phase cells following exposure to CPT, where chromatin structure is believed to be less inhibitory to repair (Figure 3.10 and 3.16). 53BP1 has previously been portrayed as a pro-NHEJ factor while recent studies have indicated that it actively inhibits resection and therefore HR (Xie *et al*, 2007; Bunting *et al*, 2010; Bouwman *et al*, 2010). In contrast to these findings, my results indicate that 53BP1 function is required for HR specifically in G2 phase cells and that as in G1, it mediates repair via localised KAP1 phosphorylation.

In contrast to 53BP1, the requirement for MDC1 in G2 phase HR goes beyond mediating KAP1 phosphorylation and thus cannot be overcome by KAP1 depletion (Figure 3.7). By monitoring different HR intermediates I observed that MDC1 is

dispensable for resection (RPA foci) but required for Rad51 loading (Rad51 foci) when KAP1 is depleted (Figures 3.8-3.9). Consistent with MDC1 playing a direct role in Rad51 loading, MDC1 depletion perturbs Rad51 foci in EU as well as in S-phase following CPT treatment (Figure 11 and Lobrich et al unpublished). It is not currently clear how MDC1 enables Rad51 loading. There is evidence that MDC1 directly interacts with Rad51 and that this interaction is required for HR through the retention of Rad51 in chromatin (Zhang *et al*, 2005). Another possibility is that MDC1 mediates Rad51 loading via the recruitment of downstream factors such as Rad18 that has been shown to be required for Rad51 loading through its interaction with Rad51c (Huang *et al*, 2009). Future experiments are required to determine the exact role of MDC1 in Rad51 filament formation during HR in both the S and G2 phases.

ATM and CtIP have previously been shown to be required for the initiation of resection in G2 phase (Shibata *et al*, 2011). In this chapter, using a flow cytometry approach, I investigated the requirement of ATM, CtIP and the mediator proteins in RPA retention in S-phase cells following CPT treatment (Figure 3.16). Although no RPA foci are observed in ATMi treated G2 phase cells following IR, ATMi treated S-phase cells showed normal RPA retention after CPT treatment (Figure 3.16). In contrast, CtIP depletion led to a significant reduction in RPA retention in S-phase cells following CPT treatment. These results indicate that CtIP is required for resection in both the S and G2 phases, but that its phosphorylation by ATM is only required for resection in G2 phase (Li *et al*, 2000). I propose that the phosphorylation of CtIP by ATM functions to target CtIP to DSBs where it functions in the initiation of resection. Consistent with this, ATMi treated cells or cells expressing phosho-mutant CtIP fail to form CtIP foci in G2 phase following IR (Shibata *et al*, 2011). In S-phase, when a replication fork stall/collapses, ssDNA forms that becomes coated by RPA and leads to ATR activation (Shechter *et al*, 2004). It is possible that ssDNA at these regions leads to the recruitment of CtIP independently of ATM, where it then functions in the elongation of ssDNA. It is also possible that another kinase such as ATR or DNA-PK can redundantly phosphorylate CtIP following its recruitment to stalled/collapsed replication forks. To gain insight into this process, I inhibited the function of ATM, ATR and DNA-PK individually and in conjunction (Figure 3.15). By using a combination of inhibitors and caffeine, I observed that while inhibition of ATM or DNA-PK alone does not impact on RPA retention after CPT, combined inhibitor treatment led to a reduction in RPA retention that became greater still by the addition of

caffeine to inhibit ATR (Figure 3.15). These findings indicate that the PIKK kinases ATM, DNA-PK and ATR are required for ssDNA formation during HR repair/recovery of stalled/collapsed replication forks. Further experiments are required to address how they regulate this process. Monitoring CtIP foci in S-phase cells following CPT treatment can provide insight into whether they regulate the process via CtIP recruitment. It is possible that they are dispensable for CtIP recruitment but that their function is required for the recruitment of other factors important for this process, as has previously been shown for MRE11 (Trenz *et al*, 2006). Although further work is needed to elucidate how resection is controlled in S-phase, the mediator proteins 53BP1, MDC1 and H2AX appear to be dispensable for this process since RPA retention after CPT is not affected by their depletion (Figure 3.16).

One-ended DSBs arising from collapsed replication forks are preferentially repaired by HR and lead to replication fork restoration (Roseaulin *et al*, 2008; Hanada *et al*, 2007; Helleday *et al*, 2007). It is thought that NHEJ can not accurately repair these lesions as they are one-ended and cannot be repaired in the same way as two-ended DSBs in the G1 and G2 phases (Helleday *et al*, 2007). One model is that the sensitivity of HR and FA mutant cells to S-phase induced DNA damage, is due to erroneous repair of one-ended DSBs by NHEJ resulting in ligation to distant one-ended DSBs and therefore genomic rearrangements (D'Andrea & Grompe, 2003; Helleday *et al*, 2007). There is evidence from several metabolic processes that 53BP1 function is required for long-range re-joining events (Difilippantonio *et al*, 2008; Dimitrova *et al*, 2008; Bothmer *et al*, 2011). In this chapter I attempted to assess whether long-range re-joining events could be observed in BRCA1 depleted cells exposed to MMS. To achieve this I used a construct containing a 53BP1 fragment required for its focal accumulation fused to an mCherry fluorescent tag (Dimitrova *et al*, 2008). MMS treatment led to DSBs specifically in S-phase cells, and the mCherry-BP1 construct localised to these regions (Figure 3.18). However, under these experimental conditions, BRCA1 depletion did not lead to an increase in long-range fusion events or to an increase in the mobility of the mCherry-BP1 IRIF as assessed by LCI. Caution must be taken when interpreting these findings as further validation and analysis of this experimental system is required.

Aberrant repair of one-ended DSBs arising from DNA damage in S-phase, is an attractive model for the genomic instability of BRCA and FA mutant cells. Moreover, if re-joining of distant one-ended DSBs does take place it will be interesting to address whether 53BP1 is required for this process. Recent studies in which the HR defect of

BRCA1 deficient cells is overcome by 53BP1 depletion indicate that 53BP1 blocks HR by inhibiting resection and that BRCA1 function is required to overcome this (Bunting *et al*, 2010; Bouwman *et al*, 2010). It is therefore possible that 53BP1 inhibits HR and promotes erroneous NHEJ in S-phase in BRCA1 deficient cells, thus contributing to the genomic instability of these cells.

7.2: Chapter 4: The role of ubiquitin signalling in Homologous Recombination

7.2.1: Major conclusions from Chapter 4

- RIDDLE patient cells are defective in G2 phase HR.
- RNF8 and RNF168 have distinct roles in G2 phase HR.
- Proteasome inhibition affects G2 phase resection.
- RNF8/RNF168 depletion or proteasome inhibition does not affect S-phase resection.
- BRCA1 is required for G2 phase HR.
- The BRCT domain but not the RING domain of BRCA1 is required for G2 phase HR.

In chapter 4, I investigated the role of ubiquitin signalling in HR. By using cultured fibroblasts isolated from a RIDDLE syndrome patient, I demonstrated that RNF168 is required for DSB repair also in G2 phase (Figure 4.1) (Stewart *et al*, 2007; 2009). The repair defect in G2 phase affected DSBs repaired with slow kinetics, which in chapter 3,

I demonstrated represent DSBs that are repaired by HR. Consistent with this, using RIDDLE patient cells I observed an RPA and Rad51 foci formation defect in G2 phase, indicating that RNF168 is required for efficient repair by HR (Figure 4.1). In G1, RNF168 mediates the repair of DSBs located at HC regions by ubiquitylating downstream targets leading to 53BP1 recruitment and subsequently the localised KAP1 phosphorylation necessary for repair (Noon *et al*, 2010). Similarly in G2, when KAP1 was depleted in RIDDLE cells, I observed normal RPA and Rad51 foci formation as well as normal γ-H2AX foci clearance (Figure 4.2). In summary, RNF168 mediates HR in G2 by promoting KAP1 dependent HC relaxation but has no direct role in the HR pathway.

The amplification of ubiquitin signals at DSBs that are required for 53BP1 and BRCA1 retention are carried out by RNF168, but the initial ubiquitin modification of histones at DSBs is carried out by RNF8 (Mailand *et al*, 2007; Doil *et al*, 2009). In G1, RNF8 is required for 53BP1 recruitment and therefore for HC DSB repair by mediating HC relaxation via KAP1 phosphorylation (Noon *et al*, 2010). Here, I have demonstrated that RNF8 is also required for HC DSB repair in G2 phase, but that in G2 the requirement for RNF8 cannot be overcome by KAP1 depletion (Figure 4.3). Moreover, I demonstrated that RNF8 depletion leads to a severe defect in RPA and Rad51 foci formation thus revealing an important role for RNF8 in these processes (Figure 4.3). To investigate whether ubiquitin signalling is required for HR, I used the proteasome inhibitor epoxomicin and observed deficient RPA foci formation in G2 (Figure 4.8). Importantly, neither RNF8 knockdown nor epoxomicin treatment affected RPA retention in S-phase cells after CPT treatment, indicating that ubiquitin signalling is dispensable for resection in S-phase (Figure 4.8).

In summary, my data demonstrate a requirement for ubiquitin signalling in resection and Rad51 loading during DSB repair by HR in G2 phase. Surprisingly, there is a differential requirement between RNF8 and RNF168 for the formation of these HR intermediates. Whereas the role of RNF168 can be overcome by KAP1 depletion, that of RNF8 cannot (Figures 4.2-4.3). How RNF8 promotes resection is unclear but its ubiquitin ligase function is likely to be required. Two independent studies have demonstrated that RNF8 but not RNF168 is required for the formation of K48 linked ubiquitin chain IRIF at DSB sites and for the accumulation of these ubiquitin conjugates at laser induced DNA damage tracks (Feng & Chen, 2012; Meerang *et al*, 2011). The formation of K48 linked ubiquitin chains on a target substrate target it for degradation

by the 26S proteasome. (Ramadan & Meerang, 2011). RNF8 was recently shown to target Ku80 for proteasomal degradation through K48 ubiquitylation (Feng & Chen, 2012). The removal of factors modified by K48 linked ubiquitin chains from DSB sites by the proteasome appears to be important for 53BP1, BRCA1 and Rad51 recruitment (Meerang *et al*, 2011; Mallette & Richard, 2012). Consistent with the notion that the formation of K48 linked ubiquitin chains are important for HR, the depletion of RNF8 but not RNF168 supresses HR also when measured by a GFP-reporter assay, supporting the data from this chapter depicting distinct roles for RNF8 and RNF168 in HR (Ramadan & Meerang, 2011). Based on these findings and my data from this chapter, I propose a model whereby RNF8 promotes resection in G2 phase HR by ubiquitylating downstream targets and regulating the formation of K48 ubiquitin chains. RNF168 is dispensable for this process but is required for the amplification of K63 linked ubiquitin modifications that are required for 53BP1 recruitment/retention and therefore localised KAP1 phosphorylation.

BRCA1 is another ubiquitin ligase that has been implicated in HR (Moynahan *et al*, 1999; Schlegel *et al*, 2006). However there is conflicting evidence as to whether the ubiquitin ligase activity of BRCA1 is required for its role in HR. It was previously suggested that BRCA1 ubiquitylates its binding partner CtIP and that this is required for the association of CtIP with chromatin and therefore for ssDNA formation (Yu *et al*, 2006). However, another study indicated that the ubiquitin ligase activity of BRCA1 is dispensable for HR (Reid *et al*, 2008). A more recent study supported the notion that BRCA1 E3 ligase activity is dispensable for HR and went on to show that it is also dispensable for the tumour suppressor function of BRCA1 (Shakya *et al*, 2011; Greenberg, 2011). Here, I demonstrate that BRCA1 activity is required for slowly repaired DSBs in G2 and that its requirement cannot be overcome by KAP1 depletion (Figure 4.9). Moreover, I showed that BRCA1 depletion also leads to an RPA and Rad51 foci formation defect in G2 that cannot be overcome by KAP1 depletion (Figure 4.9). Finally, I demonstrated the E3 ubiquitin ligase activity of BRCA1 is dispensable for G2 phase HR whereas it BRCT domain is required. Deciphering how BRCA1 facilitates these processes was the main focus of my work in chapter 5.

7.3: Chapter 5: BRCA1 repositions 53BP1 during homologous recombination in G2 to enable resection at heterochromatin

7.3.1 Major conclusions from Chapter 5

- BRCA1 is required for HR at HC-DSBs in G2 but is dispensable for HC relaxation.
- BRCA1 functions in HR downstream of CtIP/MRE11 in resection.
- 53BP1 depletion rescues the HR defect of BRCA1 knockdown cells in G2.
- 53BP1 pATM and ubiquitin chains undergo BRCA1 dependent repositioning in G2.
- The BRCT but not the RING domain of BRCA1 is required for 53BP1 repositioning during HR.
- The deubiquitinating enzyme POH1 is required for resection and 53BP1 dissociation from chromatin in G2.

In chapter 4, I demonstrated that BRCA1 is required for RPA and Rad51 foci formation in G2 phase cells following IR treatment. In this chapter, I aimed to gain insight into the role of BRCA1 in these processes. First, I tested whether BRCA1 depletion affects γ-H2AX foci clearance following IR in G1 and G2 (Figure 5.1). Consistent with previous studies and my data showing a role for BRCA1 in HR, I observed a DSB repair defect in late repairing DSBs in G2. Importantly, no repair defect was observed in G1 phase cells indicating that BRCA1 is dispensable for NHEJ but also for KAP1 mediated HC relaxation. I confirmed this by showing that BRCA1 is dispensable for pKAP1 foci formation, indicating a distinct role to the mediator proteins in HR (Figure 5.2).

Previous work from out laboratory has demonstrated that CtIP is required for the initiation of resection and commitment to repair by HR (Shibata *et al*, 2011). In addition, the nuclease activity of MRE11 is also required for the initiation of resection and is thought to achieve this by removing Ku from DNA ends (Mimitou & Symington, 2011). In the absence of either of these factors, resection fails to initiate and repair by

HR cannot ensue. Interestingly, when cells fail to initiate resection they can return to NHEJ and repair the lesions via this pathway and no DSB repair defect is observed (Figures 5.3-5.4). Here, I demonstrate that BRCA1 functions in a DNA resection step that is downstream of the CtIP/MRE11 dependent initiation of resection. Consequently, when BRCA1 is depleted HR cannot progress, and since resection is initiated, NHEJ can no longer repair the lesions thus leading to a DSB repair defect (Figure 5.3). The notion that BRCA1 functions downstream of CtIP and MRE11 in resection is supported by the fact that CtIP or MRE11 depletion can rescue the repair defect of BRCA1 depleted cells (Figure 5.3-5.4). Under these conditions, resection fails to initiate and repair ensues by NHEJ thus making BRCA1 function dispensable (Figures 5.3-5.5).

Recent studies have indicated that BRCA1 functions in HR to overcome an inhibitory barrier posed by 53BP1 on DNA resection (Bunting *et al*, 2010; Bouwman *et al*, 2010). However, my data from chapter 3, suggest that in G2 phase HR, 53BP1 does not inhibit HR but rather facilitates the process by mediating the KAP1 dependent chromatin relaxation required for HR repair of DSBs at HC regions. Here I asked whether 53BP1 depletion could rescue the requirement for BRCA1 in HR also in G2 phase. Surprisingly, I observed that when KAP1 is depleted, thus making 53BP1 dispensable for HR, depletion of 53BP1 did rescue the HR defect of BRCA1 depleted cells (Figure 5.6). These results indicate that 53BP1 has dual roles in G2 phase HR. It promotes HR by mediating KAP1 phosphorylation but it also inhibits HR by blocking the initiation of resection.

A recent study demonstrated that RNF169 antagonises the recruitment of 53BP1 and BRCA1 to DSBs by binding to ubiquitylated histones (Poulsen *et al*, 2012). One possibility is that by delaying the recruitment of 53BP1 to DSBs, RNF169 promotes the CtIP/MRE11 dependent initiation of resection. Once 53BP1 is recruited, BRCA1 is then required to promote the elongation step of resection by overcoming the inhibitory role of 53BP1 on this process. It is currently unclear how BRCA1 achieves this. In this chapter, I observed that 53BP1 becomes repositioned in G2 phase in a BRCA1 dependent manner (Figure 5.8). Moreover, using enhanced resolution microscopy and 3D modelling, I observed that 53BP1 disassociates from chromatin in the IRIF core, leading to an inner region devoid of 53BP1 (Figure 5.9). Importantly, I demonstrated that BRCA1 forms IRIF internally to 53BP1 and is required for the formation of this region devoid of 53BP1 where RPA foci form (Figure 5.10 and 5.15). One interpretation of these findings is that BRCA1 overcomes the inhibitory function of

53BP1 on resection by repositioning 53BP1 away from the DSB ends and by promoting its dissociation from chromatin regions where resection takes place.

Histone H2A ubiquitylation is required for the recruitment of 53BP1 to DSB sites (Huen *et al*, 2007; Mailand *et al*, 2007; Doil *et al*, 2009). Given this, I investigated whether 53BP1 repositioning coincided with the repositioning of FK2 IRIF, which depict ubiquitin chains. I observed that FK2 IRIF become repositioned in a BRCA1 dependent manner and that they strongly co-localise with 53BP1 foci up to 8 hours post IR (Figures 5.13-5.15). Moreover, pATM foci also become repositioned and strongly co-localise with 53BP1 foci, consistent with the role of 53BP1 in tethering activated ATM at DSBs to maintain chromatin relaxation via pKAP1 (Figures 5.14-5.15) (Noon *et al*, 2010). These results suggest that on-going ubiquitylation events away from the DSB ends might be driving the repositioning of 53BP1. Since BRCA1 is required for this process, I tested whether its ubiquitin ligase activity is required to reposition 53BP1. However, MEFs expressing ubiquitin ligase mutant BRCA1 indicated that this isn't the case since 53BP1 is repositioned normally in these cells following IR treatment (Figure 5.16).

Since the BRCT domain of BRCA1 is required for its tumour suppressor function and for efficient RPA foci formation (Figure 3.9), I tested whether it is required for 53BP1 repositioning (Shakya *et al*, 2011). Using MEFs with mutated BRCT domains, I demonstrated that the BRCT domain of BRCA1 is required for 53BP1 repositioning in G2 (Figure 5.16). BRCA1 forms several complexes via its BRCT domains, with varying roles in the DDR (Huen *et al*, 2009). To test whether BRCA1 repositions 53BP1 via its BRCT binding partners, I monitored 53BP1 foci volume in G2 following depletion of BACH1, BRCC36 or RAP80 but observed normal 53BP1 volume expansion (Figure 5.17).

The expansion of 53BP1 away from DSB ends is likely to be driven by on-going histone ubiquitylation but 53BP1 also needs to disassociate from the inner region of the IRIF to allow resection to. I reasoned that this might require the function of a DUB since a hollow core also forms in FK2 IRIF suggesting that DUBing takes place (Figure 5.15). I first tested whether BRCC36 is required for this since it possesses DUB enzymatic activity and is a member of the BRCA1a complex (Diagram 5.1). However, BRCC36 did not impact on 53BP1 repositioning or disassociation from chromatin while depletion of BRCC36 has been shown to lead to more resection rather than less (Figure 5.17) (Hu *et al*, 2011).

The DUB enzyme, POH1, is a component of the 19S subunit of the proteasome, but recent findings indicate it also functions in the DDR (Morris et al unpublished). I tested whether POH1 is required for 53BP1 disassociation from chromatin and therefore for resection. Strikingly, POH1 depletion led to a severe RPA and Rad51 foci formation defect and a failure to form a hollow core in 53BP1 IRIF despite normal IRIF expansion (Figure 5.18). Moreover, POH1 depleted cells failed to form a hollow core in FK2 IRIF indicating that POH1 is required for this process. One interpretation of these results is that the DUB activity of POH1 is required to remove ubiquitin modifications from DSB ends thus leading to the disassociation of 53BP1, which is required for resection. In support of such a model, ubiquitin modifications have previously been found to be inhibitory to resection as they are bound by RAP80 in order to prevent excessive resection. Consequently, depletion of RAP80 or its binding partners BRCC36 and Abraxas, leads to increased resection. It appears that POH1 functions to overcome the inhibitory function of RAP80 on resection by DUBing ubiquitylated histones at DSB ends. This model is supported by the fact that depletion of RAP80, BRCC36 or Abraxas, overcomes the requirement for POH1 in resection and in the disassociation of 53BP1 from DSB ends (Figures 5.18). However, the Rad51 foci formation defect of POH1 depleted cells could not be rescued by RAP80 or BRCC36 co-depletion indicating that POH1 might also have a direct downstream role in Rad51 loading (Figure 5.18c). Consistent with this, unpublished work from the Morris laboratory has shown that POH1 is required for the recruitment of the BRCA2-co-factor DSS1 to DSB sites. Moreover, POH1 was shown to form a complex with BRCA2 and BRCA1 following hydroxyurea treatment. These findings suggest that the 19S proteasome, which contains POH1, interacts with factors that promote Rad51 loading.

My data from this chapter looking at the interplay of BRCA1 and 53BP1during G2 phase HR have revealed a complex regulatory system involving on-going ubiquitylation and de-ubiquitylation events. 53BP1 seems to protect DNA ends from resection by binding to methylated histones following its recruitment by histone ubiquitylation. The amplification of ubiquitin modifications at DSBs acts as a binding platform for the RAP80 complex that in turn protects these regions from rampant resection (Sobhian *et al*, 2007; Hu *et al*, 2011). At the subset of DSBs that are to be repaired by HR, BRCA1 and POH1 co-operate to overcome the barriers posed to resection by RAP80 and 53BP1. The BRCT domain of BRCA1 is required to drive 53BP1 repositioning away from DSB ends in a process likely to be dependent on novel

ubiquitylation events even if BRCA1 is not the E3 ligase carrying out these modifications. In conjunction, POH1 is required for the formation of a hollow inner core in FK2 and 53BP1 IRIF that is required for RPA foci formation. This is likely to be achieved by DUBing ubiquitylating histones leading to the disassociation of 53BP1 and RAP80 from chromatin and thus overcoming their inhibitory role on resection. It is not currently clear how BRCA1 and POH1 co-operate in this process. Future experiments investigating functional interactions between these factors should provide valuable information. Moreover, further experiments are required to demonstrate that POH1 DUB enzymatic activity is indeed required for G2 phase resection and HR.

7.4: Chapter 6: Transcriptional silencing at DSBs requires ATM and RNF8 as well as the chromatin remodellers BAF180 and CHD7.

7.4.1: Major conclusions from Chapter 6.

- RNF8 is required is for efficient DSB repair in EU and functions in the same pathway as ATM leading to transcriptional silencing in *cis* to DSBs.

- The PBAF chromatin-remodelling complex is required for DSB repair in EU and for transcriptional repression in *cis* to DNA DSBs.

- BAF180 is recruited to DSB containing laser tracks and this does not depend on phosphorylation by ATM.

- The chromatin remodeller CHD7 is required for DSB repair in EU and for transcriptional repression in *cis* to DNA DSBs.

In this chapter, I aimed to build on findings by the Greenberg laboratory, which previously demonstrated that ATM functions to silence transcription in *cis* to DSBs by maintaining histone ubiquitylation modifications (Shanbhag *et al*, 2010). These modifications inhibit transcription and are carried out by RNF8 and amplified by

RNF168 (Doil *et al*, 2009). Consequently, depletion of RNF8 and RNF168 leads to deficient transcriptional silencing is *cis* to DSBs (Shanbhag *et al*, 2010). Here, I investigated whether deficient transcriptional silencing results in a DSB repair defect. However, previous experiments in RNF8 depleted cells did not reveal a repair defect at times as early as 1h post IR (Noon *et al*, 2010). I decided to investigate the role of RNF8 in the repair of DSBs at very early times post IR(>1h) when repair takes place specifically in EU, which contains transcriptionally active regions (Figure 6.1). RNF8 depletion led to a repair defect/delay at very early times post IR but this was not detectable by 1h post IR (Figure 6.3). This repair defect coincided with a defect in transcriptional silencing in *cis* to DSBs raising the possibility that a failure to carry out this process leads to defective/delayed DSB repair (Figure 6.3). Alternatively, this repair defect might be the consequence of deficient chromatin decondensation at the DSB sites, a process that was recently found to be RNF8 and CHD4 dependent (Luijsterburg *et al*, 2012).

Next I investigated whether chromatin remodelling is required to achieve ATM dependent transcriptional silencing. By depleting individual components of the PBAF chromatin-remodelling complex in the U20S transcription reporter cells, I uncovered a role for this complex in transcriptional silencing in *cis* to DSBs (Figure 6.4). In addition, depletion of either the BAF180 or BRG1 subunits led to a repair defect at very early times post IR that was identical in magnitude to that observed following RNF8 depletion (Figure 6.5). My interpretation of these results is that PBAF and RNF8 function in the same pathway leading to transcriptional silencing in *cis* to DSBs.

To gain insight into the role of the PBAF complex in transcriptional silencing I monitored its accumulation to laser induced DNA damage tracks containing DSBs. BAF180, contains two BAH domains that are important for its association with chromatin and likely target the complex to chromatin. Therefore, the BAF180 subunit was cloned into a GFP-vector and its recruitment to DNA damage tracks was investigated. I observed that BAF180 forms ‘weak’ tracks following laser micro-irradiation but is recruited with fast kinetics and reaches maximum intensity within 60s post IR (Figures 6.6-6.7). ATM phosphorylates BAF180 in response to DNA damage but mutating this phosphorylation site did not prevent BAF180 from being recruited along the DNA damage tracks. The functional importance of this phosphorylation is currently unclear. Future experiments looking at DSB repair and transcriptional silencing following DSB induction in cells expressing phosphomutant BAF180 are

likely to be informative. It also remains to be seen whether the BAH domains of BAF180 are important for its recruitment to laser induced DNA damage tracks. The recruitment of BAF180 to DNA damage sites occurs with fast kinetics indicating that it is likely to function upstream of the RNF8 dependent ubiquitin modifications. One possibility is that PBAF functions upstream of RNF8 to remodel nucleosomes into a configuration that is favourable to ubiquitin modification. Further experiments are needed to prove or disprove whether this is how PBAF promotes transcriptional silencing in *cis* to DSBs.

In this chapter I also investigated the role of the chromatin remodeller CHD7 in transcriptional silencing in *cis* to DSBs. CHD7 co-operates with PBAF in neuronal crest formation and is also phosphorylated by ATM after DNA damage (Bajpai *et al*, 2010; Matsuoka *et al*, 2007). Following CHD7 depletion I observed a DSB repair defect/delay at very early times post IR (Figure 6.10). Moreover, I also observed a defect in transcriptional silencing following DSB induction that was similar in magnitude to that seen after PBAF depletion (Figure 6.11). It remains to be seen whether PBAF and CHD7 cooperate to silence transcription in *cis* to DSBs and how this is achieved. Uncovering a role for these chromatin remodellers in DSB repair via transcriptional silencing could be significant since CHD7 is mutated in CHARGE syndrome while BAF180 is frequently mutated in cancers.

7.5: Final summary

In recent years, major discoveries in the DDR field have uncovered a vastly complex and multifaceted system that functions to maintain genomic stability. The ‘nuts and bolts’ of the DNA DSB repair pathways have been well studied and characterised but how these pathways are regulated is now becoming clear. Following the induction of DNA damage, the appropriate repair pathway must be deployed, repair must take place within the context of chromatin, and it must interface with processes such as replication and transcription. Pivotal in the regulation of these processes are post-translational modifications, which provide control over function, localisation, interactions and more.

In this thesis, my work focused on several aspects of the DDR to DSBs. First I studied the role of the mediator proteins in HR in the G2 phase of the cell cycle. I described roles for these proteins in facilitating the chromatin modifications required for

HR to take place at HC regions. Work from our laboratory had previously described the importance of modifying chromatin for repair at HC in G1, and here I progressed these studies by studying HC repair in G2. Chromatin modifications at DSBs where repair by HR takes place are likely to extend onto the undamaged template used for repair. In this thesis I have not provided evidence for this model and it remains to be seen if this is the case.

Since the discovery of a non-proteasomal function for the ubiquitin signalling pathway, significant discoveries have been made into the role of this modification in the DDR. In this thesis I demonstrated that ubiquitin signalling is important for chromatin modifications through its role in recruiting factors such as 53BP1. In addition, ubiquitin signalling plays a direct role in HR since RNF8 depletion or treatment with a proteasome inhibitor leads to defective DNA resection.

One of the main reasons leading to conflicting data in the literature is that factors in the DDR can either inhibit or promote a given process depending on the given circumstances. In this thesis I have described a dual role for 53BP1 in HR. 53BP1 can promote HR at HC regions by mediating chromatin relaxation, but it also inhibits HR by blocking resection. I also provide insight into the intricate mechanisms regulating DSB repair pathway choice as well as to how processes such as resection are negatively and positively regulated so that a delicate balance is achieved.

Finally, I have progressed important findings showing that transcriptional silencing takes place in *cis* to DSBs. There are many unresolved questions regarding how this is achieved but my data indicate that chromatin remodelling is likely to play a key role. Perhaps unsurprisingly, ATM appears to be a key regulatory player in this process, adding another dimension to its multifunctional role in the DDR.

References

Abraham RT (2004) PI 3-kinase related kinases: “big” players in stress-induced signaling pathways. *DNA Repair (Amst.)* **3:** 883–887

Acs K, Luijsterburg MS, Ackermann L, Salomons FA, Hoppe T & Dantuma NP (2011) The AAA-ATPase VCP/p97 promotes 53BP1 recruitment by removing L3MBTL1 from DNA double-strand breaks. *Nat. Struct. Mol. Biol.* **18:** 1345–1350

Ahnesorg P, Smith P & Jackson SP (2006) XLF interacts with the XRCC4-DNA ligase IV complex to promote DNA nonhomologous end-joining. *Cell* **124:** 301–313

Al-Hakim A, Escribano-Diaz C, Landry M-C, O'Donnell L, Panier S, Szilard RK & Durocher D (2010) The ubiquitous role of ubiquitin in the DNA damage response. *DNA Repair (Amst.)* **9:** 1229–1240

Alderton GK, Joenje H, Varon R, Børglum AD, Jeggo PA & O'Driscoll M (2004) Seckel syndrome exhibits cellular features demonstrating defects in the ATR-signalling pathway. *Hum Mol Genet* **13:** 3127–3138

Almeida KH & Sobol RW (2007) A unified view of base excision repair: lesion-dependent protein complexes regulated by post-translational modification. *DNA Repair (Amst.)* **6:** 695–711

Arnaudeau C, Lundin C & Helleday T (2001) DNA double-strand breaks associated with replication forks are predominantly repaired by homologous recombination involving an exchange mechanism in mammalian cells. *J. Mol. Biol.* **307:** 1235–1245

Bajpai R, Chen DA, Rada-Iglesias A, Zhang J, Xiong Y, Helms J, Chang C-P, Zhao Y, Swigut T & Wysocka J (2010) CHD7 cooperates with PBAF to control multipotent neural crest formation. *Nature* **463:** 958–962

Bakkenist CJ & Kastan MB (2003) DNA damage activates ATM through intermolecular autophosphorylation and dimer dissociation. *Nature* **421:** 499–506

Baldeyron C, Jacquemin E, Smith J, Jacquemont C, De Oliveira I, Gad S, Feunteun J, Stoppa-Lyonnet D & Papadopoulo D (2002) A single mutated BRCA1 allele leads to impaired fidelity of double strand break end-joining. *Oncogene* **21:** 1401–1410

Bannister AJ & Kouzarides T (2011) Regulation of chromatin by histone modifications. *Cell Res.* **21:** 381–395

Barford D (1996) Molecular mechanisms of theprotein serine/threonine phosphatases. *Trends Biochem Sci* **21:** 407–412

Bartek J, Lukas C & Lukas J (2004) Checking on DNA damage in S phase. *Nat. Rev. Mol. Cell Biol.* **5:** 792–804

Bekker-Jensen S & Mailand N (2010) Assembly and function of DNA double-strand break repair foci in mammalian cells. *DNA Repair (Amst.)* **9:** 1219–1228

Bekker-Jensen S, Rendtlew Danielsen J, Fugger K, Gromova I, Nerstedt A, Lukas C, Bartek J, Lukas J & Mailand N (2010) HERC2 coordinates ubiquitin-dependent assembly of DNA repair factors on damaged chromosomes. *Nat. Cell Biol.* **12:** 80–6; sup pp 1–12

Bennardo N, Cheng A, Huang N & Stark JM (2008) Alternative-NHEJ Is a Mechanistically Distinct Pathway of Mammalian Chromosome Break Repair. *PLoS Genet.* **4:** e1000110

Berger SL (2007) The complex language of chromatin regulation during transcription. *Nature* **447:** 407–412

Berkovich E, Monnat RJ & Kastan MB (2007) Roles of ATM and NBS1 in chromatin structure modulation and DNA double-strand break repair. *Nat. Cell Biol.* **9:** 683–690

Beucher A, Birraux J, Tchouandong L, Barton O, Shibata A, Conrad S, Goodarzi AA, Krempler A, Jeggo PA & Löbrich M (2009) ATM and Artemis promote homologous recombination of radiation-induced DNA double-strand breaks in G2. *EMBO J.* **28:** 3413–3427

Bothmer A, Robbiani DF, Di Virgilio M, Bunting SF, Klein IA, Feldhahn N, Barlow J, Chen H-T, Bosque D, Callen E, Nussenzweig A & Nussenzweig MC (2011) Regulation of DNA end joining, resection, and immunoglobulin class switch recombination by 53BP1. *Mol. Cell* **42:** 319–329

Bothmer A, Robbiani DF, Feldhahn N, Gazumyan A, Nussenzweig A & Nussenzweig MC (2010) 53BP1 regulates DNA resection and the choice between classical and alternative end joining during class switch recombination. *J. Exp. Med.* **207:** 855–865

Botuyan MV, Lee J, Ward IM, Kim J-E, Thompson JR, Chen J & Mer G (2006) Structural basis for the methylation state-specific recognition of histone H4-K20 by 53BP1 and Crb2 in DNA repair. *Cell* **127:** 1361–1373

Bouwman P, Aly A, Escandell JM, Pieterse M, Bartkova J, van der Gulden H, Hiddingh S, Thanasoula M, Kulkarni A, Yang Q, Haffty BG, Tommiska J, Blomqvist C, Drapkin R, Adams DJ, Nevanlinna H, Bartek J, Tarsounas M, Ganesan S & Jonkers J (2010) 53BP1 loss rescues BRCA1 deficiency and is associated with triple-negative and BRCA-mutated breast cancers. *Nat. Struct. Mol. Biol.* **17:** 688–695

Brown EJ & Baltimore D (2003) Essential and dispensable roles of ATR in cell cycle arrest and genome maintenance. *Genes Dev.* **17:** 615–628

Brownlee PM, Chambers AL, Oliver AW & Downs JA (2012) Cancer and the bromodomains of BAF180. *Biochem. Soc. Trans.* **40:** 364–369

Brunton H, Goodarzi AA, Noon AT, Shrikhande A, Hansen RS, Jeggo PA & Shibata A (2011) Analysis of human syndromes with disordered chromatin reveals the impact of heterochromatin on the efficacy of ATM-dependent G2/M checkpoint arrest. *Mol. Cell. Biol.* **31:** 4022–4035

Bryant HE, Schultz N, Thomas HD, Parker KM, Flower D, Lopez E, Kyle S, Meuth M, Curtin NJ & Helleday T (2005) Specific killing of BRCA2-deficient tumours with inhibitors of poly(ADP-ribose) polymerase. *Nature* **434:** 913–917

Bunting SF, Callen E, Wong N, Chen H-T, Polato F, Gunn A, Bothmer A, Feldhahn N, Fernandez-Capetillo O, Cao L, Xu X, Deng C-X, Finkel T, Nussenzweig M, Stark JM & Nussenzweig A (2010) 53BP1 inhibits homologous recombination in Brca1-deficient cells by blocking resection of DNA breaks. *Cell* **141:** 243–254

Burrows AE, Smogorzewska A & Elledge SJ (2010) Polybromo-associated BRG1-associated factor components BRD7 and BAF180 are critical regulators of p53 required for induction of replicative senescence. *Proc. Natl. Acad. Sci. U.S.A.* **107:** 14280–14285

Busino L, Chiesa M, Draetta GF & Donzelli M (2004) Cdc25A phosphatase: combinatorial phosphorylation, ubiquitylation and proteolysis. *Oncogene* **23:** 2050–2056

Caldecott KW (2003) XRCC1 and DNA strand break repair. *DNA Repair (Amst.)* **2:** 955–969

Caldecott KW (2007) Mammalian single-strand break repair: mechanisms and links with chromatin. *DNA Repair (Amst.)* **6:** 443–453

Cancer Genome Atlas Research Network (2011) Integrated genomic analyses of ovarian carcinoma. *Nature* **474:** 609–615

Cao L, Kim S, Xiao C, Wang R-H, Coumoul X, Wang X, Li WM, Xu XL, De Soto JA, Takai H, Mai S, Elledge SJ, Motoyama N & Deng C-X (2006) ATM-Chk2-p53 activation prevents tumorigenesis at an expense of organ homeostasis upon Brca1 deficiency. *EMBO J.* **25:** 2167–2177

Cao L, Xu X, Bunting SF, Liu J, Wang R-H, Cao LL, Wu JJ, Peng T-N, Chen J, Nussenzweig A, Deng C-X & Finkel T (2009) A selective requirement for 53BP1 in the biological response to genomic instability induced by Brca1 deficiency. *Mol. Cell* **35:** 534–541

Chambers AL, Brownlee PM, Durley SC, Beacham T, Kent NA & Downs JA (2012) The Two Different Isoforms of the RSC Chromatin Remodeling Complex Play Distinct Roles in DNA Damage Responses. *PLoS ONE* **7:** e32016

Chapman JR, Sossick AJ, Boulton SJ & Jackson SP (2012) BRCA1-associated exclusion of 53BP1 from DNA damage sites underlies temporal control of DNA repair. *J. Cell. Sci.*

Chou DM, Adamson B, Dephoure NE, Tan X, Nottke AC, Hurov KE, Gygi SP, Colaiácovo MP & Elledge SJ (2010) A chromatin localization screen reveals poly (ADP ribose)-regulated recruitment of the repressive polycomb and NuRD complexes to sites of DNA damage. *Proc. Natl. Acad. Sci. U.S.A.* **107:** 18475–18480

Christmann MM, Tomicic MTM, Roos WPW & Kaina BB (2003) Mechanisms of

human DNA repair: an update. *Toxicology* **193:** 3–34

Chun HH & Gatti RA (2004) Ataxia–telangiectasia, an evolving phenotype. *DNA Repair (Amst.)* **3:** 1187–1196

Clapier CR & Cairns BR (2009) The biology of chromatin remodeling complexes. *Annu. Rev. Biochem.* **78:** 273–304

Clarke CL, Sandle J, Jones AA, Sofronis A, Patani NR & Lakhani SR (2006) Mapping loss of heterozygosity in normal human breast cells from BRCA1/2 carriers. *Br. J. Cancer* **95:** 515–519

Coleman KA & Greenberg RA (2011) The BRCA1-RAP80 complex regulates DNA repair mechanism utilization by restricting end resection. *J. Biol. Chem.* **286:** 13669–13680

Cong Y-S, Wright WE & Shay JW (2002) Human telomerase and its regulation. *Microbiol. Mol. Biol. Rev.* **66:** 407–25, table of contents

Conrad S, Künzel J & Löbrich M (2011) Sister chromatid exchanges occur in G2-irradiated cells. *Cell Cycle* **10:** 222–228

Cooper EM, Cutcliffe C, Kristiansen TZ, Pandey A, Pickart CM & Cohen RE (2009) K63-specific deubiquitination by two JAMM/MPN+ complexes: BRISC-associated Brcc36 and proteasomal Poh1. *EMBO J.* **28:** 621–631

Costantini S, Woodbine L, Andreoli L, Jeggo PA & Vindigni A (2007) Interaction of the Ku heterodimer with the DNA ligase IV/Xrcc4 complex and its regulation by DNA-PK. *DNA Repair (Amst.)* **6:** 712–722

Craig JM (2004) Heterochromatin?many flavours, common themes. *Bioessays* **27:** 17–28

Critchlow SE, Bowater RP & Jackson SP (1997) Mammalian DNA double-strand break repair protein XRCC4 interacts with DNA ligase IV. *Curr. Biol.* **7:** 588–598

D'Andrea A & Grompe M (2003) The Fanconi anaemia/BRCA pathway. *Nat Rev Cancer*

Deckbar D, Birraux J, Krempler A, Tchouandong L, Beucher A, Walker S, Stiff T, Jeggo P & Löbrich M (2007) Chromosome breakage after G2 checkpoint release. *J. Cell Biol.* **176:** 749–755

Deckbar D, Jeggo PA & Löbrich M (2011) Understanding the limitations of radiation-induced cell cycle checkpoints. *Crit. Rev. Biochem. Mol. Biol.* **46:** 271–283

Deckbar D, Stiff T, Koch B, Reis C, Löbrich M & Jeggo PA (2010) The limitations of the G1-S checkpoint. *Cancer Res.* **70:** 4412–4421

Denslow SA & Wade PA (2007) The human Mi-2/NuRD complex and gene regulation. *Oncogene* **26:** 5433–5438

Difilippantonio S, Gapud E, Wong N, Huang C-Y, Mahowald G, Chen H-T, Kruhlak MJ, Callen E, Livak F, Nussenzweig MC, Sleckman BP & Nussenzweig A (2008) 53BP1 facilitates long-range DNA end-joining during V(D)J recombination. *Nature* **456:** 529–533

Dillon N & Festenstein R (2002) Unravelling heterochromatin: competition between positive and negative factors regulates accessibility. *Trends Genet.* **18:** 252–258

Dimitrova N, Chen Y-CM, Spector DL & de Lange T (2008) 53BP1 promotes non-homologous end joining of telomeres by increasing chromatin mobility. *Nature* **456:** 524–528

Doil C, Mailand N, Bekker-Jensen S, Menard P, Larsen DH, Pepperkok R, Ellenberg J, Panier S, Durocher D, Bartek J, Lukas J & Lukas C (2009) RNF168 binds and amplifies ubiquitin conjugates on damaged chromosomes to allow accumulation of repair proteins. *Cell* **136:** 435–446

Downs JA, Nussenzweig MC & Nussenzweig A (2007) Chromatin dynamics and the preservation of genetic information. *Nature* **447:** 951–958

El-Khamisy SF, Saifi GM, Weinfeld M, Johansson F, Helleday T, Lupski JR & Caldecott KW (2005) Defective DNA single-strand break repair in spinocerebellar ataxia with axonal neuropathy-1. *Nature* **434:** 108–113

Elgin SCR & Grewal SIS (2003) Heterochromatin: silence is golden. *Curr. Biol.* **13:** R895–8

Eskeland R, Leeb M, Grimes GR, Kress C, Boyle S, Sproul D, Gilbert N, Fan Y, Skoultchi AI, Wutz A & Bickmore WA (2010) Ring1B compacts chromatin structure and represses gene expression independent of histone ubiquitination. *Mol. Cell* **38:** 452–464

Falck J, Mailand N, Syljuâsen RG, Bartek J & Lukas J (2001) The ATM-Chk2-Cdc25A checkpoint pathway guards against radioresistant DNA synthesis. *Nature* **410:** 842–847

Fanning E, Klimovich V & Nager AR (2006) A dynamic model for replication protein A (RPA) function in DNA processing pathways. *Nucleic Acids Res* **34:** 4126–4137

Fattah F, Lee EH, Weisensel N, Wang Y, Lichter N & Hendrickson EA (2010) Ku regulates the non-homologous end joining pathway choice of DNA double-strand break repair in human somatic cells. *PLoS Genet.* **6:** e1000855

Faucher D & Wellinger RJ (2010) Methylated H3K4, a transcription-associated histone modification, is involved in the DNA damage response pathway. *PLoS Genet.* **6**

Feng L & Chen J (2012) The E3 ligase RNF8 regulates KU80 removal and NHEJ repair. *Nat. Struct. Mol. Biol.* **19:** 201–206

Forget AL & Kowalczykowski SC (2010) Single-molecule imaging brings Rad51 nucleoprotein filaments into focus. *Trends Cell Biol.* **20:** 269–276

Fortini P & Dogliotti E (2007) Base damage and single-strand break repair: mechanisms and functional significance of short- and long-patch repair subpathways. *DNA Repair (Amst.)* **6:** 398–409

Friedberg EC (2001) How nucleotide excision repair protects against cancer. *Nat Rev Cancer* **1:** 22–33

Fujimuro M, Sawada H & Yokosawa H (1994) Production and characterization of monoclonal antibodies specific to multi-ubiquitin chains of polyubiquitinated proteins. *FEBS Lett.* **349:** 173–180

Galanty Y, Belotserkovskaya R, Coates J, Polo S, Miller KM & Jackson SP (2009) Mammalian SUMO E3-ligases PIAS1 and PIAS4 promote responses to DNA double-strand breaks. *Nature* **462:** 935–939

Garcia V, Phelps SEL, Gray S & Neale MJ (2011) Bidirectional resection of DNA double-strand breaks by Mre11 and Exo1. *Nature* **479:** 241–244

Gareau JR & Lima CD (2010) The SUMO pathway: emerging mechanisms that shape specificity, conjugation and recognition. *Nat. Rev. Mol. Cell Biol.* **11:** 861–871

Gatz SA, Ju L, Gruber R, Hoffmann E, Carr AM, Wang Z-Q, Liu C & Jeggo PA (2011) Requirement for DNA ligase IV during embryonic neuronal development. *J. Neurosci.* **31:** 10088–10100

Goodarzi AA, Kurka T & Jeggo PA (2011) KAP-1 phosphorylation regulates CHD3 nucleosome remodeling during the DNA double-strand break response. *Nat. Struct. Mol. Biol.* **18:** 831–839

Goodarzi AA, Noon AT, Deckbar D, Ziv Y, Shiloh Y, Löbrich M & Jeggo PA (2008) ATM signaling facilitates repair of DNA double-strand breaks associated with heterochromatin. *Mol. Cell* **31:** 167–177

Goodarzi AA, Yu Y, Riballo E, Douglas P, Walker SA, Ye R, Härer C, Marchetti C, Morrice N, Jeggo PA & Lees-Miller SP (2006) DNA-PK autophosphorylation facilitates Artemis endonuclease activity. *EMBO J.* **25:** 3880–3889

Goodship J, Gill H, Carter J, Jackson A, Splitt M & Wright M (2000) Autozygosity mapping of a seckel syndrome locus to chromosome 3q22. 1-q24. *Am. J. Hum. Genet.* **67:** 498–503

Goodwin GH & Nicolas RH (2001) The BAH domain, polybromo and the RSC chromatin remodelling complex. *Gene* **268:** 1–7

Gottlieb TM & Jackson SP (1993) The DNA-dependent protein kinase: requirement for DNA ends and association with Ku antigen. *Cell* **72:** 131–142

Gowen LC, Johnson BL, Latour AM, Sulik KK & Koller BH (1996) Brca1 deficiency results in early embryonic lethality characterized by neuroepithelial abnormalities. *Nat. Genet.* **12:** 191–194

Greenberg RA (2011) BRCA1, Everything But the RING? *Science* **334:** 459–460

Grewal SIS & Jia S (2007) Heterochromatin revisited. *Nat Rev Genet* **8:** 35–46

Groth P, Orta ML, Elvers I, Majumder MM, Lagerqvist A & Helleday T (2012) Homologous recombination repairs secondary replication induced DNA double-strand breaks after ionizing radiation. *Nucleic Acids Res*

Guenatri M, Bailly D, Maison C & Almouzni G (2004) Mouse centric and pericentric satellite repeats form distinct functional heterochromatin. *J. Cell Biol.* **166:** 493–505

Haince J-F, McDonald D, Rodrigue A, Déry U, Masson J-Y, Hendzel MJ & Poirier GG (2008) PARP1-dependent kinetics of recruitment of MRE11 and NBS1 proteins to multiple DNA damage sites. *J. Biol. Chem.* **283:** 1197–1208

Halazonetis TD, Gorgoulis VG & Bartek J (2008) An oncogene-induced DNA damage model for cancer development. *Science* **319:** 1352–1355

Hanada K, Budzowska M, Davies SL, van Drunen E, Onizawa H, Beverloo HB, Maas A, Essers J, Hickson ID & Kanaar R (2007) The structure-specific endonuclease Mus81 contributes to replication restart by generating double-strand DNA breaks. *Nat. Struct. Mol. Biol.* **14:** 1096–1104

Harley CB, Futcher AB & Greider CW (1990) Telomeres shorten during ageing of human fibroblasts. *Nature* **345:** 458–460

Harper JW & Elledge SJ (2007) The DNA damage response: ten years after. *Mol. Cell* **28:** 739–745

Helleday T (2003) Pathways for mitotic homologous recombination in mammalian cells. *Mutation Research/Fundamental and Molecular Mechanisms of Mutagenesis* **532:** 103–115

Helleday T (2003) Pathways for mitotic homologous recombination in mammalian cells. *Mutat Res* **532:** 103–115

HELLEDAY T, LO J, VANGENT D & ENGELWARD B (2007) DNA double-strand break repair: From mechanistic understanding to cancer treatment. *DNA Repair (Amst.)* **6:** 923–935

Herbig U & Sedivy JM (2006) Regulation of growth arrest in senescence: telomere damage is not the end of the story. *Mech. Ageing Dev.* **127:** 16–24

Herbig U, Jobling WA, Chen BPC, Chen DJ & Sedivy JM (2004) Telomere shortening triggers senescence of human cells through a pathway involving ATM, p53, and p21(CIP1), but not p16(INK4a). *Mol. Cell* **14:** 501–513

Hermeking H, Lengauer C, Polyak K, He TC, Zhang L, Thiagalingam S, Kinzler KW & Vogelstein B (1997) 14-3-3 sigma is a p53-regulated inhibitor of G2/M progression. *Mol. Cell* **1:** 3–11

Hirao A, Kong YY, Matsuoka S, Wakeham A, Ruland J, Yoshida H, Liu D, Elledge SJ & Mak TW (2000) DNA damage-induced activation of p53 by the checkpoint

kinase Chk2. *Science* **287:** 1824–1827

Hoeijmakers JH (2001) Genome maintenance mechanisms for preventing cancer. *Nature* **411:** 366–374

Holthausen JT, Wyman C & Kanaar R (2010) Regulation of DNA strand exchange in homologous recombination. *DNA Repair (Amst.)* **9:** 1264–1272

Hu Y, Scully R, Sobhian B, Xie A, Shestakova E & Livingston DM (2011) RAP80-directed tuning of BRCA1 homologous recombination function at ionizing radiation-induced nuclear foci. *Genes Dev.* **25:** 685–700

Huang B, Eberstadt M, Olejniczak ET, Meadows RP & Fesik SW (1996) NMR structure and mutagenesis of the Fas (APO-1/CD95) death domain. *Nature* **384:** 638–641

Huang J, Huen MSY, Kim H, Leung CCY, Glover JNM, Yu X & Chen J (2009) RAD18 transmits DNA damage signalling to elicit homologous recombination repair. *Nat. Cell Biol.* **11:** 592–603

Huber LJ, Yang TW, Sarkisian CJ, Master SR, Deng CX & Chodosh LA (2001) Impaired DNA damage response in cells expressing an exon 11-deleted murine Brca1 variant that localizes to nuclear foci. *Mol. Cell. Biol.* **21:** 4005–4015

Huen MSY, Grant R, Manke I, Minn K, Yu X, Yaffe MB & Chen J (2007) RNF8 transduces the DNA-damage signal via histone ubiquitylation and checkpoint protein assembly. *Cell* **131:** 901–914

Huen MSY, Sy SM-H & Chen J (2009) BRCA1 and its toolbox for the maintenance of genome integrity. *Nat. Rev. Mol. Cell Biol.* **11:** 138–148

Huertas P & Jackson SP (2009) Human CtIP mediates cell cycle control of DNA end resection and double strand break repair. *J. Biol. Chem.* **284:** 9558–9565

Ismail IH, Andrin C, McDonald D & Hendzel MJ (2010) BMI1-mediated histone ubiquitylation promotes DNA double-strand break repair. *J. Cell Biol.* **191:** 45–60

Jackson SP & Bartek J (2009) The DNA-damage response in human biology and disease. *Nature* **461:** 1071–1078

Janssen N, Bergman JEH, Swertz MA, Tranebjaerg L, Lodahl M, Schoots J, Hofstra RMW, van Ravenswaaij-Arts CMA & Hoefsloot LH (2012) Mutation update on the CHD7 gene involved in CHARGE syndrome. *Hum. Mutat.* n/a–n/a

Jasin M (2002) Homologous repair of DNA damage and tumorigenesis: the BRCA connection. *Oncogene* **21:** 8981–8993

Jeggo PA & Löbrich M (2006) Contribution of DNA repair and cell cycle checkpoint arrest to the maintenance of genomic stability. *DNA Repair (Amst.)* **5:** 1192–1198

Jeggo PA, Geuting V & Löbrich M (2011) The role of homologous recombination in radiation-induced double-strand break repair. *Radiother Oncol* **101:** 7–12

Jensen RB, Carreira A & Kowalczykowski SC (2010) Purified human BRCA2 stimulates RAD51-mediated recombination. *Nature* **467:** 678–683

Johnson LN (2009) The regulation of protein phosphorylation. *Biochem. Soc. Trans.* **37:** 627

Kass EM, Moynahan ME & Jasin M (2010) Loss of 53BP1 is a gain for BRCA1 mutant cells. *Cancer Cell* **17:** 423–425

Kastan MB & Bartek J (2004) Cell-cycle checkpoints and cancer. *Nature* **432:** 316–323

Kasten MM, Clapier CR & Cairns BR (2011) SnapShot: Chromatin Remodeling:SWI/SNF. *Cell* **144:** 310–310.e1

Kent NA, Chambers AL & Downs JA (2007) Dual chromatin remodeling roles for RSC during DNA double strand break induction and repair at the yeast MAT locus. *J. Biol. Chem.* **282:** 27693–27701

Kolas NK, Chapman JR, Nakada S, Ylanko J, Chahwan R, Sweeney FD, Panier S, Mendez M, Wildenhain J, Thomson TM, Pelletier L, Jackson SP & Durocher D (2007) Orchestration of the DNA-damage response by the RNF8 ubiquitin ligase. *Science* **318:** 1637–1640

Kong X, Mohanty SK, Stephens J, Heale JT, Gomez-Godinez V, Shi LZ, Kim J-S, Yokomori K & Berns MW (2009) Comparative analysis of different laser systems to study cellular responses to DNA damage in mammalian cells. *Nucleic Acids Res* **37:** e68

Kruhlak M, Crouch EE, Orlov M, Montaño C, Gorski SA, Nussenzweig A, Misteli T, Phair RD & Casellas R (2007) The ATM repair pathway inhibits RNA polymerase I transcription in response to chromosome breaks. *Nature* **447:** 730–734

Lane DP (1992) Cancer. p53, guardian of the genome. *Nature* **358:** 15–16

Langerak P, Mejia-Ramirez E, Limbo O & Russell P (2011) Release of Ku and MRN from DNA ends by Mre11 nuclease activity and Ctp1 is required for homologous recombination repair of double-strand breaks. *PLoS Genet.* **7:** e1002271

Larsen DH, Poinsignon C, Gudjonsson T, Dinant C, Payne MR, Hari FJ, Rendtlew Danielsen JM, Menard P, Sand JC, Stucki M, Lukas C, Bartek J, Andersen JS & Lukas J (2010) The chromatin-remodeling factor CHD4 coordinates signaling and repair after DNA damage. *J. Cell Biol.* **190:** 731–740

Lavin MF (2007) ATM and the Mre11 complex combine to recognize and signal DNA double-strand breaks. *Oncogene* **26:** 7749–7758

Lavin MF (2008) Ataxia-telangiectasia: from a rare disorder to a paradigm for cell signalling and cancer. *Nat. Rev. Mol. Cell Biol.* **9:** 759–769

Lee J-H, Goodarzi AA, Jeggo PA & Paull TT (2010) 53BP1 promotes ATM activity through direct interactions with the MRN complex. *EMBO J.* **29:** 574–585

Li S, Ting NS, Zheng L, Chen PL, Ziv Y, Shiloh Y, Lee EY & Lee WH (2000) Functional link of BRCA1 and ataxia telangiectasia gene product in DNA damage response. *Nature* **406:** 210–215

Liang F & Jasin M (1996) Ku80-deficient cells exhibit excess degradation of extrachromosomal DNA. *J. Biol. Chem.* **271:** 14405–14411

Liang F, Romanienko PJ, Weaver DT, Jeggo PA & Jasin M (1996) Chromosomal double-strand break repair in Ku80-deficient cells. *Proc. Natl. Acad. Sci. U.S.A.* **93:** 8929–8933

Liao H, Winkfein RJ, Mack G, Rattner JB & Yen TJ (1995) CENP-F is a protein of the nuclear matrix that assembles onto kinetochores at late G2 and is rapidly degraded after mitosis. *J. Cell Biol.* **130:** 507–518

Lim DS, Kim ST, Xu B, Maser RS, Lin J, Petrini JH & Kastan MB (2000) ATM phosphorylates p95/nbs1 in an S-phase checkpoint pathway. *Nature* **404:** 613–617

Lips J & Kaina B (2001) DNA double-strand breaks trigger apoptosis in p53-deficient fibroblasts. *Carcinogenesis* **22:** 579–585

Liu J, Doty T, Gibson B & Heyer W-D (2010) Human BRCA2 protein promotes RAD51 filament formation on RPA-covered single-stranded DNA. *Nat. Struct. Mol. Biol.* **17:** 1260–1262

Lombard DB, Chua KF, Mostoslavsky R, Franco S, Gostissa M & Alt FW (2005) DNA repair, genome stability, and aging. *Cell* **120:** 497–512

Lord CJ & Ashworth A (2012) The DNA damage response and cancer therapy. *Nature* **481:** 287–294

Löbrich M, Shibata A, Beucher A, Fisher A, Ensminger M, Goodarzi AA, Barton O & Jeggo PA (2010) gammaH2AX foci analysis for monitoring DNA double-strand break repair: strengths, limitations and optimization. *Cell Cycle* **9:** 662–669

Luijsterburg MS, Acs K, Ackermann L, Wiegant WW, Bekker-Jensen S, Larsen DH, Khanna KK, van Attikum H, Mailand N & Dantuma NP (2012) A new non-catalytic role for ubiquitin ligase RNF8 in unfolding higher-order chromatin structure. *EMBO J.* 1–17

Lukas C, Melander F, Stucki M, Falck J, Bekker-Jensen S, Goldberg M, Lerenthal Y, Jackson SP, Bartek J & Lukas J (2004a) Mdc1 couples DNA double-strand break recognition by Nbs1 with its H2AX-dependent chromatin retention. *EMBO J.* **23:** 2674–2683

Lukas J, Lukas C & Bartek J (2004b) Mammalian cell cycle checkpoints: signalling pathways and their organization in space and time. *DNA Repair (Amst.)* **3:** 997–1007

Lundin C, Erixon K, Arnaudeau C, Schultz N, Jenssen D, Meuth M & Helleday T (2002) Different roles for nonhomologous end joining and homologous recombination following replication arrest in mammalian cells. *Mol. Cell. Biol.* **22:**

5869–5878

Lundin C, Schultz N, Arnaudeau C, Mohindra A, Hansen LT & Helleday T (2003) RAD51 is involved in repair of damage associated with DNA replication in mammalian cells. *J. Mol. Biol.* **328:** 521–535

Ma Y, Pannicke U, Schwarz K & Lieber MR (2002) Hairpin opening and overhang processing by an Artemis/DNA-dependent protein kinase complex in nonhomologous end joining and V(D)J recombination. *Cell* **108:** 781–794

Mailand N, Bekker-Jensen S, Faustrup H, Melander F, Bartek J, Lukas C & Lukas J (2007) RNF8 ubiquitylates histones at DNA double-strand breaks and promotes assembly of repair proteins. *Cell* **131:** 887–900

Mailand N, Falck J, Lukas C, Syljuâsen RG, Welcker M, Bartek J & Lukas J (2000) Rapid destruction of human Cdc25A in response to DNA damage. *Science* **288:** 1425–1429

Maison C & Almouzni G (2004) HP1 and the dynamics of heterochromatin maintenance. *Nat. Rev. Mol. Cell Biol.* **5:** 296–305

Mallette FA & Richard S (2012) K48-linked ubiquitination and protein degradation regulate 53BP1 recruitment at DNA damage sites. *Cell Res.* 1–3

Mallette FA, Mattiroli F, Cui G, Young LC, Hendzel MJ, Mer G, Sixma TK & Richard S (2012) RNF8- and RNF168-dependent degradation of KDM4A/JMJD2A triggers 53BP1 recruitment to DNA damage sites. *EMBO J.* **31:** 1865–1878

Marfella CGA & Imbalzano AN (2007) The Chd family of chromatin remodelers. *Mutation Research/Fundamental and Molecular Mechanisms of Mutagenesis* **618:** 30–40

Matsuoka S, Ballif BA, Smogorzewska A, McDonald ER, Hurov KE, Luo J, Bakalarski CE, Zhao Z, Solimini N, Lerenthal Y, Shiloh Y, Gygi SP & Elledge SJ (2007) ATM and ATR Substrate Analysis Reveals Extensive Protein Networks Responsive to DNA Damage. *Science* **316:** 1160–1166

Maya R, Balass M, Kim ST, Shkedy D, Leal JF, Shifman O, Moas M, Buschmann T, Ronai Z, Shiloh Y, Kastan MB, Katzir E & Oren M (2001) ATM-dependent phosphorylation of Mdm2 on serine 395: role in p53 activation by DNA damage. *Genes Dev.* **15:** 1067–1077

McVey M & Lee SE (2008) MMEJ repair of double-strand breaks (director's cut): deleted sequences and alternative endings. *Trends in Genetics* **24:** 529–538

Meerang M, Ritz D, Paliwal S, Garajova Z, Bosshard M, Mailand N, Janscak P, Hübscher U, Meyer H & Ramadan K (2011) The ubiquitin-selective segregase VCP/p97 orchestrates the response to DNA double-strand breaks. *Nat. Cell Biol.* **13:** 1376–1382

Melino G, Bernassola F, Ranalli M, Yee K, Zong WX, Corazzari M, Knight RA, Green DR, Thompson C & Vousden KH (2004) p73 Induces apoptosis via PUMA

transactivation and Bax mitochondrial translocation. *J. Biol. Chem.* **279:** 8076–8083

Meng L, Mohan R, Kwok BH, Elofsson M, Sin N & Crews CM (1999) Epoxomicin, a potent and selective proteasome inhibitor, exhibits in vivo antiinflammatory activity. *Proc. Natl. Acad. Sci. U.S.A.* **96:** 10403–10408

Metzler-Guillemain C, Luciani J, Depetris D, Guichaoua MR & Mattei MG (2003) HP1beta and HP1gamma, but not HP1alpha, decorate the entire XY body during human male meiosis. *Chromosome Res.* **11:** 73–81

Miklos GL & John B (1979) Heterochromatin and satellite DNA in man: properties and prospects. *Am. J. Hum. Genet.* **31:** 264–280

Miller KM, Tjeertes JV, Coates J, Legube G, Polo SE, Britton S & Jackson SP (2010) Human HDAC1 and HDAC2 function in the DNA-damage response to promote DNA nonhomologous end-joining. *Nat. Struct. Mol. Biol.* **17:** 1144–1151

Mimitou EP & Symington LS (2009a) Nucleases and helicases take center stage in homologous recombination. *Trends Biochem Sci* **34:** 264–272

Mimitou EP & Symington LS (2009b) DNA end resection: many nucleases make light work. *DNA Repair (Amst.)* **8:** 983–995

Mimitou EP & Symington LS (2011) DNA end resection--Unraveling the tail. *DNA Repair (Amst.)* **10:** 344–348

Mimori T & Hardin JA (1986) Mechanism of interaction between Ku protein and DNA. *J. Biol. Chem.* **261:** 10375–10379

Miné-Hattab J & Rothstein R (2012) Increased chromosome mobility facilitates homology search during recombination. *Nat. Cell Biol.*

Minter-Dykhouse K, Ward I, Huen MSY, Chen J & Lou Z (2008) Distinct versus overlapping functions of MDC1 and 53BP1 in DNA damage response and tumorigenesis. *J. Cell Biol.* **181:** 727–735

Misteli T & Soutoglou E (2009) The emerging role of nuclear architecture in DNA repair and genome maintenance. *Nat. Rev. Mol. Cell Biol.* **10:** 243–254

Mohammad DH & Yaffe MB (2009) 14-3-3 proteins, FHA domains and BRCT domains in the DNA damage response. *DNA Repair (Amst.)* **8:** 1009–1017

Mohrmann L & Verrijzer CP (2005) Composition and functional specificity of SWI2/SNF2 class chromatin remodeling complexes. *Biochim. Biophys. Acta* **1681:** 59–73

Moreno-Herrero F, de Jager M, Dekker NH, Kanaar R, Wyman C & Dekker C (2005) Mesoscale conformational changes in the DNA-repair complex Rad50/Mre11/Nbs1 upon binding DNA. *Nature* **437:** 440–443

Morris JR, Boutell C, Keppler M, Densham R, Weekes D, Alamshah A, Butler L,

Galanty Y, Pangon L, Kiuchi T, Ng T & Solomon E (2009) The SUMO modification pathway is involved in the BRCA1 response to genotoxic stress. *Nature* **462:** 886–890

Morrison AJ & Shen X (2009) Chromatin remodelling beyond transcription: the INO80 and SWR1 complexes. *Nat. Rev. Mol. Cell Biol.* **10:** 373–384

Moshous D, Callebaut I, de Chasseval R, Corneo B, Cavazzana-Calvo M, Le Deist F, Tezcan I, Sanal O, Bertrand Y, Philippe N, Fischer A & de Villartay JP (2001) Artemis, a novel DNA double-strand break repair/V(D)J recombination protein, is mutated in human severe combined immune deficiency. *Cell* **105:** 177–186

Moynahan ME, Chiu JW, Koller BH & Jasin M (1999) Brca1 controls homology-directed DNA repair. *Mol. Cell* **4:** 511–518

Moynahan ME, Pierce AJ & Jasin M (2001) BRCA2 is required for homology-directed repair of chromosomal breaks. *Mol. Cell* **7:** 263–272

Murawska M (2011) CHD chromatin remodelers and the transcription cycle. *Transcription*

Murr R, Loizou JI, Yang Y-G, Cuenin C, Li H, Wang Z-Q & Herceg Z (2006) Histone acetylation by Trrap-Tip60 modulates loading of repair proteins and repair of DNA double-strand breaks. *Nat. Cell Biol.* **8:** 91–99

Müller WG, Walker D, Hager GL & McNally JG (2001) Large-scale chromatin decondensation and recondensation regulated by transcription from a natural promoter. *J. Cell Biol.* **154:** 33–48

Nimonkar AV, Ozsoy AZ, Genschel J, Modrich P & Kowalczykowski SC (2008) Human exonuclease 1 and BLM helicase interact to resect DNA and initiate DNA repair. *Proc. Natl. Acad. Sci. U.S.A.* **105:** 16906–16911

Noon AT, Shibata A, Rief N, Löbrich M, Stewart GS, Jeggo PA & Goodarzi AA (2010) 53BP1-dependent robust localized KAP-1 phosphorylation is essential for heterochromatic DNA double-strand break repair. *Nat. Cell Biol.* **12:** 177–184

O'Connell BC & Harper JW (2007) Ubiquitin proteasome system (UPS): what can chromatin do for you? *Curr. Opin. Cell Biol.* **19:** 206–214

O'Driscoll M, Cerosaletti KM, Girard PM, Dai Y, Stumm M, Kysela B, Hirsch B, Gennery A, Palmer SE, Seidel J, Gatti RA, Varon R, Oettinger MA, Neitzel H, Jeggo PA & Concannon P (2001) DNA ligase IV mutations identified in patients exhibiting developmental delay and immunodeficiency. *Mol. Cell* **8:** 1175–1185

O'Driscoll M, Gennery AR, Seidel J, Concannon P & Jeggo PA (2004) An overview of three new disorders associated with genetic instability: LIG4 syndrome, RS-SCID and ATR-Seckel syndrome. *DNA Repair (Amst.)* **3:** 1227–1235

O'Driscoll M, Ruiz-Perez VL, Woods CG, Jeggo PA & Goodship JA (2003) A splicing mutation affecting expression of ataxia-telangiectasia and Rad3-related protein (ATR) results in Seckel syndrome. *Nat. Genet.* **33:** 497–501

Ogi T, Limsirichaikul S, Overmeer RM, Volker M, Takenaka K, Cloney R, Nakazawa Y, Niimi A, Miki Y, Jaspers NG, Mullenders LHF, Yamashita S, Fousteri MI & Lehmann AR (2010) Three DNA polymerases, recruited by different mechanisms, carry out NER repair synthesis in human cells. *Mol. Cell* **37:** 714–727

Okano S, Lan L, Caldecott KW, Mori T & Yasui A (2003) Spatial and temporal cellular responses to single-strand breaks in human cells. *Mol. Cell. Biol.* **23:** 3974–3981

Panier S & Durocher D (2009) Regulatory ubiquitylation in response to DNA double-strand breaks. *DNA Repair (Amst.)* **8:** 436–443

Patterson-Fortin J, Shao G, Bretscher H, Messick TE & Greenberg RA (2010) Differential regulation of JAMM domain deubiquitinating enzyme activity within the RAP80 complex. *J. Biol. Chem.* **285:** 30971–30981

Pei H, Zhang L, Luo K, Qin Y, Chesi M, Fei F, Bergsagel PL, Wang L, You Z & Lou Z (2011) MMSET regulates histone H4K20 methylation and 53BP1 accumulation at DNA damage sites. *Nature* **470:** 124–128

Petermann E & Helleday T (2010) Pathways of mammalian replication fork restart. *Nat. Rev. Mol. Cell Biol.* **11:** 683–687

Pierce AJ, Hu P, Han M, Ellis N & Jasin M (2001) Ku DNA end-binding protein modulates homologous repair of double-strand breaks in mammalian cells. *Genes Dev.* **15:** 3237–3242

Plans V, Scheper J, Soler M, Loukili N, Okano Y & Thomson TM (2006) The RING finger protein RNF8 recruits UBC13 for lysine 63-based self polyubiquitylation. *J. Cell. Biochem.* **97:** 572–582

Polo SE & Jackson SP (2011) Dynamics of DNA damage response proteins at DNA breaks: a focus on protein modifications. *Genes Dev.* **25:** 409–433

Polo SE, Kaidi A, Baskcomb L, Galanty Y & Jackson SP (2010) Regulation of DNA-damage responses and cell-cycle progression by the chromatin remodelling factor CHD4. *EMBO J.* **29:** 3130–3139

Pommier Y (1996) Eukaryotic DNA topoisomerase I: genome gatekeeper and its intruders, camptothecins. *Semin. Oncol.* **23:** 3–10

Pommier Y, Leo E, Zhang H & Marchand C (2010) DNA topoisomerases and their poisoning by anticancer and antibacterial drugs. *Chem. Biol.* **17:** 421–433

Postow L, Ghenoiu C, Woo EM, Krutchinsky AN, Chait BT & Funabiki H (2008) Ku80 removal from DNA through double strand break-induced ubiquitylation. *J. Cell Biol.* **182:** 467–479

Poulsen M, Lukas C, Lukas J, Bekker-Jensen S & Mailand N (2012) Human RNF169 is a negative regulator of the ubiquitin-dependent response to DNA double-strand breaks. *J. Cell Biol.*

Powell SN & Kachnic LA (2008) Therapeutic exploitation of tumor cell defects in

homologous recombination. *Anticancer Agents Med Chem* **8:** 448–460

Rahal EA, Henricksen LA, Li Y, Williams RS, Tainer JA & Dixon K (2010) ATM regulates Mre11-dependent DNA end-degradation and microhomology-mediated end joining. *Cell Cycle* **9:** 2866–2877

Ramadan K & Meerang M (2011) Degradation-linked ubiquitin signal and proteasome are integral components of DNA double strand break repair: New perspectives for anti-cancer therapy. *FEBS Lett.* **585:** 2868–2875

Ramaekers CHMA & Wouters BG (2011) Regulatory functions of ubiquitin in diverse DNA damage responses. *Curr. Mol. Med.* **11:** 152–169

Rass U, Compton SA, Matos J, Singleton MR, Ip SCY, Blanco MG, Griffith JD & West SC (2010) Mechanism of Holliday junction resolution by the human GEN1 protein. *Genes Dev.* **24:** 1559–1569

Reid LJ, Shakya R, Modi AP, Lokshin M, Cheng J-T, Jasin M, Baer R & Ludwig T (2008) E3 ligase activity of BRCA1 is not essential for mammalian cell viability or homology-directed repair of double-strand DNA breaks. *Proc. Natl. Acad. Sci. U.S.A.* **105:** 20876–20881

Riballo E, Kühne M, Rief N, Doherty A, Smith GCM, Recio M-J, Reis C, Dahm K, Fricke A, Krempler A, Parker AR, Jackson SP, Gennery A, Jeggo PA & Löbrich M (2004) A pathway of double-strand break rejoining dependent upon ATM, Artemis, and proteins locating to gamma-H2AX foci. *Mol. Cell* **16:** 715–724

Riballo E, Woodbine L, Stiff T, Walker SA, Goodarzi AA & Jeggo PA (2009) XLF-Cernunnos promotes DNA ligase IV-XRCC4 re-adenylation following ligation. *Nucleic Acids Res* **37:** 482–492

Rogakou EP, Boon C, Redon C & Bonner WM (1999) Megabase chromatin domains involved in DNA double-strand breaks in vivo. *J. Cell Biol.* **146:** 905–916

Rogakou EP, Pilch DR, Orr AH, Ivanova VS & Bonner WM (1998) DNA double-stranded breaks induce histone H2AX phosphorylation on serine 139. *J. Biol. Chem.* **273:** 5858–5868

Roos WP & Kaina B (2006) DNA damage-induced cell death by apoptosis. *Trends in Molecular Medicine* **12:** 440–450

Roseaulin L, Yamada Y, Tsutsui Y, Russell P, Iwasaki H & Arcangioli B (2008) Mus81 is essential for sister chromatid recombination at broken replication forks. *EMBO J.* **27:** 1378–1387

Rouleau M, Patel A, Hendzel MJ, Kaufmann SH & Poirier GG (2010) PARP inhibition: PARP1 and beyond. *Nat Rev Cancer* **10:** 293–301

Rulten SL, Cortes-Ledesma F, Guo L, Iles NJ & Caldecott KW (2008) APLF (C2orf13) is a novel component of poly(ADP-ribose) signaling in mammalian cells. *Mol. Cell. Biol.* **28:** 4620–4628

Rulten SL, Fisher AEO, Robert I, Zuma MC, Rouleau M, Ju L, Poirier G, Reina-San-Martin B & Caldecott KW (2011) PARP-3 and APLF Function Together to Accelerate Nonhomologous End-Joining. *Mol. Cell* **41:** 33–45

Saar K, Chrzanowska KH, Stumm M, Jung M, Nürnberg G, Wienker TF, Seemanová E, Wegner RD, Reis A & Sperling K (1997) The gene for the ataxia-telangiectasia variant, Nijmegen breakage syndrome, maps to a 1-cM interval on chromosome 8q21. *Am. J. Hum. Genet.* **60:** 605–610

Saintigny Y, Delacôte F, Varès G, Petitot F, Lambert S, Averbeck D & Lopez BS (2001) Characterization of homologous recombination induced by replication inhibition in mammalian cells. *EMBO J.* **20:** 3861–3870

Saleh-Gohari N, Bryant HE, Schultz N, Parker KM, Cassel TN & Helleday T (2005) Spontaneous homologous recombination is induced by collapsed replication forks that are caused by endogenous DNA single-strand breaks. *Mol. Cell. Biol.* **25:** 7158–7169

Sankaran S, Starita LM, Simons AM & Parvin JD (2006) Identification of domains of BRCA1 critical for the ubiquitin-dependent inhibition of centrosome function. *Cancer Res.* **66:** 4100–4107

Sarkaria JN, Busby EC, Tibbetts RS, Roos P, Taya Y, Karnitz LM & Abraham RT (1999) Inhibition of ATM and ATR kinase activities by the radiosensitizing agent, caffeine. *Cancer Res.* **59:** 4375–4382

Sartori AA, Lukas C, Coates J, Mistrik M, Fu S, Bartek J, Baer R, Lukas J & Jackson SP (2007) Human CtIP promotes DNA end resection. *Nature* **450:** 509–514

Schlegel BP, Jodelka FM & Nunez R (2006) BRCA1 promotes induction of ssDNA by ionizing radiation. *Cancer Res.* **66:** 5181–5189

Schnetz MP, Bartels CF, Shastri K, Balasubramanian D, Zentner GE, Balaji R, Zhang X, Song L, Wang Z, Laframboise T, Crawford GE & Scacheri PC (2009) Genomic distribution of CHD7 on chromatin tracks H3K4 methylation patterns. *Genome Res.* **19:** 590–601

Schultz DC, Friedman JR & Rauscher FJ (2001) Targeting histone deacetylase complexes via KRAB-zinc finger proteins: the PHD and bromodomains of KAP-1 form a cooperative unit that recruits a novel isoform of the Mi-2alpha subunit of NuRD. *Genes Dev.* **15:** 428–443

Seiler DM, Rouquette J, Schmid VJ, Strickfaden H, Ottmann C, Drexler GA, Mazurek B, Greubel C, Hable V, Dollinger G, Cremer T & Friedl AA (2011) Double-strand break-induced transcriptional silencing is associated with loss of tri-methylation at H3K4. *Chromosome Res.* **19:** 883–899

Shakya R, Reid LJ, Reczek CR, Cole F, Egli D, Lin CS, deRooij DG, Hirsch S, Ravi K, Hicks JB, Szabolcs M, Jasin M, Baer R & Ludwig T (2011) BRCA1 Tumor Suppression Depends on BRCT Phosphoprotein Binding, But Not Its E3 Ligase Activity. *Science* **334:** 525–528

Shanbhag NM, Rafalska-Metcalf IU, Balane-Bolivar C, Janicki SM & Greenberg RA (2010) ATM-dependent chromatin changes silence transcription in *cis* to DNA double-strand breaks. *Cell* **141:** 970–981

Shao RG, Cao CX, Zhang H, Kohn KW, Wold MS & Pommier Y (1999) Replication-mediated DNA damage by camptothecin induces phosphorylation of RPA by DNA-dependent protein kinase and dissociates RPA: DNA-PK complexes. *EMBO J.* **18:** 1397–1406

Shao Z, Davis AJ, Fattah KR, So S, Sun J, Lee K-J, Harrison L, Yang J & Chen DJ (2012) Persistently bound Ku at DNA ends attenuates DNA end resection and homologous recombination. *DNA Repair (Amst.)* **11:** 310–316

Shechter D, Costanzo V & Gautier J (2004) Regulation of DNA replication by ATR: signaling in response to DNA intermediates. *DNA Repair (Amst.)* **3:** 901–908

Sherr CJ & Roberts JM (1999) CDK inhibitors: positive and negative regulators of G1-phase progression. *Genes Dev.* **13:** 1501–1512

Shibata A, Barton O, Noon AT, Dahm K, Deckbar D, Goodarzi AA, Löbrich M & Jeggo PA (2010) Role of ATM and the damage response mediator proteins 53BP1 and MDC1 in the maintenance of G(2)/M checkpoint arrest. *Mol. Cell. Biol.* **30:** 3371–3383

Shibata A, Conrad S, Birraux J, Geuting V, Barton O, Ismail A, Kakarougkas A, Meek K, Taucher-Scholz G, Löbrich M & Jeggo PA (2011) Factors determining DNA double-strand break repair pathway choice in G2 phase. *EMBO J.* **30:** 1079–1092

Shiloh Y (2003) ATM and related protein kinases: safeguarding genome integrity. *Nat Rev Cancer* **3:** 155–168

Shiotani B & Zou L (2009) Single-stranded DNA orchestrates an ATM-to-ATR switch at DNA breaks. *Mol. Cell* **33:** 547–558

Smeenk G, Wiegant WW, Vrolijk H, Solari AP, Pastink A & van Attikum H (2010) The NuRD chromatin-remodeling complex regulates signaling and repair of DNA damage. *J. Cell Biol.* **190:** 741–749

Smith GC, Cary RB, Lakin ND, Hann BC, Teo SH, Chen DJ & Jackson SP (1999) Purification and DNA binding properties of the ataxia-telangiectasia gene product ATM. *Proc. Natl. Acad. Sci. U.S.A.* **96:** 11134–11139

Sobhian B, Shao G, Lilli DR, Culhane AC, Moreau LA, Xia B, Livingston DM & Greenberg RA (2007) RAP80 targets BRCA1 to specific ubiquitin structures at DNA damage sites. *Science* **316:** 1198–1202

Stark JM, Hu P, Pierce AJ, Moynahan ME, Ellis N & Jasin M (2002) ATP hydrolysis by mammalian RAD51 has a key role during homology-directed DNA repair. *J. Biol. Chem.* **277:** 20185–20194

Stark JM, Pierce AJ, Oh J, Pastink A & Jasin M (2004) Genetic steps of mammalian homologous repair with distinct mutagenic consequences. *Mol. Cell. Biol.* **24:**

9305–9316

Stewart GS (2009) Solving the RIDDLE of 53BP1 recruitment to sites of damage. *Cell Cycle* **8:** 1532–1538

Stewart GS, Panier S, Townsend K, Al-Hakim AK, Kolas NK, Miller ES, Nakada S, Ylanko J, Olivarius S, Mendez M, Oldreive C, Wildenhain J, Tagliaferro A, Pelletier L, Taubenheim N, Durandy A, Byrd PJ, Stankovic T, Taylor AMR & Durocher D (2009) The RIDDLE syndrome protein mediates a ubiquitin-dependent signaling cascade at sites of DNA damage. *Cell* **136:** 420–434

Stewart GS, Stankovic T, Byrd PJ, Wechsler T, Miller ES, Huissoon A, Drayson MT, West SC, Elledge SJ & Taylor AMR (2007) RIDDLE immunodeficiency syndrome is linked to defects in 53BP1-mediated DNA damage signaling. *Proc. Natl. Acad. Sci. U.S.A.* **104:** 16910–16915

Stiff T, O'Driscoll M, Rief N, Iwabuchi K, Löbrich M & Jeggo PA (2004) ATM and DNA-PK function redundantly to phosphorylate H2AX after exposure to ionizing radiation. *Cancer Res.* **64:** 2390–2396

Strauss C & Goldberg M (2011) Recruitment of proteins to DNA double-strand breaks: MDC1 directly recruits RAP80. *Cell Cycle* **10:** 2850–2857

Stucki M & Jackson SP (2006) gammaH2AX and MDC1: anchoring the DNA-damage-response machinery to broken chromosomes. *DNA Repair (Amst.)* **5:** 534–543

Stucki M, Clapperton JA, Mohammad D, Yaffe MB, Smerdon SJ & Jackson SP (2005) MDC1 directly binds phosphorylated histone H2AX to regulate cellular responses to DNA double-strand breaks. *Cell* **123:** 1213–1226

Sun J, Lee KJ, Davis AJ & Chen DJ (2012) Human Ku70/80 Protein Blocks Exonuclease 1-mediated DNA Resection in the Presence of Human Mre11 or Mre11/Rad50 Protein Complex. *J. Biol. Chem.* **287:** 4936–4945

Svejstrup JQ (2002) Mechanisms of transcription-coupled DNA repair. *Nat. Rev. Mol. Cell Biol.* **3:** 21–29

Sy SM-H, Jiang J, Dong S-S, Lok GT-M, Wu J, Cai H, Yeung ESL, Huang J, Chen J, Deng Y & Huen MSY (2011) Critical roles of ring finger protein RNF8 in replication stress responses. *J. Biol. Chem.* **286:** 22355–22361

Syljuåsen RG (2007) Checkpoint adaptation in human cells. *Oncogene* **26:** 5833–5839

Symington LS & Gautier J (2011) Double-strand break end resection and repair pathway choice. *Annu. Rev. Genet.* **45:** 247–271

Sørensen CS, Syljuåsen RG, Falck J, Schroeder T, Rönnstrand L, Khanna KK, Zhou B-B, Bartek J & Lukas J (2003) Chk1 regulates the S phase checkpoint by coupling the physiological turnover and ionizing radiation-induced accelerated proteolysis of Cdc25A. *Cancer Cell* **3:** 247–258

Tafani M, Karpinich NO, Hurster KA, Pastorino JG, Schneider T, Russo MA & Farber

JL (2002) Cytochrome c release upon Fas receptor activation depends on translocation of full-length bid and the induction of the mitochondrial permeability transition. *J. Biol. Chem.* **277:** 10073–10082

Takai H, Smogorzewska A & de Lange T (2003) DNA damage foci at dysfunctional telomeres. *Curr. Biol.* **13:** 1549–1556

Tang L, Nogales E & Ciferri C (2010) Structure and function of SWI/SNF chromatin remodeling complexes and mechanistic implications for transcription. *Prog. Biophys. Mol. Biol.* **102:** 122–128

Taylor AMR, Groom A & Byrd PJ (2004) Ataxia-telangiectasia-like disorder (ATLD)—its clinical presentation and molecular basis. *DNA Repair (Amst.)* **3:** 1219–1225

Taylor WR & Stark GR (2001) Regulation of the G2/M transition by p53. *Oncogene* **20:** 1803–1815

Thomson TM & Guerra-Rebollo M (2010) Ubiquitin and SUMO signalling in DNA repair. *Biochem. Soc. Trans.* **38:** 116–131

Trempe J-F (2011) Reading the ubiquitin postal code. *Current Opinion in Structural Biology* **21:** 792–801

Trenz K, Smith E, Smith S & Costanzo V (2006) ATM and ATR promote Mre11 dependent restart of collapsed replication forks and prevent accumulation of DNA breaks. *EMBO J.* **25:** 1764–1774

Trojer P & Reinberg D (2007) Facultative Heterochromatin: Is There a Distinctive Molecular Signature? *Mol. Cell* **28:** 1–13

Ulrich HD & Walden H (2010) Ubiquitin signalling in DNA replication and repair. *Nat. Rev. Mol. Cell Biol.* 1–11

Urnov FD (2002) A feel for the template: zinc finger protein transcription factors and chromatin. *Biochem. Cell Biol.* **80:** 321–333

van Attikum H & Gasser SM (2009) Crosstalk between histone modifications during the DNA damage response. *Trends Cell Biol.* **19:** 207–217

van Dierendonck JH, Wijsman JH, Keijzer R, van de Velde CJ & Cornelisse CJ (1991) Cell-cycle-related staining patterns of anti-proliferating cell nuclear antigen monoclonal antibodies. Comparison with BrdUrd labeling and Ki-67 staining. *Am. J. Pathol.* **138:** 1165–1172

Varela I, Tarpey P, Raine K, Huang D, Ong CK, Stephens P, Davies H, Jones D, Lin M-L, Teague J, Bignell G, Butler A, Cho J, Dalgliesh GL, Galappaththige D, Greenman C, Hardy C, Jia M, Latimer C, Lau KW, et al (2011) Exome sequencing identifies frequent mutation of the SWI/SNF complex gene PBRM1 in renal carcinoma. *Nature* **469:** 539–542

Vissers LELM, van Ravenswaaij CMA, Admiraal R, Hurst JA, de Vries BBA, Janssen

IM, van der Vliet WA, Huys EHLPG, de Jong PJ, Hamel BCJ, Schoenmakers EFPM, Brunner HG, Veltman JA & van Kessel AG (2004) Mutations in a new member of the chromodomain gene family cause CHARGE syndrome. *Nat. Genet.* **36:** 955–957

Wang B & Elledge SJ (2007) Ubc13/Rnf8 ubiquitin ligases control foci formation of the Rap80/Abraxas/Brca1/Brcc36 complex in response to DNA damage. *Proc. Natl. Acad. Sci. U.S.A.* **104:** 20759–20763

Wang H, Wang L, Erdjument-Bromage H, Vidal M, Tempst P, Jones RS & Zhang Y (2004) Role of histone H2A ubiquitination in Polycomb silencing. *Nature* **431:** 873–878

Wang M, Wu W, Wu W, Rosidi B, Zhang L, Wang H & Iliakis G (2006) PARP-1 and Ku compete for repair of DNA double strand breaks by distinct NHEJ pathways. *Nucleic Acids Res* **34:** 6170–6182

Wang XW, Zhan Q, Coursen JD, Khan MA, Kontny HU, Yu L, Hollander MC, O'Connor PM, Fornace AJ & Harris CC (1999) GADD45 induction of a G2/M cell cycle checkpoint. *Proc. Natl. Acad. Sci. U.S.A.* **96:** 3706–3711

Wu LC, Wang ZW, Tsan JT, Spillman MA, Phung A, Xu XL, Yang MC, Hwang LY, Bowcock AM & Baer R (1996) Identification of a RING protein that can interact in vivo with the BRCA1 gene product. *Nat. Genet.* **14:** 430–440

Xia W, Nagase S, Montia AG, Kalachikov SM, Keniry M, Su T, Memeo L, Hibshoosh H & Parsons R (2008) BAF180 is a critical regulator of p21 induction and a tumor suppressor mutated in breast cancer. *Cancer Res.* **68:** 1667–1674

Xie A, Hartlerode A, Stucki M, Odate S, Puget N, Kwok A, Nagaraju G, Yan C, Alt FW, Chen J, Jackson SP & Scully R (2007) Distinct roles of chromatin-associated proteins MDC1 and 53BP1 in mammalian double-strand break repair. *Mol. Cell* **28:** 1045–1057

Xu X, Qiao W, Linke SP, Cao L, Li WM, Furth PA, Harris CC & Deng CX (2001) Genetic interactions between tumor suppressors Brca1 and p53 in apoptosis, cell cycle and tumorigenesis. *Nat. Genet.* **28:** 266–271

Xu Y & Price BD (2011) Chromatin dynamics and the repair of DNA double strand breaks. *Cell Cycle* **10:** 261–267

Xu Y, Sun Y, Jiang X, Ayrapetov MK, Moskwa P, Yang S, Weinstock DM & Price BD (2010) The p400 ATPase regulates nucleosome stability and chromatin ubiquitination during DNA repair. *J. Cell Biol.* **191:** 31–43

Yarden RI, Pardo-Reoyo S, Sgagias M, Cowan KH & Brody LC (2002) BRCA1 regulates the G2/M checkpoint by activating Chk1 kinase upon DNA damage. *Nat. Genet.* **30:** 285–289

Yazdi PT, Wang Y, Zhao S, Patel N, Lee EY-HP & Qin J (2002) SMC1 is a downstream effector in the ATM/NBS1 branch of the human S-phase checkpoint. *Genes Dev.* **16:** 571–582

You Z, Chahwan C, Bailis J, Hunter T & Russell P (2005) ATM activation and its recruitment to damaged DNA require binding to the C terminus of Nbs1. *Mol. Cell. Biol.* **25:** 5363–5379

You Z, Shi LZ, Zhu Q, Wu P, Zhang Y-W, Basilio A, Tonnu N, Verma IM, Berns MW & Hunter T (2009) CtIP links DNA double-strand break sensing to resection. *Mol. Cell* **36:** 954–969

Yu X & Chen J (2004) DNA damage-induced cell cycle checkpoint control requires CtIP, a phosphorylation-dependent binding partner of BRCA1 C-terminal domains. *Mol. Cell. Biol.* **24:** 9478–9486

Yu XX, Fu SS, Chen JJ5 (2006) BRCA1 ubiquitinates its phosphorylation-dependent binding partner CtIP. *Genes Dev.* **20:** 1721–1726

Yuan SS, Lee SY, Chen G, Song M, Tomlinson GE & Lee EY (1999) BRCA2 is required for ionizing radiation-induced assembly of Rad51 complex in vivo. *Cancer Res.* **59:** 3547–3551

Yun MH & Hiom K (2009) CtIP-BRCA1 modulates the choice of DNA double-strand-break repair pathway throughout the cell cycle. *Nature* **459:** 460–463

Yunis JJ & Yasmineh WG (1971) Heterochromatin, satellite DNA, and cell function. Structural DNA of eucaryotes may support and protect genes and aid in speciation. *Science* **174:** 1200–1209

Zhang J, Ma Z, Treszezamsky A & Powell SN (2005) MDC1 interacts with Rad51 and facilitates homologous recombination. *Nat. Struct. Mol. Biol.* **12:** 902–909

Zhang Y & Jasin M (2010) An essential role for CtIP in chromosomal translocation formation through an alternative end-joining pathway. *Nat. Struct. Mol. Biol.* **18:** 80–84

Zhao GY, Sonoda E, Barber LJ, Oka H, Murakawa Y, Yamada K, Ikura T, Wang X, Kobayashi M, Yamamoto K, Boulton SJ & Takeda S (2007) A critical role for the ubiquitin-conjugating enzyme Ubc13 in initiating homologous recombination. *Mol. Cell* **25:** 663–675

Zhong Q, Boyer TG, Chen P-L & Lee W-H (2002) Deficient nonhomologous end-joining activity in cell-free extracts from Brca1-null fibroblasts. *Cancer Res.* **62:** 3966–3970

Zhou BB & Elledge SJ (2000) The DNA damage response: putting checkpoints in perspective. *Nature* **408:** 433–439

Zhou W, Wang X & Rosenfeld MG (2009) Histone H2A ubiquitination in transcriptional regulation and DNA damage repair. *Int. J. Biochem. Cell Biol.* **41:** 12–15

Zhu P, Zhou W, Wang J, Puc J, Ohgi KA, Erdjument-Bromage H, Tempst P, Glass CK & Rosenfeld MG (2007) A histone H2A deubiquitinase complex coordinating histone acetylation and H1 dissociation in transcriptional regulation. *Mol. Cell* **27:**

609–621

Zhu Q, Pao GM, Huynh AM, Suh H, Tonnu N, Nederlof PM, Gage FH & Verma IM (2011) BRCA1 tumour suppression occurs via heterochromatin-mediated silencing. *Nature* **477:** 179–184

APPENDIX

BRCA1 and POH1 co-operate to reposition 53BP1 during homologous recombination in G2 to enable resection at heterochromatin

Andreas Kakarougkas[1], Amani Ismail[1], Yoko Katsuki[1], Karin Klement[2], Aaron A. Goodarzi[2], Markus Lobrich[3], Raimundo Freire[4], Atsushi Shibata[1] and Penny A. Jeggo[1*]

[1]Genome Damage and Stability Centre, University of Sussex, Brighton BN1 9 RQ

[2]Southern Alberta Cancer Research Institute, Department of Biochemistry and Molecular Biology, University of Calgary, Alberta, Canada T2N 4N1

[3]Darmstadt University of Technology, Radiation Biology and DNA Repair, 64287 Darmstadt, Germany

[4]Unidad de Investigación, Hospital Universitario de Canarias, Instituto de Tecnologías Biomédicas, Ofra s/n, 38320 La Laguna, Tenerife, Spain.

***Correspondence to: p.a.jeggo@sussex.ac.uk**

Tel: 0044 1273 678482

Fax: 0044 1273 678121.

Character count: 54,463 (excluding references)

Running Title: BRCA1 repositions 53BP1 during HR in G2.

Keywords: ATM signalling / BRCA1 / DNA double strand break repair / homologous recombination / 53BP1

Abstract. (174)

Although DNA non-homologous end-joining (NHEJ) repairs most DNA double strand breaks (DSBs) in G2 phase, DSBs at heterochromatin (HC) regions undergo repair by homologous recombination (HR). Here, we examine roles for 53BP1 and BRCA1 in DSB repair in G2. We show that 53BP1 is required for HR at HC regions in G2 by promoting phosphorylated KAP1 foci formation but conversely 53BP1 creates a barrier to HR. BRCA1 is dispensable for pKAP1 foci formation but promotes resection downstream of CtIP/MRN. BRCA1, via its BRCT domain, promotes G2-specific repositioning of 53BP1 to the foci periphery and its vacation from the core. Ubiquitin modifications but not gH2AX are similarly relocalised. RPA foci form in the 53BP1-devoid core. Depletion of the deubiquitinating enzyme and proteasome component, POH1, allows 53BP1 expansion but prevents formation of the 53BP1-devoid core and RPA foci formation. Depletion of RAP80, BRCC36 or Abraxas overcomes the need for POH1 for generation of the 53BP1-devoid core. We propose that BRCA1 promotes 53BP1 repositioning onto the undamaged template relieving the barrier to HR whilst enabling HC modifications.

Introduction

Agents such as ionising radiation (IR) generate two-ended DNA double strand breaks (DSBs) in all cell cycle phases. Additionally, one-ended DSBs can arise in S phase at stalled/collapsed replication forks (Petermann & Helleday, 2010). Cells are equipped with two major DSB repair mechanisms, DNA non-homologous end-joining (NHEJ), which occurs in all cell cycle phases and homologous recombination (HR), which uses sister homologues in late S/G2 phase (Mahaney et al, 2009; Wyman & Kanaar, 2006). NHEJ represents the major pathway repairing two-ended DSBs whilst HR exerts its main function during replication (Beucher et al, 2009; Zhang & Jasin, 2011).

Two related DNA damage response (DDR) signalling pathways respond to DSBs (Kurz & Lees-Miller, 2004). Ataxia and telangiectasia mutated (ATM) is activated by two-ended DSBs; AT and Rad3 related (ATR), in contrast, responds to single stranded (ss) regions of DNA, which arise at stalled/collapsed replication forks or following resection of double stranded (ds) DNA ends (Ciccia & Elledge, 2010; Lavin, 2008). Both kinases orchestrate assembly of DDR proteins at the damage site. ATM-dependent signalling involves ATM recruitment by the MRE11/RAD50/NBS1 (MRN) complex, H2AX phosphorylation and recruitment of the mediator protein, MDC1, which provides a step tethering MRN and ATM at the DSB (Jackson & Bartek, 2009). The ubiquitin ligases, RNF8 and RNF168, are then recruited (Panier & Durocher, 2009). Subsequent degradation of methylated histone binding proteins aids the localisation of 53BP1, another mediator protein (Acs et al, 2011; Mallette et al, 2012). This assembly can be visualised as IR-induced foci (IRIF) at DSBs. In addition to this process, which occurs in all cell cycle phases, another branch of recruited proteins that include BRCA1, Rap80, Abraxas, and BRCC36, form either uniquely or more robustly in G2 phase (Feng et al, 2010).

DSB repair is influenced by chromatin structure and cell cycle phase. In G0/G1, the majority (~ 85 %) of IR-induced DSBs, which are located in euchromatic (EC) DNA, are re-joined by NHEJ without requirement for ATM or DDR mediator proteins (Riballo et al, 2004). In contrast, the repair of DSBs located in heterochromatic (HC) regions (~ 15 %) requires ATM, H2AX, MRN, RNF8, RNF168, and 53BP1 as well as NHEJ proteins (Goodarzi et al, 2008; Noon et al, 2010). Current evidence suggests that compacted HC impedes DSB repair and that ATM promotes phosphorylation of KAP1 (pKAP1), an HC-building factor. pKAP1 forms in a pan nuclear manner and as discrete foci (pKAP1 foci). Whilst pan nuclear pKAP1 only requires activated ATM, pKAP1

foci, which form uniquely at HC-DSBs, additionally require 53BP1 and upstream DDR proteins necessary for 53BP1 recruitment (Noon et al, 2010). 53BP1 is proposed to tether ATM at DSBs, promoting concentrated pKAP-1 (i.e. pKAP-1 foci) at HC-DSBs, release of the chromatin remodelling protein, CHD3, and HC relaxation (Noon et al, 2010); (Goodarzi et al, 2011). Although ATM localises to all DSBs, it is specifically required for HC-DSB repair (although it may also promote repair of other DSB sub-fractions such as those undergoing transcription) (Shanbhag et al, 2010). In addition to these differing genetic requirements for HC versus EC-DSB repair, there are kinetic differences; EC-DSBs are repaired rapidly whilst HC-DSBs are repaired with slow kinetics (Goodarzi et al, 2008).

In G2, EC-DSBs are repaired predominantly by NHEJ (as in G1). However, HC-DSBs, in contrast to the situation in G1, undergo repair by HR (Beucher et al, 2009). ATM has at least two functions in HR; it phosphorylates KAP1 promoting HC relaxation and phosphorylates and activates CtIP, enabling DNA resection (Shibata et al, 2011). Based on these and additional findings, it has been proposed that NHEJ makes the first attempt to repair DSBs in G2 but if rapid repair does not ensue then resection occurs committing to HR. Thus, HR functions predominantly to repair the slow component of DSB repair (HC-DSBs) in G2 phase (Beucher et al, 2009). However, little is understood about events regulating the switch from NHEJ to HR.

There is also interplay between HR and NHEJ at one-ended DSBs in S phase with data suggesting that the Fanconi anaemia proteins function to prevent access of Ku, an upstream NHEJ component (Adamo et al, 2010; Pace et al, 2010). Additionally, evidence has suggested that 53BP1 and BRCA1 regulate DSB repair pathway choice (Bothmer et al, 2010; Bouwman et al, 2010; Bunting et al, 2010; Shibata et al, 2011). BRCA1 is essential for HR although it may also influence NHEJ (Baldeyron et al, 2002; Moynahan et al, 1999; Stark et al, 2004; Zhong et al, 2002). BRCA1 has been reported to enhance CtIP recruitment and resection (Chen et al, 2008; Choudhary & Li, 2002; Schlegel et al, 2006). 53BP1, in contrast, has been considered to promote NHEJ. Although 53BP1 is dispensable for most DSB repair by NHEJ, it is required for HC-DSB repair, telomere fusions, and long range V(D)J recombination re-joining (Difilippantonio et al, 2008; Dimitrova et al, 2008; Noon et al, 2010). Importantly, whilst deficiency in BRCA1 impairs resection and inhibits HR, both are regained following concomitant loss of BRCA1 and 53BP1 (Bouwman et al, 2010; Bunting et al, 2010). However, the mechanism underlying these provocative findings is unclear.

Here, we examine roles for 53BP1 and BRCA1 in HR at IR-induced two-ended DSBs in G2. We exploit G2 phase analysis since transactions at replication forks are complex to dissect and since it allows the necessity for additional chromatin modifications (e.g. HC relaxation) to be examined. We show that, contrary to previous reports, 53BP1 has a pro-HR function at HC-DSBs in G2 via its requirement for pKAP-1 foci formation. Thus, 53BP1 does not solely promote NHEJ. Next, we show that BRCA1 functions downstream of CtIP/MRN to complete resection. As in S phase, loss of 53BP1 overcomes the need for BRCA1 for HR. Using enhanced resolution and 3D imaging, we show that 53BP1 foci undergo G2-phase specific enlargement via a process requiring BRCA1's BRCT domain. Additionally, a central core devoid of 53BP1 where RPA foci form is generated. Moreover, we show that POH1, a recently characterised deubiquitinating enzyme and proteasome component, is required for generation of the 53BP1-devoid core and RPA foci (Cooper et al, 2009; Yao & Cohen, 2002). These findings provide mechanistic insight into how BRCA1 modulates 53BP1 to enable HR. We propose a model whereby BRCA1 counterbalances two opposing impacts of 53BP1, repositioning 53BP1 to relieve its barrier to resection whilst enabling 53BP1 to effect HC modifications on the undamaged template.

Results.

53BP1 is required for HR at two-ended DSBs in G2 phase.

The requirement for 53BP1 for DSB repair in G2 was initially examined by enumerating gH2AX foci in irradiated 53BP1$^{+/+}$ and $^{-/-}$ mouse embryo fibroblasts (MEFs). DSB repair was normal at 2-4 h but impaired by 6-8 h post IR (Figure 1A), which is similar to the defect observed in 53BP1$^{-/-}$ G0/G1 phase MEFs and G2 cells lacking Artemis, ATM, BRCA2, RAD51 or RAD54 (Beucher et al, 2009; Riballo et al, 2004). These findings were verified using siRNA 53BP1 in A549 cells (Figure 1B). Enumeration of RPA and Rad51 foci formation as markers of resection and HR repair in A549 cells at 2 h post IR revealed modestly diminished resection and more markedly impaired RAD51 loading following siRNA 53BP1 (Figure 1C,D). Examination of sister chromatid exchanges (SCEs) in mitotic cells derived from irradiated G2 cells (see (Beucher et al, 2009)) showed that siRNA 53BP1 abolished IR-induced SCEs (Figure 1E). Addition of an ATM inhibitor (ATMi) demonstrated that 53BP1 functions epistatically to ATM to promote HR (Figure 1B-E). We conclude that 53BP1 is essential for HR in G2 following IR since SCEs, a direct readout for HR, and gH2AX foci loss are similarly diminished by either siRNA 53BP1 or ATMi addition.

53BP1 is specifically required for HR at HC-DSBs.

We previously suggested that, after g- or X-ray exposure, HR in G2 phase arises predominantly at HC-DSBs, which are repaired with slow kinetics due to a barrier created by the HC superstructure (Beucher et al, 2009; Shibata et al, 2011). Previous studies have shown that densely staining DAPI regions do not efficiently reflect chromocentres in late G2 (Goodarzi et al, 2009). To consolidate the notion that HR occurs predominantly at HC-DSBs, we used confocal microscopy and immunofluorescence staining for the heterochromatic markers, H3K9me3 and H4K20me3, to visualise chromocentres in G2. At 8 h post IR in WT cells, >71 % of RPA foci overlap with H3K9me3 or H4K20me3 positive chromatin; when both HC markers were used (to enhance HC demarcation), >88% of RPA foci co-localise with HC (Figure 2A-D). We previously showed that ~15-20% of DSBs undergo resection in control G2 cells with the level of resected DSBs increasing following loss of NHEJ proteins, demonstrating that HR can occur at EC-DSBs (Shibata et al, 2011). Here, we observed that in 2BN cells, which lack the NHEJ component, XLF, the additional RPA

foci persisting 8 h post IR (compared to control) predominantly occur in H3K9me3 or H4K20me3 negative chromatin (i.e. euchromatin) (Figure 2A-D).

Next, we examined the relationship between pKAP1 foci and HR in G2 phase. In G1 cells, we observed that pKAP1 foci only form at the subset of DSBs repaired with slow kinetics, shown to represent HC-DSBs (Noon et al, 2010). Previously, we were unable to detect pKAP1 foci in G2 cells due to partial dispersal of KAP1 from chromocentres in late G2/mitosis (Goodarzi et al, 2009)**.** Here, using siRNA MeCP2, which enhances the size of IRIF **(**Brunton et al, 2011), we could visualise pKAP1 foci in G2 cells and found that RPA foci substantially co-localise with pKAP1 and 53BP1 foci (Figure 2E). Additionally, following combined Ku80+DNA-PKcs siRNA (siRNA DNA-PK) this overlap is greatly diminished. Since RPA foci co-localise with the HC markers, H3K9me3/H4K20me3, this supports the notion that pKAP1 foci predominantly form at HC-DSBs in G2 (as in G1 phase). Together, this analysis strongly suggests that HR occurs primarily at HC-DSBs in WT cells but can arise at EC-DSBs when DNA-PK is absent. We also observed that pKAP1 foci do not form in G2 (as in G1) cells following 53BP1+MeCP2 siRNA (Figure 2F). Moreover, we observed normal RPA foci and gH2AX foci loss at EC-DSBs following siRNA 53BP1 providing evidence that 53BP1 is dispensable for HR at EC-DSBs (Supplementary Figure 2A). Thus, there is a direct correlation between 53BP1's requirement for pKAP1 foci formation and HR consistent with a causal relationship.

To consolidate the notion that 53BP1 is required for HR via a function in promoting HC relaxation, we examined whether HC relaxation (by knockdown of HC components) can overcome the requirement for 53BP1 for DSB repair in G2 phase. Strikingly, siRNA KAP-1 restored normal gH2AX foci loss, resection (as judged by RPA foci numbers), RAD51 loading and SCE formation to 53BP1 depleted G2 cells (Supplementary Figure 3). Knockdown of HP1 (a,b+g) similarly overcame the need for 53BP1 for G2 phase DSB repair (Supplementary Figure 3E).

Collectively, these findings substantiate and extend previous data suggesting that after IR, HR occurs predominantly at HC regions. We propose that HC represents a partial barrier to resection and a full barrier to the completion of HR (SCEs) at DSBs in G2 and that 53BP1 promotes pKAP-1 foci formation to relieve that barrier. However, HR can occur efficiently without 53BP1at HC-DSBs following siRNA of critical HC components (KAP1 or HP1) or at EC-DSBs. Moreover, 53BP1 is dispensable for NHEJ since the fast DSB repair process (NHEJ) takes place in 53BP1$^{-/-}$ cells (Figure

1A). This strongly suggests that 53BP1 is dispensable for HR and NHEJ but can promote either process by impacting on HC.

BRCA1 is required for HR at HC-DSBs in G2.

Having examined 53BP1's role in DSB repair, we next examined the requirement for BRCA1. Firstly, we observed normal pKAP-1 foci formation in G2 phase cells following siRNA BRCA1+MeCP2 in contrast to the defect observed following siRNA 53BP1 (Figure 2F) suggesting that BRCA1 is dispensable for pKAP1-mediated HC relaxation. Next, we examined DSB repair in cells depleted for BRCA1. In G1 cells, we observed normal gH2AX foci loss post IR (fast and slow components) following siRNA BRCA1 (Figure 3A). In contrast, we reproducibly observed defective DSB repair in BRCA1-depleted G2 cells detectable as a failure to undergo the slow DSB repair process (Figure 3B). The fact that the slow DSB repair process in G1 (HC-DSB repair) is BRCA1 independent is consistent with the finding above that BRCA1 is dispensable for pKAP1 foci formation. The failure to repair the slow component of DSB repair in G2 (which, we argue, represents HR) is consistent with the substantial evidence that BRCA1 is essential for HR (Baldeyron et al, 2002; Moynahan et al, 1999; Stark et al, 2004; Zhong et al, 2002). Consistent with the notion that BRCA1's role in DSB repair in G2 represents a direct function in HR rather than HC-relaxation, we found that combined siRNA BRCA1+KAP1 did not overcome the repair defect caused by siRNA BRCA1 (Figure 3B).

BRCA1 functions downstream of CtIP/MRN.

Previous studies have shown that CtIP is required for resection during HR (Chen et al, 2008; Choudhary & Li, 2002; Schlegel et al, 2006). We previously observed that in G2, CtIP depletion inhibits RPA foci formation and HR but efficient DSB repair ensues by NHEJ (Shibata et al, 2011). That repair occurs by NHEJ is demonstrated by its dependence on XLF, an NHEJ factor (Shibata et al, 2011) (see also Figure 3C,E). However, impaired repair is observed in G2 following siRNA BRCA1 suggesting that BRCA1 may function downstream of CtIP, possibly at a stage post commitment to HR. To investigate the order of BRCA1 and CtIP function, we examined whether CtIP depletion could rescue the G2 repair defect following siRNA BRCA1. As previously, we observed normal DSB repair following siRNA CtIP (Shibata et al, 2011) (Figure 3C). Strikingly, siRNA CtIP+BRCA1 relieved the defect observed following siRNA

BRCA1 alone (Figure 3C). We propose that CtIP functions upstream of BRCA1 to initiate resection, committing to repair by HR. BRCA1, in contrast, functions to complete resection. Since initiation of resection (the step committing to HR) occurs in the absence of BRCA1, DSB repair can no longer ensue by NHEJ.

Next, we examined whether siRNA CtIP or BRCA1 could rescue the repair defect in cells lacking BRCA2, a protein required for loading of RAD51, a downstream step in HR (Pellegrini et al, 2002). We anticipated that if BRCA1 functions downstream of CtIP-dependent initiation of resection, siRNA CtIP but not BRCA1 would rescue the BRCA2 repair defect. Consistent with this notion, whilst siRNA CtIP rescued the repair defect caused by siRNA BRCA2, joint siRNA BRCA1+BRCA2 showed defective DSB repair (Figure 3C).

We also examined the impact of siRNA MRE11, which, like CtIP, is required for the initiation of resection (Mimitou & Symington, 2011). However, MRE11 has an additional downstream role as a component of the MRN complex, promoting HC-DSB repair via pKAP-1 foci formation (Noon et al, 2010). Thus, MRN, like 53BP1, is required for HC relaxation. We examined how these distinct roles impacted upon BRCA1 depletion. In G2, siRNA MRE11 conferred a DSB repair defect similar to that observed in HR deficient cells but combined siRNA MRE11+KAP-1 allowed normal DSB repair (most likely by NHEJ) (Figure 3D)**.** Support for the notion that DSB repair does not occur by HR is provided by the fact that efficient DSB repair was also observed following triple siRNA BRCA2, MRE11+KAP-1 (Figure 3C). Thus, if the requirement for MRE11 for HC-relaxation is bypassed by KAP1 siRNA, then depletion of MRE11 or CtIP yield similar phenotypes. Thus, we conclude that MRE11 has an additional role in the initiation of resection. Consistent with this, a normal level of DSB repair was also observed following siRNA MRE11+KAP-1+BRCA1 (Figure 3D). Collectively these findings strongly suggest that CtIP/MRN functions to initiate resection whereas BRCA1 has a downstream role promoting resection post the initiation step.

To gain further insight into the position of BRCA1 function, we examined RPA and RAD51 foci formation. Consistent with other findings, siRNA BRCA1 causes a modest decrease in RPA and RAD51 foci numbers (Figure 3E-F**)** (Chen et al, 2008; Choudhary & Li, 2002; Schlegel et al, 2006). siRNA CtIP causes a marked decrease in both endpoints. As expected, siRNA BRCA2 does not impair resection but prevents RAD51 foci formation (Shibata et al, 2011). Importantly, RPA and RAD51 foci

numbers remained low following siRNA BRCA1+CtIP or BRCA2+CtIP consistent with the evidence that DSB repair ensues by NHEJ and not HR (Shibata et al, 2011), and that both BRCA1 and BRCA2 function downstream of CtIP-dependent initiation of resection (Figure 3E-F).

siRNA MRE11 reduced RPA foci numbers although less dramatically than observed after siRNA CtIP, which we attribute to inefficient siRNA. Importantly, combined siRNA MRE11+KAP-1 did not enhance RPA foci numbers, in contrast to our finding with 53BP1, demonstrating an additional role of MRE11 in resection. Further, triple siRNA MRE11+KAP-1+BRCA2 conferred reduced RPA foci numbers compared to siRNA BRCA2 alone consistent with the notion that the DSB repair observed in Figure 3C occurs by NHEJ not HR. Following siRNA BRCA1+BRCA2 the level of RPA foci numbers were low compared to siRNA BRCA2 alone arguing that BRCA1 functions upstream of BRCA2, yet DSB repair is precluded (Figure 3E).

Collectively, we interpret these findings as showing that MRE11/CtIP has an upstream role in initiating resection, which commits to repair by HR. If prevented, DSB repair can ensue by NHEJ. In contrast, BRCA1 has a downstream role in HR. Since diminished RPA foci numbers are evident following siRNA BRCA1, we propose that BRCA1 has a role in completing resection downstream of CtIP/MRN-dependent initiation.

Combined siRNA 53BP1+BRCA1 restores HR at two ended DSBs.

Previous findings have shown that combined depletion of 53BP1 and BRCA1 enables resection and HR to proceed following replication stalling (Bouwman et al, 2010; Bunting et al, 2010). We examined whether this is similarly observed at IR-induced DSBs in G2. Perhaps surprisingly, combined knockdown of 53BP1 and BRCA1 does not restore RPA or RAD51 foci formation or DSB repair (Figure 4A-C). However, consistent with 53BP1's role in promoting HC relaxation, triple knockdown of 53BP1, BRCA1 and KAP-1 restored all these end points to control levels (NB SCE formation was not examined following triple knockdown due to a diminished mitotic index) (Figure 4A-C). These findings demonstrate that 53BP1 has two functions in G2; a positive role in promoting HC relaxation and an inhibitory function that is overcome by BRCA1. Further, they verify that analysis of G2 phase DSB repair is a suitable system to probe the role of BRCA1 in overcoming the barrier posed by 53BP1.

53BP1 undergoes repositioning at IRIF during HR.

We observed that 53BP1 IRIF in G2 cells enlarge at later times post IR compared to IRIF in G1. We exploited enhanced resolution microscopy and 3D processing to quantify IRIF size and organization. In G1 cells, we did not detect any substantial increase in IRIF volume post IR using a-53BP1, whereas a doubling in 53BP1 foci volume was observed from 0.5 to 8 h in G2 (Figure 5A,C). Importantly, siRNA BRCA1 did not affect IRIF volume in G1 cells but precluded the enlargement in G2, with IRIF volume resembling that observed in G1 (Figure 5B, C). We also observed that, whereas 53BP1 was localised as a tight sphere in G1 and at 30 min post IR in G2, in striking contrast, it became repositioned by 8 h post IR in G2, vacating the central core and relocalising to the periphery of enlarged IRIF (Figure 6B and Supplementary Figure 4A). Strikingly, 53BP1 repositioning did not occur following siRNA BRCA1 (Figure 6C). Further, in control cells at both 0.5 and 8 h post IR, BRCA1 localised internally to 53BP1 (Figure 6A,B). To gain insight into the progression of HR, we next examined the relative localisation of RPA. Strikingly, RPA localised to the IRIF core that became devoid of 53BP1 with BRCA1 being located between 53BP1 and RPA (Figure 6B). A similar relative localisation of 53BP1 to BRCA1 was recently reported and RPA localisation to the IRIF core is consistent with a report of a micro compartment of single strand DNA binding proteins within the centre of micro irradiated laser tracks (Bekker-Jensen et al, 2006; Chapman et al, 2012).

Ubiquitin chains but not gH2AX relocalise with 53BP1.

53BP1 localises to IRIF via RNF8-RNF168-dependent H2A ubiquitylation (Pei et al, 2011). We predicted that 53BP1 repositioning to IRIF periphery might necessitate enlargement of the region encompassing ubiquitin chains. Using 3D imaging with a-FK2 antibodies at 8 h post IR in G2 cells, we observed that the IRIF core became depleted of the a-FK2 signal, which instead strongly co-localised with 53BP1 (Figure 6A,B and Supplementary Figure 4B). Thus, FK2 co-localised with 53BP1 at 0.5 and 8 h post IR in G2. In stark contrast, whereas gH2AX localises externally to 53BP1 at 0.5h post IR, it does not relocalise and hence becomes positioned internally to 53BP1 by 8 h post IR in G2 (Figure 6A,B). However, gH2AX is also lost from the core, where RPA foci form.

To assess whether the inability of 53BP1 foci to enlarge in BRCA1 depleted cells might be a consequence of the reduced resection (assessed as RPA foci numbers)

observed following BRCA1 siRNA, we examined 53BP1 foci in cells depleted for Artemis, an endonuclease required for resection in G2 phase, since Artemis siRNA results in a similar decrease in RPA foci numbers to that observed following BRCA1 siRNA (Beucher et al, 2009). Notably, we observed a similar two-fold increase in 53BP1 foci volume in G2 cells to that seen in control cells (Figure 6D)**.** Additionally, 53BP1 depletion did not rescue either the diminished RPA foci numbers or DSB repair in Artemis-depleted G2 cells (Supplementary Figure 5A-B). This strongly suggests that BRCA1 directly promotes 53BP1 relocalisation during HR rather than relocalisation being an indirect consequence of impaired resection**.**

To gain insight into the domains of BRCA1 required for 53BP1 repositioning, we exploited MEFs homozygously expressing *WT BRCA1*, $BRCA1^{FH\text{-}126A}$, which inactivates the E3 ligase activity, or $BRCA1^{S1598F}$, which disrupts the BRCT phospho-recognition domain (Shakya et al, 2011). Analysis using these cells has shown that BRCA1's BRCT domain is required for HR monitored by an I-Sce1 plasmid assay (Shakya et al, 2011). Consistent with these findings, we observed that RPA and RAD51 foci formation is diminished in $BRCA1^{S1598F}$ MEFs but occurs normally in $BRCA1^{FH\text{-}126A}$ MEFs (Figure 7A,B). Furthermore, although foci expansion was less marked in MEFs compared to the human cells, expansion was evident and occurs normally in MEFs expressing *WT* or $BRCA1^{FH126A}$ but not in $BRCA1^{S1598F}$ MEFs (Figure 7C). Thus, we conclude that BRCA1's BRCT domain is required for 53BP1 repositioning in G2 phase.

POH1 is dispensable for 53BP1 repositioning but is required for its vacation from the central core; interface with the RAP80/BRCC36/Abraxas complex.

Several proteins interact with BRCA1's BRCT domain including CtIP, BACH1 and a complex encompassing RAP80-BRCC36-Abraxas, (Cantor et al, 2001; Hu et al, 2011; Sobhian et al, 2007; Wang et al, 2007; Yu et al, 1998). Since we observed that CtIP functions upstream of BRCA1 in the initiation step of HR, we considered it unlikely that CtIP is the factor mediating BRCA1 function in 53BP1 repositioning. Normal 53BP1 foci enlargement and repositioning was observed following siRNA RAP80, BRCC36 or BACH1 (Supplementary Figure 6). Since the process involves repositioning of ubiquitin chains, we reasoned that it might require the function of a deubiquitin ligase (DUB) but surprisingly BRCC36 did not appear to be required. We, therefore, examined the requirement for POH1, a recently described component of the

DNA damage response required for HR (Butler et al, manuscript submitted). Although 53BP1 and FK2 chains expanded normally following siRNA POH1, strikingly they did not vacate the core region nor were RPA foci observed in the core (Figure 8A,B). Consistent with this, RPA foci numbers were markedly reduced following siRNA POH1 (Figure 8C). These findings show that POH1 is required for resection. To consolidate this using non-foci analysis, we also observed that IR-induced RPA phosphorylation is POH1-dependent (Supplementary Figure 7A). Recent studies have proposed that RAP80 suppresses resection by binding to and protecting ubiquitin chains on chromatin from degradation by DUBs. Since depletion of RAP80, BRCC36 or Abraxas leads to enhanced resection, we examined the impact of combined POH1 and either siRNA RAP80, BRCC36 or Abraxas (Coleman & Greenberg, 2011; Hu et al, 2011). In all cases, as expected we observed normal 53BP1 enlargement but surprisingly a central core devoid of ubiquitin chains and 53BP1 was now visible (Figure 8A,B). Moreover, RPA was detected in the core and RPA foci numbers returned to normal levels, although the foci appeared slightly smaller than in control cells (Figure 8B, C). Additionally, we examined RAD51 foci formation following siRNA POH1. As expected from the dramatic reduction in RPA foci, siRNA POH resulted in markedly reduced RAD51 foci formation. Unexpectedly, however, siRNA POH1+BRCC36 did not restore RAD51 foci formation despite promoting the recovery of RPA foci (Supplementary Figure 7B). Thus, we conclude that POH1 has an additional function in promoting RAD51 loading that is likely distinct to its role in creating a 53BP1-devoid core to IRIF.

Discussion.

Here, we gain mechanistic insight into functions of BRCA1 and 53BP1 in HR by examining repair of two-ended DSBs in G2 following IR. Previously, we have shown that in G1 phase, DSBs are repaired with two component kinetics, that the slow component represents the repair of HC-DSBs and that 53BP1 promotes HC-DSB repair by enabling pKAP1 foci formation. DSBs are also repaired with fast and slow kinetics in G2 phase. However, in G2 the slow component represents HR with evidence suggesting that the DSBs repaired by HR are predominantly HC-DSBs. Here, we provide further evidence to support that notion. Using H3K9me3 and H4K20me3 to identify chromodomains in G2, we show that RPA foci form predominantly at such domains. Additionally, visualisation of pKAP1 foci in G2 following siMeCP2 shows that they are 53BP1-dependent and predominantly co-localise with RPA foci. However, depletion of NHEJ components allows RPA foci to form at non-HC regions; under such conditions RPA foci do not co-localise with pKAP1 foci.

Surprisingly, in contrast to previous suggestions that 53BP1 promotes NHEJ, we show that it is required for HR at HC-DSBs in G2 but is dispensable for HR at the non-HC-DSBs, which arise following depletion of DNA-PK. Further, the role of 53BP1 in HR correlates with its requirement for pKAP1 foci formation. Thus, although not a core HR protein, we suggest that 53BP1 can indirectly promote HR (in the presence of BRCA1) via a role in enabling HC-relaxation. The fact that HR can proceed without 53BP1 following depletion of HC components (KAP1 or HP1) supports this suggestion. This role of 53BP1 may be dispensable during replication, where HC may dismantle.

We show that BRCA1 specifically confers a DSB repair defect in G2 but, unlike 53BP1, is dispensable for pKAP1 foci formation. A recent study reported that BRCA1 loss impacts upon heterochromatinization (Zhu et al, 2011). We previously observed normal DSB repair rates in other human syndromes with disordered heterochromatin (e.g. Rett Syndrome) but such cells display a diminished requirement for ATM for HC-DSB repair (Brunton et al, 2011; Goodarzi et al, 2008). The specific requirement for BRCA1 in G2 is, therefore, a distinct phenotype. Further, we have observed that BRCA1-depleted cells display the anticipated DSB repair defect following ATMi addition in G1 and G2**.** Thus, any change in HC structure caused by BRCA1 depletion does not impact upon the need for ATM for HC-DSB repair. We reveal that BRCA1 functions downstream of CtIP/MRN-dependent initiation of resection to promote full

resection. In assessing resection, we acknowledge that our resection assay (RPA foci formation) has limitations. Surprisingly, following either BRCA1 or 53BP1 siRNA, RPA foci numbers are reduced without any detectable change in size**.** We suggest that RPA foci size may not reflect the magnitude of resection but rather there may be a threshold size for detection. Notwithstanding this limitation, we interpret reduced RPA foci numbers as a read out for impaired resection. Studies with *S. cerevisiae* have revealed that resection occurs in two steps; initially, the yeast homologues of CtIP/MRN remove a short oligonucleotide producing an intermediate with a 3' overhang. End processing then occurs by a process involving the yeast homologues of ExoI or BLM (Mimitou & Symington, 2011). Our findings support this model and suggest that BRCA1 promotes a step downstream of MRN/CtIP.

We show that MRN has dual roles in end-processing; an upstream role where it functions with CtIP and a downstream role as a mediator protein, promoting HC-relaxation (Mimitou & Symington, 2011; Noon et al, 2010). To examine the upstream role, we relieve the need for HC relaxation by depleting KAP1. Importantly, depletion of CtIP alone or Mre11+KAP1 reduces RPA foci formation but not DSB repair. We recently showed that CtIP depletion allows DSB repair by NHEJ in G2 (Shibata et al, 2011). Strikingly, depletion of CtIP alone or MRN+KAP1 also rescues the repair defect conferred by BRCA2 depletion in G2. In contrast, BRCA1 depletion cannot rescue repair in BRCA2-depleted cells. Thus, we propose that the CtIP-MRN initiating step of resection that commits to repair by HR is BRCA1-independent and that BRCA1 is required for a downstream step completing resection. Interestingly, as shown here and previously, BRCA1 is dispensable for resection since resection occurs when BRCA1 and 53BP1 are concordantly depleted (Bouwman et al, 2010; Bunting et al, 2010).

We demonstrate two distinct and somewhat opposing impacts of 53BP1 at IRIF in G2. Firstly, as discussed above, 53BP1 promotes HC relaxation, identical to its role in G1 phase, although in G2, HC-DSBs undergo repair by HR rather than a process involving NHEJ proteins (Beucher et al, 2009; Noon et al, 2010). In contrast to this role of 53BP1 in promoting HR, we show that, consistent with findings in S phase cells, 53BP1 can block HR in the absence of BRCA1 (Bouwman et al, 2010; Bunting et al, 2010). This impact is distinct to its role in HC relaxation since HR stalls in BRCA1 depleted cells even following siRNA KAP1. Based on the phenotype of BRCA1 depleted cells, 53BP1 appears to provide a modest barrier to RPA foci formation, a

larger barrier to RAD51 loading but a full barrier to the completion of HR (SCE formation and DSB repair).

BRCA1 promotes relocalisation of 53BP1 in G2 creating a core devoid of 53BP1. Enhanced imaging analysis has provided mechanistic insight into how BRCA1 overcomes the barrier posed by 53BP1, namely by promoting 53BP1 relocalisation to the periphery of enlarged IRIF and creating a core devoid of 53BP1. Strikingly, 53BP1 foci at DSBs undergoing HR increase in volume relative to G1 cells. Ubiquitin chains detected by FK2 similarly increase in volume but gH2AX does not. Whilst this could represent an enlargement along the DNA molecule, the volume increase occurs in three dimensions (i.e. spherically) rather than longitudinally raising the possibility that it represents 53BP1 repositioning to encompass the undamaged template. Since HC confers a barrier to steps of HR, HC changes on the undamaged template will likely be required. We propose that BRCA1 promotes 53BP1 repositioning onto the undamaged template during HR, enabling the requisite chromatin modifications, including HC relaxation (Supplementary Figure 6). However, 53BP1 repositioning also creates a core devoid of 53BP1, enabling RPA foci formation and subsequent RAD51 loading. 53BP1, therefore, exerts two opposing impacts on HR; promoting HR via HC relaxation and inhibiting HR at IRIF. BRCA1 counterbalances these two opposing impacts.

We show that this process requires BRCA1 BRCT domain but not the ring finger motif. Recent studies have shown that BRCA1 BRCT interacts with a RAP80/BRCC36/Abraxas complex. Although it has been proposed that RAP80 helps to recruit BRCA1, we observed that loss of RAP80, BRCC36 or Abraxas does not impair 53BP1 repositioning. This is consistent with other studies showing that loss of these proteins does not impair but enhances HR (Coleman & Greenberg, 2011; Hu et al, 2011). However, we found that the DUB, POH1, is required for formation of the core devoid of 53BP1 and ubiquitin chains, and for RPA foci formation. A recent study has shown that POH1 and the proteasome are required for HR (Butler et al, manuscript submitted). Significantly, the POH1-dependent 53BP1-devoid core also lacks ubiquitin moieties and gH2AX suggesting that its generation could require proteasome-dependent degradation. Interestingly, 53BP1 expansion to the foci periphery is POH1-independent demonstrating that it likely represents new recruitment of 53BP1 and not histone shuffling.

Our findings demonstrate that BRCA1 BRCT has two distinct functions; (i) it promotes new 53BP1 recruitment to the foci periphery and (ii) it creates a core in the IRIF devoid of 53BP1 that enables RPA recruitment. This latter process is POH1-dependent and serves to relieve an inhibitory barrier posed by the RAP80/BRCC36/Abraxas complex. One possibility is that BRCA1 serves to recruit POH1 and/or other proteasome components. Interestingly, BRCA1 immunoprecipitates with BRCA1 although further work is required to assess the significance of this interaction (Butler et al. manuscript submitted). Combined loss of POH1 and either RAP80, BRCC36 or Abraxas leads to recovery of a 53BP1-devoid core and RPA recruitment. Coupled with recent evidence suggesting that RAP80 binds ubiquitin chains and protects them from rampant deubiquitylation, we suggest that BRCA1 regulates a timely switch enabling POH1-dependent deubiquitylation and possibly proteasome-mediated degradation (Coleman & Greenberg, 2011; Hu et al, 2011). Interestingly, recent work has shown that RNF169, represents a further ubiquitin ligase that functions in the DNA damage response (Poulsen et al, 2012). RNF169, however, appears to function in an atypical manner and can compete with and limit both 53BP1 and RAP80 recruitment to RNF8/168-ubiquitylated chromatin. Whether RNF169 functions to promote access of POH1 to the ubiquitin chains remains to be determined. The role that BRCA1 plays in allowing additional 53BP1 recruitment at IRIF periphery is unclear but is POH1 independent.

Model for the roles of 53BP1 and BRCA1 in HR.

We propose that since HR in irradiated G2 cells occurs predominantly at HC-DSBs, chromatin modifications (particularly pKAP1 foci) on the undamaged and damaged template are required. BRCA1 facilitates this by promoting the repositioning of ubiquitin modifications and 53BP1, enabling ATM to remain tethered at DSBs as resection ensues (Supplementary Figure 8A). Additionally, 53BP1 repositioning creates a core devoid of ubiquitin modifications and 53BP1. Although ubiquitin modifications do not appear to restrict HR, the presence of 53BP1 itself is inhibitory. This process may occur more dramatically in G2 either because BRCA1 shows greater expression in G2 than in G1, because resection is CDK regulated and occurs more readily and/or because a sister chromatid is present.

In summary, we provide mechanistic insight into events that regulate the conversion from NHEJ to HR at two-ended DSBs in G2. We propose that cells counter-

balance distinct events that restrict resection and Rad51 loading. HC super-structure represents one such barrier, which is overcome by 53BP1-dependent KAP1 phosphorylation (Supplementary Figure 8A). However, 53BP1 and RAP80 also create a barrier to resection and RAD51 loading. We propose that BRCA1 promotes 53BP1 repositioning to the foci periphery enabling continued HC relaxation. Additionally, BRCA1 together with POH1 create a core devoid of 53BP1 where RPA loading occurs. This latter role relieves the barrier posed by RAP80 since depletion of RAP80 overcomes the need for POH1 to create the 53BP-devoid core (Supplementary Figure 8B).

Materials and Methods

Cell Culture and irradiation

A549 and 1BrhTERT cells were cultured in DMEM with 10% FCS, L-glutamine, penicillin and streptomycin. Cells were incubated at 37°C in a humidified 95% air and 5% CO2 atmosphere.

Cells were irradiated by exposure to a ^{137}Cs. For G2 experiments 4µl of 2.95mM Aphidicolin was added prior to IR to prevent S-phase cells from progressing into G2. ATMi Ku-55933(Calbiochem) was added as indicated.

Small interfering RNA (siRNA) knockdown conditions

siRNA-mediated knockdown was achieved using HiPerFect Transfection Reagent (Qiagen, Hilden, Germany) following the manufacturer's instructions. 100 pmol of siRNA duplexes per 2 x 10^5 of logarithmically growing cells were used. Cells were then grown for 72 hours prior to IR. 53BP1(5´-AGAACGAGGAGACGGUA AUAGUGGG-3´), KAP-1 (5'CAGUGCUGCACUAGCUGUGA GGAUA-3') BRCA1(5'-GGAACCUGUCUCCACAAAG-3') POH1(5'-AGAGUUGGAUGGAAGGUUU-3') and Abraxas (5'-CATCGACTGGAACATTCCTTATATA-3') siRNA oligonucleotides were StealthTM RNAi oligos from Invitrogen. 53BP1,BRCA1, Ku70, DNAPK, Artemis, BRCA2, Mre11, BRCC36, RAP80, POH1 and CtiP siRNA oligonucleotides were obtained from the Dharmacon SMARTpool.

Immunofluorescence

Cells plated on glass slides were fixed for 10 min with fixative (3% (w/v) PFA, 2% (w/v) sucrose, 1X PBS) and permeabilized for 1 min with 0.2 % Triton X-100 in PBS. When staining for RPA and Rad51 foci, pre extraction was performed by treatment with 0.2 % Triton X-100 in PBS for 0.5-1 min prior to PFA fixation. Cells were rinsed with PBS and incubated with primary antibody diluted in PBS + 2% (w/v) BSA for 1 h at room temperature (RT). Cells were washed three times, incubated with secondary antibody (diluted in PBS + 2% (w/v) BSA) for 30 min at RT in the dark, incubated with 4',6-diamidino-2-phenylindole (DAPI) for 10 min and washed three times with PBS.

Slides were mounted using Vectashield and visualised/analysed using a Nikon-e400 microscope and imaged using an Applied Precision® Delta Vision® RT Olympus IX70 deconvolution microscope and softWoRx® Suite software. In each sample a minimum of 30 cells was scored blindly and error bars represent the s.d between three experiments.

Z stack imaging and 3D modelling

Z-stack imaging was carried out using an Applied Precision® Delta Vision® RT Olympus IX70 deconvolution microscope and softWoRx® Suite software. Z-stacks were set at 2 μm and individual nuclei imaged using 100x magnification. Following deconvolution by the **Huygens Professional** image processing software package **(**PSF-Theoretical, Max iterations- 400, Quality change threshold- 0.01), IRIF volume quantification was undertaken using the 'surface' tool of the BitPlane Imaris software.

Sister Chromatid Exchanges:

2 x 10^5 logarithmically cells were grown for 48 h in 10 μM BrdU before IR. 0.2μg/ml Colcemid (plus 1mM caffeine to overcome the G2/M arrest) was added from 8 -12 h post-IR to collect mitotic cells. SCEs were scored in > 800 chromosomes from 3 experiments per data point. Staining was according to standard protocols. Aphidicolin (Sigma-Aldrich, Poole, UK) was added at 1 mg/ml immediately before IR. ATM inhibitor (KU55933, Calbiochem), was added at 20 mM 20 minutes prior to IR.

Antibodies

The primary antibodies used were: γH2AX and 53BP1 (Upstate Technology, Billerica, USA) at 1:800, 53BP1 (Bethyl, Cambridge, England) at 1:800), RPA (Calbiochem, Billerica, USA) at 1:800, RPA (Lifespan Biosciences, Suffolk, UK) at 1:100), Phospho RPA32 (S4/S8) (Bethyl, Cambridge, UK), Ku80 (Cell signalling), Rad51(Santa-Cruz Biootechnology**,** Santa Cruz, USA) at 1:200, p-histone H3 (p-H3) Ser10 (Upstate Biotechnology, Buckingham, UK.) at 1:500; FK2 (Millipore, Billerica, USA.) at 1:400; H3K9me3 and H4K20me3 (Abcam, Cambridge, UK), at 1:800**)**. The anti-rabbit polyclonal BRCA1 antibody was raised against human BRCA1 amino acid residues 1250-1650. The corresponding cDNA fragment was cloned into the pET-28 expression vector (Novagen, Billerica, USA) and the recombinant protein fused to a

histidine tag was purified using Ni-NTA resin (Qiagen, Hilden, Germany) following the manufacturer's instructions. The following secondary antibodies were: FITC (Sigma Aldrich, Poole, UK.) at 1:200, CY3 (Sigma Aldrich, Poole, UK.) at 1:200), Alexa 488, Alexa647 and Alexa 555 (Invitrogen, Grand Island, USA.) all at 1:400.

Analysis of RPA foci overlap with HC in G2.

1BR3 hTERT (WT) and 2BN hTERT (XLF mutated) cells were irradiated with 3 Gy IR and maintained in aphidicolin (as above). Cells were harvested 8 hr later, extracted 30s with 0.2% triton X100 (in PBS) and fixed and immunostained for RPA (p34 subunit, RPA2) and Histone H3 Trimethylated K9 (H3K9me3) or Histone H4 Trimethylated K20 (H4K20me3). Z-stacks were captured using a Confocal Zeiss LSM510meta microscope. Overlap between RPA foci and HC markers were quantified by ImageJ software with the 'Colocalisation Analysis' plugin. Mean values represent 15-20 cells in each of three experiments for each condition.

Acknowledgements.

We thank Drs. A. Carr, E.Hoffman and H. Hochegger for help with image analysis, and Dr. T. Ludwig for providing BRCA1 MEFs. The PAJ laboratory is supported by an MRC programme grant, the Association for International Cancer Research, the Wellcome Research Trust and the EMF Biological Research Trust. The M.L. laboratory is supported by the Deutsche Forschungsgemeinschaft (Lo 677/4-3) and the Bundesministerium für Bildung und Forschung (02S8335, 02S8355, 03NUK001C, 02NUK016D). RF is supported by grants from the Spanish Ministry of Science and Innovation (SAF2010-22357 and CONSOLIDER-Ingenio 2010 CDS2007-0015). AAG is supported by grants from the Canadian Institutes of Health Research and the Alberta Cancer Foundation.

Author contributions.

AK and AI carried out most experimental work aided by AS and YK. RF provided BRCA1 antibodies. KK and AAG carried out the chromocentre analysis. ML, RF AS and PAJ contributed to discussions underlying the project and its development. AK and PAJ played the major role in manuscript preparation with contributions from ML, RF and AS.

References.

Acs K, Luijsterburg MS, Ackermann L, Salomons FA, Hoppe T, Dantuma NP (2011) The AAA-ATPase VCP/p97 promotes 53BP1 recruitment by removing L3MBTL1 from DNA double-strand breaks. *Nature structural & molecular biology* 18: 1345-1350

Adamo A, Collis SJ, Adelman CA, Silva N, Horejsi Z, Ward JD, Martinez-Perez E, Boulton SJ, La Volpe A (2010) Preventing nonhomologous end joining suppresses DNA repair defects of Fanconi anemia. *Mol Cell* 39: 25-35

Baldeyron C, Jacquemin E, Smith J, Jacquemont C, De Oliveira I, Gad S, Feunteun J, Stoppa-Lyonnet D, Papadopoulo D (2002) A single mutated BRCA1 allele leads to impaired fidelity of double strand break end-joining. *Oncogene* 21: 1401-1410.

Bekker-Jensen S, Lukas C, Kitagawa R, Melander F, Kastan MB, Bartek J, Lukas J (2006) Spatial organization of the mammalian genome surveillance machinery in response to DNA strand breaks. *J Cell Biol* 173: 195-206

Beucher A, Birraux J, Tchouandong L, Barton O, Shibata A, Conrad S, Goodarzi AA, Krempler A, Jeggo PA, Lobrich M (2009) ATM and Artemis promote homologous recombination of radiation-induced DNA double-strand breaks in G2. *EMBO J* 28: 3413-3427

Bothmer A, Robbiani DF, Feldhahn N, Gazumyan A, Nussenzweig A, Nussenzweig MC (2010) 53BP1 regulates DNA resection and the choice between classical and alternative end joining during class switch recombination. *J Exp Med* 207: 855-865

Bouwman P, Aly A, Escandell JM, Pieterse M, Bartkova J, van der Gulden H, Hiddingh S, Thanasoula M, Kulkarni A, Yang Q, Haffty BG, Tommiska J, Blomqvist C, Drapkin R, Adams DJ, Nevanlinna H, Bartek J, Tarsounas M, Ganesan S, Jonkers J (2010) 53BP1 loss rescues BRCA1 deficiency and is associated with triple-negative and BRCA-mutated breast cancers. *Nat Struct Mol Biol* 17: 688-695

Brunton H, Goodarzi AA, Noon AT, Shrikhande A, Hansen RS, Jeggo PA, Shibata A (2011) Analysis of Human Syndromes with Disordered Chromatin Reveals the Impact of Heterochromatin on the Efficacy of ATM-Dependent G2/M Checkpoint Arrest. *Mol Cell Biol* 31: 4022-4035

Bunting SF, Callen E, Wong N, Chen HT, Polato F, Gunn A, Bothmer A, Feldhahn N, Fernandez-Capetillo O, Cao L, Xu X, Deng CX, Finkel T, Nussenzweig M, Stark JM, Nussenzweig A (2010) 53BP1 inhibits homologous recombination in Brca1-deficient cells by blocking resection of DNA breaks. *Cell* 141: 243-254

Cantor SB, Bell DW, Ganesan S, Kass EM, Drapkin R, Grossman S, Wahrer DC, Sgroi DC, Lane WS, Haber DA, Livingston DM (2001) BACH1, a novel helicase-like protein, interacts directly with BRCA1 and contributes to its DNA repair function. *Cell* 105: 149-160.

Chapman JR, Sossick AJ, Boulton SJ, Jackson SP (2012) BRCA1-associated exclusion of 53BP1 from DNA damage sites underlies temporal control of DNA repair. *Journal of cell science*

Chen L, Nievera CJ, Lee AY, Wu X (2008) Cell cycle-dependent complex formation of BRCA1.CtIP.MRN is important for DNA double-strand break repair. *J Biol Chem* 283: 7713-7720

Choudhary SK, Li R (2002) BRCA1 modulates ionizing radiation-induced nuclear focus formation by the replication protein A p34 subunit. *J Cell Biochem* 84: 666-674

Ciccia A, Elledge SJ (2010) The DNA damage response: making it safe to play with knives. *Mol Cell* 40: 179-204

Coleman KA, Greenberg RA (2011) The BRCA1-RAP80 complex regulates DNA repair mechanism utilization by restricting end resection. *The Journal of biological chemistry* 286: 13669-13680

Cooper EM, Cutcliffe C, Kristiansen TZ, Pandey A, Pickart CM, Cohen RE (2009) K63-specific deubiquitination by two JAMM/MPN+ complexes: BRISC-associated Brcc36 and proteasomal Poh1. *The EMBO journal* 28: 621-631

Difilippantonio S, Gapud E, Wong N, Huang CY, Mahowald G, Chen HT, Kruhlak MJ, Callen E, Livak F, Nussenzweig MC, Sleckman BP, Nussenzweig A (2008) 53BP1 facilitates long-range DNA end-joining during V(D)J recombination. *Nature*

Dimitrova N, Chen YC, Spector DL, de Lange T (2008) 53BP1 promotes non-homologous end joining of telomeres by increasing chromatin mobility. *Nature*

Feng L, Wang J, Chen J (2010) The Lys63-specific deubiquitinating enzyme BRCC36 is regulated by two scaffold proteins localising in different subcellular compartments. *J Biol Chem* 285: 30982-30988

Goodarzi AA, Kurka T, Jeggo PA (2011) KAP-1 phosphorylation regulates CHD3 nucleosome remodeling during the DNA double-strand break response. *Nat Struct Mol Biol* 18: 831-839

Goodarzi AA, Noon AT, Deckbar D, Ziv Y, Shiloh Y, Lobrich M, Jeggo PA (2008) ATM signaling facilitates repair of DNA double-strand breaks associated with heterochromatin. *Mol Cell* 31: 167-177

Goodarzi AA, Noon AT, Jeggo PA (2009) The impact of heterochromatin on DSB repair. *Biochem Soc Trans* 37: 569-576

Hu Y, Scully R, Sobhian B, Xie A, Shestakova E, Livingston DM (2011) RAP80-directed tuning of BRCA1 homologous recombination function at ionizing radiation-induced nuclear foci. *Genes Dev* 25: 685-700

Jackson SP, Bartek J (2009) The DNA-damage response in human biology and disease. *Nature* 461: 1071-1078

Kurz EU, Lees-Miller SP (2004) DNA damage-induced activation of ATM and ATM-dependent signaling pathways. *DNA Repair (Amst)* 3: 889-900

Lavin MF (2008) Ataxia-telangiectasia: from a rare disorder to a paradigm for cell signalling and cancer. *Nat Rev Mol Cell Biol* 9: 759-769

Mahaney BL, Meek K, Lees-Miller SP (2009) Repair of ionizing radiation-induced DNA double-strand breaks by non-homologous end-joining. *Biochem J* 417: 639-650

Mallette FA, Mattiroli F, Cui G, Young LC, Hendzel MJ, Mer G, Sixma TK, Richard S (2012) RNF8- and RNF168-dependent degradation of KDM4A/JMJD2A triggers 53BP1 recruitment to DNA damage sites. *The EMBO journal* 31: 1865-1878

Mimitou EP, Symington LS (2011) DNA end resection--unraveling the tail. *DNA Repair (Amst)* 10: 344-348

Moynahan ME, Chiu JW, Koller BH, Jasin M (1999) Brca1 controls homology-directed DNA repair. *Mol Cell* 4: 511-518

Noon AT, Shibata A, Rief N, Lobrich M, Stewart GS, Jeggo PA, Goodarzi AA (2010) 53BP1-dependent robust localised KAP-1 phosphorylation is essential for heterochromatic DNA double-strand break repair. *Nat Cell Biol* 12: 177-184

Pace P, Mosedale G, Hodskinson MR, Rosado IV, Sivasubramaniam M, Patel KJ (2010) Ku70 corrupts DNA repair in the absence of the Fanconi anemia pathway. *Science* 329: 219-223

Panier S, Durocher D (2009) Regulatory ubiquitylation in response to DNA double-strand breaks. *DNA Repair (Amst)* 8: 436-443

Pei H, Zhang L, Luo K, Qin Y, Chesi M, Fei F, Bergsagel PL, Wang L, You Z, Lou Z (2011) MMSET regulates histone H4K20 methylation and 53BP1 accumulation at DNA damage sites. *Nature* 470: 124-128

Pellegrini L, Yu DS, Lo T, Anand S, Lee M, Blundell TL, Venkitaraman AR (2002) Insights into DNA recombination from the structure of a RAD51-BRCA2 complex. *Nature* 420: 287-293.

Petermann E, Helleday T (2010) Pathways of mammalian replication fork restart. *Nat Rev Mol Cell Biol* 11: 683-687

Poulsen M, Lukas C, Lukas J, Bekker-Jensen S, Mailand N (2012) Human RNF169 is a negative regulator of the ubiquitin-dependent response to DNA double-strand breaks. *The Journal of cell biology* 197: 189-199

Riballo E, Kuhne M, Rief N, Doherty A, Smith GC, Recio MJ, Reis C, Dahm K, Fricke A, Krempler A, Parker AR, Jackson SP, Gennery A, Jeggo PA, Lobrich M (2004) A pathway of double-strand break rejoining dependent upon ATM, Artemis, and proteins locating to gamma-H2AX foci. *Mol Cell* 16: 715-724

Schlegel BP, Jodelka FM, Nunez R (2006) BRCA1 promotes induction of ssDNA by ionizing radiation. *Cancer Res* 66: 5181-5189

Shakya R, Reid LJ, Reczek CR, Cole F, Egli D, Lin CS, deRooij DG, Hirsch S, Ravi K, Hicks JB, Szabolcs M, Jasin M, Baer R, Ludwig T (2011) BRCA1 tumor suppression depends on BRCT phosphoprotein binding, but not its E3 ligase activity. *Science* 334: 525-528

Shanbhag NM, Rafalska-Metcalf IU, Balane-Bolivar C, Janicki SM, Greenberg RA (2010) ATM-dependent chromatin changes silence transcription in *cis* to DNA double-strand breaks. *Cell* 141: 970-981

Shibata A, Conrad S, Birraux J, Geuting V, Barton O, Ismail A, Kakarougkas A, Meek K, Taucher-Scholz G, Lobrich M, Jeggo PA (2011) Factors determining DNA double-strand break repair pathway choice in G2 phase. *EMBO J* 30: 1079-1092

Sobhian B, Shao G, Lilli DR, Culhane AC, Moreau LA, Xia B, Livingston DM, Greenberg RA (2007) RAP80 targets BRCA1 to specific ubiquitin structures at DNA damage sites. *Science* 316: 1198-1202

Stark JM, Pierce AJ, Oh J, Pastink A, Jasin M (2004) Genetic steps of mammalian homologous repair with distinct mutagenic consequences. *Mol Cell Biol* 24: 9305-9316

Wang B, Matsuoka S, Ballif BA, Zhang D, Smogorzewska A, Gygi SP, Elledge SJ (2007) Abraxas and RAP80 form a BRCA1 protein complex required for the DNA damage response. *Science* 316: 1194-1198

Wyman C, Kanaar R (2006) DNA double-strand break repair: all's well that ends well. *Annu Rev Genet* 40: 363-383

Yao T, Cohen RE (2002) A cryptic protease couples deubiquitination and degradation by the proteasome. *Nature* 419: 403-407

Yu X, Wu LC, Bowcock AM, Aronheim A, Baer R (1998) The C-terminal (BRCT) domains of BRCA1 interact in vivo with CtIP, a protein implicated in the CtBP pathway of transcriptional repression. *The Journal of biological chemistry* 273: 25388-25392

Zhang Y, Jasin M (2011) An essential role for CtIP in chromosomal translocation formation through an alternative end-joining pathway. *Nat Struct Mol Biol* 18: 80-84

Zhong Q, Boyer TG, Chen PL, Lee WH (2002) Deficient nonhomologous end-joining activity in cell-free extracts from Brca1-null fibroblasts. *Cancer Res* 62: 3966-3970

Zhu Q, Pao GM, Huynh AM, Suh H, Tonnu N, Nederlof PM, Gage FH, Verma IM (2011) BRCA1 tumour suppression occurs via heterochromatin-mediated silencing. *Nature* 477: 179-184

Figure 1

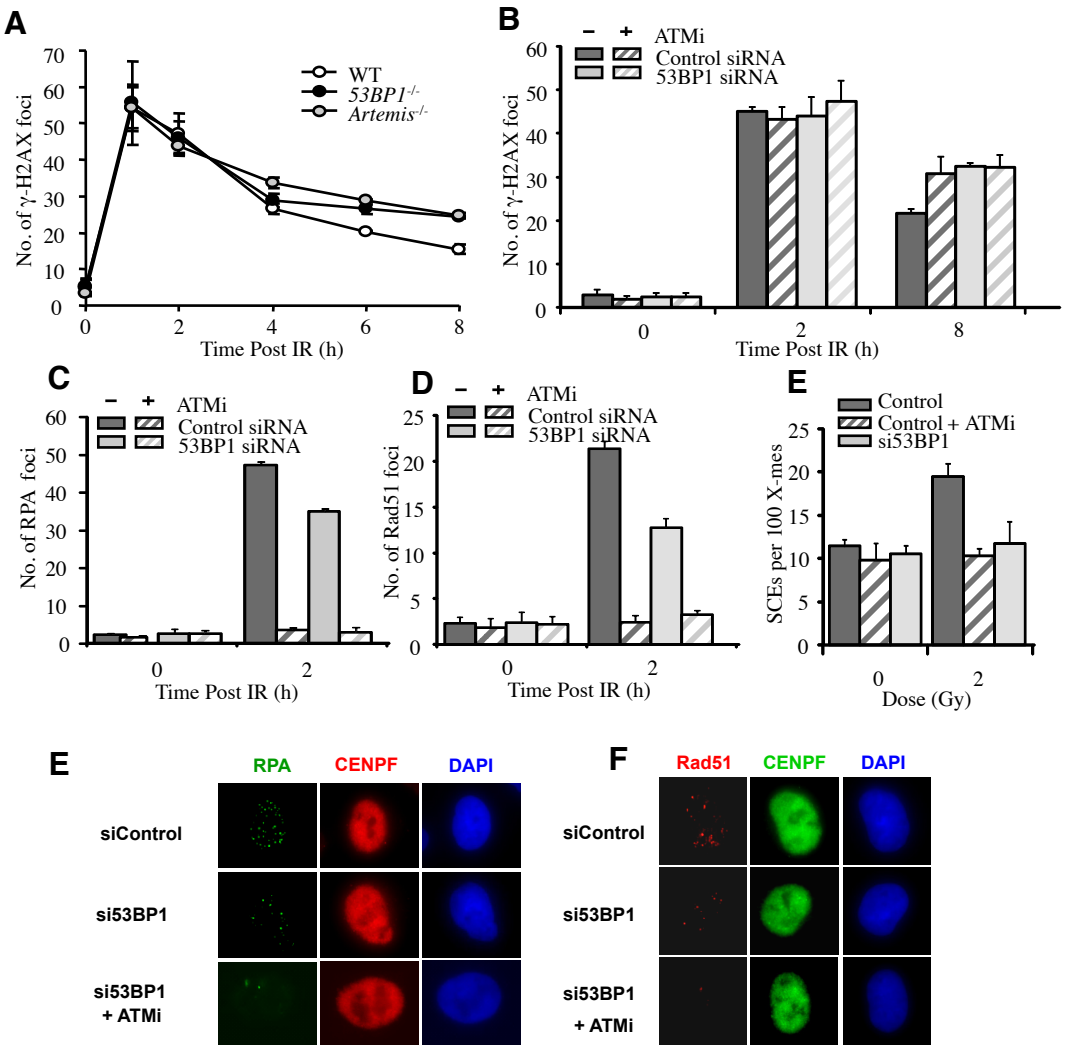
A
No. of γ-H2AX foci
Time Post IR (h)
WT
53BP1-/-
Artemis-/-
B
ATMi
Control siRNA
53BP1 siRNA
No. of γ-H2AX foci
Time Post IR (h)
C
ATMi
Control siRNA
53BP1 siRNA
No. of RPA foci
Time Post IR (h)
D
ATMi
Control siRNA
53BP1 siRNA
No. of Rad51 foci
Time Post IR (h)
E
Control
Control + ATMi
si53BP1
SCEs per 100 X-mes
Dose (Gy)
E
RPA
CENPF
DAPI
siControl
si53BP1
si53BP1 + ATMi
F
Rad51
CENPF
DAPI
siControl
si53BP1
si53BP1 + ATMi

Figure 2

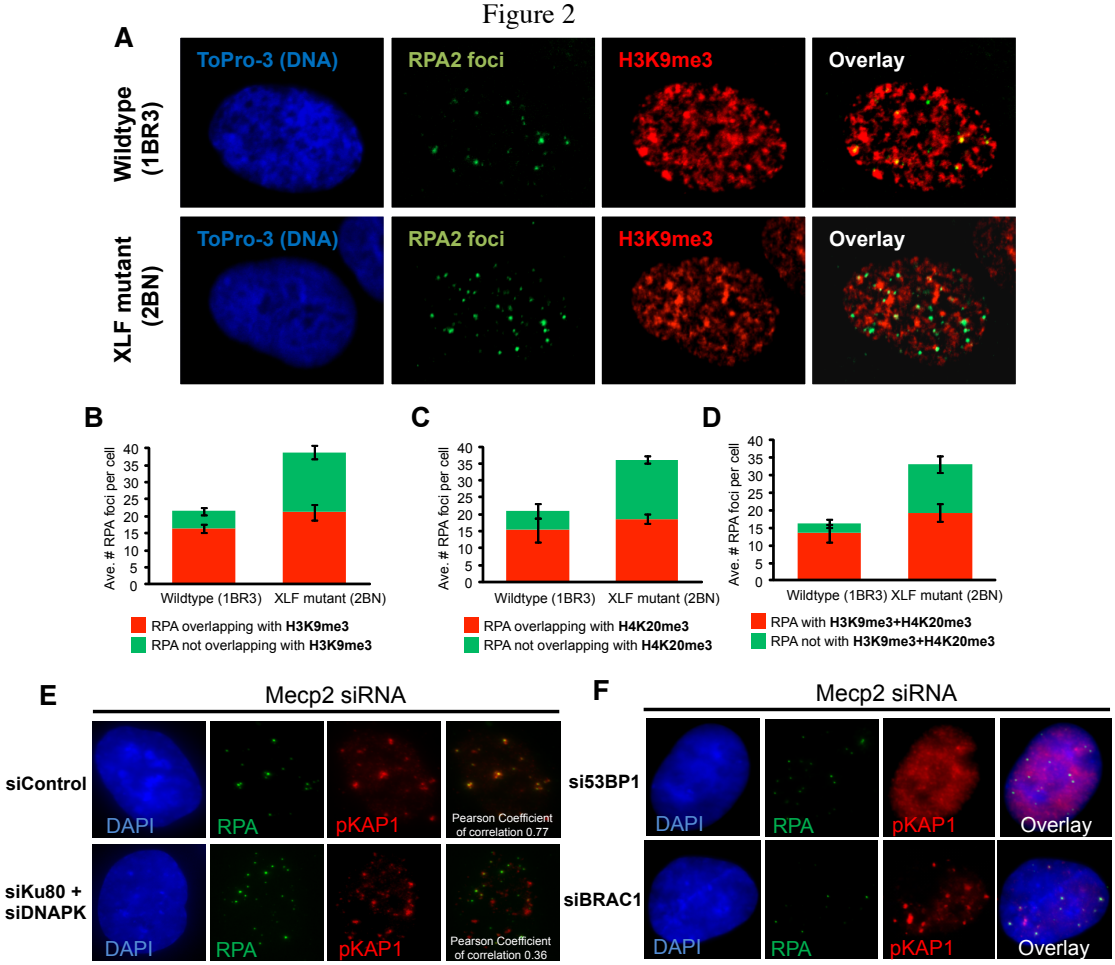
A
Wildtype (1BR3)
XLF mutant (2BN)
ToPro-3 (DNA)
RPA2 foci
H3K9me3
Overlay
B
Ave. # RPA foci per cell
Wildtype (1BR3)
XLF mutant (2BN)
RPA overlapping with H3K9me3
RPA not overlapping with H3K9me3
C
RPA overlapping with H4K20me3
RPA not overlapping with H4K20me3
D
Wildtype (1BR3) XLF mutant (2BN)
RPA with H3K9me3+H4K20me3
RPA not with H3K9me3+H4K20me3
E
Mecp2 siRNA
siControl
siKu80 + siDNAPK
DAPI
RPA
pKAP1
Pearson Coefficient of correlation 0.77
Pearson Coefficient of correlation 0.36
F
Mecp2 siRNA
si53BP1
siBRAC1
Overlay

Figure 3

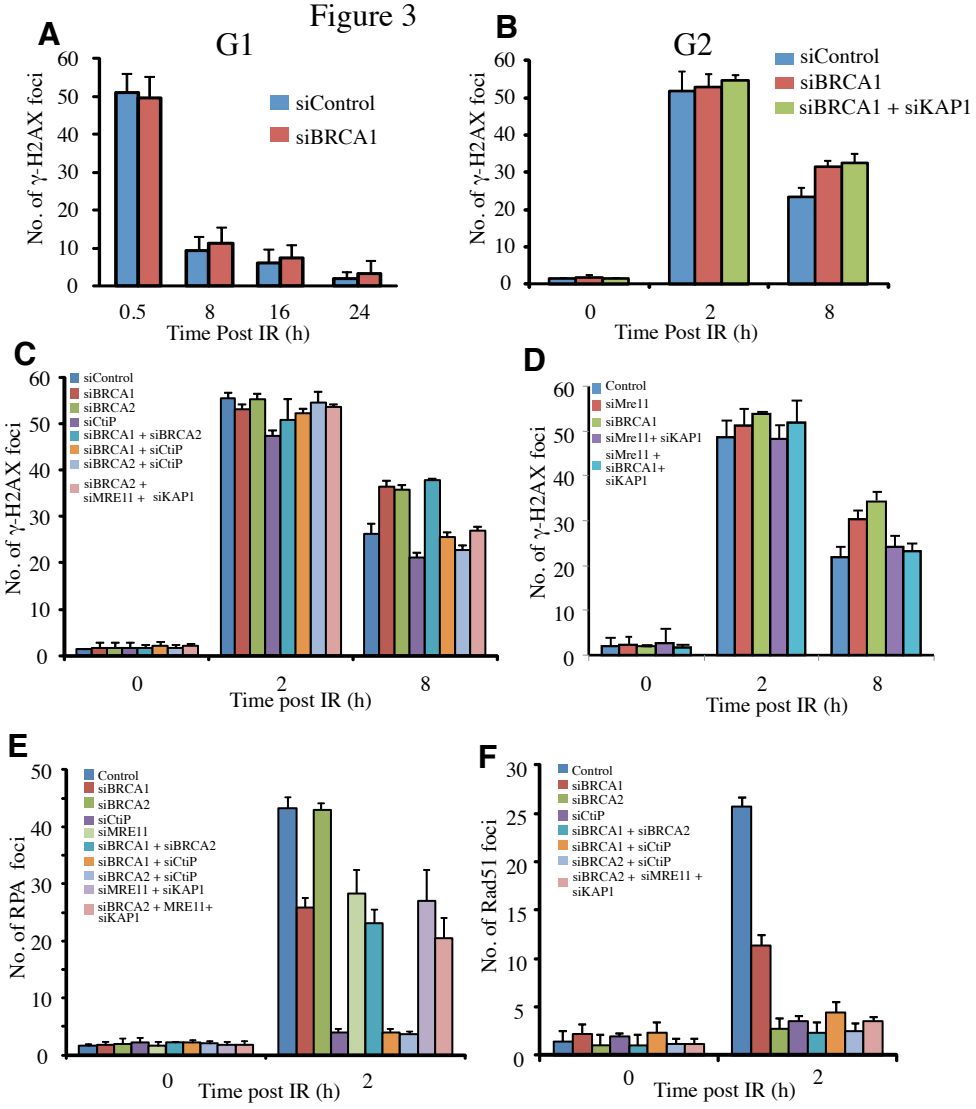
A
G1
siControl
siBRCA1
No. of γ-H2AX foci
Time Post IR (h)
B
G2
siControl
siBRCA1
siBRCA1 + siKAP1
No. of γ-H2AX foci
Time Post IR (h)
C
siControl
siBRCA1
siBRCA2
siCtiP
siBRCA1 + siBRCA2
siBRCA1 + siCtiP
siBRCA2 + siCtiP
siBRCA2 + siMRE11 + siKAP1
No. of γ-H2AX foci
Time post IR (h)
D
Control
siMre11
siBRCA1
siMre11+ siKAP1
siMre11 + siBRCA1+ siKAP1
No. of γ-H2AX foci
Time post IR (h)
E
Control
siBRCA1
siBRCA2
siCtiP
siMRE11
siBRCA1 + siBRCA2
siBRCA1 + siCtiP
siBRCA2 + siCtiP
siMRE11 + siKAP1
siBRCA2 + MRE11+ siKAP1
No. of RPA foci
Time post IR (h)
F
Control
siBRCA1
siBRCA2
siCtiP
siBRCA1 + siBRCA2
siBRCA1 + siCtiP
siBRCA2 + siCtiP
siBRCA2 + siMRE11 + siKAP1
No. of Rad51 foci
Time post IR (h)

Figure 4

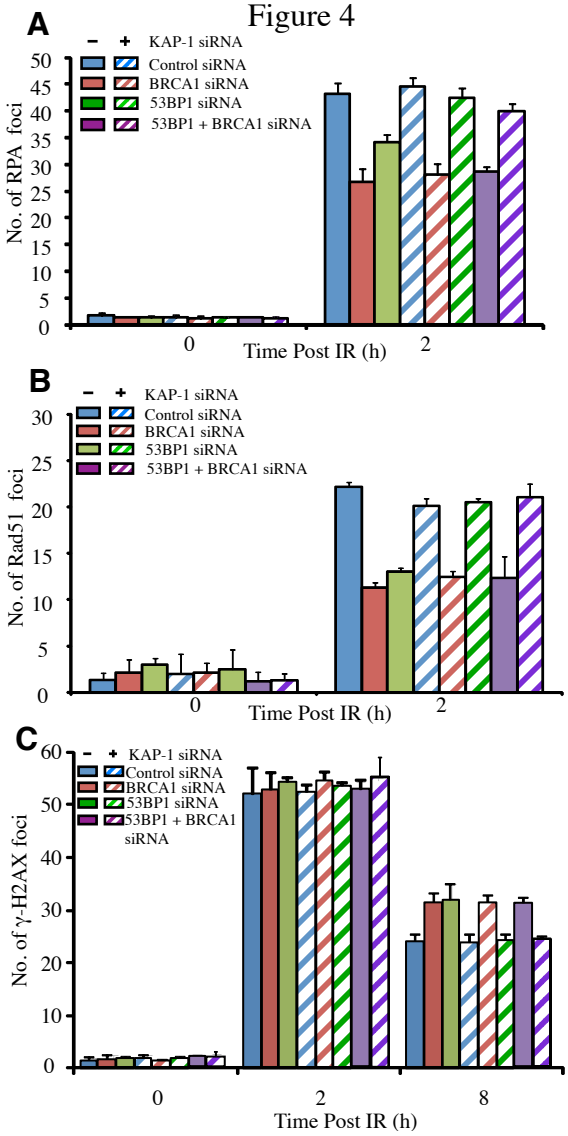
A
– + KAP-1 siRNA
Control siRNA
BRCA1 siRNA
53BP1 siRNA
53BP1 + BRCA1 siRNA
No. of RPA foci
0 5 10 15 20 25 30 35 40 45 50
0
2
Time Post IR (h)
B
– + KAP-1 siRNA
Control siRNA
BRCA1 siRNA
53BP1 siRNA
53BP1 + BRCA1 siRNA
No. of Rad51 foci
0 5 10 15 20 25 30
0
2
Time Post IR (h)
C
– + KAP-1 siRNA
Control siRNA
BRCA1 siRNA
53BP1 siRNA
53BP1 + BRCA1 siRNA
No. of γ-H2AX foci
0 10 20 30 40 50 60
0
2
8
Time Post IR (h)

Figure 5

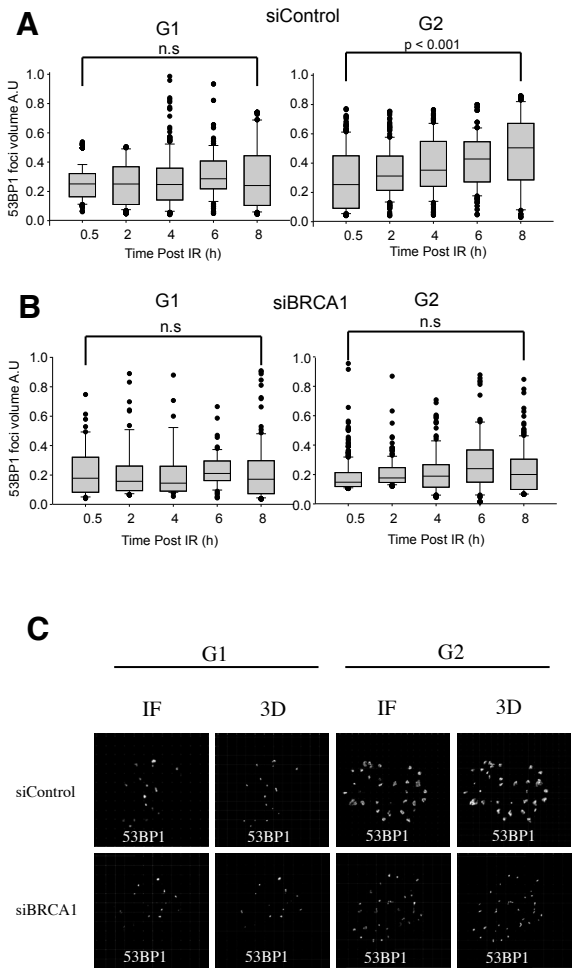
A
siControl
G1
n.s
G2
p < 0.001
53BP1 foci volume A.U
Time Post IR (h)
B
siBRCA1
G1
n.s
G2
n.s
53BP1 foci volume A.U
Time Post IR (h)
C
G1
G2
IF
3D
IF
3D
siControl
siBRCA1
53BP1

Figure 6

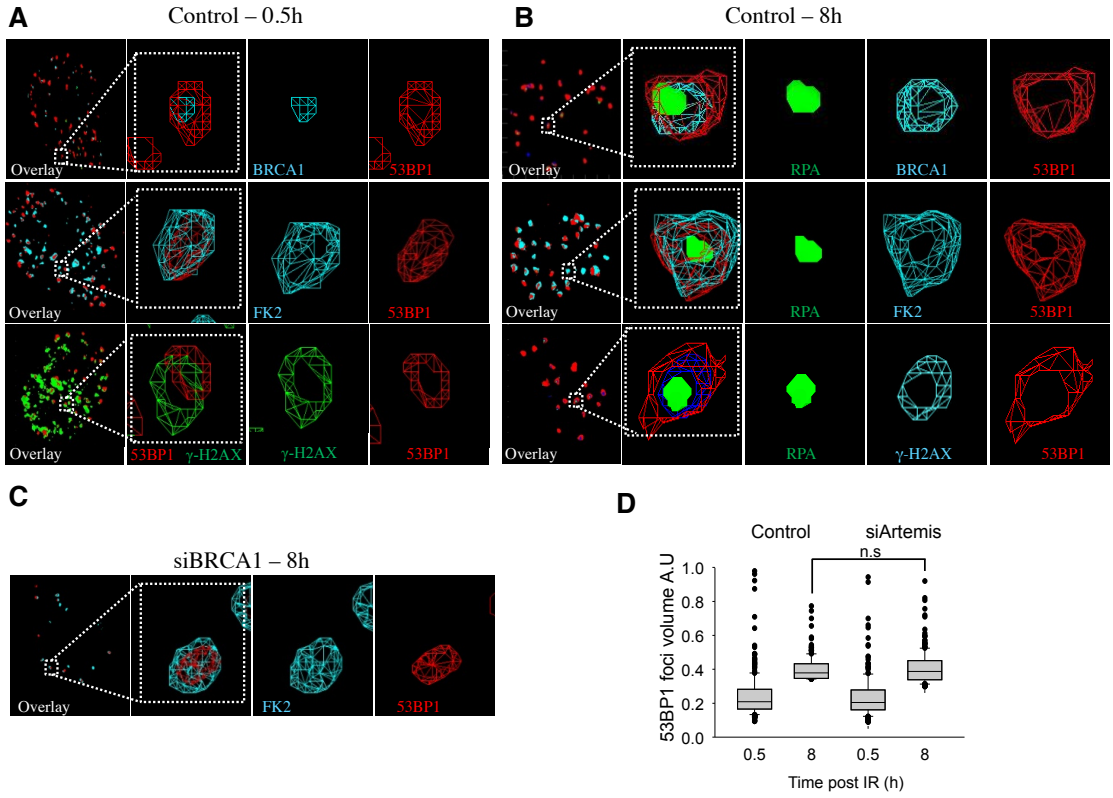
A
Control – 0.5h
Overlay
BRCA1
53BP1
Overlay
FK2
53BP1
Overlay
53BP1 γ-H2AX
γ-H2AX
53BP1
B
Control – 8h
Overlay
RPA
BRCA1
53BP1
Overlay
RPA
FK2
53BP1
Overlay
RPA
γ-H2AX
53BP1
C
siBRCA1 – 8h
Overlay
FK2
53BP1
D
Control
siArtemis
n.s
53BP1 foci volume A.U
1.0
0.8
0.6
0.4
0.2
0.0
0.5
8
0.5
8
Time post IR (h)

Figure 7

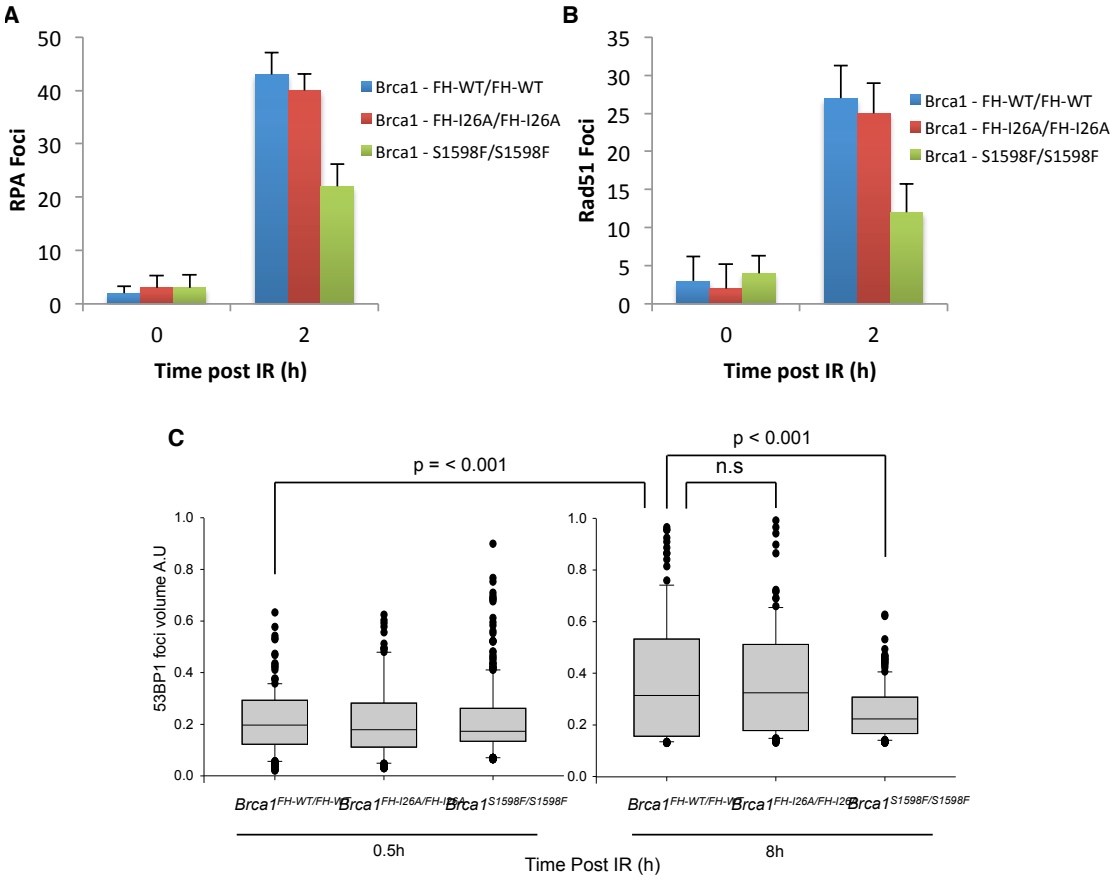
A
RPA Foci
50
40
30
20
10
0
0
2
Time post IR (h)
Brca1 - FH-WT/FH-WT
Brca1 - FH-I26A/FH-I26A
Brca1 - S1598F/S1598F
B
Rad51 Foci
35
30
25
20
15
10
5
0
0
2
Time post IR (h)
Brca1 - FH-WT/FH-WT
Brca1 - FH-I26A/FH-I26A
Brca1 - S1598F/S1598F
C
p = < 0.001
p < 0.001
n.s
53BP1 foci volume A.U
1.0
0.8
0.6
0.4
0.2
0.0
Brca1FH-WT/FH-WT
Brca1FH-I26A/FH-I26A
Brca1S1598F/S1598F
0.5h
8h
Time Post IR (h)

Figure 8

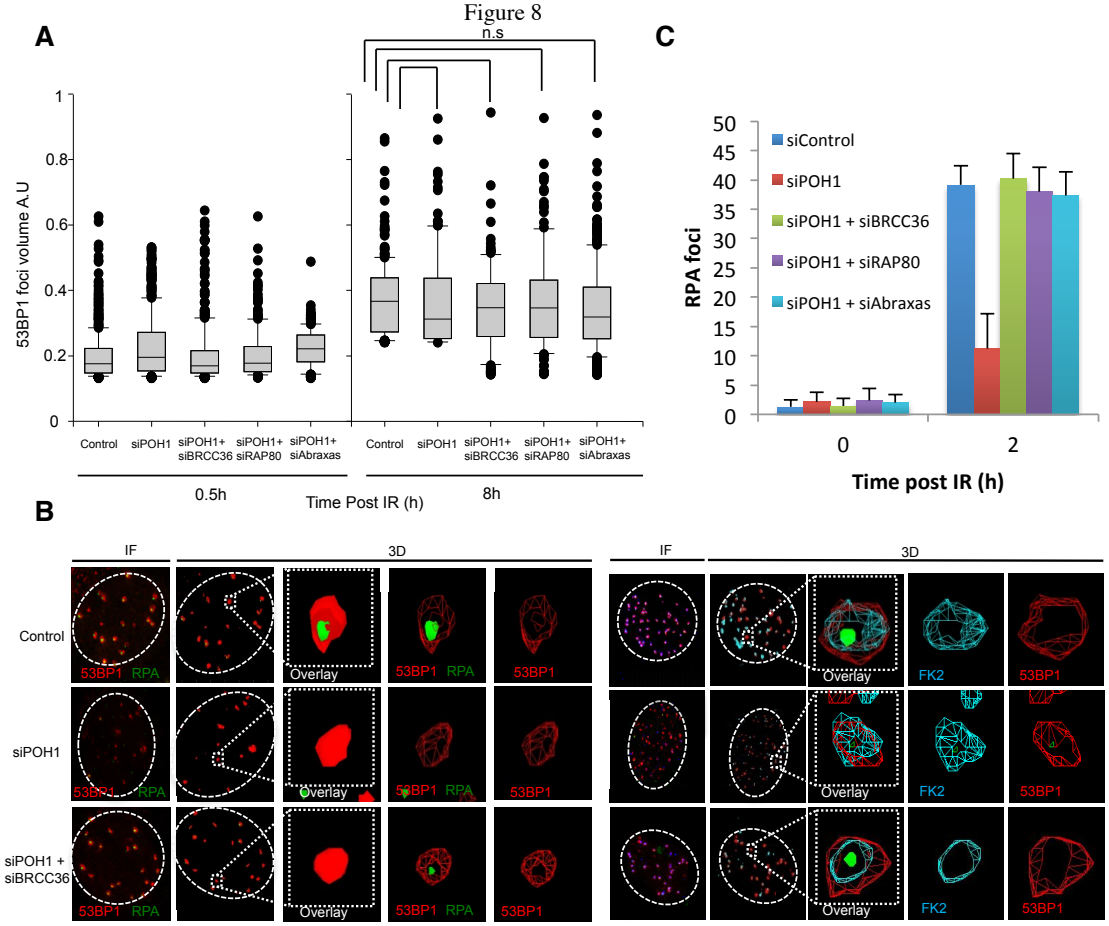
A
n.s
53BP1 foci volume A.U
1
0.8
0.6
0.4
0.2
0
Control
siPOH1
siPOH1+ siBRCC36
siPOH1+ siRAP80
siPOH1+ siAbraxas
0.5h
8h
Time Post IR (h)
C
RPA foci
50
45
40
35
30
25
20
15
10
5
0
siControl
siPOH1
siPOH1 + siBRCC36
siPOH1 + siRAP80
siPOH1 + siAbraxas
0
2
Time post IR (h)
B
IF
3D
Control
siPOH1
siPOH1 + siBRCC36
53BP1
RPA
Overlay
FK2

Figure legends.

Figure 1. 53BP1 promotes DSB repair by HR in G2 phase.

A) Wild type (WT), 53BP1$^{-/-}$ and Artemis$^{-/-}$ MEFs were exposed to 3 Gy IR and gH2AX foci enumerated to 8 h post IR. G2 cells were identified by CENPF staining (Shibata et al, 2011). Aphidicolin was added prior to IR to prevent S phase cells progressing into G2 during analysis in all experiments. Control experiments verified that this does not affect HR in G2 phase (Beucher et al, 2009; Shibata et al, 2011).
B) gH2AX foci were enumerated in A549 cells with or without siRNA 53BP1 following 3 Gy IR. Similar results to those observed using MEFs were obtained. ATM inhibitor (ATMi) was added as indicated. C-D) RPA foci (C), RAD51 foci (D) and SCEs generated from G2 phase cells (E). RPA and RAD51 foci were enumerated at 2 h and SCEs scored at the first metaphase post 3 Gy IR, either with or without ATMi and 53BP1 siRNA. Control experiments have shown that RPA and RAD51 foci numbers reach a maximum ~ 2 h post IR (Shibata et al, 2011). All results represent the mean and s.d. of 3 experiments. Results shown were obtained using a single 53BP1 oligonucleotide; identical results were obtained using a pool of 53BP1 oligonucleotides distinct to the single oligonucleotide (Supplementary Figure 1). Knockdown efficiency is shown in Supplementary Figure 1. Thus, a DSB repair defect in G2 cells lacking 53BP1 is shown in deficient MEFs and following two siRNA conditions. Direct evidence for defective HR is shown by SCE and supported by foci analysis. E-F) Representative images of IF analysis.

Figure 2. 53BP1 is specifically required for HR at HC-DSBs.

A) Visualisation of H3K9me3 and RPA foci in G2 cells.
Proliferating 1BR3hTERT and 2BN hTERT (XLF deficient) cells were exposed to 3 Gy IR in the presence of aphidicolin. 8 h post IR cells were extracted and immunostained for RPA2 (green), H3K9me3 (red) and DNA (ToPro03, blue). Slides were imaged in 3D by confocal microscopy. The figure shows a 2D representation of the 3D images.
B-D) The experiment in (A) was repeated with either H3K9me3, H4K20me3 or H3K9me3+H4K20me3 in the red channel. The overlap between RPA and HC markers was quantified by computer analysis and results represent mean values for 3 experiments for each condition.
E) Co-localisation of RPA and pKAP1 IRIF in G2 phase. 1BRhTERT cells were harvested 8 h post 3 Gy IR in the presence of aphidocolin and immunostained with the

indicated antibodies. Analysis was undertaken in G2 cells; S phase cells were excluded from analysis by the pan-nuclear RPA staining caused by aphidicolin addition. G1 cells do not show RPA foci. G2 phase cells have low chromatin bound KAP-1 making pKAP1 foci analysis difficult (Goodarzi et al, 2009). To visualise pKAP-1 in G2 cells, cells were subjected to MeCP2 siRNA, which we previously observed caused increased foci expansion and visualisation of pKAP1 in G2 (Brunton et al, 2011). Co-localisation between pKAP1 and RPA was undertaken using softWoRx® Suite software. The Pearson Coefficient of Correlation indicates how closely two intensities colocalise on a pixel-by-pixel basis (full colocalisation is 1.0). RPA foci show significant overlap with pKAP1. Similar analysis was carried out after combined Ku80+DNA-PKcs siRNA (DNA-PK siRNA). Under these conditions the overlap between RPA and pKAP1 was substantially reduced. F) 53BP1 but not BRCA1 is required for pKAP1 IRIF in G2 phase

F). Analysis was carried out as in 2E following siRNA MeCP2+ 53BP1 or +BRCA1. 53BP1 is required for pKAP1 foci formation but is dispensable for pan-nuclear KAP1 phosphorylation (Noon et al, 2010).

Figure 3. BRCA1 is dispensable for HC-DSB repair in G1 phase but functions downstream of CtIP/MRN in G2 to promote resection during HR repair of HC-DSBs.

A-B) A549 cells were exposed to 3 Gy IR and gH2AX foci enumerated in G1 and G2 with or without siRNA BRCA1 and KAP-1. G2 and G1 cells were identified as in Figure 1. Results shown are with a single BRCA1 oligonucleotide; identical results were obtained using a distinct pool of oligonucleotides**.** Aphidicolin was added as previously described. The efficiency of triple knockdown is shown in Supplementary Figure 1**.** The efficacy of CtIP knockdown using three distinct oligonucleotides was shown previously (Shibata et al, 2011). Also, using the same conditions, we observed that resection and RAD51 foci formation was restored by transfection with CtIP cDNA. (C-F) Enumeration of gH2AX (C and D), RPA (E) andRAD51 (F) foci in G2 phase A549 cells post 3 Gy IR following treatment with the indicated siRNAs. Results represent the mean and s.d. of 3 experiments.

Figure 4. Combined loss of BRCA1, 53BP1 and KAP1 allows DSB repair by HR.

A549 cells were treated with the indicated siRNAs, exposed to 3 Gy IR and examined for RPA (A), RAD51 (B) or gH2AX (C) foci at the indicated times. Results are shown in samples with or without siRNA KAP1 to expose the necessity to have relaxed HC to observe HR in G2 phase. Results represent the mean and s.d. of 3 experiments.

Figure 5. Analysis of IRIF in G1 and G2 cells using enhanced resolution microscopy.

A-B) Analysis of 53BP1 foci volume in A549 cells following exposure to 3 Gy IR. The 53BP1 foci volume was assessed by 3 dimensional imaging using an Applied Precision® Delta Vision® RT Olympus IX70 deconvolution microscope and softWoRx® Suite software at the indicated times in G1 and G2 phase cells (see Materials and Methods for details). G2 cells were identified by CENPF staining. Analysis was undertaken in untreated cells (A) and following treatment with siRNA BRCA1 (B). The data represent the median, lower and upper quartiles from at least 10 nuclei from each of three experiments. Error bars represent the minimum and maximum valid values. Maximum valid values, determined as the highest datum still within 1.5 x the interquartile range of the upper quartile, were used to eliminate abnormally large values arising from foci 'clumping' and resolution limitations (depicted as individual points). Statistical analysis was carried out using the Mann Whitney Rank Sum test. Data were deemed to be significant when a p value < 0.05 was obtained. BRCA1 depletion was confirmed by immunostaining. Typical results are shown in Supplementary Figure 4A. C) Representative images of nuclei immunostained for 53BP1 at 8 h after 3 Gy IR in G1 and G2 with or without siRNA BRCA1. Left panels are immunofluorescence images; right panels show the computer generated 3D structures used for foci volume quantification in panels (A) and (B). We and others have observed foci enlargement in G1 phase with time. However, although observed, this did not cause a significant increase in the volume assessment made here and is distinct (and smaller) than the marked increase in volume observed in G2 phase cells.

Figure 6: **BRCA1 promotes relocalisation of 53BP1 in G2 creating a core devoid of 53BP1 and ubiquitin chains.**

A-B) Analysis of G2 A549 cells at 0.5 (A) and 8 (B) h post 3 Gy IR. Following immunostaining with the indicated antibodies (53BP1, BRCA1, RPA, FK2 and

gH2AX), 3D IRIF analysis was undertaken using softWoRx® Suite. The red and green signals represent 53BP1 and RPA, respectively; the blue signal is as indicated. 'Wireframe' images are displayed allowing 3D visualisation. Foci volume enlarges from 0.5- 8 h post IR generating an expanded core lacking 53BP1. BRCA1 localises internally to 53BP1 and RPA lies within the core**.** G1 images are shown in Figure 5C. They were indistinguishable from G2 images at 0.5 h. C) Images following siRNA BRCA1 8 h post IR. The foci at 0.5 h were similar to those at 8 h. No detectable BRCA1 signal was observed following BRCA1 knockdown. D) 53BP1 foci volume estimations following siRNA Artemis. Analysis was undertaken as in Figure 5. Artemis knockdown was verified by demonstrating a G2 repair defect (Supplementary Figure 5A).

Figure 7. The BRCT but not the RING domain of BRCA1 is required for resection, Rad51 loading and 53BP1 repositioning during HR in G2.

A*) BRCA1*$^{FH\text{-}WT/FH\text{-}WT}$, *BRCA1*$^{FH\text{-}I26A/FH\text{-}I26A}$ and *BRCA1*$^{S1598F/S1598F}$ MEFs were irradiated with 3Gy IR in the presence of aphidocolin. Cells were harvested 8 h post IR and immunostained with DAPI, RPA and p-H3 antibodies to identify G2 cells. RPA foci were enumerated in p-H3^{+} cells. B) As for A) but Rad51 foci were enumerated 2 h post 3Gy IR. In A-B), foci were enumerated in 30 cells per time-point and the data represent the mean and s.d. of 3 experiments. C) Analysis of 53BP1 foci volume in G2 phase *Brca1*$^{FH\text{-}WT/FH\text{-}WT}$, *BRCA1*$^{FH\text{-}I26A}$ and *BRCA1*$^{FH\text{-}S1598F}$ MEFs 0.5 and 8h following 3Gy IR. Analysis was carried out as in Figure 5A. Statistical analysis was carried out using the Mann Whitney Rank Sum test. Data were deemed significant when p was < 0.05.

Figure 8. POH1 promotes resection in G2 by overcoming the inhibitory barriers of 53BP1 and RAP80.

A) 53BP1 foci volume was estimated in A549 cells treated with the indicated siRNA at 0.5 and 8 h following 3Gy IR. Statistical analysis was carried out using the Mann-Whitney rank sum test. Data were deemed to be significant when a p value < 0.05 was obtained. B) A549 cells were immunostained with the indicated antibodies 8 h post 3Gy IR. G2 cells were selected by CENPF^{+} staining. The far left panels are a projection of the immunofluorescence (IF) Z-stacked images acquired on an Applied Precision® Delta Vision® RT Olympus IX70 deconvolution microscope. 3D model conversions of these images using the softWoRx® Suite are shown in the subsequent panels. Individual

foci from cells treated with the indicated siRNA were magnified and displayed either as solid or wireframe structures. Wireframe images allow visualisation of the hollow core in 53BP1 and FK2 IRIF where RPA foci form. A devoid core of 53BP1 or FK2 does not form following siRNA POH1 but is visible following siRNA BRCC36+POH1. A single oligonucleotide to POH1 was used for this experiment but similar results were obtained using a pool of siRNA POH1 oligonucleotides. C) A549 cells were treated with the indicated siRNA, and exposed to 3 Gy IR. Cells were processed as in Figure 1. RPA foci were enumerated in 30 cells per time-point and data represent the mean and s.d. of 3 experiments.

Supplementary figure 1

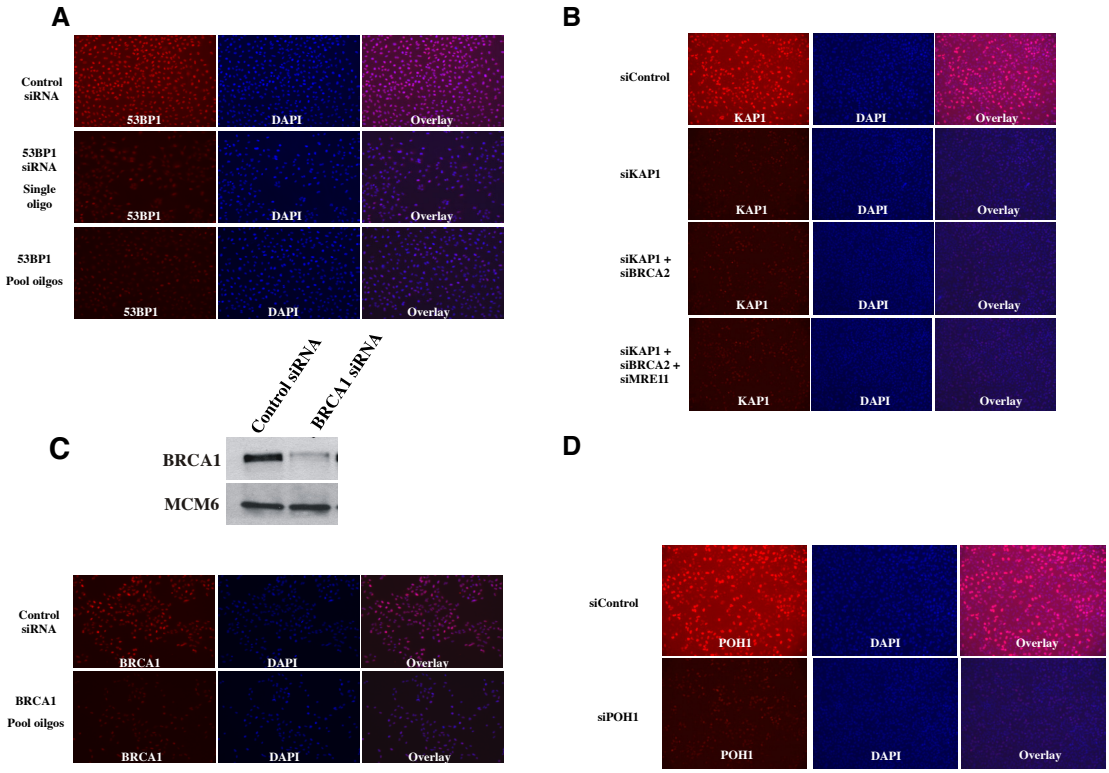

Supplementary figure 2

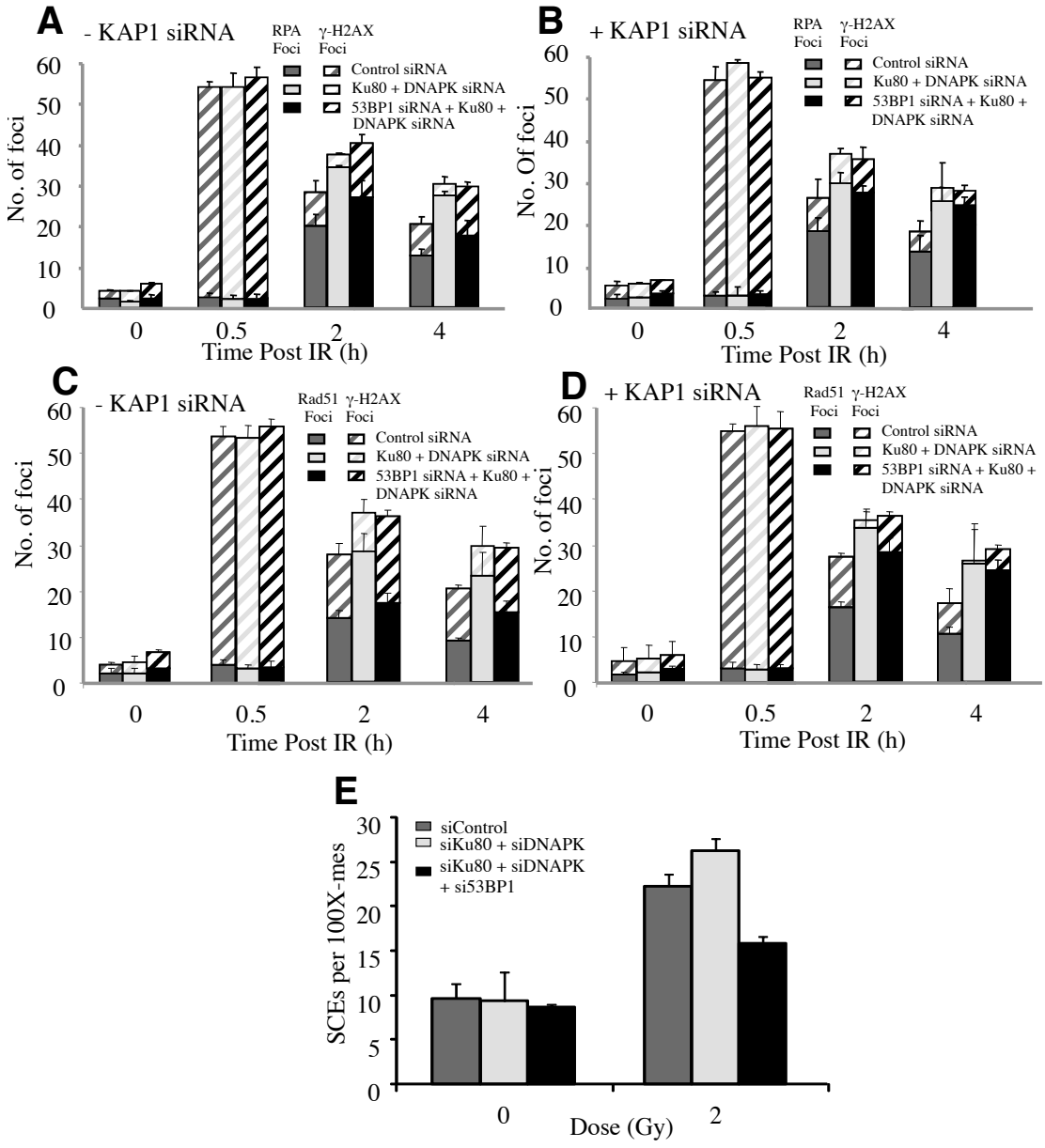

Supplementary figure 3

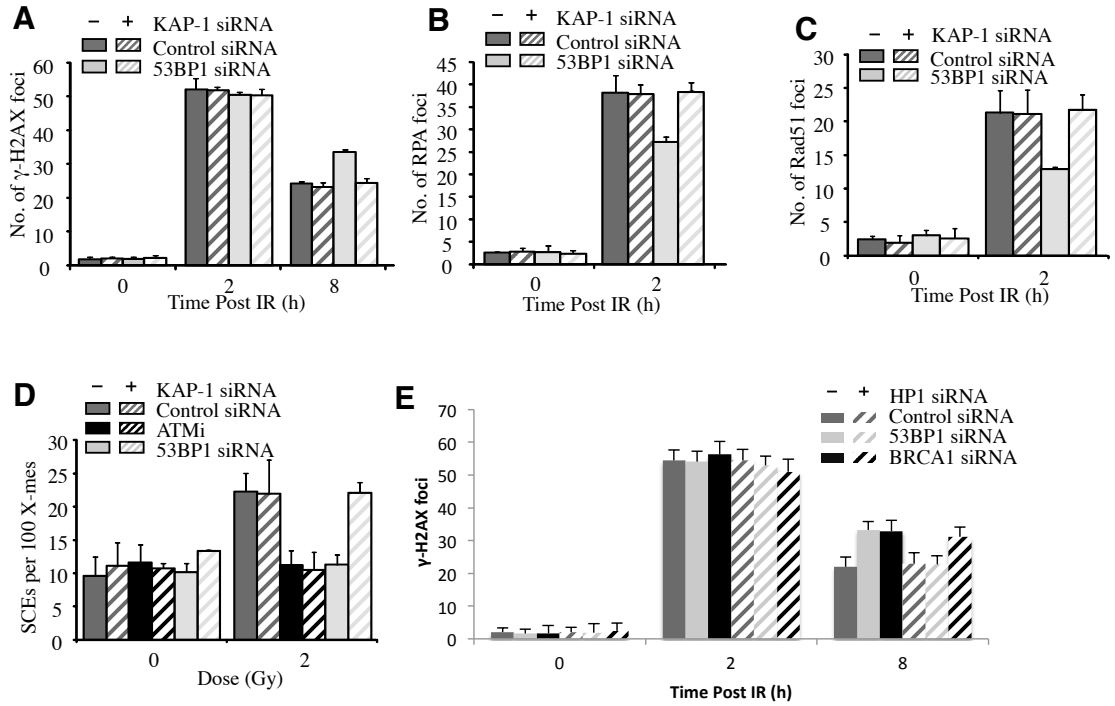

Supplementary figure 4

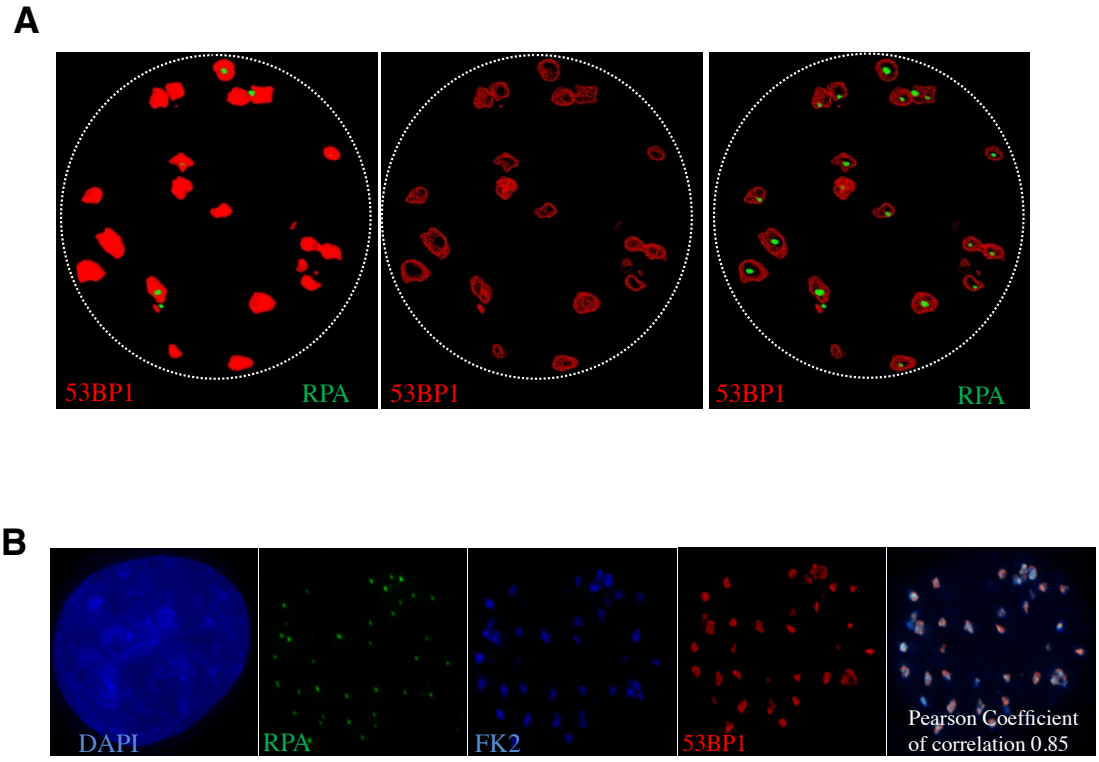

Supplementary figure 5

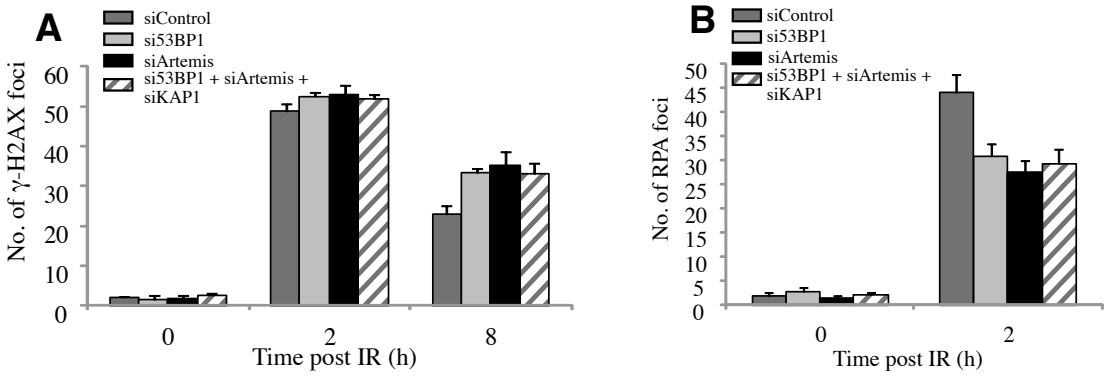

Supplementary figure 6

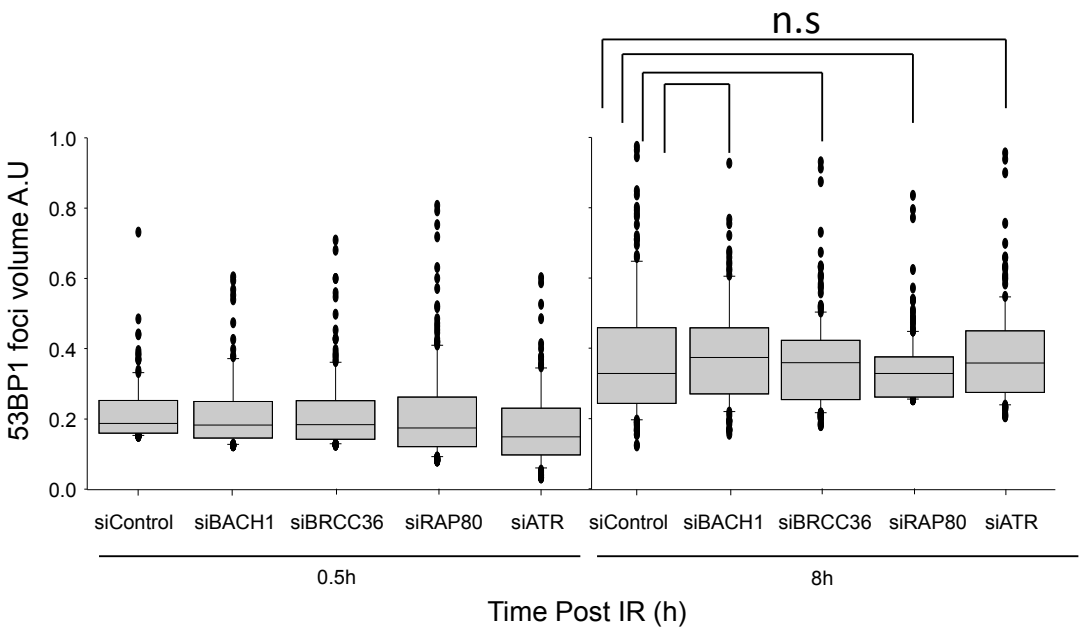

Supplementary figure 7

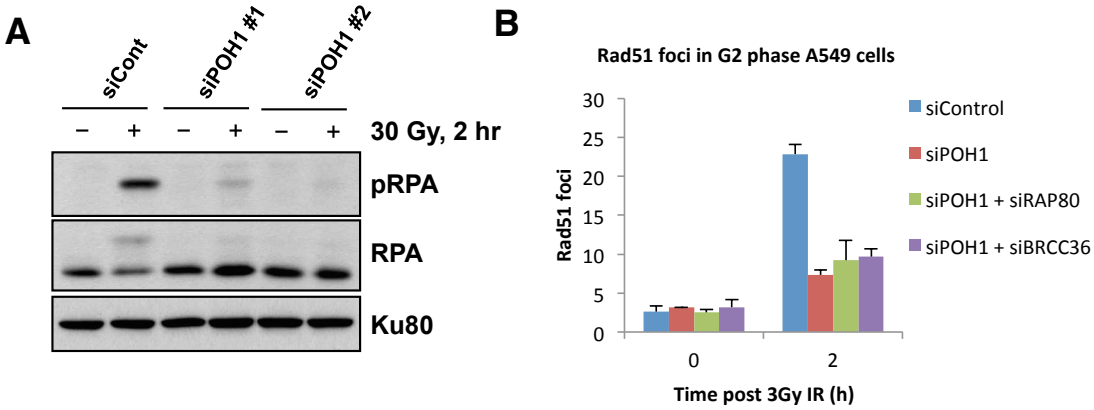

Supplementary figure 8

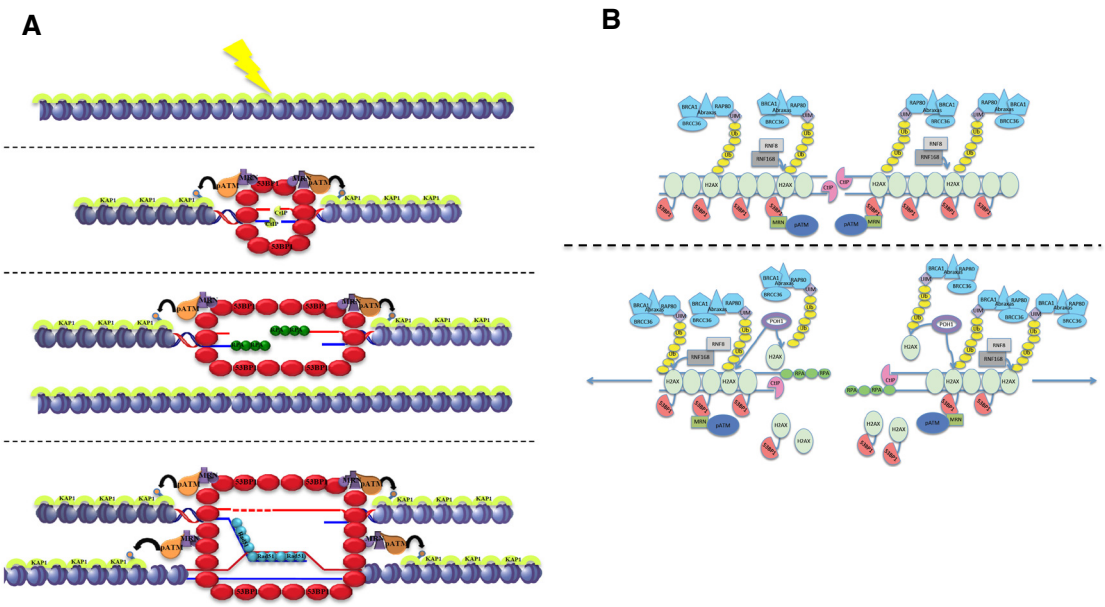

Supplementary Figure 1: Controls for siRNA knockdown efficiencies.
100 pmol of siRNA duplexes per 2 x 10^5 logarithmically growing cells were used for each knockdown. Cells were then grown for 72 h prior to fixation and immunostaining/immunoblotting with the indicated antibodies. A) Knockdown efficiency in A549 cells following treatment with either a single or a pool of 53BP1 siRNA oligonucleotides (the single oligonucleotide was distinct to any in the pool). B) As above but knockdown efficiency of KAP-1 siRNA was assessed under single, double and triple knockdown conditions. C) BRCA1 single and pool oligonucleotide knockdown efficiency was assessed by immunoblotting and immunostaining. For immunoblotting, MCM6 was used as a loading control. D) Knockdown efficiency of POH1 following treatment with a single POH1 siRNA oligonucleotide. Similar results were also obtained using a pool of distinct siRNA POH1 oliognucleotides.

Supplementary Figure 2: 53BP1 is dispensable for resection and RAD51 loading at euchromatic DSBs in cells lacking DNA-PK components.
A-B) RPA and gH2AX foci were enumerated in G2 cells at the indicated times after exposure to 1 Gy IR in A549 cells subjected to control siRNA, siRNA Ku80+DNA-Pkcs or siRNA 53BP1+Ku80+DNA-PKcs either without (A) or with (B) KAP1 siRNA. C-D) As shown for panels A-B but RAD51 foci are shown instead of RPA foci. Solid and hashed columns represent RPA (or RAD51) and gH2AX foci, respectively. Results following 53BP1 siRNA alone are given in Figure 2. Results represent the mean and s.d. of 3 experiments.

Since DNA-PK component proteins (Ku70, Ku80 and DNA-PKcs) are highly expressed in human cells, siRNA depletion of these proteins is inefficient. We, therefore, carried out combined Ku80 and DNA-PKcs siRNA (labelled Ku80+DNA-PK siRNA). Following Ku80+DNA-PKsiRNA, DSB repair is slowed and increased RPA and Rad51 foci numbers are observed (A and C) and increased G2 phase SCEs arise (E*)* i.e. euchromatic (EC) DSB repair by HR is increased. siRNA Ku80+DNA-PK+ 53BP1 compared with to siRNA Ku80+DNA-PK (i.e. without 53BP1 siRNA) revealed a modest reduction in RPA foci (A,B), RAD51 foci (C,D) or SCEs (E). This reduction was similar to that observed in cells treated only with siRNA 53BP1 (see Figure 1 main text). As in Figure 1, the magnitude of the reduction was greater for RAD51 than for RPA foci. Further, following additional depletion of KAP-1 (i.e. DNA-PK/53BP1/KAP-1 siRNA) RPA foci numbers were identical to that observed in cells

subjected to DNA-PK siRNA alone (B). Similar results were obtained monitoring RAD51 foci (C and D). (NB SCE analysis was not carried out following quadruple siRNA since this impacted on cell proliferation). Collectively, these results suggest that 53BP1 is dispensable for HR at EC-DSBs but promotes HR at HC-DSBs via its role in promoting HC relaxation. E) Sister chromatid exchanges in G2 phase A549 cells following exposure to 2 Gy IR. Following treatment with the indicated siRNA oligos, 2 x 10^5 logarithmically growing cells were cultured for 48 h in 10 μM BrdU before IR. 0.2μg/ml Colcemid (plus 1mM caffeine to overcome the G2/M arrest) was added from 8 -12 h post-IR to collect mitotic cells. SCEs were scored in at least 800 chromosomes from 3 independent experiments per data point. Staining was according to standard protocols. Results represent the mean and s.d of 3 experiments. These results show a small increase in SCEs following siRNA of Ku80+DNA-PKcs demonstrating that some DSBs are repaired by HR. SCE frequency is also increased compared following Ku80+DNA-PKcs+53BP1 siRNA but the increase is smaller compared to that observed in control cells. This is consistent with the notion that 53BP1 is dispensable for HR at EC-DSBs but is required for HR at HC-DSBs. SCE formation after quadruple knock-down that included KAP1siRNA was not pursued since there was a significant impact on mitotic frequency.

Figure 3. The defect in HR in 53BP1 siRNA cells can be relieved by KAP1 or HP1 siRNA.

gH2AX (A), RPA (B) or RAD51 (C) foci were enumerated at the times indicated following exposure of A549 cells to 3 Gy IR with or without siRNA KAP-1. Panel D) shows the quantification of SCEs in mitotic cells arising from irradiated G2 phase cells. In all panels results represent the mean and s.d. of 3 experiments. All results shown were obtained using a pool of 53BP1 oligonucleotides and these are used hereafter as substantial protein knockdown was achieved (Supplementary Figure 1A). The efficiency of siRNA KAP-1 is shown in Supplementary Figure 1B. E) A549 cells were treated with control, 53BP1 or BRCA1 siRNA with or without siRNA to all three isoforms of HP1 (α,β,γ) and were irradiated with 3Gy IR. Sample preparation and gH2AX enumeration was carried out as in A).

For all endpoints, siRNA KAP1 or HP1 relieved the defects observed by siRNA 53BP1.

Supplementary figure 4: **Analysis of 53BP1, RPA and FK2 IRIF.**

A) 3D model of G2 phase A549 cell harvested 8h post 3 Gy IR and immunostained with the indicated antibodies. The left panel is a 'solid' representation of both 53BP1 and RPA signals. In the middle and right panels, 53BP1 signal is shown as 'wireframe' depicting the hollow center of 53BP1 foci where RPA foci form. B) A549 Cells were immunostained with the indicated antibodies 8 h post 3Gy IR and colocalization between 53BP1 and FK2 was carried out using softWoRx® Suite software. The Pearson Coefficient of Correlation indicates how closely the two intensities are colocalized on a pixel-by-pixel basis (full colocalization is 1.0)

Supplementary figure 5: 53BP1 depletion does not alleviate the requirement of Artemis in G2 phase DSB repair.

A549 cells were treated with the indicated siRNA, exposed to 3 Gy IR and examined for gH2AX (A) and RPA foci (B) at the indicated times. 53BP1 depletion did not rescue either the diminished RPA foci formation or DSB repair in G2 cells depleted for Artemis. Results represent the mean and s.d. of 3 experiments.

Supplementary Figure 6. The BRCA1 interacting proteins BACH1, RAP80 and BRCC36 as well as ATR function are dispensable for 53BP1 repositioning during HR.

Analysis 53BP1 foci volume in A549 cells treated with the indicated siRNA. The cells were irradiated with 3Gy and harvested at 0.5h and 8h post IR. The volume of 53BP1 foci was assessed by 3 dimensional imaging using an Applied Precision® Delta Vision® RT Olympus IX70 deconvolution microscope and softWoRx® Suite software at the indicated times (see materials and methods for details of image processing). The data represent the median and lower and upper quartiles from at least 10 nuclei from each of three experiments. Error bars represent the minimum and maximum valid values determined as the highest datum still within 1.5 the interquartile range of the upper quartile. These were used to eliminate abnormally large values (depicted as single points) arising from foci 'clumping' and resolution limitations. Statistical analysis was carried out using the Mann Whitney Rank Sum test. Data where deemed to be significant when a p value < 0.05 was obtained.

Supplementary Figure 7: POH1 depletion impairs resection and Rad51 foci

formation following IR.

A) Cells subjected to POH1 siRNA display impaired IR-induced RPA phosphorylation. To monitor resection following IR, phosphorylation of RPA on Ser 4 and Ser 8 was examined by Western Blotting. A549 cells were irradiated with 30 Gy following siRNA transfection, and whole cell extracts were prepared at 2 h post IR. Depletion of siRNA POH1 resulted in significantly reduced pRPA formation. The results are shown using a single POH1 siRNA oligonucleotide and a pool of POH1 siRNA oligonucleotides (see Materials and Methods).

B) A549 cells were treated with the indicated siRNA and 72 h later were exposed to 3Gy IR. Rad51 foci were scored in G2 phase cells as determined by CENP-F +ve staining. Results represent the mean and s.d. of 2 experiments. siRNA POH1 resulted in markedly reduced RAD51 foci but there was only a small rescue following siRNA RAP80 or BRCC36 in contrast to the marked rescue of RPA foci (Figure 8C).

Supplementary Figure 8: **Model showing the expansion of 53BP1 foci in G2 phase and the formation of an IRIF core devoid of 53BP1 and FK2 where RPA foci form.**

A) Model showing the requirement for 53BP1 to affect HC changes on the undamaged sister chromatid. The slowly repaired DSBs that arise within regions of heterochromatin (HC) undergo resection and repair by HR (HC is depicted in green). In early G2 phase (30 min post IR), 53BP1 foci form around the DSB on a single DNA molecule similar to the situation in G1 phase. 53BP1 is likely not located at the extreme DNA end. 53BP1 interacts with RAD50 of the MRN complex; NBS1 of the MRN complex interacts with ATM. Thus, ATM tethering at the DSB is enhanced by the presence of 53BP1 foci (interactions between MRN and MDC1 or H2AX also enhance ATM tethering but 53BP1 appears to be critical for the presence of pATM foci at DSBs). ATM phosphorylates KAP-1 located at HC-DSBs in a concentrated manner producing pKAP-1 foci (note that pan-nuclear pKAP-1 also occurs at early times post IR but this is not 53BP1-dependent; in contrast the formation of pKAP-1 foci, which only form at HC-DSBs is 53BP1-dependent). This causes HC-relaxation in the vicinity of the DSB (not depicted in the figure). HC forms a partial barrier to resection that is overcome by 53BP1-ATM pKAP-1 foci formation. The presence of 53BP1 on the DNA molecule also forms a partial barrier to the completion of resection and a bigger barrier to RAD51 loading. However, neither 53BP1 nor KAP1 prevent the initiation of resection by CtIP-MRN, since they function downstream of CtIP-MRN

dependent commitment to HR and since RPA foci numbers are only partially reduced. Later in G2 (evident at 2 h), further resection ensues followed by the single stranded DNA overhang with bound RPA and/or RAD51 invading the undamaged sister template. 53BP1 foci formation expands to allow further resection and to encompass the undamaged DNA molecule, resulting in a two fold expansion in foci volume. The expansion of 53BP1 foci requires the BRCT but not the RING finger domain of BRCA1 and involves repositioning of ubiquitin modifications on histones. Thus, we propose that BRCA1 promotes deubiquitination and/or proteasome mediated protein degradation in the core region and new ubiquitin events on the damaged and, we propose, the undamaged molecule. For simplicity this has not been depicted in the figure. The presence of 53BP1 on the undamaged strand allows pKAP1 formation and hence HC relaxation on this strand, which promotes the completion of resection and/or RAD51 loading. We have depicted 53BP1 as entirely encircling the DNA molecule although its initial tethering involves interactions with methylated H4. This is consistent with evidence that 53BP1 undergoes oligomerisation and has a role in synapsis during long range V(D)J recombination (Adams et al, 2005; Difilippantonio et al, 2008). In G2 phase, 53BP1 may also enhance synapsis but this does not appear to be essential since HR can ensue in the absence of 53BP1+BRCA1. We suggest that the close association of sister chromatids in G2 phase via cohesin interactions can function redundantly to 53BP1-dependent synapsis in G2 phase. Thus, 53BP1-dependent synapsis is only essential for long-range translocation events in G1 phase.

B) Model showing the role of POH1 in removing 53BP1 from the foci core region. Previous studies have demonstrated that 53BP1 and RAP80 form a restrictive barrier to resection by binding to methylated and ubiquitylated histones at DSBs. The BRCT domain of BRCA1 is required for 53BP1 repositioning away from the DSB ends as well as for the formation of an IRIF core devoid of 53BP1 where resection occurs. Similarly, the BRCT domain of BRCA1 is also required for the formation of an IRIF central core devoid of ubiquitin modifications. We propose that BRCA1 achieves this via the recruitment of the deubiquitinating enzyme POH1which functions to promote the removal of 53BP1 and ubiquitin chains but is dispensable for 53BP1 repositioning to the foci periphery. POH1 DUBing might lead to histone degradation thus exposing DNA to the nucleases which carry out the elongation step in resection.